Toward the Development of Sustainable Polymers – Zinc and Iron Complexes for Poly(carbonate), Poly(ether) and Poly(ester) Synthesis

By

Timothy Simon Anderson

A thesis submitted to the School of Graduate Studies

in partial fulfillment of the requirements for the degree of

Doctor of Philosophy

Department of Chemistry

Memorial University of Newfoundland

July 2021

St. John's Newfoundland

Abstract

In recent decades, significant effort has been put toward the development of sustainable polymers to compliment or replace the materials currently in use. Two major classes of interest are poly(carbonate)s and poly(ester)s. The allure of these stems from the materials that are used to synthesize them. Copolymerization of carbon dioxide and epoxides is one method of synthesizing poly(carbonate) and carbon dioxide levels in our atmosphere continue to rise – a result of anthropogenic activity – therefore, utilizing the small molecule for various transformations is convenient and necessary. The most common epoxides used in poly(carbonate) synthesis are produced from petroleum but there are naturally sourced compounds as well. Similarly, poly(ester) is produced mainly in the form of poly(ethylene terephthalate) but recently, naturally sourced reagents (i.e. lactide) have begun commercial production. The synthesis of the polymers is often facilitated through metal-based catalysts that encourage controlled reactivity between the substrates.

In this work, a zinc amino-bis(phenolate) complex was investigated for catalytic activity toward carbon dioxide and cyclohexene oxide copolymerization in the presence of benzyl alcohol co-catalyst producing poly(ether-*co*-carbonate) with high molecular weights containing both ether and carbonate linkages. The catalyst was active at 1 bar carbon dioxide – a trait shared by some of the most active catalysts in this area. The complex also exhibited activity toward copolymerization of carbon dioxide and limonene oxide – a naturally sourced

epoxide. Poly(limonene carbonate) typically exhibits physical properties more similar to commercially produced bisphenol-A poly(carbonate)s.

Iron complexes were also examined for carbon dioxide and epoxide coupling as part of a collaboration between the groups of Drs. Kerton and Kozak with my own contributions studying three Fe(III) amino-bis(phenolate) complexes. Toward cyclohexene oxide and carbon dioxide coupling in the presence of bis(triphenylphosphine)iminium chloride co-catalyst, only cyclic cyclohexene carbonate was observed in low yields. However, the activity of two of the complexes toward lactide ring-opening polymerization was high. Furthermore, co- and terpolymerization reactions involving lactide, phthalic anhydride and epoxides produced poly(ester-*co*-ether)s with narrow dispersities.

A zinc alkylperoxo complex was synthesized and structurally characterized. This could be applied toward the epoxidation of *a-ß* unsaturated ketones and subsequent copolymerization with carbon dioxide in one-pot in low yields. This represents the first instance of poly(carbonate) synthesis from epoxide-devoid starting materials in one-pot.

Acknowledgements

I would first like to offer a sincere thank you my supervisor, Dr. Christopher Kozak, for taking me into his research group and helping me to flourish into the chemist I am today. His patience with me cannot be overstated, and he has always encouraged me to be a greater scientist and person. He has been an exceptional mentor, educator, leader, source of support, and is someone who seems to share in my philosophy that a day that is spent without a laugh is a day wasted. Here, I would also like to thank Dr. Francesca Kerton for all of her advice and guidance and infectious desire to learn more.

Next, I would like to thank Dr. Bob Helleur and Dr. Sunil Pansare for their advice and guidance as committee members. Thank you to Dr. Celine Schneider for all of her help with NMR spectroscopy, Dr. Louise Dawe and Dr. Mike Katz for X-ray crystallography, Linda Windsor and Dr. Stefana Egli for their aid with MALDI-TOF MS, and to Adam Beaton for assisting with TGA and DSC.

Thank you to NSERC (Dr. Kozak's research grant), the Department of Chemistry, School of Graduate Studies and the Graduate Student Union here at Memorial University, as well as Dr. Liqin Chen and Mitacs for the funding that made all of this work possible.

I'd also like to thank all of the members of the Green Chemistry and Catalysis Group with whom I have had the privilege to know over the years. A special shout out to Kori, Juliana, Jen, Kenson, Kaijie and Hart, who have always made the best days brighter and the worst days easy. A special thank you as well to all of the wonderful staff in the chemistry department, past and present.

Finally, thank you to my parents, Bud and Cathy Anderson, and my siblings Matt, Kerri, Ryan and Kelsey for their unending love and support. Thank you as well to my good friends Heff, Jon, Dare, Matt, Josh, May and Lucas for being there for me all along the way. I could never have gotten to where I am today without the support of everybody listed here, and many others, and for which I will be forever grateful.

Table of Contents

List of Figures

List of Schemes

List of Tables

List of Abbreviations and Units

°C: degrees Centigrade

Å: Ångstroms (10^{-10} m)

AGE: allyl glycidyl ether

ATR: attenuated total reflectance

bar: 100 kilopascals

BAr^F: tetrakis(3,5-bis(trifluoromethyl)phenyl)borate

BBL: *ß*-butyrolactone

BDI: *ß*-diketiminate

BPA: bisphenol-A

C1: single carbon

CA: complexing agent

CBO: *cis*-butylene oxide

CHC: cyclohexene carbonate

CHEO: cyclohexyl ethylene oxide

CHO:cyclohexene oxide

CPO: cyclopentene oxide

Đ: dispersity (M_w/M_n)

DBU: 1,8-diazabicyclo[5.4.0]undec-7-ene

DGA: diglycolic anhydride

DHBA: 2,3-dihydroxybenzoic acid

DMAP: 4-(dimethylamino)pyridine

DMCC: double metal cyanide complex

DOSY: diffusion ordered spectroscopy

DSC: differential scanning calorimetry

E_a: activation energy

ECH: epichlorohydrin

Fc: ferrocenium

g: gram(s)

GO: glycidol

GPC: gel permeation chromatography

h: hour(s)

HPLC: high performance liquid chromatography

Hz: hertz

IBO: isobutylene oxide

iPrOH: isopropyl alcohol

IR: infrared

K: degree(s) Kelvin

kJ: kilojoule(s)

LA: lactide

LDO: limonene dioxide

LO: limonene oxide

LPV: low pressure/vacuum

m/z: mass to charge ratio

MA: maleic anhydride

MALDI-TOF: matrix-assisted laser desorption/ionization time-of-flight

*m*CPBA: *meta*-chloroperoxybenzoate

min: minute(s)

mL: millilitre(s) (10^{-3} L)

M_n: number average molecular weight

mol: moles

MS: mass spectrometry

M_w: weight average molecular weight

NA: naphthalic anhydride

NMR: nuclear magnetic resonance

Ac: acetate

PA: phthalic anhydride

PC: poly(carbonate)

PCHC: poly(cyclohexene carbonate)

PCL: poly(caprolactone)

PCPE: poly(cyclopentyl ether)

PET: poly(ethyleneterephthlalate)

PGE: phenylglycidyl ether

PHB: poly(hydroxybutyrate)

phosfen: 10-di(2-*t*-butyl-6-diphenyl-phosphiniminophenoxy)ferrocene

PLA: poly(lactic acid)

PLC: poly(limonene carbonate)

PMDETA: pentamethyldiethylenetriamine

PO: propylene oxide

PPC: poly(propylene carbonate)

ppm: parts per million

rac: racemic

ROCOP: ring-opening copolymerization

ROP: ring-opening polymerization

s: seconds

SA: succinic anhydride

salan: *N*,*N*'-bis(phenolato)-1,2-diaminoethane

salen: *N*,*N*'-bis(salicylidene)ethylenediamine

SO: styrene oxide

TBA: tributylamine

TBD: 1,5,7-triazabicyclo[4.4.0]dec-5-ene

TEEDA: *N*,*N*,*N*′,*N*′-tetraethylethylenediamine
TEMPO: (2,2,6,6-tetramethylpiperidin-1-yl)oxyl

TFA: trifluoroacetate

T_g: glass transition temperature

TGA: thermogravimetric analysis

THF: tetrahydrofuran

TMEDA: tetramethylethylenediamine

TMS: tetramethylsilane

TO: turnovers

TOF: turnover frequency

TON: turnover number

UV-vis: ultraviolet-visible

v/*v*: volume by volume

VCHO: vinyl cyclohexene oxide

vs: versus

ε-CL: epsilon caprolactone

μL: microlitres (10^{-6} L)

μm: micrometre (10^{-6} m)

List of Appendices

Chapter 1

Statement of Co-Authorship

Section 1.3 has been published as part of *Copolymerization of carbon dioxide and epoxides by metal coordination complexes* in Coordination Chemistry Reviews, **2018**, *376*, 565-587.

Authors: Christopher M. Kozak, Kenson Ambrose & Timothy S. Anderson

The third author (Timothy S. Anderson) contributed to all aspects of Section 4 of this published review including literature review, manuscript preparation and the addressing of peer-reviewed comments.

The second author (Kenson Ambrose) contributed to all aspects of Section 2 including literature review, manuscript preparation and the addressing of peer-reviewed comments.

The corresponding author (Christopher M. Kozak) is the principal investigator and provided the initial idea of the review. Dr. Kozak contributed to writing all sections of the review and entirely for all sections not mentioned above including conducting the literature review, manuscript preparation and submission, and co-author supervision.

Introduction

1.1. Polymerization reactions

Polymers encompass a diverse array of compounds utilized throughout our modern-day society. Their expansive set of physical characteristics make them suitable for a myriad of applications and thus they are ubiquitous throughout our day-to-day lives. They are not, however, purely synthetic. In Nature, polymers are found in many forms, from the cellulose that causes rigidity in plants, to the protective silk chrysalises of a butterfly, to the very DNA in all living beings on Earth. We have been able to harness the versatility of polymers, allowing us to form numerous materials ranging from flexible thin films to rigid protective casings and anything in between. The refinement of polymer production toward a particular function has been nearly perfected. There are, of course, many types of polymers and it is the chemical composition and arrangement of groups in their chains that directly influence their properties. The individual repeating units that make up a polymer have drastic effects on these metrics. Polyolefins, particularly poly(ethylene), poly(propylene), and poly(vinyl chloride), are produced more than other polymer compounds for commercial applications and remain some of the most well-defined as a result, but the robustness of the materials also limit their ability to be broken down environmentally.

1.2. Environmental impact

The bioaccumulation of plastics and microplastics can have a profound impact on many ecosystems and, as per a recent report by Auta and coworkers, sampling from any environment on Earth will be contaminated with these materials.[1] Microplastics are one such contaminant, the result of polymer weathering, and have been found deep in the Marianas Trench and atop mountains. The effect of this pollution goes beyond the superficial: wildlife, particularly in oceans and lakes, are often found with substantial amounts of plastic waste in the digestive tracts of their carcasses. A 2020 review covered reports of the effects of these materials on human health and they are suspected of causing neurodegenerative diseases, immune disorders and cancers due to the potential of surface reactivity, but these reports are not conclusive and further study is required to draw firm conclusions.[2] Another prominent example is that of poly(carbonate) decomposition releasing bisphenol-A (BPA), one of the two major components in commercial synthesis of poly(carbonate), into environmental ecosystems. Studies have suggested that BPA is an endocrine mimic and thus overexposure and bioaccumulation could result in negative side effects, particularly reproductive health and metabolic diseases.[3] A recent study commissioned by Environment and Climate Change Canada found that less than 10% of consumer plastics are recycled in any fashion and a staggering 86% end up in landfills. It would be naïve to assume that there is a single answer to the growing problem of environmental waste accumulation of polymers. Several avenues must be pursued and among them is the development of new materials with reduced or eliminated environmental impact, either through benign (bio)degradation or efficient recycling techniques.

1.3. Catalysis

A central theme of the work reported in this thesis will revolve around catalysis, particularly organometallic, homogeneous catalysis. This principle allows for the synthesis of materials that might otherwise be extremely difficult or impossible under other means by lowering the energy input required to facilitate the reactions. Although it is difficult to predict the financial impact catalysis has on our economies, the *U.S. Pacific Northwest National Laboratories* places the value of all commercial and industrial catalytic processes at $10 trillion annually as of 2015.[4] The importance of catalysis stretches far beyond the economic realm and is of critical importance in biological systems in the forms of enzymes or other systems. Enzymes are biological catalysts primarily composed of proteins that are essential for the survival of complex life.[5] The ability to carefully control highly reactive species (catalase to H_2O_2) or activation of compounds with limited reactivity (carbonic anhydrase to CO_2) highlight some of the potential of catalysis.[6-7] Although many enzymes are entirely organic, these two examples each contain a metal that is fundamental to their reactivity, iron and zinc respectively. It has been estimated that one-third of all enzymes and proteins contain metals in some capacity that is related to their biological activity.[8] Synthetic organometallic and inorganic catalysis have further demonstrated the efficacy of metal-based catalysis for an enormous number of reactions, with olefin metathesis, olefin hydrogenation and carbon–carbon and carbon–heteroatom cross-coupling being among the most prevalent and applicable to many synthetic disciplines.[9-16]

The development of first-row transition metal complexes to supplant their precious-metal analogues is of great interest owing to the relative abundance and associated economic cost. The reactivity of the 3d metals is often different to their 4d and 5d counterparts, typically a result of differing electronic or bonding environments.[11,15-17] Manipulation of these properties through judicious ligand design is the most powerful technique currently available for enhancing the activity of 3d transition-metal catalysts. Reviewing all of the efforts to develop earth-abundant metal-catalyzed transformations would be a colossal task and so this thesis will instead focus on catalysts for poly(ester), poly(ether) and poly(carbonate) production.

1.4. Source of monomers for polymer synthesis

The three classes of polymers to be discussed in this thesis will be poly(ester)s, poly(ether)s and poly(carbonate)s, and as such monomers pertaining to these materials will be highlighted, namely cyclic esters, cyclic anhydrides and epoxides. The majority of polymer feedstocks are sourced from non-renewable petrochemicals. Poly(ester)s are one of the most widely produced polymer sub-types and production has been dominated by poly(ethylene terephthalate) (PET), ranked fourth in commercial production and among the common make-up of single-use plastics.[18] The production of poly(ethylene terephthalate) can be traced back to petroleum refinement by-products along with so many other commercialized polymers. In academic polymer research, there has been a push to diversify these feedstocks to include naturally sourced compounds or encourage alternate production of products currently produced via non-renewable reaction pathways. As an example, epichlorohydrin

(ECH) had been commercially produced from oxidation of allyl chloride, but as of 2011, bio-based ECH production from glycerol has been commercialized. A small selection of epoxides discussed in this thesis is shown in Fig. 1.1. Those highlighted in red are sourced from petroleum. Those in orange can be produced from biomass-derived sources but are commercially produced from petrochemical feedstocks. The epoxides in green are obtained from biomass-derived starting materials. Arguably the most popular naturally sourced epoxide is limonene oxide (LO) which can be produced by the oxidation of limonene, a terpene present in citrus zests. As of 2015, roughly 20,000 tons of zests are produced as waste from the citrus industry in the United States and thus a useful compound from these materials presents an excellent candidate for waste management.[19] For polymer synthesis specifically, limonene oxide is structurally analogous to the widely studied cyclohexene oxide, while containing an unsaturated bond in what would be the backbone of the polymer. Furthermore, limonene oxide contains three stereocentres meaning polymer tacticity can be influenced and have dramatic effects on the physical properties of the material. Examples of the exploitation of the functionality and particulars of the control over polymer properties will be discussed later.

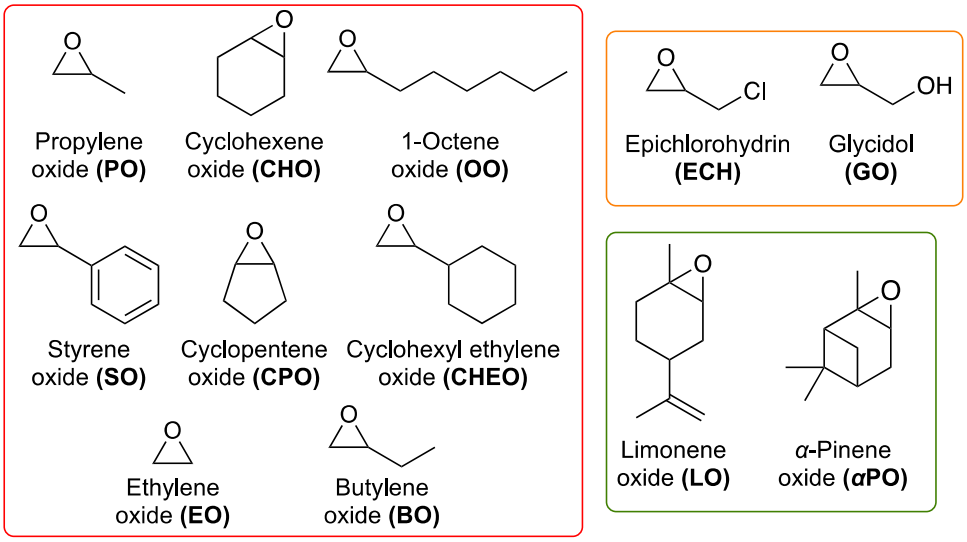

Fig. 1.1: Examples of epoxides utilized in ring-opening polymerization of epoxides and CO_2/epoxide copolymerization reactions. The left set are sourced from non-renewable feedstocks, the top right set are commercially produced from non-renewables but can be sourced from renewables and the bottom right are synthesized from renewable materials.

1.5. Polymers from renewable feedstocks

As mentioned above, a large majority of the monomers used to synthesize most industrially produced polymer products are sourced from non-renewable sources, primarily the oil refinement process. Specifically, this includes polyolefins, poly(styrene), poly(ethylene terephthalate), and poly(vinyl chlorides). Not only are these materials non-renewable, but the resulting polymers are often effectively non-degradable in the environment. Both industrially and in academia there are a growing number of companies and research groups that have begun to focus on utilizing renewable materials for polymer synthesis, including the Kerton

and Kozak groups at Memorial University of Newfoundland. Companies such as Novomer, Covestro, and NatureWorks are producing polymers of several varieties from renewable feedstocks. Among these monomers, lactide, the cyclic di-ester derived from lactic acid and its resulting polymer are the most well understood. Poly(lactide) synthesis has been extensively studied throughout the 1990s and 2000s. Lactic acid (LA) can be sourced from biomass such as corn via fermentation of carbohydrates and then converted into lactide via intermolecular esterification, intramolecular esterification of LA oligomers, and/or depolymerization of those oligomers.[20-21] Lactic acid production is observed commercially in the process of Ingeo synthesis, a poly(lactide) produced by NatureWorks that has been used as films, rigid packaging materials, non-woven fibres and durable protective casings.[22-23] Other monomers in the epoxide and anhydride families will be discussed in their respective sections below. The term (bio)degradable will be used throughout this work and although the definition in polymer chemistry is "…polymers that require enzymes of microorganisms for hydrolytic or oxidative degradation…" which would preclude poly(lactide) or other materials that can degrade under environmentally natural conditions (photodegradation, hydrolysis, etc.), it will nevertheless be used to include such materials as well when the degradation products are not considered harmful.[24]

1.6. Multicomponent polymerization reactions

To this point in the thesis, several examples of polymers made from a single monomer have been described. Polymers can also be prepared that incorporate different monomers into polymeric repeating units within a single chain. The resulting polymers are

named according to the number of individual components and their relative arrangement to one another. Homopolymers, copolymers and terpolymers (one-, two- and three-component polymers) will be discussed in this thesis (Fig. 1.2). Polymer **A** represents a polymer composed of a single repeating unit, a homopolymer. **B** is a copolymer with a distinct split between segments, a block copolymer. Similarly, **C** is an alternating block copolymer and **D** a perfectly alternating copolymer. **E** represents a random copolymer, where there is no control over monomer insertion. **F** is a block terpolymer consisting of three different monomer types. **G** represents an alternating terpolymer. **H** shows a random terpolymer. With well-defined segments of different polymeric chains, the physical properties of the materials can be altered according to that make-up. For example, limited control over the glass transition temperature – T_g, the temperature range at which a polymer changes from a rigid material to a more viscous or fluidic state – of poly(propylene carbonate) (30 – 40 °C) can be achieved through molecular weight control alone which makes the biocompatible polymer unsuitable for biomedical applications due to the similarity to human body temperature.[25] By incorporating a separate block of poly(cyclohexene carbonate), this can be increased to 65 – 70 °C, which may provide a suitable material for these biomedical purposes.[26]

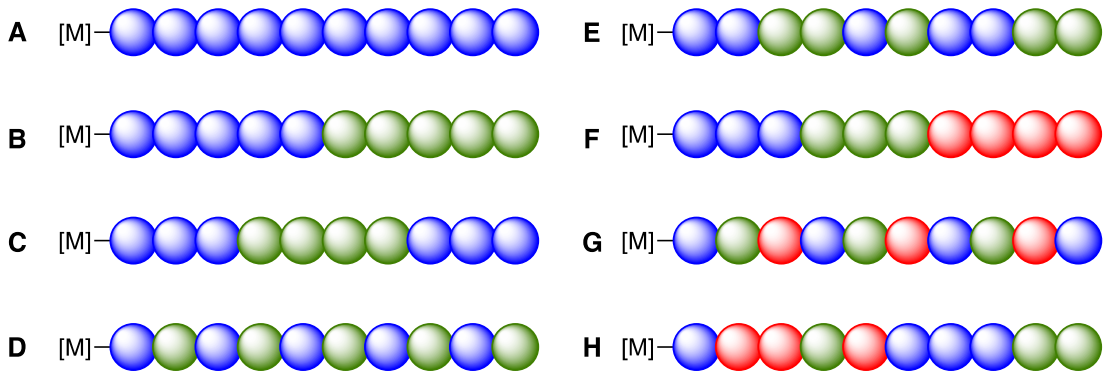

Fig. 1.2: Selected possible polymer compositions bound to a metal, [M], where each coloured sphere represents a different monomer type.

It is important also to consider polymer lengths and how the catalyst can influence them. Two terms used to describe such classes are "living" and "immortal" polymerizations. Living polymerizations are those where the rate of initiation is rapid and much higher than the rate of propagation, and where no termination or chain-transfer processes are observed. This results in uniform polymer lengths for any particular reaction, and there will always be equimolar or fewer individual polymers than initiating species. Immortal polymerizations are those that result in more individual polymer chains than initiators, and propagation cannot be halted by addition of protic compounds that would "kill" a living system. Instead, chain-transfer is common, rapid, and reversible; that is the source of a new polymer chain, but chain-transfer with a previously growing chain can occur and continue propagating. Although this appears chaotic, the rapid rate of chain-transfer coupled with slower propagation results in relatively monodisperse molecular weights.[27] This was first reported in 1985 by Inoue and coworkers.[28] In this work, an aluminum porphyrin catalyst in the presence

of methanol produced narrowly disperse polymer and the total number of polymer chains corresponded approximately with the number of initiating species (Al–Cl catalyst) plus the number of chain transfer agents (MeOH) present. Increasing the chain transfer agent loading up to 50 equivalents per Al produced corroborating results. In systems that exhibit living or immortal behaviour, polymer lengths can be influenced by increasing monomer loading relative to the catalytic species.

1.7. Carbon dioxide as a reagent

Atmospheric levels of carbon dioxide have reached unprecedented heights in modern history with concentrations over 417 ppm as of May, 2020.[29] The increasing levels have been tied to industrialization that began in the 18th century with most pre-industrial estimates of CO_2 concentration around 280 ppm. The Intergovernmental Panel on Climate Change (IPCC) reported in 2013-2014 that greenhouse gas emission increase is one of the major factors contributing to climate change and CO_2 is one of the major contributors.[30] The increased production does, however, provide us with a convenient source of a C1 feedstock that can be utilized as a reagent for several transformations.[31] A number of these reactions are shown in Fig. 1.3 and the industrialized processes are denoted by a dollar sign. CO_2 is also non-toxic and recyclable, which allows us access to carbon neutral syntheses of useful materials. Although the valorization of CO_2 and other greenhouse gasses alone cannot solve the growing issue of climate change,[32] development of new processes and materials that effectively store them can help to reduce their impact alongside measures more geopolitical in nature. However, CO_2 is a very thermodynamically stable molecule, and as such can be

difficult to utilize as a reagent. Despite this, several catalysts have been developed that exhibit excellent activity for many reactions under mild conditions. Although CO_2 has a structurally simple nature, there are several coordination modes through which it can interact with a metal centre which has allowed for the development of catalysts with many different metals.

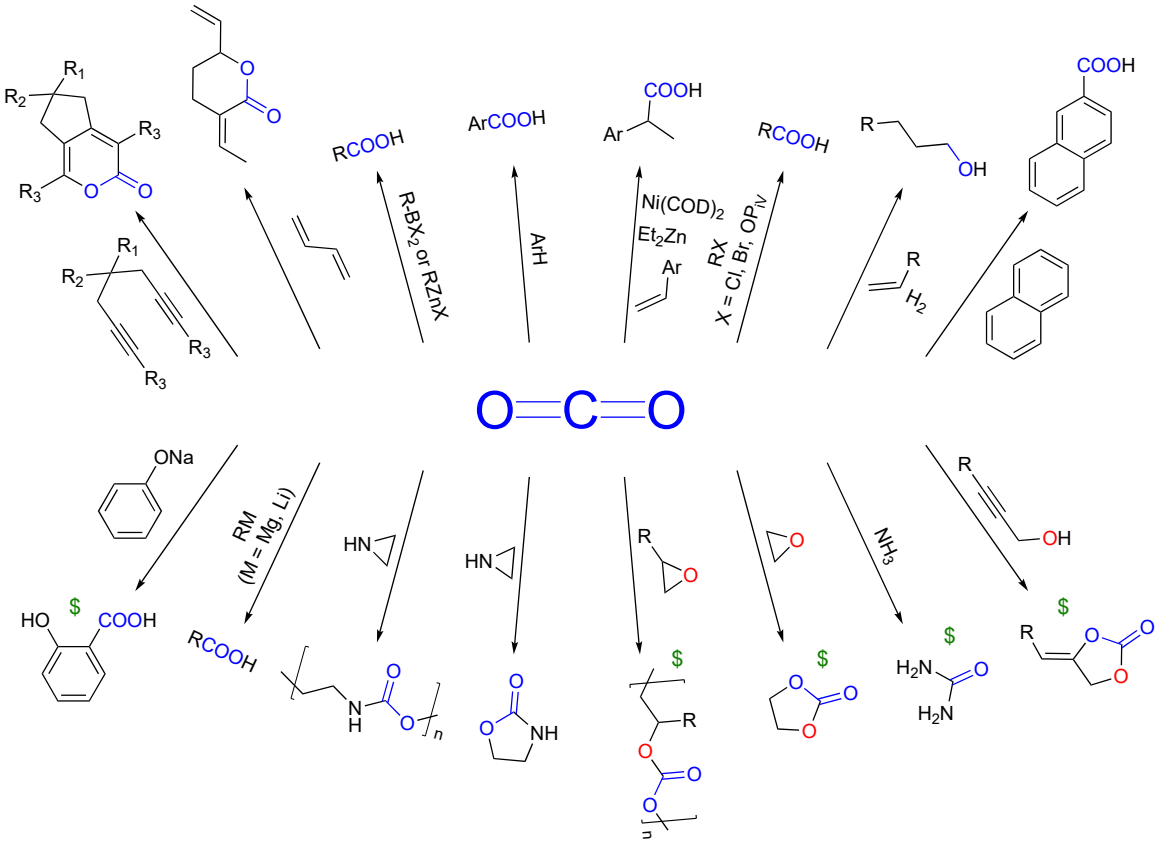

Fig. 1.3: Select reactions involving CO_2 that have been reported as of 2015. The processes denoted with a dollar sign have been industrialized.[31]

As of 2015, five processes have been industrialized that use CO_2 as a reactant: carboxylation of sodium phenoxide, CO_2 and epoxide copolymerization, coupling of CO_2 with ethylene oxide and alkynes to form cyclic carbonate, and urea production.[31,33]

Academically, several other reactions have been developed that incorporate CO_2, but the scope is limited by the low reactivity of the species. Most of these transformations involve highly reactive intermediates generated via metal catalysts. Typical coupling partners include alkynes, aziridines, or aromatic systems. The problems associated with the high reactivity of some of these substrates alongside the limited reactivity of CO_2 can be mitigated through the use of suitable organometallic catalysts. The activation of CO_2 is paramount to its use as a reagent and stabilization of reactive intermediates by these organometallic compounds is essential for controlled synthesis. For polymer chemistry, an ideal use of CO_2 would be homopolymerization but this reaction requires prohibitively intense conditions of 4×10^5 bar and 1800 K and poly(CO_2) readily depolymerizes.[34-35] For current polymer synthesis, the practical use of CO_2 is copolymerization with other monomers.

1.8. Copolymerization of CO_2 and epoxides

Typical polymerization and CO_2 coupling processes are shown in Scheme 1.1. In this specific instance, a zinc complex is the catalytic initiator. In path **A** ring-opening polymerization (ROP) of epoxides is shown forming poly(ether) and **B** is the copolymerization between CO_2 and epoxides to give poly(carbonate)s. The ring-opening of the epoxide generates the zinc-alkoxide where CO_2 is able to insert, forming the carbonate. This then acts as the nucleophile toward the ring-opening of another epoxide monomer. The R group (shown as an orange sphere) represents a growing polymer chain, which can be composed of ether or carbonate segments. In cycle **C**, it is possible for the carbonate intermediate to "back-bite" and cyclize to form a cyclic carbonate molecule. This can occur

during polymerization to yield an alkoxide as well and is sometimes a competing side-reaction. There are several possible back-biting mechanisms and the metal mediated reaction is shown in Scheme 1.1.[36] Cyclic carbonates are often seen as an unwanted by-product of copolymerization reactions, but they themselves are useful as aprotic solvents with high boiling points, as additives in fuels to improve octane value and reduce carbon particulates, as electrolyte solvents for batteries, and as more environmentally sustainable reagents and monomers. For polymer synthesis the cyclic moiety can itself be ring-opened to form poly(carbonate).[37-38] The reactions are facilitated by a nucleophile (X in Scheme 1.1) which may be internal or introduced externally in the form of a co-catalyst should the internal nucleophilic groups lack the ability to ring-open a monomer. Similarly, introduction of co-catalyst may indeed enhance turnover significantly.[39-42] Although these additives can be catalytically active on their own, metal complexes are able to activate the monomers through coordination and enhance electrophilicity. Typically, increased loading of such co-catalysts shifts selectivity toward cyclic carbonate formation.[43] Notably, the presence of excess anion may result in anionic carbonate intermediates that favour the back-biting process.[36]

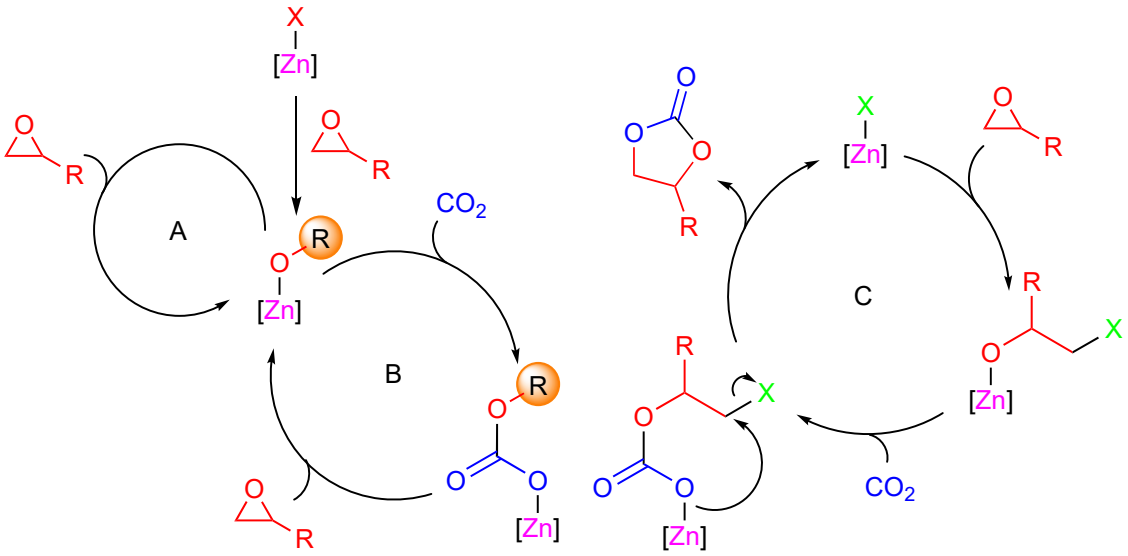

Scheme 1.1: Possible catalytic cycles in CO_2 and epoxide copolymerization/coupling.

Commercial production of poly(carbonate) involves reaction of bisphenol-A with phosgene. BPA is a suspected endocrine disruptor[44] and phosgene is a highly toxic gas and thus an alternative method of poly(carbonate) synthesis from more benign materials is desirable.[45] In 1969, Inoue and co-workers discovered that epoxides could be coupled with CO_2 to form poly(carbonate).[46] The development of well-defined catalysts began in the 1970s when Inoue reported the first single-site catalyst: an aluminum tetraphenylporphyrin complex **1.1** (Fig. 1.4).[47] This catalyst produced poly(propylene carbonate) (PPC) with a molecular weight of 3,900 g mol^{-1} over 19 days at 20 °C and 8 bar CO_2 with narrow dispersity of 1.15 and 40% selective for carbonate linkages. Although slow, this marked the first example of well-controlled poly(carbonate) production from CO_2. Inoue continued to research the topic with related metalloporphyrin complexes of aluminum throughout the 1980s.[48-50] In 1999, the Ree group reported copolymerization with the same species as in Fig.

1.4, but with a chloride ligand rather than a methoxyl group and tetrabutylammonium bromide (Bu_4NBr) as a co-initiator.[51] Here, PPC of 1,900 g mol^{-1} was produced with 75% selectivity for carbonate linkages and dispersity of 1.10 at 20 °C and 52 bar CO_2. A chromium porphyrin complex **1.2** (Fig. 1.5) with 4-(dimethylamino)pyridine (DMAP) was also reported as an effective catalyst for CHO and CO_2 copolymerization but the polymer was not characterized.[52] The limited polymer molecular weights have led to the design of related tunable ligands.

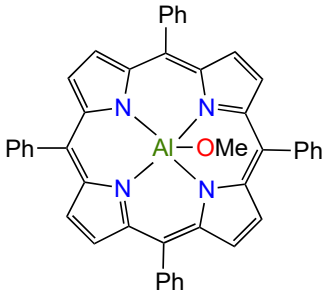

1.1

Fig. 1.4: Aluminum porphyrin complex **1.1** reported by Inoue in 1978 for PO and CO_2 copolymerization.[47]

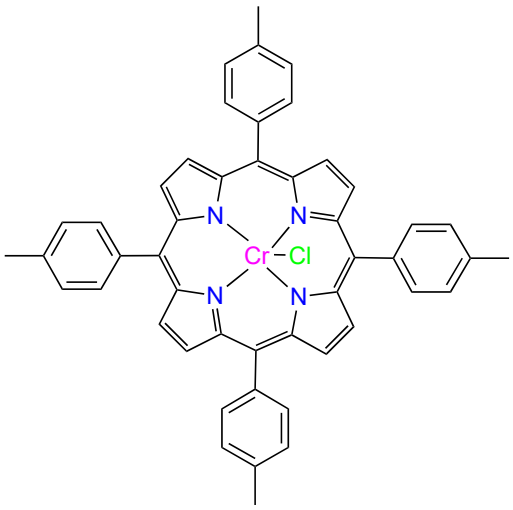

1.2

Fig. 1.5: Chromium porphyrin catalyst for CHO and CO_2 copolymerization.[52]

Salicylaldimine (salen) ligands are perhaps the most pivotal development for CO_2 and epoxide copolymerization reactions. Jacobsen first reported chromium (**1.3**) and cobalt (**1.4**) salen complexes for the asymmetric ring-opening of epoxides (Fig. 1.6).[53] This was followed up in the form of a patent by Jacobsen utilizing **1.3** for PCC production.[54] It was around this time that there was an explosion of sorts in the CO_2 and epoxide coupling fields. Many groups began utilizing the core structures of the salen type ligands with subtle and pronounced variations to the *N*,*N*' tether and aryl substituents which has continued into the present day and been reviewed extensively.[39,42,55-56]

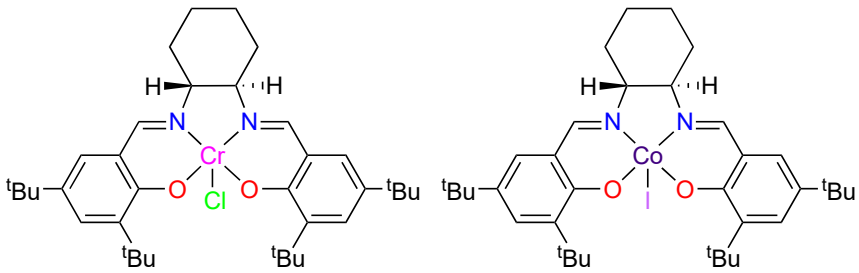

Fig. 1.6: Chromium- and cobalt-salen complexes reported by Jacobsen for asymmetric ROP of epoxides. Compound **1.3** was later utilized for CHO and CO_2 copolymerization.[53]

Further efforts to diversify the ligands suitable for copolymerization have involved the manipulation of the electronic properties of the metals through "reduction" of salen type ligands to "salans" with amino donating functionality. This in turn has created a flexibility otherwise not present in porphyrin or salen ligands and will be referred to regularly throughout this thesis.

In 1995, Darensbourg and Holtcamp had found that a bis(2,6-diphenylphenoxide)zinc·$(Et_2O)_2$ homogeneous compound was highly active toward CHO and CO_2 copolymerization at 55 bar CO_2 and 80 °C, producing polymer with 91% selectivity for carbonate linkages, 38,000 g mol^{-1} and a broad dispersity of 4.5, TOF = 2.4 h^{-1}.[57] This was a key discovery for zinc catalysis as heterogeneous systems with limited reproducibility and polymer control, inspired by Inoue's initial report, represented most zinc-catalyzed CO_2 and epoxide copolymerization up to this point.[58] Subsequently, studies on the influence of steric bulk of the phenoxide ligands were performed and determined to have little effect on the performance of the catalysts, with the bis(2,4,6-

trimethylphenoxide)zinc·$(C_5H_5N)_2$ achieving the highest TOF of 9.6 h^{-1}.[59] The strength of the binding between the ancillary ligands and the metal were discussed, but they appeared to have no bearing on the polymerization results.

Several other zinc-phenoxide species were investigated with limited success, but it was in 1998 that Coates reported the first (BDI)Zn(OAc) dimeric species for CHO and CO_2 copolymerization, reaching 31,000 g mol^{-1} and 97% selectivity for carbonate linkages and narrow dispersity of 1.11, TOF = 247 h^{-1}.[60] This was the most active catalyst at the time and several subsequent reports from the group emphasized the importance of the initiating groups, the electronics of the system and the steric effects imposed by the ligands.[61-64]

Though the process is well-defined and several companies have begun to produce CO_2-based poly(carbonate) with a wide array of glass transition temperatures, the polymers remain less widely used due to a lack of functionality present on most epoxides.[65] One potential response is to utilize epoxides which contain groups that can be functionalized post-polymerization. Vinylcyclohexene oxide (VCHO) and limonene oxide (LO) are at the forefront of these efforts. VCHO is structurally similar to CHO and thus an excellent candidate for comparison of reactivity and physical properties of the resulting poly(carbonate), and LO is the quintessential example of a renewable feedstock for CO_2 and epoxide copolymerization. The vinylic groups can be functionalized in several ways, often through well-known reactions such as cross-metathesis and alkene hydrothiolation or hydrosilylation.[66-69] In 2016, Kleij reported the first catalytic terpolymerization of CHO and LO. Good control over the process was achieved and the resulting terpolymer exhibited

glass transition temperatures between pure poly(cyclohexene carbonate) and poly(limonene carbonate) as anticipated.[66] This study also demonstrated the ability to functionalize the unsaturation of the limonene monomer allowing for post-polymerization functionalization. Due to the relatively ordered polymers they were able to synthesize in this study, they sought to cross-link these polymers with 1,2-ethanedithiol in an attempt to improve the thermal properties of the materials far beyond the capacity of the poly(carbonate) terpolymers alone with T_g as high as 150 °C achieved.

1.9. Zinc-catalyzed CO_2 and epoxide copolymerization

Zinc catalysts for CO_2/epoxide copolymerization reactions have had great historical significance since the initial discoveries by Inoue.[46,70] Since the late 1990s, reports of more reactive and well-defined homogenous zinc-based systems became more abundant. A pioneering discovery was reported by Coates and co-workers in 1998 of very highly active zinc catalysts supported by bulky *β*-diketiminate (BDI) ligands.[60] Since then research in zinc catalysts for CO_2/epoxide copolymerization has grown significantly and the area has been the subject of several excellent reviews.[39-41,71-73] Herein, I aim to highlight the exceptional zinc-based catalytic systems reported from 2013 to present. Exemplary work has recently focused on development of multimetallic and multinuclear catalysts, which typically show high activity due to cooperative effects of two active metal sites. Also, there have been several recent reports of computational and kinetic studies on reaction mechanisms.[74-78]

In 2013, Rieger and co-workers reported the most active zinc catalyst for the copolymerization of CO_2 with cyclohexene oxide to date. The homogeneous dinuclear zinc complex possessed a tethered BDI ligand system (**1.5**, Fig. 1.7) giving a TOF of 7600 h^{-1} at 100 °C and 20 bar, selective for poly(carbonate) formation.[79] The dinuclear system showed enhanced control and activity toward copolymerization compared to mononuclear analogs. Cooperation between two metal centers is necessary as ring-opening of the epoxide and CO_2 insertion are competitive rate-determining steps. This system was only poorly active toward PO copolymerization, which is proposed to be due to stronger bonding between the PO and the metal center compared to CHO. The activity of this system could be improved through modification of the electronic properties of the ligand by adding electron-withdrawing groups. Catalyst **1.6** (Fig. 1.7) could achieve a TOF of 155,000 h^{-1} at 100 °C, 30 bar CO_2 in 20 min in 5 mL toluene. A conversion of 85% was obtained containing 88% carbonate linkages and a dispersity of 1.7.[80]

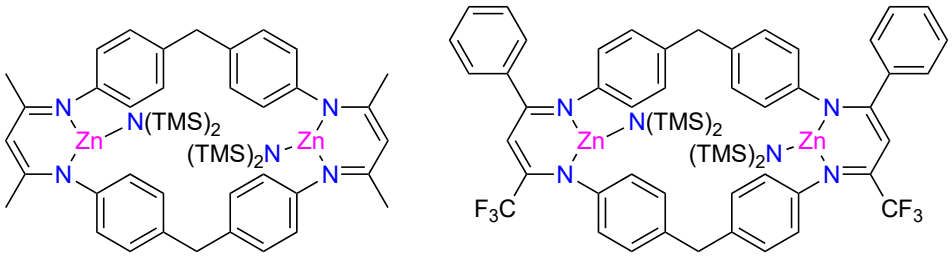

1.5 **1.6**

Fig. 1.7: Dinuclear zinc catalysts for copolymerization of CO_2 and CHO.[79-80]

In 2014, Meng and co-workers utilized mono- and tri-zinc species with a variety of Schiff base and salen ligands for CO_2/CHO copolymerization (**1.7 – 1.10**, Fig. 1.8).[81] Their objective was to observe the effect of electron-donating and withdrawing substituents on the

aromatic rings (**1.7**), effect of internal (acetate) and external (chloride) anions, and mono- versus multinuclear character of these catalysts for CO_2/CHO copolymerization. As shown in Rieger's work[79], the multimetallic systems were more effective at copolymerization reactions than monometallic systems. The trimetallic systems **1.8a** and **1.8b** exhibited the highest activities, yielding molecular weights of 25,000 and 45,000 g mol^{-1} respectively, at 0.1 mol% catalyst loading, 80 °C, 50 bar and 22 h. Using **1.8a**, 90% selectivity for poly(cyclohexene carbonate) (PCHC) was obtained with 98% carbonate linkages at 70 °C and 50 bar CO_2 over 22 h. Molecular weights of up to 45.5 kg mol^{-1} were obtained, but dispersities were broad (between 2.22 and 9.82). Reaction conditions could be controlled to favor narrower dispersities, but this sacrificed selectivity for poly(carbonate) formation. Mechanistic investigations on **1.8a** and **1.8b** were reported showing first order dependence on catalyst loading, CO_2 pressure and epoxide concentration.[82-83] The related zinc complexes, **1.9** and **1.10**, were found to be entirely inactive to carbonate formation.

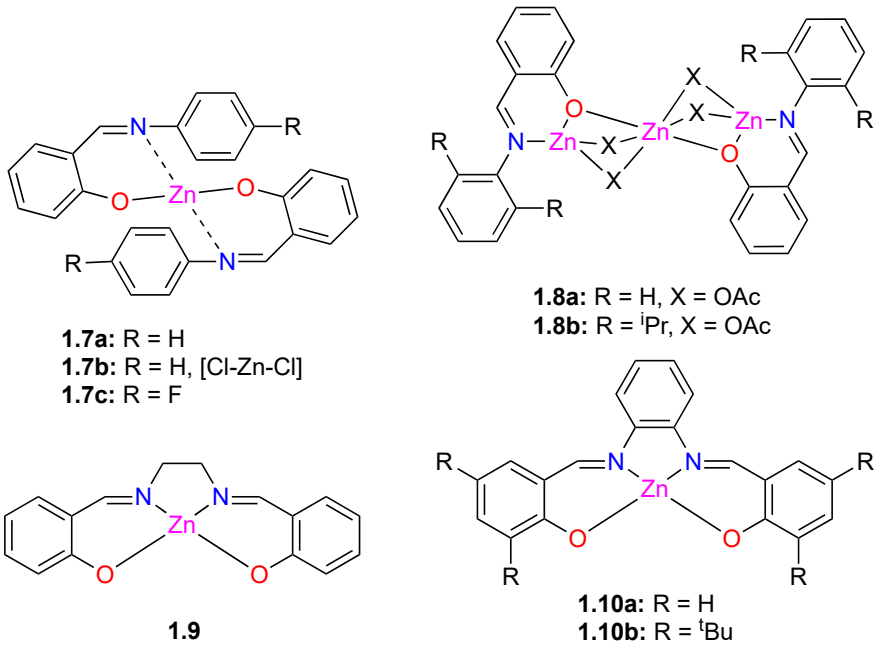

Fig. 1.8: Schiff-base-derived zinc systems studied for CHO and CO_2 copolymerization.[81]

A zinc(II)-cobalt(III) double metal cyanide complex (**1.11**, Fig. 1.9) catalyzed formation of poly(carbonate)s using epoxides with varying alkyl chain length, degree of substitution, and bulk (representative epoxides are given in Fig. 1.1).[84] This is the first example of ring-opening of branched epoxides for copolymerization with CO_2. Catalyst **1.11** was able to achieve poly(carbonate) formation with each epoxide to varying success at conditions of 40 bar CO_2 and 50 – 60 °C. Molecular weights covered a large range from 9,000 to 93,200 g mol^{-1}, and the dispersity is varied as well, though all were broad, ranging from 2.0 to 5.0. This system does not require the use of an external nucleophile. The bulky and long chain epoxides (DDO, ^{i}BuO, ^{t}BuEO, Fig. 1.9, and CHEO as shown in Fig. 1.1) gave almost exclusively perfectly alternating poly(carbonate)s while SO and HO (Fig. 1.9) exhibited less CO_2 incorporation. Smaller aliphatic chains (EO, PO and BO) exhibited poorer selectivity for poly(carbonate) formation. The long aliphatic chains led to a decrease in glass transition temperatures, down to as low as –38 °C whereas the bulkier epoxides such as CHEO led to a much higher glass transition temperature of 84 °C.

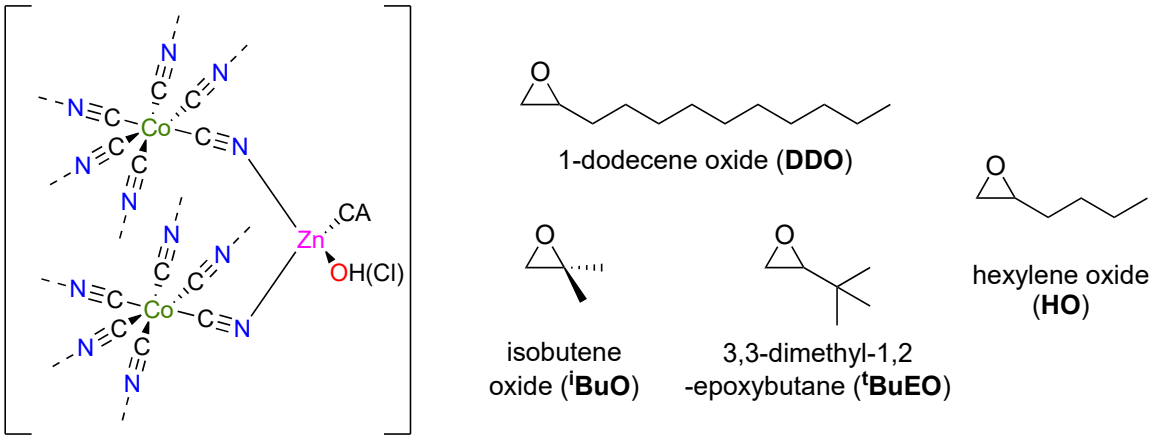

1.11

Fig. 1.9: Proposed ground state structure of the active site of Zn-Co^{III} double metal cyanide complex (DMCC) employed as catalyst for epoxide/CO_2 copolymerization. CA is a "complexing agent", either H_2O or ^tBuOH.[84]

Yuan, Yao and co-workers reported the use of zinc-yttrium, **1.12**, and zinc-neodymium, **1.13**, cooperative systems (Fig. 1.10).[85] Pulsed-gradient spin-echo NMR experiments confirmed that the multinuclear complexes do not dissociate into mononuclear species in solution. At 25 °C and 7 bar CO_2, 0.1 mol% loading of **1.13** achieved 98% yield of PCHC with no evidence of ether linkages and molecular weights nearing 300,000 g mol^{-1} with a dispersity of 1.65. Increased reaction temperature led to systematic decreases in polymer molecular weights. This system was completely inactive for styrene oxide and propylene oxide. A proposed mechanism for the copolymerization is shown in Scheme 1.2. The results of their studies suggested nearly perfectly alternating copolymerization; thus, poly(ether) formation is highly unfavoured even at relatively low pressures (7 bar) of CO_2. Stabilization of the reactive alkoxides or carbonates and coordination of the epoxides is

shared between the three metal centers, providing an advantageous environment for polymer formation. It was suggested that one of the neodymium centers activates the epoxide while the remaining two metals are bound to the carbonate end of the growing polymer chain. The high activity at room temperature described for this system can likely be attributed to a cooperative effect between the three metals.

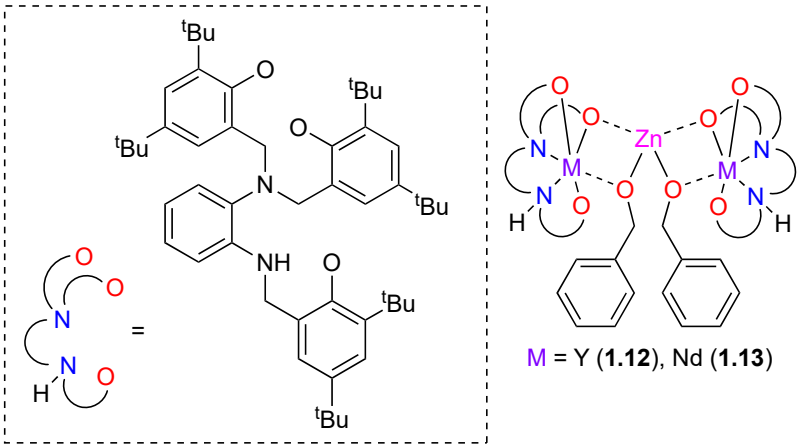

Fig. 1.10: Trinuclear Zn/Y and Zn/Nd complexes utilized for the copolymerization of CHO and CO_2.[85]

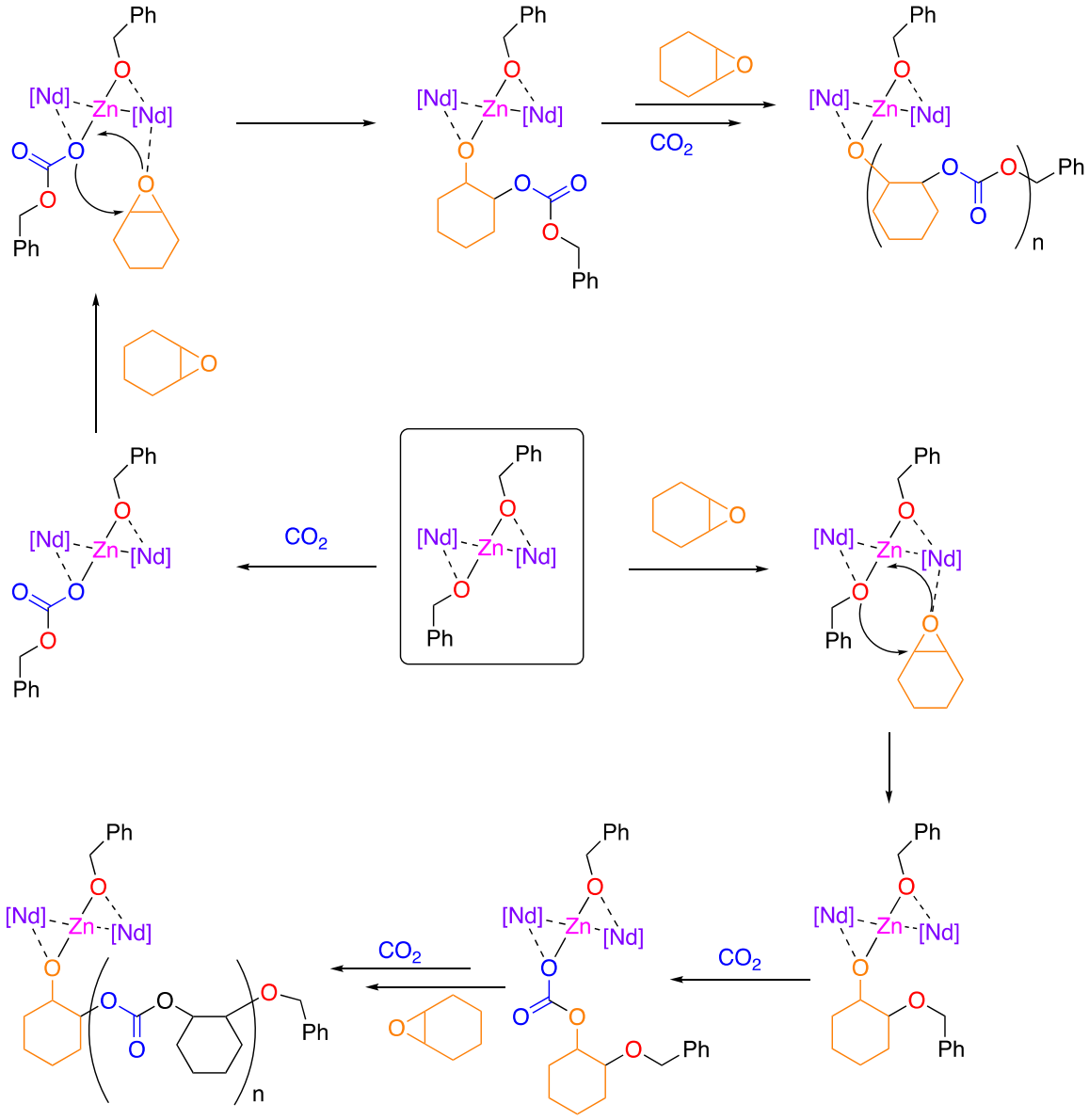

Scheme 1.2: Mechanisms proposed for the CO_2/CHO copolymerization catalyzed by trinuclear zinc-neodymium species **1.13**.[85] [Nd]-Zn-[Nd] refers to the compound **1.13** in Fig. **1.10** with ligands and zinc connectivity omitted to illustrate the mechanism clearly.

In 2018, Werner and co-workers screened the catalytic activity of organozinc species of the formula ZnR_2 (R = ethyl, butyl, isopropyl, cyclohexyl and phenyl) for the

copolymerization of cyclohexene oxide with CO_2.[86] The reactions were poorly controlled with dispersities up to 5.0 and molecular weights ranging from 10,000 to 22,000 g mol^{-1} at 0.5 mol% catalyst loading in 2 mL toluene at 20 bar CO_2 and 100 °C. Incorporation of CO_2 was moderate to high (77 – 90%) for each of these systems. The exception was $ZnEt_2$ under argon, which yielded high molecular weight (76,400 g mol^{-1}) poly(ether) with a dispersity of 2.2 with <1% PC. Reactions at 50 bar proved to be most effective at poly(carbonate) synthesis, whereas decreasing the pressure to 5 bar led to lower yields, turnover numbers and degree of carbonate linkages as well as a general decrease in polymer molecular weights. Cyclic carbonate formation (7 – 10%) was observed at higher temperatures but none was formed at 60 °C with only a small decrease in turnover number. Introduction of a co-catalyst (tetrabutylammonium bromide (Bu_4NBr), bis(triphenylphosphine)iminium chloride (PPNCl), 1,8-diazabicyclo[5.4.0]undec-7-ene (DBU) or 1,5,7-triazabicyclo[4.4.0]dec-5-ene (TBD)), led to increased cyclic carbonate formation (12 – 82% yield), or a mixture with oligomers of 270 – 590 g mol^{-1} molecular weight. With DMAP as the co-catalyst, no significant conversion was observed.

Ko and co-workers reported the use of mono- and dinuclear zinc complexes coordinated to different bis(benzotriazole iminophenolate) ligands for CO_2 and epoxide coupling and copolymerization (**1.14** and **1.15**, Fig. 1.11).[87] In the absence of co-catalyst, **1.15** was able to achieve 11% conversion of CHO after 24 h (62.5 mmol% catalyst, 20.7 bar CO_2, 120 °C), with 55% selectivity for poly(carbonate). Compound **1.14** gave similar results of 18% conversion and 53% selectivity for poly(carbonate). Each reported >99% carbonate linkages. Compound **1.14** was further examined in the presence of 10 equiv. of Bu_4NBr co-

catalyst. Under the above conditions, 99% conversion to *cis*-CHC was achieved after 14 h at 113 TO h^{-1}.

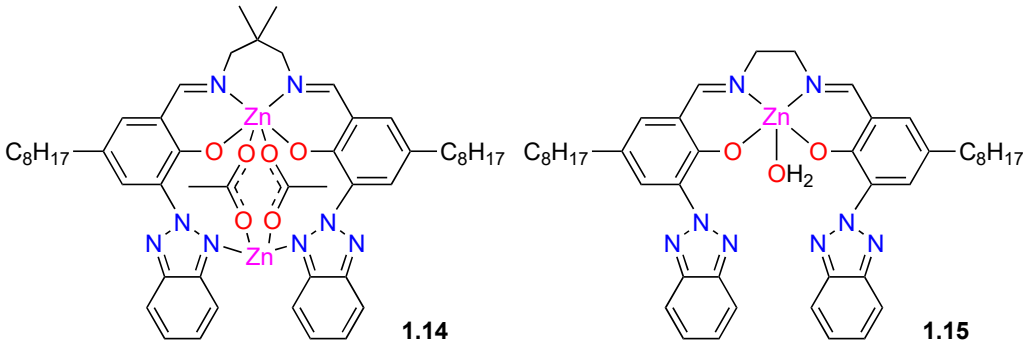

Fig. 1.11: Mono- and dinuclear zinc compounds used in the copolymerization of CO_2 and CHO.[87]

In 2017, Rieger and co-workers investigated a Lewis acidic BDI-zinc complex **1.16** (Fig. 1.12) toward copolymerization and terpolymerization of CO_2 with a variety of different epoxides, namely PO, ECH, CHO, LO, SO, and OO (Fig. 1.1).[25] In the copolymerization between LO and CO_2 catalyzed by 0.4 mol% 55 at 30 bar CO_2, 40 °C, 6.5 h in 2 mL of toluene, 100% selectivity for poly(limonene carbonate) (PLC) was achieved in 59% yield at 120 TO h^{-1}. This was the most active system for the production of PLC to date and produced polymers having molecular weights up to 145,300 g mol^{-1} and dispersities as low as 1.3. Two terpolymerization reactions were performed at room temperature and 30 bar CO_2. LO and PO in a 250:600 ratio with respect to catalyst gave 98% selectivity for poly(carbonate) in 40% yield after 6 h at 55 TO h^{-1}. The composition of the product was 51% PLC with 47% poly(propylene carbonate) groups with a molecular weight of 95,000 g mol^{-1} and dispersity of 1.4. A small amount of cyclic propylene carbonate (2%) was

produced. Terpolymerization of CHO and PO was conducted in a 1:1 ratio and gave 65% yield after 14 h, showing 99% selectivity for polymer, which showed a 59:40 ratio of PCHC:PPC blocks (1% conversion to cyclic propylene carbonate), a molecular weight of 272,000 g mol^{-1} and a dispersity of 1.3 with activity of TO 46 h^{-1}. Earlier that year, Rieger and co-workers utilized **1.16** as a catalyst for the one-pot synthesis of block and terpolymers of CO_2, epoxides (CHO and CPO), and *β*-butyrolactone (BBL) controlled by CO_2.[88] Three reaction pathways could be obtained by conducting the reaction at 40 bar, 3 bar, and 0 bar CO_2 pressure. High CO_2 pressure inhibited BBL incorporation and poly(carbonate) formation is rapid, whereas the absence of CO_2 results in only the ring opening of BBL, which was comparatively slow. No poly(ether) formation was observed. Consequently, low pressures of CO_2 reduced the rate of poly(carbonate) formation to that of BBL ring-opening, resulting in random monomer incorporation during propagation. True block terpolymers could be obtained by polymerizing BBL in the absence of CO_2 where upon pressurizing to 40 bar led to formation of poly(carbonate) blocks. Relatively high molecular weights and narrow dispersities were achieved for all reaction conditions with variations in molecular weights attributed to reaction time or rate limitation due to monomer ring-opening. Copolymerization of epoxide mixtures with CO_2 were investigated. CPO exhibits similar ring-strain to CHO and provides similar activity, but is much less studied, likely due to a much higher cost than CHO. Similar terpolymerization activity was observed, however, rather than block terpolymers resulting from intermittent pressurization, small amounts of poly(hydroxybutyrate) (PHB) and poly(cyclopentyl ether) (PCPE) linkages could be identified via ^{1}H NMR, suggesting the resulting polymers were in fact gradient copolymers. The synthesis of strictly poly(cyclopentene carbonate) at 40 bar CO_2 led to the highest reported

TOF for this monomer of 3,200 h^{-1}, giving a polymer molecular weight of 122 kg mol^{-1} with 99% carbonate incorporation.

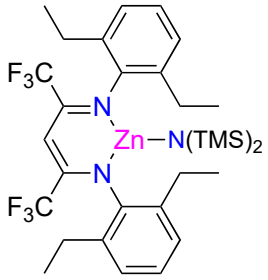

1.16

Fig. 1.12: *β*-Diketiminatozinc complex used for copolymerization and terpolymerization reactions of CO_2 with various epoxides.[25]

The Williams group reported two catalytic systems involving hetero-bimetallic complexes of titanium and zinc with a tetraamino-bis(phenolate) macrocyclic ligand (**1.17** and **1.18**, Fig. 1.13).[89] These two compounds were tested for activity toward CHO and CO_2 copolymerization at 1 bar of CO_2 and 80 °C with no external co-catalyst as the alkoxide co-ligands were suitable initiators for ring-opening of the epoxide monomers. Molecular weights were low (1750 – 2190 g mol^{-1}) and dispersities were moderately narrow (1.35 – 1.37). The mono-titanium precursor was found to be completely inactive for polymerization.

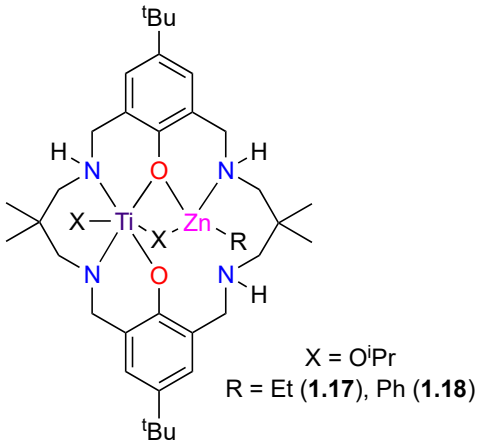

Fig. 1.13: Macrocyclic hetero-dinuclear species used for copolymerization of CO_2 and CHO.[89]

In 2018, Okuda, Mashima and co-workers reported hetero-metallic trizinc-lanthanide complexes with macrocyclic ligands for CHO and CO_2 copolymerizations (**1.19**, Fig. 1.14).[90] The acetate groups rapidly shift with outer-sphere acetate anions, providing ample initiating groups for polymerization. Although triflate and nitrate anions were tested for this system, only the acetate derivative was able to catalyze copolymerization. The complex with acetate and lanthanum provided poly(carbonate) with >99% carbonate linkages. Studies of the effect of the lanthanide metal (La, Ce, Pr, Nd, Sm, Eu, Gd and Dy) on the process showed the largest lanthanides led to the highest activity (TOF 310 – 370 h^{-1}, molecular weight of 14,000 g mol^{-1} at 0.05 mol% catalyst loading and 10 bar CO_2, giving carbonate content >99%). All polymers obtained showed narrow dispersities regardless of the lanthanide ion used. The acetate end-groups of the poly(carbonate)s could be easily replaced by ammonium benzoate, yielding an ammonium alkoxide end-groups and regenerating the zinc carboxylate necessary for initiation. This is the first reported telomerization of poly(carbonate)s.

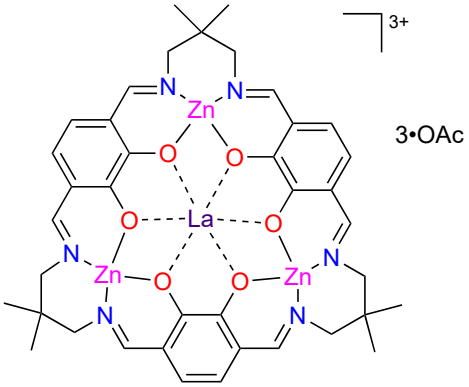

1.19

Fig. 1.14: Macrocyclic trizinc-lanthanum catalyst for CHO and CO_2 copolymerization reactions. Acetates are coordinated to the metal centers in a combination of bridging and monodentate modes and undergo rapid exchange in solution.[90]

In 2017, a proline-based dizinc catalyst, **1.20**, was reported for copolymerization reactions involving CHO (Fig. 1.15).[91] This species showed moderate activity toward poly(carbonate) synthesis at 1 bar CO_2 with CHO at 80 °C, giving TON between 808 and 1684 (TOF of 88 – 149 h^{-1}) with selective yields of poly(carbonate) up to 97%. Poly(cyclohexene carbonate) molecular weights were between 1,400 and 2,700 g mol^{-1} with dispersities between 1.22 and 1.29. It is proposed that the active dizinc bis-ligand complexes are able to rapidly undergo interconversion to at least 5 different isomers at the conditions of reactivity.

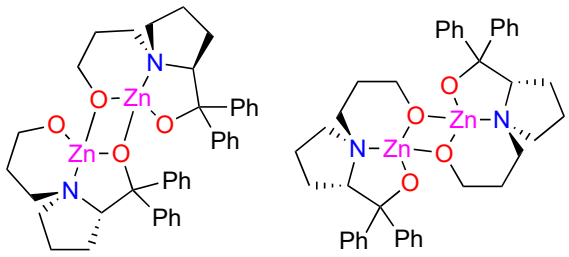

1.20a **1.20b**

Fig. 1.15: Two isomers of dizinc proline-based tridentate ligand complexes.[91]

In 2016, the use of the zinc-scorpionate species (**1.21** – **1.26**, Fig. 1.16) for CHO and CO_2 copolymerization was reported.[92] The influence of catalyst choice (varying R and X group), temperature, pressure and time was studied and showed **1.25** to be the most active at 80 °C, 40 bar CO_2 with 1 mol% catalyst loading. This provided a conversion of 89% within 16 h, of which 90% of the product was PCHC having M_n of 14,100 g mol^{-1} with narrow dispersity (1.08) with the remaining product being cyclohexene carbonate. Performing the reaction over temperature ranges from 60 to 100 °C showed polymer molecular weights generally increased with temperature while dispersities narrowed. Selectivity for poly(carbonate), however, decreased with increasing temperature, instead favoring cyclic carbonate formation. Decreasing the pressure from 50 to 10 bar had detrimental effects on overall conversion, poly(carbonate) incorporation and turnover frequency. Turnover frequencies were low, reaching up to 5.56 TO h^{-1}.

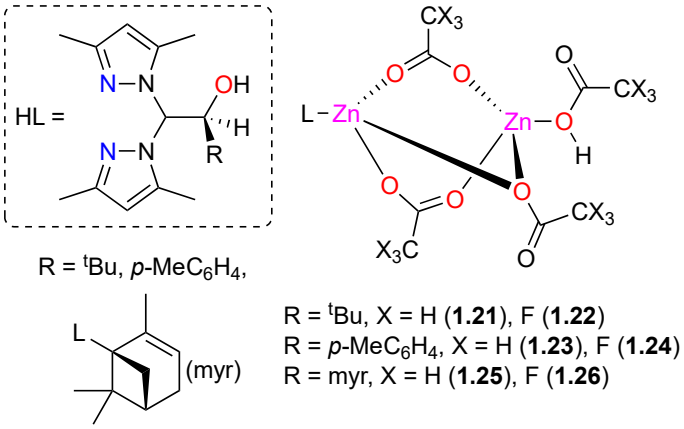

Fig. 1.16: Heteroscorpionate ligand and zinc complexes utilized for CO_2 and CHO coupling.[92]

In 2015, Williams and co-workers reported the synthesis of ABA block copolymers from *ε*-caprolactone (*ε*-CL), CHO and CO_2 catalyzed by a dizinc, macrocyclic aminophenolate catalyst (**1.27a**, Fig. 1.17).[93] In a bulk mixture of the monomers at 80 °C, 1 bar of CO_2 and varied catalyst loadings, copolymerization of the epoxide with CO_2 occurred first and resulted in the formation of hydroxyl-terminated PCHC, while *ε*-CL ring-opening polymerization began only after CO_2 depressurization to produce a tri-block copolymer. These polymers had molecular weights of 4,000 – 13,800 g mol^{-1} and dispersities ranging from 1.33 to 1.49. Reactions containing only the lactone monomer did not produce polymer, instead only proceeding in the presence of epoxide and the absence of CO_2. The initiator for ROP of *ε*-CL was proposed to be the *in situ* generated alkoxide from the ring-opened CHO monomer giving a catalyst capable of selectively forming polymers with well-defined ABA block composition and narrow dispersities.

A subsequent report by Williams in 2016 reported the chemoselective polymerization to form copoly(esters) and copoly(ester-carbonates).[94] The reaction mixtures consisted of lactone, epoxide, and CO_2, as well as lactone, phthalic anhydride, and epoxide, catalyzed by **1.27b** (Fig. 1.17). As mentioned previously, ROP of *ε*-CL only occurs in the presence of CHO, suggesting the initiation of *ε*-CL ROP requires the formation of a zinc alkoxide. When CO_2 is introduced to the system, only PCHC is formed. Increasing the lactone content inhibited poly(carbonate) formation, which was proposed to be due to competitive binding between the lactone and the epoxide. Introduction of CO_2 after initiation of lactone ROP also led to termination of further PCL formation. Phthalic anhydride (PA), *ε*-CL and epoxide ring-opening copolymerization was also examined as the catalyst was previously shown to catalyze the formation of perfectly alternating poly(ester)s from PA and CHO.[95] In a bulk mixture of all three monomers, the rapid formation of PCHPE occurred selectively, and once PA was entirely consumed, *ε*-CL ROP was able to proceed, forming highly controlled block copoly(ester)s with dispersities ranging from 1.42 to 1.57. Molecular weights were controlled through monomer composition ratios, ranging from 2,600 to 22,500 g mol^{-1} and agreeing with computational predictions. A subsequent report from Mathers, Williams and co-workers reported terpolymerization reactions between CHO, a bio-derived anhydride (BCA1) and CO_2, catalyzed by **1.27b** or magnesium derivatives of the macrocyclic ancillary ligand in Fig. 1.17.[96] In bulk mixtures of all three monomers the selectivity for poly(ester) formation vs. poly(carbonate) or poly(ether) formation was heavily dependent upon the metal. The zinc compounds exhibited selectivity for poly(ester) formation until exhaustion of the anhydride monomer, which was subsequently followed by epoxide/CO_2 copolymer formation. This is the first reported example of preferential epoxide/anhydride ROCOP

over CO_2/epoxide copolymerization. Conversely, the magnesium compound favored epoxide/CO_2 copolymer in the presence of CO_2, while poly(ester) was formed in its absence. All reactions involving the three monomers were performed under 1 bar of CO_2, 100 °C, catalyst/anhydride/CHO ratio of 1:100:1000.

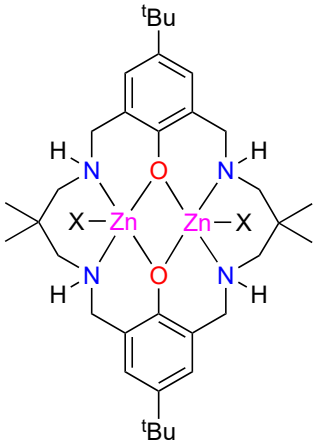

1.27a X = CF_3CO_2
1.27b X = OAc

Fig. 1.17: Macrocyclic dizinc catalysts for copolymerization of CO_2, CHO, *ε*-CL, and PA. Each acetate or trifluoroacetate anion bridges the two zinc centers.[93-94,96]

Zinc-catalyzed copolymerization reactions continue to be a widely studied branch of 3d metal catalyzed copolymerization. In fact, significant findings such as the increased activity of homo- and hetero-multinuclear systems and highly selective copolymerization reactions at 1 bar of CO_2 continue to suggest that zinc is an attractive metal for catalyst design toward these transformations. Judicious ligand design to enhance cooperation between a zinc center and one or more other metal centers will continue to advance the field of copolymerization reactions involving CO_2 and epoxides alongside other monomers, particularly anhydrides. Work has begun to shift toward the synthesis of terpolymers and

block copolymers – requiring robust catalytic systems that can facilitate reactivity with a large variety of monomers. Earlier reports of multimetallic systems containing zinc suggest that they will be well-suited to this task. Regarding monomers, those possessing groups that can be functionalized post-polymerization, such as limonene oxide, will prove valuable as there are many catalytic systems that allow for control of molecular weights of copolymers, but the one-pot functionalization of these polymers is desirable for fine-tuning their physical properties. For example, the BDI-zinc complex developed by Coates and co-workers in 2004 was optimized by Hauenstein, Agarwal, and Greiner in 2016 for the synthesis of PLC.[58,97] Post-polymerization functionalization allowed for fine-tuning of glass transition temperatures, T_g, Young's modulus, and tensile strength. In 2016 Sablong, Koning and Li reported BDI-zinc catalyzed copolymerization of CO_2 and limonene dioxide, LDO, and the post-polymerization functionalization at the unreacted pendent epoxide.[98] These poly(carbonate)s were highly tolerant to functional group modification, resulting in polymers containing thiols, carboxylic acids and cyclic carbonates. Significant modification of T_g with little effect on M_n and dispersity suggest broader implications for polymer functionalization. Research building upon these findings should prove valuable in an academic setting and find industrial application for the development of new and renewable polymers.

1.10. Zinc amino-phenolate complexes for polymerization catalysis

Several different metals have been shown to be active for the polymerization catalysis discussed thus far, and among the most active are zinc catalysts. Clearly the choice of ligand differentiates an exceptional catalyst from an inactive one and it is here that nearly limitless

design space is opened. The previous section provided examples of some of these systems, particularly those designed by the Williams group, for CO_2 and epoxide copolymerization. The Kozak group has worked with amino-phenolate ligands coordinated to several different metals due to their highly tunable steric and electronic properties. This has allowed for the development of active catalysts for different polymerization processes and other coupling reactions. Chapter 2 will discuss the amino-bis(phenolate) zinc catalyzed ring-opening polymerization of epoxides and copolymerization of epoxides and CO_2, and this work was published in 2019.

1.11. Poly(ester)s

Poly(ester)s represent a broad class of everyday materials, present in objects such as clothing, home furnishings, safety belts, plastic bottles, display monitors, holographic photopolymers and many others. As mentioned above, the commercial production of poly(ester)s is dominated by poly(ethylene terephthalate). In efforts to shift toward renewable substrates, research has primarily focused on poly(lactide) but the use of cyclic anhydrides as comonomers for poly(ester) synthesis has grown significantly. Cyclic anhydrides can provide desirable improvements to the thermal properties of the polymers in which they become enchained, typically through increased glass transition temperatures, and thus provide potential alternatives to polymers currently employed for myriad applications with high rigidity and deformation resistance.[96,99-100] The common anhydrides for copolymerization include maleic anhydride (MA) and derivatives of MA coupled with naturally occurring terpenes (*a*-phellandrene, *a*-terpinene), and phthalic anhydride (PA). Unfortunately,

commercial production of both MA and PA still relies on petrochemicals, so although they are antithetical to the renewable theme of biorenewable polymer formation, they are crucial to the development of complex multi-component polymer processes.

1.12. Copoly(ester) and terpoly(ester) synthesis

As research examining poly(lactide) itself has been covered extensively,[21,101] research in poly(ester) synthesis has begun to shift into copolymer and terpolymer syntheses. Of course, lactide is not the only suitable monomer for poly(ester) formation. Notably, anhydrides have been used to great effect for co- and terpolymerization reactions as they cannot sequentially ring-open due to the nature of the carboxylate nucleophile.[73] This allows for the synthesis of highly controlled copolymers from cyclic anhydrides and other monomers. Poly(ester-*co*-ether) and poly(ester-*co*-carbonate) are of particular interest as the individual polymers, poly(lactide), poly(ether) and poly(carbonate), have been well studied up to this point. Using cyclic anhydrides as monomers allows for fine control over the polymerization process and will widen the scope of uses for the resulting materials.

1.13. Cyclic anhydrides as co-monomers

Introducing cyclic anhydrides as a comonomer to other well-established polymerization reactions is of interest to enhance the physical characteristics of the polymer and diversify the applications therein. There have been several reports that highlight the improvement of the thermal properties when different anhydride comonomers were

introduced to systems with epoxides, but the prevalence of reports on the subject has increased in recent years.[96,99-100,102-103] Poly(ester) production has been dominated by lactone ROP, but the scope of lactones suitable for polymerization is very limited and the introduction of other monomers did not improve the polymer product's properties appreciably.[103] Alternatively, anhydrides are much more varied and coupling with another versatile functionality in epoxides broadens that scope enormously and alternating copolymerization often allows for finer control of the process. Furthermore, introducing functionalization in the monomers is much more accessible and post-polymerization functionalization has proven to be an important tool for renewable polymer development.

1.14. Poly(ester-*co*-ether) synthesis from epoxides and cyclic anhydrides

The first report on the metal complex-catalyzed copolymerization of cyclic anhydrides with epoxides was published by Inoue in 1985, although uncontrolled copolymerization has been known since the 1960s.[73,104-105] They observed the alternating copolymerization of PA with PO catalyzed by an aluminum porphyrin system similar in design to that in Fig. 1.4, finding success with (L)Al-Cl and (L)Al-OCO^{t}Bu. Reactions also required onium salt co-catalysts and little to no polymerization was observed when only the aluminum species or onium salt were used. Complete conversion of PA could be observed with either the aluminum chloride or aluminum carboxylate porphyrin species with narrow dispersity of 1.1. The observed molecular weights based upon substrate to catalyst loading were approximately half of those anticipated for single-site polymerization. This suggested a

dual-site polymerization catalyst with chains propagating from each face of the complex and producing twice the number of chains with twice the monomer consumed per catalyst.

In addition to aluminum, chromium and cobalt-porphyrin complexes have been utilized for epoxide-anhydride ring-opening copolymerization (ROCOP). Duchateau extensively studied the chromium complexes in Fig. 1.18 and found that the introduction of a co-catalyst (DMAP) was essential for achieving high activity and control with either.[106] A number of different anhydrides could be used, and perfectly alternating copolymers could be obtained within 3 h (neat) or 6 h (solution) in most cases with 0.004 mol% catalyst loading. Molecular weights varied between 1,300 – 19,250 g mol^{-1} and dispersities were low to moderate (1.2 – 1.6). All reactions were performed at 100 °C. They proposed that chain-transfer reactions during polymerization due to adventitious water were the cause of the molecular weight discrepancies. Notably, each catalyst afforded similar results under the same conditions but in some cases, polymers produced using **1.29** would exhibit ether linkages while those produced using **1.28** were perfectly alternating polymer. This is perhaps due to increased fluxionality of **1.29** reducing the activation energy for epoxide ring-opening – the supposed rate-limiting step.

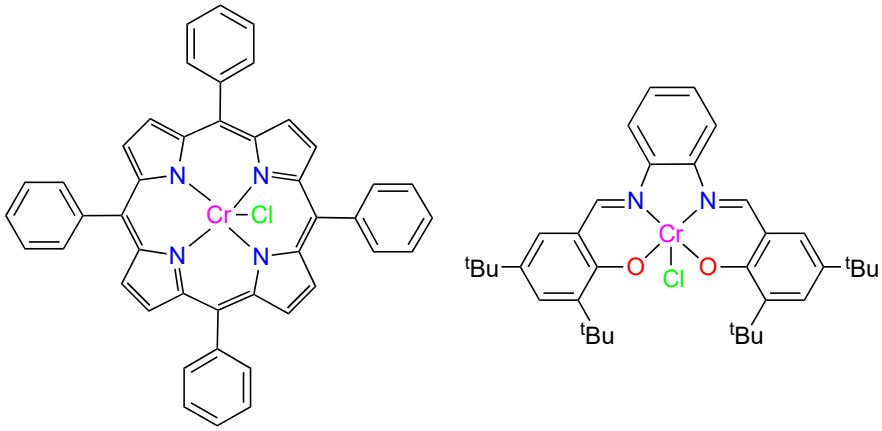

1.28 **1.29**

Fig. 1.18: Cr-porphyrin complex reported by Duchateau for CHO-anhydride copolymerization.[106]

After this report, Duchateau had studied the effect of different metal-salen complexes and the influence of the diamine "backbone" on the polymerization activity.[107] Unsurprisingly, the efficacy was affected by not only the ligand structure and the metal (Cr, Co and Al) but by co-catalyst choice (DMAP, *N*-MeIm, TBD, several phosphines and PPNCl) and ratio to metal complex. Generally speaking, species **1.29** was the most effective for these systems with the finest control over poly(ester) selectivity. Among the numerous co-catalysts examined, PPNCl was found to be the most effective and at 1:1 loading with metal complex, reached an M_n of 15,000 g mol^{-1} (0.002 mol%) of perfectly alternating copolymer, dispersity of 1.1. Increasing the loading of PPNCl decreased the molecular weight. DMAP was found to be nearly as effective but impurities in the material appear to have resulted in chain-transfer events that decreased molecular weights.

Although early indications were that salan/salen complexes required co-catalysts, binary catalytic systems, Coates and co-workers reported similar cobalt and chromium salen species (Fig. 1.19) that were active toward maleic anhydride-epoxide ROCOP even in the absence of co-catalyst.[108] Complex **1.30** at 45 °C converted 12% of propylene oxide with no evidence of ether linkages over 15 h (0.0025 mol%) while **1.31** was able to convert 47% with no ether linkages under the same conditions. By diluting the reaction mixture in toluene, **1.31** was able to achieve complete conversion again with no ether linkages, a first for metal-salen catalyzed copoly(ester) formation without co-catalyst. The molecular weight was near the expected value (17,000 g mol^{-1}) and the dispersity was a moderate 1.6. High selectivity was observed using **1.31** with several other epoxides and conversions were all ≥ 90% with consistently high molecular weights (21,000 – 33,000 g mol^{-1}) and similar dispersity (1.1 – 1.7) under the conditions above in hexanes. The dispersity could be narrowed significantly by introduction of ^{i}PrOH chain transfer agent at 1.5 – 4.5 mol% with respect to maleic anhydride. Increasing the relative abundance led to a decrease in dispersity and a decrease in polymer molecular weight.

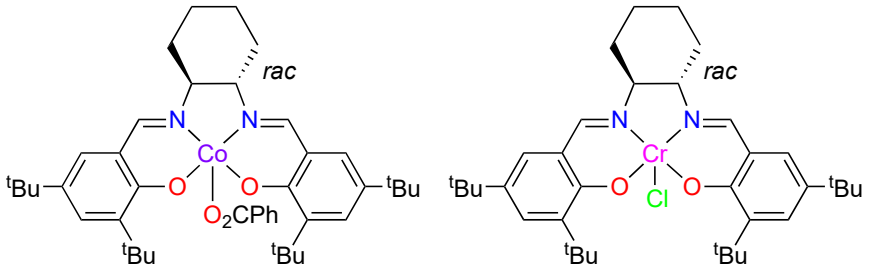

1.30 **1.31**

Fig. 1.19: Cobalt- and chromium-salen complexes reported by Coates for maleic anhydride and epoxide copolymerization.[108]

Coates and co-workers continued to expand the scope of these reactions by applying (BDI)zinc catalysts that had demonstrated exceptional activity toward CO_2 and epoxide copolymerization within the decade prior (Fig. 1.20).[58,60,109] Similar to the report above, a variety of epoxides CHO, VCHO, PO, LO, *cis*-butylene oxide (CBO), isobutylene oxide (IBO)) and three cyclic anhydrides, diglycolic anhydride (DGA), maleic anhydride (MA) and succinic anhydride (SA), were used. It was found that the electronic effect of the R^3 group was of paramount importance for reactions involving DGA and CHO, requiring the CN of **1.33**, **1.35** or **1.36** to achieve activity, otherwise the complex was degraded through reaction of the ligand with DGA. The aryl substituents R^1 and R^2 were also of importance to activity although to a lesser degree, with the asymmetric **1.35** proving to be the most active toward DGA/CHO copolymerization, yielding 79% conversion to copolymer, molecular weight of 23,000 g mol^{-1} and dispersity of 1.2 (0.33 mol% catalyst loading, 50 °C in 1.2 mL toluene, 2 h). **1.35** was further studied with the other epoxides and anhydrides listed above. Compound **1.35** proved effective toward perfectly alternating copolymerization of all epoxides with DGA, as well as CHO and VCHO with SA and LO with MA at optimized conditions. High molecular weights were obtained for each and dispersities ranged from 1.1 – 1.5. Larger polymer masses could be observed via GPC and were attributed to hydrolyzed anhydride acting as an initiator.

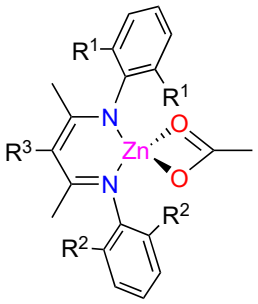

1.32 - $R^1 = R^2 = Et$, $R^3 = H$
1.33 - $R^1 = R^2 = Et$, $R^3 = CN$
1.34 - $R^1 = R^2 = Et$, $R^3 = Me$
1.35 - $R^1 = {}^iPr$, $R^2 = Et$, $R^3 = CN$
1.36 - $R^1 = R^2 = {}^iPr$, $R^3 = CN$

Fig. 1.20: BDI-zinc catalysts reported by Coates and co-workers for epoxide and anhydride copolymerization.[109]

Many 3d transition metal complexes have demonstrated exceptional activity toward copolymerization reactions, but thus far iron catalysts have not been discussed. The reports above highlight the ability of ligand design to influence the activity of the catalysts and more recently several reports of iron-catalyzed polymerizations have begun to surface.

1.15. Iron catalysis

Iron use in civilization can be traced back nearly 6000 years and has remained a staple material in several forms throughout our history. Organometallic catalysts involving iron have a long and storied past, particularly in the field of cross-coupling through C–H and C–O bond activation for which it is best known, but there are numerous other transformations that iron catalysis is well suited toward.[110-114] Abundant, the most common of the transition metals on Earth, and consequently inexpensive, iron is typically biocompatible and environmentally benign and is among the more important metals for naturally occurring biocatalysis making it suitable for catalyst design that follows green chemistry principles.

Additionally, it is not uncommon to find iron compounds with metal oxidation states ranging from -2 to +5, thus not only capable of functioning as the traditional Lewis Acid catalysts but also nucleophilic species as well. In fact, taking advantage of the redox capabilities of the metal is an entire field in and of itself.[115] As with other metal catalysts, both homogeneous and heterogeneous catalysts have been developed with iron. Of the heterogeneous variety, the most widely studied are iron nanoparticles. Interestingly, there have been reports of catalytic activity of proposed homogeneous systems being attributed instead to iron nanoparticles formed *in situ*. An enormous number of homogeneous iron-based catalysts have been developed and the most pertinent of which will be discussed in later sections.

1.16. Trace metal impurities in iron catalysis

Despite the myriad of successes observed for iron catalysts there is one important caveat to mention regarding its activity that was discovered in a report looking at the Suzuki coupling reaction.[116] It was determined that after rigorous purification of the Fe(II) and Fe(III) pyridine complexes used therein, no catalytic activity was observed. In actuality, trace palladium acetate was the catalytic species achieving quantitative conversion even at 1,000,000 molar equivalents of the starting material. A few years later, Buchwald and Bolm reported findings that lower purity $FeCl_3$ performed arylation reactions in greater yields than the higher purity catalysts.[117] They suggest copper impurities are responsible for the improved performance. Very recently, amine-catalyzed Suzuki couplings were reported and

quickly disputed, as palladium impurity from the amine synthesis, undetectable by inductively coupled plasma mass spectrometry, was the true catalyst.[118-119] As it stands, metal contamination in iron salts and even prepared iron catalysts is not uncommon, and thus rigorous purification is essential when designing new iron-based catalysts.

1.17. Iron catalysts for polymerization reactions

In recent years, there have been several reports on the efficacy of iron-based catalysts towards the copolymerization reactions discussed above, competitive with the other 3d metal catalysts that have so far dominated the field. The generally benign nature of iron complexes provides a compelling motivation to develop catalysts for commodity product synthesis to reduce damage caused by environmental metal-leaching from refuse.[120-121] In fact, iron-catalyzed olefin polymerization was first reported in 1998 by Brookhart and Gibson.[122] However, reports of iron-catalyzed CO_2/epoxide and epoxide/anhydride copolymerization have, until recently, been rare. Perhaps unsurprisingly, the prevalence of reports on CO_2/epoxide coupling has increased alongside reports of iron-catalyzed CO_2 reduction, although iron-ligand-CO_2 interactions have been known at least since the discovery of carbaminohemoglobin in 1928.[123] The coupling of CO_2 with epoxides from an iron-containing catalyst was first reported in a patent in 1985 by Kruper and Swart in the form of a double metal cyanide complex of zinc and iron.[124] Detailed studies of these types of systems were later reported by Darensbourg where it was found that epoxide activation likely occurs at the zinc-sites rather than iron, suggesting limitations on the ability of iron to initiate coupling reactions of this ilk.[125-126]

1.18. Iron catalyzed CO_2 coupling

Similar to the other transition metal catalysts, a single-site iron *N*-heterocyclic macrocyclic species was the first compound (**1.37**) reported for CO_2 and epoxide coupling – PO and CO_2 to form propylene carbonate by Marquis and Sanderson of the Texaco Chemical Company in 1992 (Fig. 1.21).[127] An exciting result, the catalyst required rather intense conditions of 180 °C at 0.5 mol% catalyst loading, supporting the hypothesis that iron initiated coupling with CO_2 required much higher energy input than similar 3d metal analogues (i.e. Cr(III)).

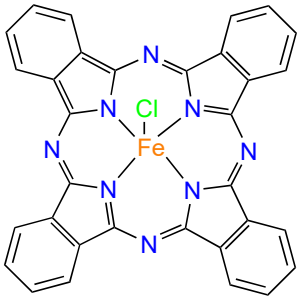

1.37

Fig. 1.21: Iron-phthalocyanine complex patented by Texaco Chemical Company in 1992.[127]

In 2000, He and co-workers reported a compound closely related to **1.37** but devoid of halide and thus in the Fe(II) oxidation state.[128] This species, as well as Al-Cl, Mg, Ni and Co variants, were applied toward coupling of CO_2 with EO, PO, ECH, and SO. Unsurprisingly, the catalyst was inactive toward coupling without the addition of co-catalyst nucleophile. However, when tributylamine (TBA) was introduced (4.5 equiv), cyclic

carbonate could be formed from each epoxide at 140 °C in 5 h with 2 equiv CO_2 per epoxide. While the activity toward PO was weak (6% conversion), SO and EO reached 60% and 65% respectively, and ECH could reach 91% conversion in just 30 min. As TBA exhibited poor activity in the absence of metal catalyst, this demonstrated that iron compounds could potentially achieve conversions on par with other metals in similar timeframes although the conditions were still rather harsh, and the Al and Mg analogues performed better in this study.

Recently, three iron-porphyrin catalysts (Fig. 1.22) were reported for cyclic carbonate formation from SO and CO_2 at 1 bar pressure. These compounds were also studied alongside magnesium- and zinc-chloride complexes and **1.38a** was found to be nearly as active as either, with just slight reductions in yield and TOF (h^{-1}). At 1.8 mol% catalyst loading, 2.3 mol% Bu_4NBr co-catalyst loading, 1 bar CO_2 and 70 °C, complete conversion to styrene carbonate could be observed in 5 h for **1.38a**, while **1.38b** and **c** achieved 73% and 90% respectively in 4 h. Evidently, the aryl-substituents impacted the activity significantly. Although the iron analogues were less active or slower than the Mg or Zn species under the same conditions, the observation of complete conversion at just 1 bar CO_2 represents an exceptional step forward for iron-*N*-heterocyclic catalysts that have thus far required fairly harsh conditions for CO_2 coupling reactions. Selectivity toward cyclic carbonate rather than polymer is unsurprising at higher temperatures as it is the thermodynamic product of the reaction. Cyclic carbonate production by iron catalysts of other design have been reviewed elsewhere.[43,129-130] As optimization of catalyst design has improved and conditions became milder, reports on CO_2 and epoxide copolymerization have increased in prevalence.

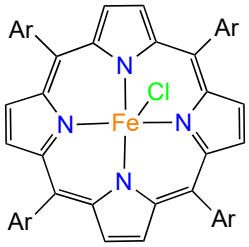

1.38
a: Ar = *p*-OMe-C_6H_4
b: Ar = *o*,*p*-OMe-C_6H_3
c: Ar = *m*,*p*-OMe-C_6H_3

Fig. 1.22: Iron-porphyrin complexes reported by Safari and co-workers in 2017.[131]

1.19. Iron-catalyzed copolymerization of CO_2 and epoxides

One of the earlier important reports on iron-catalyzed copolymerization published by the Williams group in 2011.[132] They employed a dimetallic iron complex supported by a macrocyclic amino-phenolate ligand similar to those of compounds **1.17** and **1.18** (Fig. 1.23). In neat CHO at 80 °C, 0.1 mol% **1.39** achieved 70% conversion to perfectly alternating poly(cyclohexene carbonate) in 24 h at 10 bar CO_2. The molecular weight was 11,700 g mol^{-1} with dispersity of 1.13, with trace amounts of *trans*-cyclohexene carbonate (CHC). Reducing the pressure to 1 bar and increasing reaction time to 48 h resulted in 29% conversion but selectivity toward poly(carbonate) of 66%. The molecular weight of this material was very low (2,000 g mol^{-1}) and the dispersity was relatively high at 1.55, and 7% conversion to *trans*-CHC was observed. Reducing catalyst loading to 0.01 mol% reduced conversion significantly (25%) but again perfectly alternating copolymer was produced at high molecular weight (17,200 g mol^{-1}) and very narrow dispersity of 1.03. However, a bimodal molecular weight distribution was observed via GPC analysis of lower molecular weight polymer

(8,100 g mol^{-1}, dispersity of 1.06) and is attributed to chain-transfer facilitated by by-products of HCl reacting with CHO. HCl is produced from FeCl reaction with impurities. If PPNCl co-catalyst was introduced (1, 2, or 4 equiv) at 1 bar CO_2, selectivity switched toward *cis*-CHC. Changing the epoxide to PO or SO resulted in strictly cyclic carbonate formation. This was the first example of an iron catalyst capable of synthesizing both poly(carbonate) and cyclic carbonate selectively.

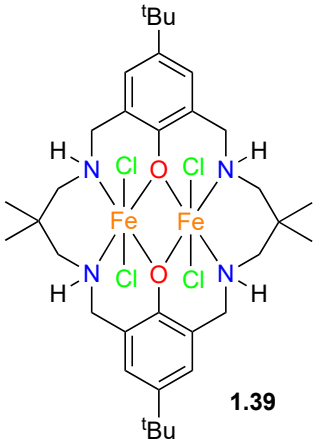

1.39

Fig. 1.23: Bimetallic iron-amino-phenolate catalyst reported by Williams for CO_2 and CHO copolymerization.[132]

Interested in controlling selectivity for either cyclic carbonate or poly(carbonate), Kleij and Pescarmona reported iron-amino-tris(phenolate) catalysts (Fig. 1.24) for cyclohexene oxide and CO_2 coupling.[133] First, **1.40a** was screened with five co-catalysts (Bu_4NF, Bu_4NCl, Bu_4NBr, Bu_4NI, PPNCl) at ratios of 10:1, 5:1 and 1:1 co-catalyst to iron complex. Reactions were performed at 0.5 mol% **1.40a**, 80 bar CO_2, 85 °C for 3 h (supercritical CO_2 conditions). Generally speaking, increasing the amount of co-catalyst led to increased selectivity for cyclohexene carbonate with the exception of Bu_4NF, where

selectivity for CHC was highest at 5 equiv, and 10 equiv resulted in mostly poly(ether) production, although this salt could not convert more than 12% under any loadings. The use of 1 equiv of both Bu_4NCl and PPNCl resulted in complete selectivity toward poly(carbonate) at 78% and 98% conversion, respectively. In all cases producing PCHC, no ether linkages were observed. As a 1:1 ratio appeared optimal, all species were tested with the co-catalysts above, as well as PPNBr and PPNI. Loadings were decreased to 0.1 mol% which reduced overall conversions. Complexes **1.40a** and **1.40b** behaved similarly in all cases suggesting that the steric differences between each are inconsequential to catalytic activity, however **1.40c** was significantly less reactive and selective than the others. They proposed that reduced solubility in supercritical conditions is the primary factor resulting in this behaviour, rather than changes in electronic environment of the catalyst, although they postulated that electrostatic repulsion may destabilize the ionic intermediates present during propagation in the relatively apolar supercritical CO_2 environment. Reduced co-catalyst loading was also examined for PPNCl and Bu_4NCl with all iron complexes but conversions were reduced in each case, although high selectivity was observed with **1.40a** and **1.40b** with PPNCl and **1.40b** with Bu_4NCl. Three polymers were characterized, those from reactions of **1.40a** and **1.40b** with 1 equiv of PPNCl, and **1.40a** with 0.25 equiv PPNCl. Bimodal molecular weight distributions were observed for each polymer: low molecular weight polymer (1,500 – 1,800 g mol^{-1}), moderate dispersities (1.18 – 1.25) and higher molecular weight polymer (~6,000 g mol^{-1}) with narrower dispersities (1.05 – 1.06). The authors proposed that adventitious water was causing chain transfer reactions and strictly anhydrous conditions were not feasible with their equipment. While molecular weights were much lower than polymers produced by other metal catalysts of the time, the selectivity toward either

product was an important find and further suggested that careful ligand design could lead to the development of better iron catalysts in the future.

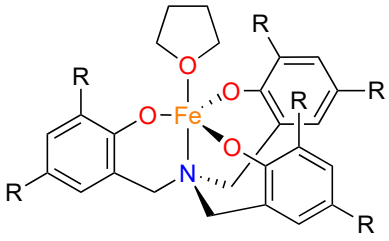

1.40
a: R = Me
b: R = ^{t}Bu
c: R = Cl

Fig. 1.24: Iron-amino-tris(phenolate) complexes reported by Kleij and Pescarmona for CO_2 and CHO copolymerization.[133]

Further developments of more recent iron-catalyzed CO_2 and epoxide copolymerization catalysts and the relatively new and limited field of iron-catalyzed epoxide and anhydride copolymerization will be discussed in detail in Chapter 4.

1.20. Alkylperoxo zinc complexes and oxidation of alkenes

In 2003, Lewiński and co-workers reported the first structurally characterized zinc-alkylperoxide (Scheme 1.3).[134] They proposed that the peroxide is formed through insertion of O_2 into the Zn–C bond of the precursor compound. Their interest was to generate this compound *in situ* and use it as an oxidant of enones to form *α,ß*-epoxy ketones. Current oxidation methods are performed with H_2O_2 or other more harmful metal oxidants such as $KMnO_4$, but these zinc compounds may provide an alternative and less aggressive method of

epoxidation. They had reported that the peroxy-zinc species was expected to be thermally unstable as other main-group metal-peroxides had exhibited pyrophoric reactivity with dioxygen and only complexes with heavier metals such as gallium and indium being isolable.[135] However, the introduction of the *β*-diketiminate ligand appeared to stabilize the dimeric species through non-covalent interactions as seen in many other single-site complexes containing this class of ligand. Unfortunately, the mechanism of the epoxidation is not well understood, and efforts to expand beyond electron-deficient olefins may not be trivial.

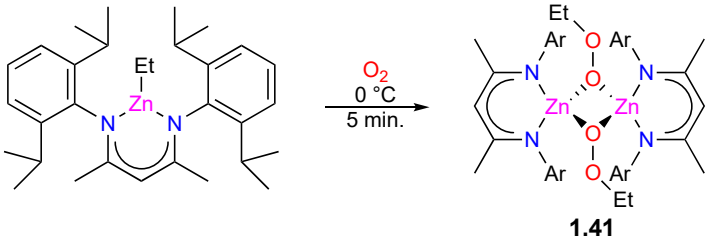

1.41

Scheme 1.3: Synthesis of the first structurally characterized alkylperoxozinc compound.

It was from this information that the idea to epoxidize enones and other unsaturated olefins and then polymerize the resulting epoxides in one pot was spawned. Efforts to replicate the work of Lewiński and co-workers will be discussed as well as isolation of a new peroxy-zinc species related to compound **2.1** in Chapter 3. This novel complex (**3.1**) was screened for epoxidation activity toward *trans*-chalcone, limonene and carvone, and copolymerization with CO_2 and the resulting epoxides (Scheme 1.4).

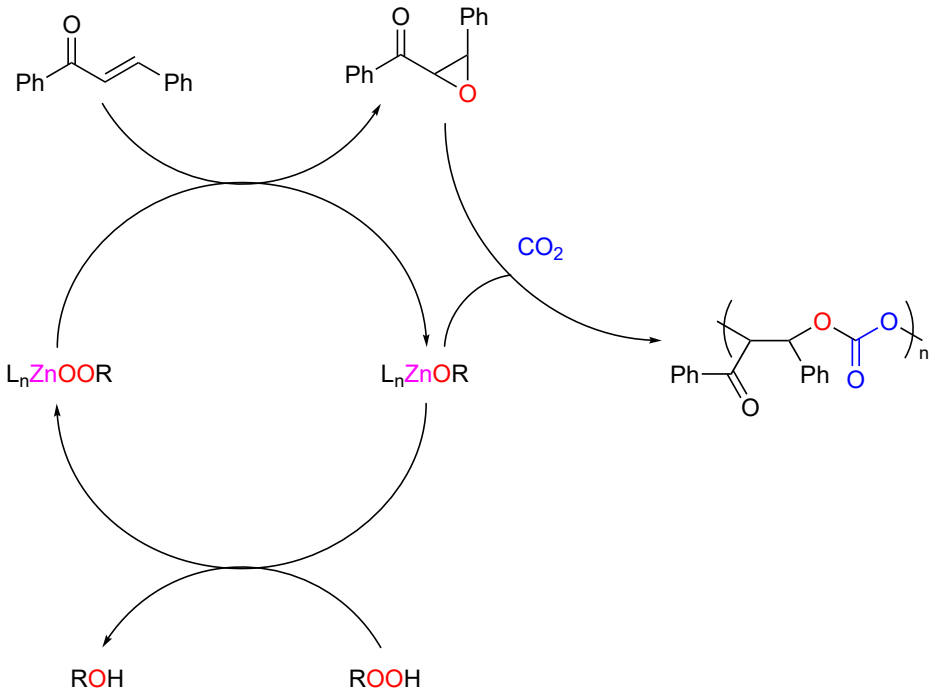

Scheme 1.4: Proposed catalytic cycle for epoxidation of *trans*-chalcone, copolymerization with CO_2, and regeneration of the alkylperoxozinc complex.

1.21. Thesis objectives

Several organometallic catalysts were to be designed, synthesized and applied toward different polymerization and coupling reactions. The primary interests were complexes of zinc and iron and the structure-activity relationships of them. Zinc catalysts were the first reported for copolymerization of CO_2 and epoxides, have historically been among the most active species and continue to be amongst the best today, particularly dinuclear complexes. The wide breadth of reports on zinc complexes for these reactions allow for the exploration of ligand design and how they influence the polymerization processes. Attempts to improve

upon literature results through synthesis of an amino-bis(phenolate)$(ZnEt)_2$ species will be presented in Chapter 2. This framework was also theorized to be suitable for stabilization of a larger tetrameric zinc peroxide species that could potentially be applied toward epoxidation of alkenes and subsequent copolymerization with CO_2 and efforts toward this goal are described in Chapter 3. Unlike zinc, cobalt or chromium, reports on iron complexes for CO_2 and epoxide copolymerization are fewer in number. Generally, iron complexes are high spin and thus substitutionally labile. This was thought to limit the design of effective metal-ligand complexes. However, recent reports of discrete iron catalysts for coupling of CO_2 with epoxides has clearly demonstrated that this limitation, if it is indeed limiting, can be overcome. Iron catalysts have also demonstrated switchable selectivity for CO_2 and epoxide coupling to form cyclic or poly(carbonate), and also switchable selectivity of monomer incorporation in poly(carbonate-*co*-ester) synthesis. Application of two previously reported complexes, amino-bis(phenolate)iron complexes, toward similar reactions were of interest and these efforts are described in Chapter 4.

1.22. References

1. Auta, H. S.; Emenike, C. U.; Fauziah, S. H., Distribution and importance of microplastics in the marine environment: A review of the sources, fate, effects, and potential solutions. *Environ. Int.* **2017**, *102*, pp 165-176.

2. Prata, J. C.; da Costa, J. P.; Lopes, I.; Duarte, A. C.; Rocha-Santos, T., Environmental exposure to microplastics: An overview on possible human health effects. *Sci. Total Environ.* **2020**, *702*, p 134455.

3. Rochester, J. R., Bisphenol A and human health: A review of the literature. *Reprod. Toxicol.* **2013**, *42*, pp 132-155.

4. Bauer, E. B., Iron Catalysis: Historic Overview and Current Trends. **2015**, *50*, pp 1-18.

5. Raymond, J.; Segrè, D., The Effect of Oxygen on Biochemical Networks and the Evolution of Complex Life. *Science* **2006**, *311*, pp 1764-1767.

6. Gaetani, G.; Galiano, S.; Canepa, L.; Ferraris, A.; Kirkman, H., Catalase and glutathione peroxidase are equally active in detoxication of hydrogen peroxide in human erythrocytes. *Blood* **1989**, *73*, pp 334-9.

7. Badger, M. R.; Price, G. D., The Role of Carbonic Anhydrase in Photosynthesis. *Annu. Rev. Plant Physiol. Plant Mol. Biol.* **1994**, *45*, pp 369-392.

8. Holm, R. H.; Kennepohl, P.; Solomon, E. I., Structural and Functional Aspects of Metal Sites in Biology. *Chem. Rev.* **1996**, *96*, pp 2239-2314.

9. Hartwig, J. F., Carbon–heteroatom bond formation catalysed by organometallic complexes. *Nature* **2008**, *455*, pp 314-322.

10. Han, F.-S., Transition-metal-catalyzed Suzuki–Miyaura cross-coupling reactions: a remarkable advance from palladium to nickel catalysts. *Chem. Soc. Rev.* **2013**, *42*, pp 5270-5298.

11. Elsby, M. R.; Baker, R. T., Strategies and mechanisms of metal–ligand cooperativity in first-row transition metal complex catalysts. *Chem. Soc. Rev.* **2020**, *49*, pp 8933-8987.

12. van der Vlugt, J. I., Cooperative Catalysis with First-Row Late Transition Metals. *Eur. J. Inorg. Chem.* **2012**, *2012*, pp 363-375.

13. Obligacion, J. V.; Chirik, P. J., Earth-abundant transition metal catalysts for alkene hydrosilylation and hydroboration. *Nat. Rev. Chem.* **2018**, *2*, pp 15-34.

14. Su, B.; Cao, Z.-C.; Shi, Z.-J., Exploration of Earth-Abundant Transition Metals (Fe, Co, and Ni) as Catalysts in Unreactive Chemical Bond Activations. *Acc. Chem. Res.* **2015**, *48*, pp 886-896.

15. Gandeepan, P.; Müller, T.; Zell, D.; Cera, G.; Warratz, S.; Ackermann, L., 3d Transition Metals for C–H Activation. *Chem. Rev.* **2019**, *119*, pp 2192-2452.

16. Peng, J.-B.; Wu, F.-P.; Wu, X.-F., First-Row Transition-Metal-Catalyzed Carbonylative Transformations of Carbon Electrophiles. *Chem. Rev.* **2019**, *119*, pp 2090-2127.

17. Nandy, A.; Chu, D. B. K.; Harper, D. R.; Duan, C.; Arunachalam, N.; Cytter, Y.; Kulik, H. J., Large-scale comparison of 3d and 4d transition metal complexes illuminates the reduced effect of exchange on second-row spin-state energetics. *Phys. Chem. Chem. Phys.* **2020**, *22*, pp 19326-19341.

18. Geyer, R.; Jambeck, J. R.; Law, K. L., Production, use, and fate of all plastics ever made. *Sci. Adv.* **2017**, *3*, p e1700782.

19. Iyer, K. A.; Zhang, L.; Torkelson, J. M., Direct Use of Natural Antioxidant-rich Agro-wastes as Thermal Stabilizer for Polymer: Processing and Recycling. *ACS. Sustain. Chem. Eng.* **2016**, *4*, pp 881-889.

20. Groot, W.; Van Krieken, J.; Sliekersl, O.; de Vos, S., Production and purification of lactic acid and lactide. *Poly(lactic acid): Structures, Production, Synthesis and Applications* **2010**, pp 1-18.

21. Wheaton, C. A.; Hayes, P. G.; Ireland, B. J., Complexes of Mg, Ca and Zn as homogeneous catalysts for lactide polymerization. *Dalton Trans.* **2009**, pp 4832-4846.

22. Merrington, A.; Smith, P. B.; Plonka, J. H.; Bubeck, R. A., *PCT Int. Appl. WO2015181029A1* **2015**.

23. NatureWorks., *http://www.natureworksllc.com/ (accessed May 17, 2020).*

24. Ikada, Y.; Tsuji, H., Biodegradable polyesters for medical and ecological applications. *Macromol. Rapid Commun.* **2000**, *21*, pp 117-132.

25. Reiter, M.; Vagin, S.; Kronast, A.; Jandl, C.; Rieger, B., A Lewis acid β-diiminato-zinc-complex as all-rounder for co- and terpolymerisation of various epoxides with carbon dioxide. *Chem. Sci.* **2017**, *8*, pp 1876-1882.

26. Shi, L.; Lu, X.-B.; Zhang, R.; Peng, X.-J.; Zhang, C.-Q.; Li, J.-F.; Peng, X.-M., Asymmetric Alternating Copolymerization and Terpolymerization of Epoxides with Carbon Dioxide at Mild Conditions. *Macromolecules* **2006**, *39*, pp 5679-5685.

27. Inoue, S., Immortal polymerization: The outset, development, and application. *J. Polym. Sci. A Polym. Chem.* **2000**, *38*, pp 2861-2871.

28. Asano, S.; Aida, T.; Inoue, S., 'Immortal' polymerization. Polymerization of epoxide catalysed by an aluminium porphyrin–alcohol system. *J. Chem. Soc., Chem. Commun.* **1985**, pp 1148-1149.

29. National Oceanic and Atmospheric Administration Trends in Atmospheric Carbon Dioxide. **2020**.

30. IPCC fourth assessment report: climate change 2013 (AR5). **2013**.

31. Liu, Q.; Wu, L.; Jackstell, R.; Beller, M., Using carbon dioxide as a building block in organic synthesis. *Nat. Commun.* **2015**, *6*, p 5933.

32. Kätelhön, A.; Meys, R.; Deutz, S.; Suh, S.; Bardow, A., Climate change mitigation potential of carbon capture and utilization in the chemical industry. *Proceedings of the National Academy of Sciences* **2019**, *116*, pp 11187-11194.

33. Bargiacchi, E.; Antonelli, M.; Desideri, U., A comparative assessment of Power-to-Fuel production pathways. *Energy* **2019**, *183*, pp 1253-1265.

34. Iota, V.; Yoo, C. S.; Cynn, H., Quartzlike Carbon Dioxide: An Optically Nonlinear Extended Solid at High Pressures and Temperatures. *Science* **1999**, *283*, p 1510.

35. Huang, J.; Worch, J. C.; Dove, A. P.; Coulembier, O., Update and Challenges in Carbon Dioxide-Based Polycarbonate Synthesis. *ChemSusChem* **2020**, *13*, pp 469-487.

36. Andrea, K. A.; Plommer, H.; Kerton, F. M., Ring-opening polymerizations and copolymerizations of epoxides using aluminum- and boron-centered catalysts. *Eur. Polym. J.* **2019**, *120*, p 109202.

37. Sakakura, T.; Kohno, K., The synthesis of organic carbonates from carbon dioxide. *Chem. Commun.* **2009**, pp 1312-1330.

38. Vicente, R.; Mata, S., Chapter 7 - Zinc-Mediated Synthesis of Heterocycles. In *Advances in Transition-Metal Mediated Heterocyclic Synthesis*, Solé, D.; Fernández, I., Eds. Academic Press: 2018; pp 285-310.

39. Darensbourg, D. J., Making Plastics from Carbon Dioxide: Salen Metal Complexes as Catalysts for the Production of Polycarbonates from Epoxides and CO_2. *Chem. Rev.* **2007**, *107*, pp 2388-2410.

40. Klaus, S.; Lehenmeier, M. W.; Anderson, C. E.; Rieger, B., Recent advances in CO_2/epoxide copolymerization—New strategies and cooperative mechanisms. *Coord. Chem. Rev.* **2011**, *255*, pp 1460-1479.

41. Coates, G. W.; Moore, D. R., Discrete metal-based catalysts for the copolymerization of CO_2 and epoxides: discovery, reactivity, optimization, and mechanism. *Angew. Chem. Int. Ed.* **2004**, *43*, pp 6618-39.

42. Kozak, C. M.; Ambrose, K.; Anderson, T. S., Copolymerization of carbon dioxide and epoxides by metal coordination complexes. *Coord. Chem. Rev.* **2018**, *376*, pp 565-587.

43. Andrea, K. A.; Kerton, F. M., Iron-catalyzed reactions of CO_2 and epoxides to yield cyclic and polycarbonates. *Polym. J. (Tokyo, Jpn.)* **2021**, *53*, pp 29-46.

44. Vandenberg, L. N.; Maffini, M. V.; Sonnenschein, C.; Rubin, B. S.; Soto, A. M., Bisphenol-A and the Great Divide: A Review of Controversies in the Field of Endocrine Disruption. *Endocr. Rev.* **2009**, *30*, pp 75-95.

45. Diller, W. F., Pathogenesis of Phosgene Poisoning. *Toxicol. Ind. Health* **1985**, *1*, pp 7-15.

46. Inoue, S.; Koinuma, H.; Tsuruta, T., Copolymerization of carbon dioxide and epoxide. *J. Polym. Sci. B.* **1969**, *7*, pp 287-292.

47. Takeda, N.; Inoue, S., Polymerization of 1,2-epoxypropane and copolymerization with carbon dioxide catalyzed by metalloporphyrins. *Makromol. Chem.* **1978**, *179*, pp 1377-1381.

48. Aida, T.; Inoue, S., Synthesis of polyether-polycarbonate block copolymer from carbon dioxide and epoxide using a metalloporphyrin catalyst system. *Macromolecules* **1982**, *15*, pp 682-684.

49. Aida, T.; Inoue, S., Activation of carbon dioxide with aluminum porphyrin and reaction with epoxide. Studies on (tetraphenylporphinato)aluminum alkoxide having a long oxyalkylene chain as the alkoxide group. *J. Am. Chem. Soc.* **1983**, *105*, pp 1304-1309.

50. Aida, T.; Ishikawa, M.; Inoue, S., Alternating copolymerization of carbon dioxide and epoxide catalyzed by the aluminum porphyrin-quaternary organic salt or -triphenylphosphine system. Synthesis of polycarbonate with well-controlled molecular weight. *Macromolecules* **1986**, *19*, pp 8-13.

51. Jung, J. H.; Ree, M.; Chang, T., Copolymerization of carbon dioxide and propylene oxide using an aluminum porphyrin system and its components. *J. Polym. Sci. A Polym. Chem.* **1999**, *37*, pp 3329-3336.

52. Kruper, W. J.; Dellar, D. D., Catalytic Formation of Cyclic Carbonates from Epoxides and CO_2 with Chromium Metalloporphyrinates. *The Journal of Organic Chemistry* **1995**, *60*, pp 725-727.

53. Jacobsen, E. N., Asymmetric Catalysis of Epoxide Ring-Opening Reactions. *Acc. Chem. Res.* **2000**, *33*, pp 421-431.

54. E. N. Jacobsen, M. T., J. F. Larrow, *PCT Int. Appl. WO00/09463* **2000**.

55. Darensbourg, D. J.; Yarbrough, J. C.; Ortiz, C.; Fang, C. C., Comparative kinetic studies of the copolymerization of cyclohexene oxide and propylene oxide with carbon dioxide in the presence of chromium salen derivatives. In situ FTIR measurements of copolymer vs cyclic carbonate production. *J. Am. Chem. Soc.* **2003**, *125*, pp 7586-7591.

56. Poland, S. J.; Darensbourg, D. J., A quest for polycarbonates provided via sustainable epoxide/CO_2 copolymerization processes. *Green Chem.* **2017**, *19*, pp 4990-5011.

57. Darensbourg, D. J.; Holtcamp, M. W., Catalytic Activity of Zinc(II) Phenoxides Which Possess Readily Accessible Coordination Sites. Copolymerization and Terpolymerization of Epoxides and Carbon Dioxide. *Macromolecules* **1995**, *28*, pp 7577-7579.

58. Byrne, C. M.; Allen, S. D.; Lobkovsky, E. B.; Coates, G. W., Alternating copolymerization of limonene oxide and carbon dioxide. *J. Am. Chem. Soc.* **2004**, *126*, pp 11404-5.

59. Darensbourg, D. J.; Holtcamp, M. W.; Struck, G. E.; Zimmer, M. S.; Niezgoda, S. A.; Rainey, P.; Robertson, J. B.; Draper, J. D.; Reibenspies, J. H., Catalytic Activity of a Series of Zn(II) Phenoxides for the Copolymerization of Epoxides and Carbon Dioxide. *J. Am. Chem. Soc.* **1999**, *121*, pp 107-116.

60. Cheng, M.; Lobkovsky, E. B.; Coates, G. W., Catalytic Reactions Involving C1Feedstocks: New High-Activity Zn(II)-Based Catalysts for the Alternating Copolymerization of Carbon Dioxide and Epoxides. *J. Am. Chem. Soc.* **1998**, *120*, pp 11018-11019.

61. Cheng, M.; Darling, N. A.; Lobkovsky, E. B.; Coates, G. W., Enantiomerically-enriched organic reagents polymer synthesis: enantioselective copolymerization of cycloalkene oxides and CO using homogeneous, zinc-based catalysts. *Chem. Commun.* **2000**, pp 2007-2008.

62. Cheng, M.; Moore, D. R.; Reczek, J. J.; Chamberlain, B. M.; Lobkovsky, E. B.; Coates, G. W., Single-Site Beta-Diiminate Zinc Catalysts for the Alternating Copolymerization of CO_2 and Epoxides: Catalyst Synthesis and Unprecedented Polymerization Activity. *J. Am. Chem. Soc.* **2001**, *123*, pp 8738-8749.

63. Moore, D. R.; Cheng, M.; Lobkovsky, E. B.; Coates, G. W., Electronic and Steric Effects on Catalysts for CO_2/Epoxide Polymerization: Subtle Modifications Resulting in Superior Activities. *Angew. Chem. Int. Ed.* **2002**, *41*, pp 2599-2602.

64. Allen, S. D.; Moore, D. R.; Lobkovsky, E. B.; Coates, G. W., High-Activity, Single-Site Catalysts for the Alternating Copolymerization of CO_2 and Propylene Oxide. *J. Am. Chem. Soc.* **2002**, *124*, pp 14284-14285.

65. Wang, Y.; Darensbourg, D. J., Carbon Dioxide-based Functional Polycarbonates: Metal Catalyzed Copolymerization of CO_2 and Epoxides. *Coord. Chem. Rev.* **2018**, *372*, pp 85-100.

66. Martin, C.; Kleij, A. W., Terpolymers Derived from Limonene Oxide and Carbon Dioxide: Access to Cross-Linked Polycarbonates with Improved Thermal Properties. *Macromolecules* **2016**, *49*, pp 6285-6295.

67. Andrea, K. A.; Kerton, F. M., Triarylborane-catalyzed formation of cyclic organic carbonates and polycarbonates. *ACS Catal.* **2019**, *9*, pp 1799-1809.

68. Andrea, K. A.; Kerton, F. M., Functionalized polycarbonates via triphenylborane catalyzed polymerization-hydrosilylation. *RSC Adv.* **2019**, *9*, pp 26542-26546.

69. Cherian, A. E.; Sun, F. C.; Sheiko, S. S.; Coates, G. W., Formation of Nanoparticles by Intramolecular Cross-Linking: Following the Reaction Progress of Single Polymer Chains by Atomic Force Microscopy. *J. Am. Chem. Soc.* **2007**, *129*, pp 11350-11351.

70. Inoue, S.; Koinuma, H.; Tsuruta, T., *Makromol. Chem.* **1969**, *130*, pp 210-220.

71. Kember, M. R.; Buchard, A.; Williams, C. K., Catalysts for CO_2/epoxide copolymerisation. *Chem. Commun.* **2011**, *47*, pp 141-63.

72. Trott, G.; Saini, P. K.; Williams, C. K., Catalysts for CO_2/epoxide ring-opening copolymerization. *Philos. Trans. Royal Soc. A* **2016**, *374*.

73. Paul, S.; Zhu, Y.; Romain, C.; Brooks, R.; Saini, P. K.; Williams, C. K., Ring-opening copolymerization (ROCOP): synthesis and properties of polyesters and polycarbonates. *Chem. Commun.* **2015**, *51*, pp 6459-79.

74. Kissling, S.; Altenbuchner, P. T.; Lehenmeier, M. W.; Herdtweck, E.; Deglmann, P.; Seemann, U. B.; Rieger, B., Mechanistic Aspects of a Highly Active Dinuclear Zinc Catalyst for the Co-polymerization of Epoxides and CO_2. *Chem. Eur. J.* **2015**, *21*, pp 8148-8157.

75. Marbach, J.; Nornberg, B.; Rahlf, A. F.; Luinstra, G. A., Zinc glutarate-mediated copolymerization of CO_2 and PO - parameter studies using design of experiments. *Catal. Sci. Tech.* **2017**, *7*, pp 2897-2905.

76. Martin, C.; Kleij, A. W., Comparing kinetic profiles between bifunctional and binary type of Zn(salen)-based catalysts for organic carbonate formation. *Beilstein J. Org. Chem.* **2014**, *10*, pp 1817-25.

77. Romain, C.; Bennington, M. S.; White, A. J.; Williams, C. K.; Brooker, S., Macrocyclic Dizinc(II) Alkyl and Alkoxide Complexes: Reversible CO_2 Uptake and Polymerization Catalysis Testing. *Inorg. Chem.* **2015**, *54*, pp 11842-51.

78. Romain, C.; Garden, J. A.; Trott, G.; Buchard, A.; White, A. J. P.; Williams, C. K., Di-Zinc-Aryl Complexes: CO_2 Insertions and Applications in Polymerisation Catalysis. *Chem. Eur. J.* **2017**, *23*, pp 7367-7376.

79. Lehenmeier, M. W.; Kissling, S.; Altenbuchner, P. T.; Bruckmeier, C.; Deglmann, P.; Brym, A. K.; Rieger, B., Flexibly tethered dinuclear zinc complexes: a solution to the entropy problem in CO_2/epoxide copolymerization catalysis? *Angew. Chem. Int. Ed.* **2013**, *52*, pp 9821-9826.

80. Kissling, S.; Lehenmeier, M. W.; Altenbuchner, P. T.; Kronast, A.; Reiter, M.; Deglmann, P.; Seemann, U. B.; Rieger, B., Dinuclear zinc catalysts with unprecedented activities for the copolymerization of cyclohexene oxide and CO_2. *Chem. Commun.* **2015**, *51*, pp 4579-4582.

81. Xu, Y.; Xiao, M.; Wang, S.; Pan, M.; Meng, Y., Activities comparison of Schiff base zinc and tri-zinc complexes for alternating copolymerization of CO_2 and epoxides. *Polym. Chem.* **2014**, *5*, p 3838.

82. Xu, Y.; Wang, S.; Lin, L.; Xiao, M.; Meng, Y., Semi-crystalline terpolymers with varying chain sequence structures derived from CO_2, cyclohexene oxide and ε-caprolactone: one-step synthesis catalyzed by tri-zinc complexes. *Polym. Chem.* **2015**, *6*, pp 1533-1540.

83. Xu, Y.; Lin, L.; He, C.-T.; Qin, J.; Li, Z.; Wang, S.; Xiao, M.; Meng, Y., Kinetic and mechanistic investigation for the copolymerization of CO_2 and cyclohexene oxide catalyzed by trizinc complexes. *Polym. Chem.* **2017**, *8*, pp 3632-3640.

84. Zhang, X.-H.; Wei, R.-J.; Zhang, Y. Y.; Du, B.-Y.; Fan, Z.-Q., Carbon Dioxide/Epoxide Copolymerization via a Nanosized Zinc–Cobalt(III) Double Metal Cyanide Complex: Substituent Effects of Epoxides on Polycarbonate Selectivity, Regioselectivity and Glass Transition Temperatures. *Macromolecules* **2015**, *48*, pp 536-544.

85. Qin, J.; Xu, B.; Zhang, Y.; Yuan, D.; Yao, Y. M., Cooperative rare earth metal-zinc based heterometallic catalysts for copolymerization of CO_2 and cyclohexene oxide. *Green Chem.* **2016**, *18*, pp 4270-4275.

86. Wulf, C.; Doering, U.; Werner, T., Copolymerization of CO_2 and epoxides mediated by zinc organyls. *RSC Adv.* **2018**, *8*, pp 3673-3679.

87. Yu, C. Y.; Chuang, H. J.; Ko, B. T., Bimetallic bis(benzotriazole iminophenolate) cobalt, nickel and zinc complexes as versatile catalysts for coupling of carbon dioxide with epoxides and copolymerization of phthalic anhydride with cyclohexene oxide. *Catal. Sci. Tech.* **2016**, *6*, pp 1779-1791.

88. Kernbichl, S.; Reiter, M.; Adams, F.; Vagin, S.; Rieger, B., CO_2-controlled one-pot synthesis of AB, ABA block, and statistical terpolymers from beta-butyrolactone, epoxides, and CO_2. *J. Am. Chem. Soc.* **2017**, *139*, pp 6787-6790.

89. Garden, J. A.; White, A. J. P.; Williams, C. K., Heterodinuclear titanium/zinc catalysis: synthesis, characterization and activity for CO_2/epoxide copolymerization and cyclic ester polymerization. *Dalton Trans.* **2017**, *46*, pp 2532-2541.

90. Nagae, H.; Aoki, R.; Akutagawa, S. N.; Kleemann, J.; Tagawa, R.; Schindler, T.; Choi, G.; Spaniol, T. P.; Tsurugi, H.; Okuda, J.; Mashima, K., Lanthanide Complexes Supported by a Trizinc Crown Ether as Catalysts for Alternating Copolymerization of Epoxide and CO_2 : Telomerization Controlled by Carboxylate Anions. *Angew. Chem. Int. Ed.* **2018**, *57*, pp 2492-2496.

91. Schutze, M.; Dechert, S.; Meyer, F., Highly Active and Readily Accessible Proline-Based Dizinc Catalyst for CO_2/Epoxide Copolymerization. *Chem. Eur. J.* **2017**, *23*, pp 16472-16475.

92. Martínez, J.; Castro-Osma, J. A.; Lara-Sánchez, A.; Otero, A.; Fernández-Baeza, J.; Tejeda, J.; Sánchez-Barba, L. F.; Rodríguez-Diéguez, A., Ring-opening copolymerisation of cyclohexene oxide and carbon dioxide catalysed by scorpionate zinc complexes. *Polym. Chem.* **2016**, *7*, pp 6475-6484.

93. Paul, S.; Romain, C.; Shaw, J.; Williams, C. K., Sequence Selective Polymerization Catalysis: A New Route to ABA Block Copoly(ester-b-carbonate-b-ester). *Macromolecules* **2015**, *48*, pp 6047-6056.

94. Romain, C.; Zhu, Y.; Dingwall, P.; Paul, S.; Rzepa, H. S.; Buchard, A.; Williams, C. K., Chemoselective polymerizations from mixtures of epoxide, lactone, anhydride, and carbon dioxide. *J. Am. Chem. Soc.* **2016**, *138*, pp 4120-31.

95. Thevenon, A.; Garden, J. A.; White, A. J.; Williams, C. K., Dinuclear Zinc Salen Catalysts for the Ring Opening Copolymerization of Epoxides and Carbon Dioxide or Anhydrides. *Inorg. Chem.* **2015**, *54*, pp 11906-15.

96. Saini, P. K.; Fiorani, G.; Mathers, R. T.; Williams, C. K., Zinc versus Magnesium: Orthogonal Catalyst Reactivity in Selective Polymerizations of Epoxides, Bio-derived Anhydrides and Carbon Dioxide. *Chem. Eur. J.* **2017**, *23*, pp 4260-4265.

97. Hauenstein, O.; Agarwal, S.; Greiner, A., Bio-based polycarbonate as synthetic toolbox. *Nat. Commun.* **2016**, *7*, p 11862.

98. Li, C.; Sablong, R. J.; Koning, C. E., Chemoselective Alternating Copolymerization of Limonene Dioxide and Carbon Dioxide: A New Highly Functional Aliphatic Epoxy Polycarbonate. *Angew. Chem. Int. Ed.* **2016**, *55*, pp 11572-6.

99. Van Zee, N. J.; Coates, G. W., Alternating Copolymerization of Propylene Oxide with Biorenewable Terpene-Based Cyclic Anhydrides: A Sustainable Route to Aliphatic Polyesters with High Glass Transition Temperatures. *Angew. Chem. Int. Ed.* **2015**, *54*, pp 2665-2668.

100. Van Zee, N. J.; Sanford, M. J.; Coates, G. W., Electronic Effects of Aluminum Complexes in the Copolymerization of Propylene Oxide with Tricyclic Anhydrides: Access to Well-Defined, Functionalizable Aliphatic Polyesters. *J. Am. Chem. Soc.* **2016**, *138*, pp 2755-2761.

101. Ajellal, N.; Carpentier, J.-F.; Guillaume, C.; Guillaume, S. M.; Helou, M.; Poirier, V.; Sarazin, Y.; Trifonov, A., Metal-catalyzed Immortal Ring-opening Polymerization of Lactones, Lactides and Cyclic Carbonates. *Dalton Trans.* **2010**, *39*, pp 8363-8376.

102. Saini, P. K.; Romain, C.; Zhu, Y.; Williams, C. K., Di-magnesium and zinc catalysts for the copolymerization of phthalic anhydride and cyclohexene oxide. *Polym. Chem.* **2014**, *5*, pp 6068-6075.

103. Sanford, M. J.; Peña Carrodeguas, L.; Van Zee, N. J.; Kleij, A. W.; Coates, G. W., Alternating Copolymerization of Propylene Oxide and Cyclohexene Oxide with Tricyclic

Anhydrides: Access to Partially Renewable Aliphatic Polyesters with High Glass Transition Temperatures. *Macromolecules* **2016**, *49*, pp 6394-6400.

104. Aida, T.; Inoue, S., Catalytic reaction on both sides of a metalloporphyrin plane. Alternating copolymerization of phthalic anhydride and epoxypropane with an aluminum porphyrin-quaternary salt system. *J. Am. Chem. Soc.* **1985**, *107*, pp 1358-1364.

105. Hilt, V. A.; Reichert, K. H.; Hamann, K., Synthese von polyestern durch copolymerisation von dicarbonsäreanhydriden und ringäthern. *Makromol. Chem.* **1967**, *101*, pp 246-270.

106. Huijser, S.; HosseiniNejad, E.; Sablong, R.; de Jong, C.; Koning, C. E.; Duchateau, R., Ring-Opening Co- and Terpolymerization of an Alicyclic Oxirane with Carboxylic Acid Anhydrides and CO_2 in the Presence of Chromium Porphyrinato and Salen Catalysts. *Macromolecules* **2011**, *44*, pp 1132-1139.

107. Hosseini Nejad, E.; van Melis, C. G. W.; Vermeer, T. J.; Koning, C. E.; Duchateau, R., Alternating Ring-Opening Polymerization of Cyclohexene Oxide and Anhydrides: Effect of Catalyst, Cocatalyst, and Anhydride Structure. *Macromolecules* **2012**, *45*, pp 1770-1776.

108. DiCiccio, A. M.; Coates, G. W., Ring-Opening Copolymerization of Maleic Anhydride with Epoxides: A Chain-Growth Approach to Unsaturated Polyesters. *J. Am. Chem. Soc.* **2011**, *133*, pp 10724-10727.

109. Jeske, R. C.; DiCiccio, A. M.; Coates, G. W., Alternating Copolymerization of Epoxides and Cyclic Anhydrides: An Improved Route to Aliphatic Polyesters. *J. Am. Chem. Soc.* **2007**, *129*, pp 11330-11331.

110. Bolm, C.; Legros, J.; Le Paih, J.; Zani, L., Iron-Catalyzed Reactions in Organic Synthesis. *Chem. Rev.* **2004**, *104*, pp 6217-6254.

111. Sun, C.-L.; Li, B.-J.; Shi, Z.-J., Direct C−H Transformation via Iron Catalysis. *Chem. Rev.* **2011**, *111*, pp 1293-1314.

112. Wei, D.; Darcel, C., Iron Catalysis in Reduction and Hydrometalation Reactions. *Chem. Rev.* **2019**, *119*, pp 2550-2610.

113. Gopalaiah, K., Chiral Iron Catalysts for Asymmetric Synthesis. *Chem. Rev.* **2013**, *113*, pp 3248-3296.

114. Bauer, I.; Knölker, H.-J., Iron Catalysis in Organic Synthesis. *Chem. Rev.* **2015**, *115*, pp 3170-3387.

115. Enthaler, S.; Junge, K.; Beller, M., Sustainable Metal Catalysis with Iron: From Rust to a Rising Star? *Angew. Chem. Int. Ed.* **2008**, *47*, pp 3317-3321.

116. Bedford, R. B.; Nakamura, M.; Gower, N. J.; Haddow, M. F.; Hall, M. A.; Huwe, M.; Hashimoto, T.; Okopie, R. A., Iron-catalysed Suzuki coupling? A cautionary tale. *Tetrahedron Lett.* **2009**, *50*, pp 6110-6111.

117. Buchwald, S. L.; Bolm, C., On the role of metal contaminants in catalyses with $FeCl_3$. *Angew. Chem. Int. Ed.* **2009**, *48*, pp 5586-5587.

118. Xu, L.; Liu, F.-Y.; Zhang, Q.; Chang, W.-J.; Liu, Z.-L.; Lv, Y.; Yu, H.-Z.; Xu, J.; Dai, J.-J.; Xu, H.-J., The amine-catalysed Suzuki–Miyaura-type coupling of aryl halides and arylboronic acids. *Nat. Catal.* **2021**, *4*, pp 71-78.

119. Mickaël, A.; Robin, B.; Callum, B.; Dietrich, B.; Jonathan, C.; Sean, D.; Jean-Charles, E.; Georgy P., G.; Ingo V., H.; Joseph, H.; Kirill A., K.; Matthew, K.; Johannes, K.; Pavel S., K.; Alastair, L.; Roberto, N.-S.; Natalie E., P.; Benjamin J. S., R.; Hazel A., S.; Dmitry V., U.; Alexander Z., V.; Mark, W.; Harry J., W., *Amine-Catalysed Suzuki–Miyaura-Type Coupling? the Identification and Isolation of the Palladium Culprits*. 2021. Accessed at https://chemrxiv.org/engage/chemrxiv/article-details/60c7566b702a9bb55e18c8e6.

120. Mendez-Sanchez, N.; Cutright, T. J.; Qiao, P., Accelerated weathering and biodegradation of E-glass polyester composites. *Int. Biodeterior. Biodegradation* **2004**, *54*, pp 289-296.

121. Krachler, M.; Shotyk, W., Trace and ultratrace metals in bottled waters: Survey of sources worldwide and comparison with refillable metal bottles. *Sci. Total Environ.* **2009**, *407*, pp 1089-1096.

122. Small, B. L.; Brookhart, M.; Bennett, A. M. A., Highly Active Iron and Cobalt Catalysts for the Polymerization of Ethylene. *J. Am. Chem. Soc.* **1998**, *120*, pp 4049-4050.

123. Henriques, O., The carbon dioxide combination in the blood. V. Physiological considerations concerning the carbhemoglobin problem. *Biochem. Z.* **1928**, *200*, pp 22-24.

124. Kruper, W. J.; Swart, D. J., U.S. Patent 4,500,704. **1985**.

125. Darensbourg, D. J.; Adams, M. J.; Yarbrough, J. C., Toward the design of double metal cyanides for the copolymerization of CO_2 and epoxides. *Inorg. Chem.* **2001**, *40*, pp 6543-4.

126. Darensbourg, D. J.; Adams, M. J.; Yarbrough, J. C.; Phelps, A. L., Synthesis and Structural Characterization of Double Metal Cyanides of Iron and Zinc: Catalyst Precursors for the Copolymerization of Carbon Dioxide and Epoxides. *Inorg. Chem.* **2003**, *42*, pp 7809-7818.

127. Marquis, E. T.; Sanderson, J. R., US Patent 5,283,356A. **1992**.

128. Ji, D.; Lu, X.; He, R., Syntheses of cyclic carbonates from carbon dioxide and epoxides with metal phthalocyanines as catalyst. *Appl. Catal. A: Gen.* **2000**, *203*, pp 329-333.

129. Andrea, K. A.; Kerton, F. M., Iron-catalyzed reactions of CO_2 and epoxides to yield cyclic and polycarbonates. *Polym. J. (Tokyo, Jpn.)* **2020**.

130. Della Monica, F.; Buonerba, A.; Capacchione, C., Homogeneous Iron Catalysts in the Reaction of Epoxides with Carbon Dioxide. *Adv. Synth. Catal.* **2019**, *361*, pp 265-282.

131. Farhadian, A.; Gol Afshani, M. B.; Babaei Miyardan, A.; Nabid, M. R.; Safari, N., A Facile and Green Route for Conversion of Bifunctional Epoxide and Vegetable Oils to Cyclic Carbonate: A Green Route to CO_2 Fixation. *ChemistrySelect* **2017**, *2*, pp 1431-1435.

132. Buchard, A.; Kember, M. R.; Sandeman, K. G.; Williams, C. K., A Bimetallic Iron(III) Catalyst for CO_2/Epoxide Coupling. *Chem. Commun.* **2011**, *47*, pp 212-214.

133. Taherimehr, M.; Al-Amsyar, S. M.; Whiteoak, C. J.; Kleij, A. W.; Pescarmona, P. P., High Activity and Switchable Selectivity in the Synthesis of Cyclic and Polymeric Cyclohexene Carbonates with Iron Amino Triphenolate Catalysts. *Green Chem.* **2013**, *15*, pp 3083-3090.

134. Lewiński, J.; Ochal, Z.; Bojarski, E.; Tratkiewicz, E.; Justyniak, I.; Lipkowski, J., First Structurally Authenticated Zinc Alkylperoxide: A Model System for the Epoxidation of Enones. *Angew. Chem. Int. Ed.* **2003**, *42*, pp 4643-4646.

135. Lewiński, J.; Zachara, J.; Grabska, E., Synthesis and Molecular Structure of (^{t}BuOO)(^{t}BuO)Al(μ-O^{t}Bu)$_2$Al(mesal)$_2$. The First Structurally Characterized (Alkylperoxo)aluminum Compound. *J. Am. Chem. Soc.* **1996**, *118*, pp 6794-6795.

Chapter 2

Ring-opening polymerization of epoxides and ring-opening copolymerization of CO_2 with epoxides by a zinc amino-bis(phenolate) catalyst

Statement of Co-Authorship

This chapter has been published under the above title in the European Polymer Journal, **2019**, *120*, 109237.

Authors: Timothy S. Anderson & Christopher M. Kozak.

The first author (Timothy S. Anderson) contributed to all aspects of the project including: experimental design and performance, literature review, data collection and analysis, manuscript preparation and the addressing of peer-reviewed comments.

The corresponding author (Christopher M. Kozak) is the principal investigator and provided the initial idea of the project. Dr. Kozak oversaw data analysis, experimental design and approach, manuscript preparation and submission, and co-author supervision.

Modifications have been made to further elaborate on the results presented.

2.1. Introduction

In the Kozak group, an amino-bis(phenolate) zinc catalyst was utilized for the ring-opening polymerization of *rac*-lactide for the synthesis of poly(ester)s.[1] The results of this work inspired me to apply this catalyst toward the ROP of epoxides and ROCOP of epoxides with CO_2. Here, the synthesis of poly(ether)s and poly(ether-*co*-carbonates) from epoxides and CO_2 using this amino-bis(phenolate) zinc complex (Scheme 2.1) with different co-catalysts will be discussed. The choice of co-catalyst influences the polymer molecular weight, degree of ether linkages, and polymer dispersity. Compound **2.1** contains an open-faced bimetallic core supported by an amino-bis(phenolate) ligand that should provide access to the coordination sites of the zinc centres.

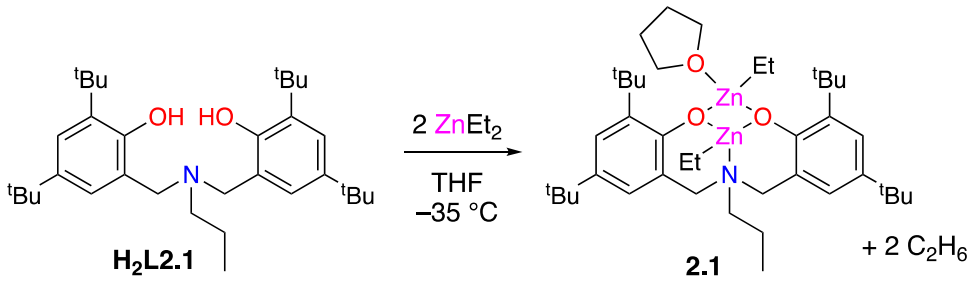

Scheme 2.1: Synthesis of **2.1**.

Copolymerization of epoxides and CO_2 to form poly(carbonate)s has been studied since Inoue's discovery of the reaction in 1969.[2] CO_2 presents a convenient, increasingly abundant, and renewable C1 feedstock for the production of several different compounds, including poly(carbonate)s as an alternative to the conventional use of bisphenol-A and

phosgene.[3-5] The physical properties of poly(carbonate)s rely heavily upon the choice of epoxide and degree of ether linkages in the polymers.[6] Several recent reports covering CO_2/epoxide copolymerization discuss the uses for these compounds in the industrial and commercial sectors.[3-9] Cyclohexene oxide (CHO) is commonly utilized for this reaction due to the resulting polymers exhibiting high glass transition temperatures (110 – 130 °C) and good tensile strength, as well as its availability as a waste product from the petroleum industry.[3,9-12] The mechanical properties and availability of poly(cyclohexene carbonate) has led to a growing number of reports on copolymerization of CO_2/epoxides over the past 15 years, with the most recent work examining renewable epoxides such as limonene oxide (LO).[12-15] More complex polymer syntheses involve the incorporation of other polymeric blocks into a single chain to form multi-block copolymers in one pot.[16-18] This can include segments of poly(carbonate) from different epoxides as well as poly(ether) segments from the ring-opening polymerization (homopolymerization) of the epoxides.[12,19]

Zinc catalysts for CO_2/epoxide copolymerization reactions are some of the most highly active and well-controlled homogeneous systems to date and they continue to be studied widely.[3,7-8,11,20] Aminophenolate ligands provide a flexible framework with highly tunable phenolate and amine environments and have demonstrated good activity toward CO_2/epoxide coupling reactions with several first row transition metals.[3,7,11,18,21-25] The Williams group reported an aminophenolate zinc species for poly(carbonate) synthesis where they employ a macrocyclic ligand giving a dinuclear catalyst achieving a turnover frequency (TOF) of 25 h^{-1} at 53% conversion and 94% selectivity for poly(carbonate) at 1 bar CO_2 and 100 °C. The activity was attributed to the presence of a bimetallic core contained within the

macrocyclic ligand framework.[11] Polymerization was believed to occur through a cooperative mechanism where the growing polymer chain shuttles between two zinc centres. Several of the more highly active systems demonstrate this behavior and thus the recent development of zinc-based catalysts in the literature has begun to focus primarily on multimetallic or multinuclear catalysts to take advantage of this cooperative effect.[17,26-29]

2.2. Complex synthesis

Compound **H_2L2.1** was synthesized according to literature procedure. [30]

Compound **2.1** was synthesized according to literature procedure (see Scheme 2.1) and purified by dissolving in pentane and filtering through a 2 cm plug of Celite and drying under vacuum.[31]

2.3. Discussion

Compound **2.1**, in the absence of co-catalyst or with two equiv of benzyl alcohol (one per zinc centre), ring-opens consecutive CHO monomers to form poly(cyclohexene oxide) (Scheme 2.2, path A). Reactions were performed from –20 to 100 °C and results are shown in Table 2.1. The solubility of the catalyst in CHO is low below 0 °C, therefore the resulting inhomogeneity of the reaction mixture hindered polymerization activity (entry 1). In the presence of a solvent, either toluene or dichloromethane at 20 °C, conversions were low (less than 30% over 3 h). Maximum conversions were achieved at 20 °C. The M_n in entries 5

and 7 agree approximately with the theoretical molecular weights (per zinc), suggesting polymerization is occurring at each metal centre and is initiated by a benzyl alkoxide generated via reaction between the ethyl zinc and the alcohol. Although it has been noted that removal of the second ethyl zinc bond via alcoholysis is challenging,[32-33] it has been observed by Coates and co-workers[29] and the formation of a larger aggregate of **2.1** via reaction with isopropyl alcohol was observed in the Kozak group.[1] Molecular weights increase with a decrease in temperature. This suggests that either the reaction of the benzyl alcohol with the zinc ethyl groups is temperature limited, or simply that more chain transfer events (either to free benzyl alcohol, adventitious water or cyclohexene diol, a known impurity in CHO[10,34]) occur at the higher temperatures (entries 2 – 6). As an *in situ*-formed metal alkoxide (or the phenolate ligand itself in the absence of added alcohol) is believed to be the initiator of epoxide ROP, the number of active growing chains depends on the number of active Zn–O sites. It may also be that the catalytic cycle follows an activated monomer mechanism. At 100 °C the conversion decreased considerably, which can be attributed to a shift in equilibrium toward dissociation of epoxide from the active species. This may result from increased prevalence of chain transfer by cyclohexane diol impurities, and thus chain termination, which is competing with polymer propagation (entry 6).[10] Representative GPC traces can be found in the appendix (Fig. A2.1 – A2.3). T_g values are within the range of 48 to 60 °C and increase with increasing molecular weights. T_g values for poly(cyclohexene oxide) of 68 – 69 °C for polymers with high molecular weights (76 – 500 kg mol^{-1}) have been reported.[35-36]

Turnover frequencies afforded by **2.1** are significantly lower than other reported homogeneous systems. Le Roux and coworkers reported ionic zinc species for the ROP of CHO in 5 mL toluene (0.1 mol% catalyst loading) at 30 °C and achieved TOF up to 60,000 h^{-1} with broad dispersities (2.9 – 5.7).[37] The aluminum aminophenolate-catalyzed ROP of CHO has been reported by Kerton and co-workers with catalyst loadings from 0.001 – 0.5 mol% per Al in neat CHO yielding narrowly disperse polymer ($Đ$ = 1.08 – 1.36) at 20 °C.[35] TOFs ranged from 60 – 3600 h^{-1} with the highest activity at 0.1 mol% Al. A bimetallic aluminum salen complex reported by Mazzeo and co-workers achieved TOFs of 28 – 5000 h^{-1} at 25 °C and 70 °C in neat CHO.[38] Activity was significantly higher at elevated temperatures and required 4 equiv of isopropyl alcohol per Al. A study comparing dinuclear and mononuclear aluminum aminophenolate complexes was reported by Yuan, Yao and co-workers in 2016.[39] It was found that dinuclear species were more active toward ROP of CHO at 30 °C in 0.3 mL hexanes with catalyst loadings between 0.01 – 0.1 mol% Al reaching a TOF of 702 h^{-1}.

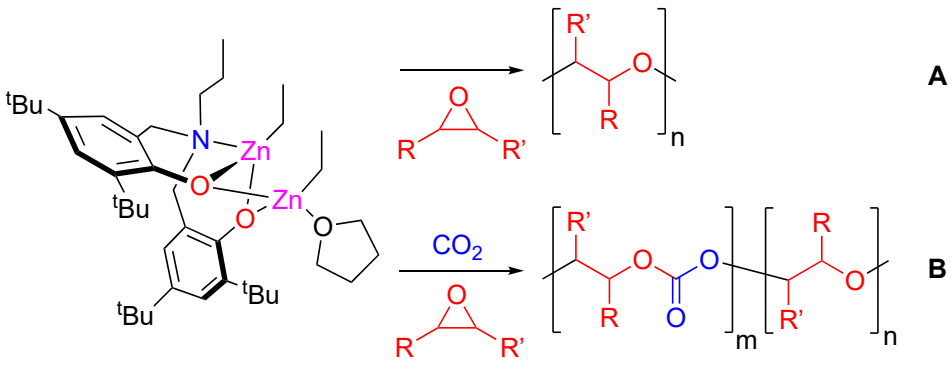

Scheme 2.2: ROP of epoxide (A) and epoxide/CO_2 ROCOP (B) catalyzed by **2.1**.

Table 2.1: Homopolymerization of CHO by **2.1** and BnOH.

Entry[a]	Temp. (°C)	Conv.[b]/ (Yield)[c] (%)	M_n (g mol^{-1}) [d]	$M_n^{th.}$ (g mol^{-1})[e]	$Đ$[d]	TOF (h^{-1})	T_g (°C) [f]
1	-20	0	-	-	-	-	-
2	0	40 (35)	19,000	3,900	1.5	40	57
3	20	65 (53)	17,800	6,400	1.9	65	60
4	40	65 (54)	11,500	6,400	1.9	65	50
5	80	63 (35)	7,400	6,200	1.9	63	50
6	100	45 (22)	8,200	4,400	1.9	45	48
7[g]	20	56 (37)	5,600	5,500	2.5	56	41

[a]Compound **2.1**, BnOH and CHO (1:2:200) stirred neat for 2 h. [b]Determined by ^{1}H NMR spectroscopy of crude reaction mixture. [c]Isolated yield. [d]Determined by triple detection GPC analysis of isolated material, dn/dc = 0.0960 mL g^{-1}. [e]Calculated M_n of poly(cyclohexene oxide) = 98.1 g mol^{-1} × ([CHO]/[BnOH]) × conversion of CHO. [f] Determined using differential scanning calorimetry. [g]Reaction opened to air for 5 min then resealed.

End-group analysis of shorter chain polymers was performed by ^{1}H NMR spectroscopy. These polymers were obtained by reducing the monomer-to-catalyst loading and monitored *in situ* by ^{1}H NMR spectroscopy. In reactions containing **2.1**:BnOH:CHO of 1:2:20, benzyl ether end groups could be observed in the ^{1}H NMR spectrum ($CDCl_3$) at δ 7.34 and 4.69 (Fig. A2.4). Furthermore, ethane was observed at δ 0.86, suggesting the BnOH protonated the Zn–Et moiety to release ethane and generate a zinc alkoxide, which then acts as the initiator for polymerization. Propylene oxide (PO), limonene oxide (LO), glycidol (GO), and epichlorohydrin (ECH) were also examined for homopolymerization but were completely inactive or provided very low conversions (0 – 20%) to poly(ether) (Table A2.1).

Epoxide/CO_2 ROCOP studies were performed at 60 °C and 40 bar with 0.5 mol% loading of **2.1** and 1.0 mol% of co-catalyst for 18 h. Using tetrabutylammonium bromide (Bu_4NBr) as the co-catalyst gave poor activity for polymerization resulting in 4% epoxide conversion. Using bis(triphenylphosphine)iminium chloride (PPNCl) as the co-catalyst resulted in 41% epoxide conversion with 96% selectivity toward carbonate linkages over ether linkages in the polymer. PPNCl is only sparingly soluble in CHO and the low concentration of chloride anions may slow the initiation process. Using BnOH as co-catalyst led to 77% epoxide conversion, but with 60% selectivity for carbonate linkages. The higher conversion and higher solubility of BnOH in CHO led me to use BnOH for reaction optimization. The produced poly(cyclohexene ether-*co*-carbonate) had a molecular weight of 107.9 kg mol^{-1} with a dispersity of 2.7 (Table 2.2, entry 1). Reducing the pressure to 20 bar resulted in little change to conversion and carbonate incorporation (entry 2). An explanation for this behavior will be discussed below. Increasing the temperature to 80 °C significantly increased carbonate content with little effect on conversion, but polymer molecular weights increased significantly (entry 3). The effect of pressure on the conversion, carbonate formation, and dispersity at 80 °C is shown in entries 4 – 7. Reactions under 1 bar of CO_2 produced poly(cyclohexene ether-*co*-carbonate) with 23% carbonate linkages and 40% conversion (entry 4) but with a much lower molecular weight than polymers obtained at higher CO_2 pressures and similar to the molecular weights of poly(ether)s described above. Interestingly, the conversion at 1 bar CO_2 is lower than that observed in the ROP reactions performed under N_2 (63%, Table 2.1, entry 5), suggesting the presence of CO_2 inhibits the ROP of CHO even at low CO_2 pressures. At 10 bar CO_2 both conversion of epoxide and CO_2 incorporation increased, as did overall polymer molecular weight (entry 5). Increasing

the pressure to 30 and 40 bar CO_2 had modest effect on conversion or carbonate incorporation. In all of these reactions, molecular weights are consistently higher than predicted for living polymerizations and dispersities are between 1.6 and 2.7. Increases or decreases in temperature at 20 bar greatly reduced the carbonate content (Table 2.3). Cyclic carbonate formation is negligible as shown by ^{1}H NMR spectroscopy and by monitoring the band at 1810 cm^{-1} via *in situ* IR spectroscopy (Fig. 2.1). The high degree of ether linkages present suggests that poly(ether) formation is not inhibited immediately upon pressurization with CO_2 (Fig. 2.1). Poly(ether) formation was found to occur initially but growth of the band at 1089 cm^{-1} halted after 20 min, whereas poly(carbonate) formation exhibited a comparatively more rapid onset of the band at 1750 cm^{-1} and continuous growth over 18 h.

Table 2.2: Effect of pressure and temperature on copolymerization of CO_2 and CHO catalyzed by **2.1** with BnOH.

Entry[a]	*P* (bar)	*T* (°C)	Conv. / (CO_3)[b] (%)	M_n[c] (g mol^{-1})	*Đ*[c]	TOF (h^{-1})	T_g[d] (°C)
1	40	60	77 (40)	107,900	2.7	9	-
2	20	60	68 (44)	275,300	1.8	8	-
3	20	80	72 (66)	352,500	1.6	8	90
4	1	80	40 (23)	12,100	1.8	4	64
5	10	80	67 (64)	287,800	1.6	7	108
6	30	80	72 (68)	304,000	1.6	8	100
7	40	80	77 (71)	307,700	1.8	9	106

[a]Reactions performed for 18 h in neat CHO under catalyst loading ratio **2.1**:BnOH:CHO of 1:2:200. [b]Determined via ^{1}H NMR spectroscopy of an aliquot from the crude reaction mixture. Cyclic carbonate observed at <1% in all cases. [c]Determined via triple detection GPC analysis of isolated material, dn/dc = 0.0701 mL g^{-1}. [d]Determined using differential scanning calorimetry.

Table 2.3: Effect of temperature on poly(ether-*co*-carbonate) formation at 20 bar CO_2.

Entry[a]	Temp. (°C)	Conv. (%)[b]	Carbonate link. (%)[b]	M_n[c] (g mol^{-1})	$Đ$[c]	TOF (h^{-1})
1	40	45	23	8,600	2.2	5
2	60	68	44	186,000	2.3	8
3	80	72	66	352,500	1.6	8
4	100	65	53	147,000	1.7	7

[a]Reactions performed for 18 h. **2.1**:BnOH:CHO (1:2:200). [b]Determined via ^{1}H NMR of aliquot from crude reaction mixture ($CDCl_3$). Cyclic carbonate observed at <1% in all cases. [c]Determined via GPC analysis of purified product.

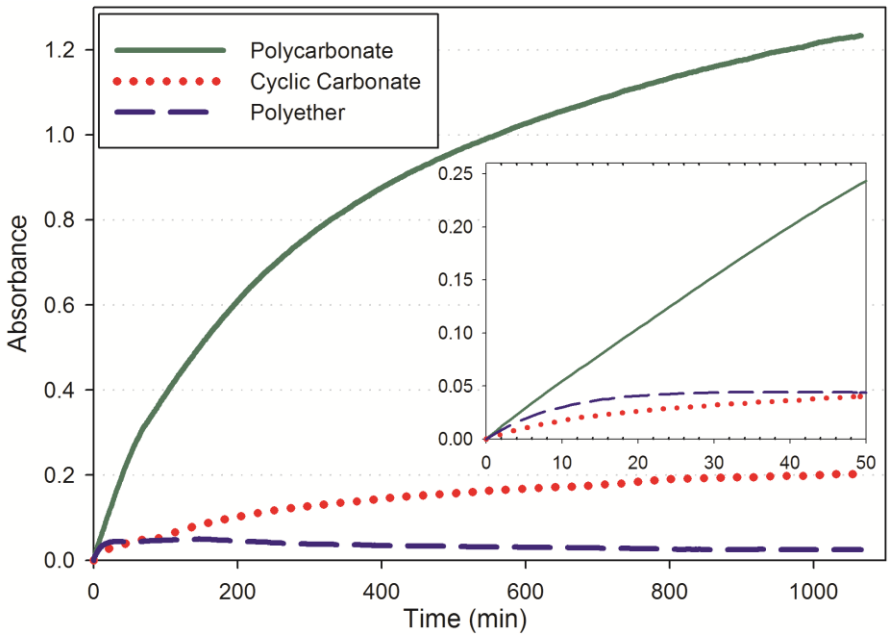

Fig. 2.1: IR absorbance vs. time profiles for polymerization described in Table 2, entry 7 (poly(carbonate) band at 1750 cm^{-1}, poly(ether) band at 1089 cm^{-1}, cyclic carbonate band at 1810 cm^{-1}). Reaction temperature is 80 °C at time = 0 min. Inset: The first 50 min of the reaction showing the inhibition of poly(ether) formation after 20 min.

The rate of poly(carbonate) formation at different pressures was examined by monitoring the growth of the band at 1750 cm^{-1} corresponding to poly(carbonate) (Fig. 2.2). A pressure of 20 bar CO_2 was optimal for the initial rate of poly(carbonate) formation. Interestingly, the reaction at 1 bar had a faster initial rate than at 30 bar, while reactions at 40 bar were the slowest. In 2011, Williams reported the formation of poly(cyclohexene carbonate) at 1 bar using a dinuclear zinc catalyst supported by a macrocyclic amino-phenolate ligand. The activation energy (E_a) was determined to be 96.8 kJ mol^{-1}.[10] A follow up study on the same catalyst determined that the lowest energy step involved in copolymerization was that of CO_2 insertion into a zinc-alkoxide bond at 47.7 kJ mol^{-1}.[16] Another study by Rieger on a tethered *ß*-diiminate dinuclear zinc catalyst examined the energy barriers of several steps in CHO/CO_2 copolymerization at 5 bar and 50 bar.[20] Experimentally, reaction order with respect to CO_2 concentration changes from first order to zero order at 25 bar. Correspondingly, the reaction order with respect to CHO concentration changed from zero order to first order. This demonstrates that at higher pressures, epoxide ring opening becomes the rate determining step, while at lower pressures CO_2 insertion is rate-limiting. As the Rieger and Williams systems are also dinuclear zinc compounds, I believe that this system may behave in a similar fashion to them, but that in the initial stages of the reaction, the ROP and ROCOP processes compete with one another until ROP is halted as the solution becomes saturated with the introduced CO_2. The slight decrease in the initial rate from 30 to 40 bar CO_2 may be attributed to CHO volume expansion as the reaction mixture absorbs CO_2, reducing the effective catalyst loading.[40] Alternatively, this could result from the effect of diffusion limitation at low CO_2 pressure. CO_2 dissolution rates

have been identified by Williams, Shaffer and co-workers to be influential on the overall kinetics of CO_2 insertion reactions.[41]

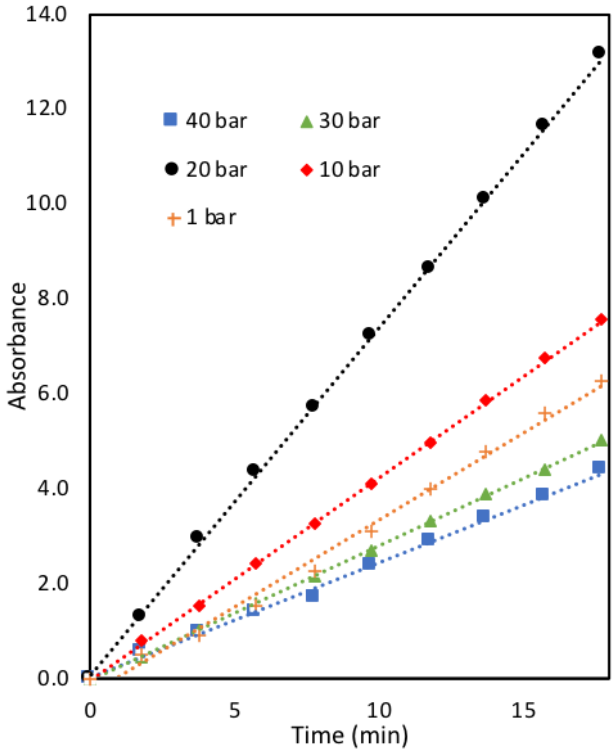

Fig. 2.2: Plots of absorbance (poly(carbonate), 1750 cm^{-1}) vs. time at pressures from 1 to 40 bar for initial 18 min of reaction. Reaction conditions: **2.1**:BnOH:CHO (1:2:200), 80 °C.

The effect of co-catalyst loading on the overall conversion for CO_2 and CHO copolymerization was examined. 1, 2, 4, and 10 equiv of BnOH with respect to **2.1** were used at 80 °C and 20 bar CO_2 (Table 2.4). A maximum conversion of 72% was achieved with 2 equiv BnOH (entry 2), which was similar to the reaction with 1 equiv (entry 1). Increasing the BnOH to 4 equiv reduced the overall conversion to 18% with 61% carbonate linkages (entry 3), while 10 equiv of BnOH appeared to deactivate the catalyst (entry 4).

Table 2.4: ROCOP of CHO/CO_2 by **2.1** with different loading of BnOH co-catalyst.

Entry[a]	Equiv BnOH	Conv. / (CO_3)[b] (%)
1	1	68 (72)
2	2	72 (66)
3	4	18 (61)
4	10	0

[a]Reactions performed for 18 h at 80 °C and 20 bar CO_2. **2.1**:CHO (1:200). [b]Determined via ^{1}H NMR of aliquot from crude reaction mixture ($CDCl_3$)

A catalyst loading of 1.0 mol% of **2.1** with 2.0 mol% BnOH at 20 bar and 80 °C gave a conversion of 75% with 67% carbonate linkages for CHO/CO_2 copolymerization, which was similar to the 72% conversion and 66% carbonate linkages obtained when using 0.5 mol% loading of **2.1** and 1.0 mol% BnOH (Table 2.2, entry 3). Reducing the catalyst loading to 0.2 mol% of **2.1** with 0.4 mol% BnOH showed a conversion of 47% with 79% selectivity for carbonate linkages. Decreasing the catalyst loading further resulted in no activity toward ROP or ROCOP. Based on these results, the ideal conditions for this system appear to be 1.0 mol% zinc complex, 2.0 mol% benzyl alcohol cocatalyst, 20 bar CO_2 and 80 °C over 18h.

Using PO as the epoxide at 40 bar and 60 °C (0.5 mol% loading of **2.1**, 1.0 mol% BnOH) showed a conversion of 19% to cyclic carbonate by ^{1}H NMR spectroscopy (Fig. A2.5). A 1:1 mixture of CHO:PO at 40 bar and 60 °C resulted in a conversion of 13% to poly(cyclohexene carbonate) with <5% to poly(propylene carbonate) as determined via ^{1}H NMR spectroscopy (Fig. A2.6). Conversions of 3% for cyclic propylene carbonate and *cis*-cyclohexene carbonate were also observed, as well as 9% conversion to poly(ether), which consisted of a 9:1 ratio of poly(cyclohexene oxide) to poly(propylene oxide). Limonene oxide

on its own was inactive toward coupling with CO_2 at 40 bar and 80 °C. It could, however, be incorporated as a co-monomer with CHO. At 80 °C and 20 bar CO_2 a 1:1 mixture of LO:CHO gave a conversion of 55% producing a polymer with a composition of 87% poly(cyclohexene carbonate) to 13% poly(limonene carbonate) linkages (Fig. A2.7). The resulting polymer possessed a molecular weight of 66,700 g mol^{-1} with a high dispersity of 3.7. The high molecular weight could correspond to catalyst deactivation from a hydroxyl-containing impurity present in the LO, reducing the effective catalyst loading.[42] Total carbonate content was 90%, which suggests the presence of LO inhibits the formation of ether linkages that are more abundant for ROCOP of CHO and CO_2 alone. The IR absorbance vs time profile monitoring the formation of different reaction products is shown in Fig. 2.3. The frequencies of the carbonyls corresponding to poly(limonene carbonate) (PLC, 1743 cm^{-1}) and PCHC (1750 cm^{-1}) overlap in the infrared spectrum, therefore resolving their individual growth over time was impossible. The rate of poly(carbonate) formation increases as the band corresponding to LO begins to decrease (1646 cm^{-1}). As no poly(limonene oxide) formation was observed, the decrease in the LO band was monitored and showed a 2 h induction period for LO ROCOP relative to PCHC formation. The resulting polymer had two observable T_g values of –20 and 132 °C (Fig. A2.9), the former is lower than typical values for PCHC or PLC (115 & 130 °C respectively)[43] while the latter is higher for that obtained for each of the pure polymers.[9,42] I attribute the T_g at -20 °C to the presence of hydroxyl containing impurity from the starting material (i.e. cyclohexene diol) acting as a plasticizer to increase the flexibility of the polymer.[44] The higher T_g of 132 °C is typically associated with a cross-linking on the poly(carbonate)[45] or reaction of the terminal alkene of the limonene units.[46] I also considered the possibility of cross-linking during

polymerization and examined the Mark-Houwink-Sakurada plot *via* GPC analysis to determine the linearity of the polymer (Fig. A2.10). The reported value for $a = 0.7$ suggests the sample is relatively linear with moderate packing, thus it can be interpreted that there are no side reactions taking place.[47] MALDI-TOF MS data were collected for this sample where poly(carbonate) and poly(ether) segments of each monomer could be identified (Fig. A2.12). The presence of the different co-monomers can be confirmed, but clearly identifying the end groups in these polymers is complicated by the multiple co-monomers along with carbonate and ether linkages. Since benzyl end groups were confirmed by ^{1}H NMR analysis of poly(ether)s as discussed above, it is likely that they are present in the poly(carbonate)s as well. Diffusion ordered spectroscopy (DOSY) showed diffusivity values for polymers within 1 order of magnitude (–5.05 to –4.95 log(cm^2 s^{-1})) suggesting a single polymer species present in solution and that there is a single polymerization process occurring (Fig. 2.4). Unreacted CHO and LO, $CDCl_3$ and TMS were also observed. Though the molecular weight distribution is broad ($Đ = 3.7$), the majority of the material is low molecular weight (Fig. A2.11), likely a result of chain termination from the aforementioned hydroxide containing impurity, as well as 1,2-cyclohexane diol present in trace quantities in CHO,[10] or trace water content.[48] This one pot synthesis of a CHO/LO copolymer differs from that reported by Schmalz, Greiner and co-workers, where the epoxide monomers were added sequentially to the reaction mixture to form true block copolymers.[12]

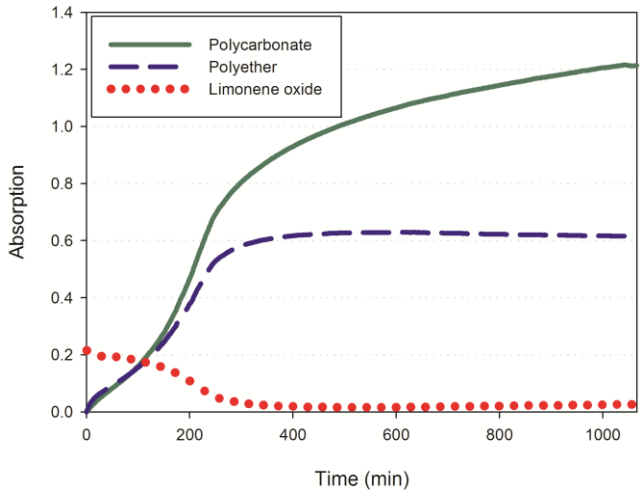

Fig. 2.3: IR absorbance vs. time for the copolymerization of CHO and LO with CO_2. The band for PCHC (1750 cm^{-1}) overlaps with the band corresponding to PLC (1743 cm^{-1}) but the rate of poly(carbonate) formation decreases once LO consumption (band at 1646 cm^{-1}) is complete.

Fig. 2.4: DOSY spectrum for LO/CHO copolymer. Polymer –5.05 to –4.95 log(cm^2 s^{-1}), $CDCl_3$ –4.56 log(cm^2 s^{-1}), CHO –4.66 log(cm^2 s^{-1}). (500 MHz, $CDCl_3$, 298K)

Due to the rapid formation of poly(cyclohexene oxide) and the inhibition of poly(ether) formation after pressurization of the reactor with CO_2 as shown by IR spectroscopy, I envisioned that block or gradient copolymers poly(cyclohexene ether-*co*-carbonate) could be synthesized by allowing homopolymerization to occur for several minutes prior to pressurization with CO_2. Rieger demonstrated that *β*-butyrolactone enchainment could be inhibited by high pressures (40 bar) of CO_2.[17] Thus, I set out to replicate this effect with poly(ether) and poly(carbonate) blocks. At 60 °C and 40 bar CO_2, two reactions were performed for 18 h. In the first instance, the reaction mixture was stirred

at 60 °C for 10 min prior to pressurization with CO_2 leading to an epoxide conversion of 65%. A second reaction was performed where the mixture was stirred for 30 min prior to pressurization, resulting in a lower total conversion of 47%. Molecular weights were similar in both products (19,000 g mol^{-1}) but the dispersity was approximately three times greater when 10 min of homopolymerization was allowed ($Đ$ = 3.1 compared to 9.1). This suggests that the homopolymerization of CHO is more controlled than poly(carbonate) formation, and that poly(ether) formation reduces overall conversions, likely due to an increase in viscosity. The Mark-Houwink-Sakurada plots for the homopolymers in Table 2.1 suggest significant packing of a randomly coiled polymer (a = 0.60 – 0.65) supporting increased viscosity. DOSY was performed on the crude material with 30 min of homopolymerization time and shows the presence of two distinct polymer compositions — one corresponding to poly(carbonate) and the other to poly(ether) suggesting that there are two polymerization processes occurring (Fig. 2.5) — and that poly(carbonate) formation is not initiated from poly(ether) chain ends. Unfortunately, homopolymerization occurs rapidly, and fine control over the two processes could not be achieved with this system. However, due to the inhibition of poly(ether) formation after CO_2 is introduced into the reaction mixtures, I propose that the interaction between zinc centres and CO_2 is controlling the kinetics of the reaction due to a more favourable interaction between zinc and CO_2 than between zinc and epoxide. Glass transition temperatures of the poly(cyclohexene ether-*co*-carbonate)s are similar to previously reported values (100 – 130 °C)[14-15] and the decrease is likely due to the prevalence of ether linkages.[3] TGA shows only one significant mass loss (Fig. 2.6).

Fig. 2.5: DOSY spectrum of poly(cyclohexene oxide) and poly(cyclohexene carbonate) synthesized via 30 min of homopolymerization prior to CO_2 pressurization (40 bar), showing two or more distinct polymer products. Poly(cyclohexene oxide) –5.99 log(cm^2 s^{-1}), poly(cyclohexene carbonate) –6.49 log(cm^2 s^{-1}), $CDCl_3$, CHO & CH_2Cl_2 –4.66 log(cm^2 s^{-1}). (500 MHz, $CDCl_3$, 298K)

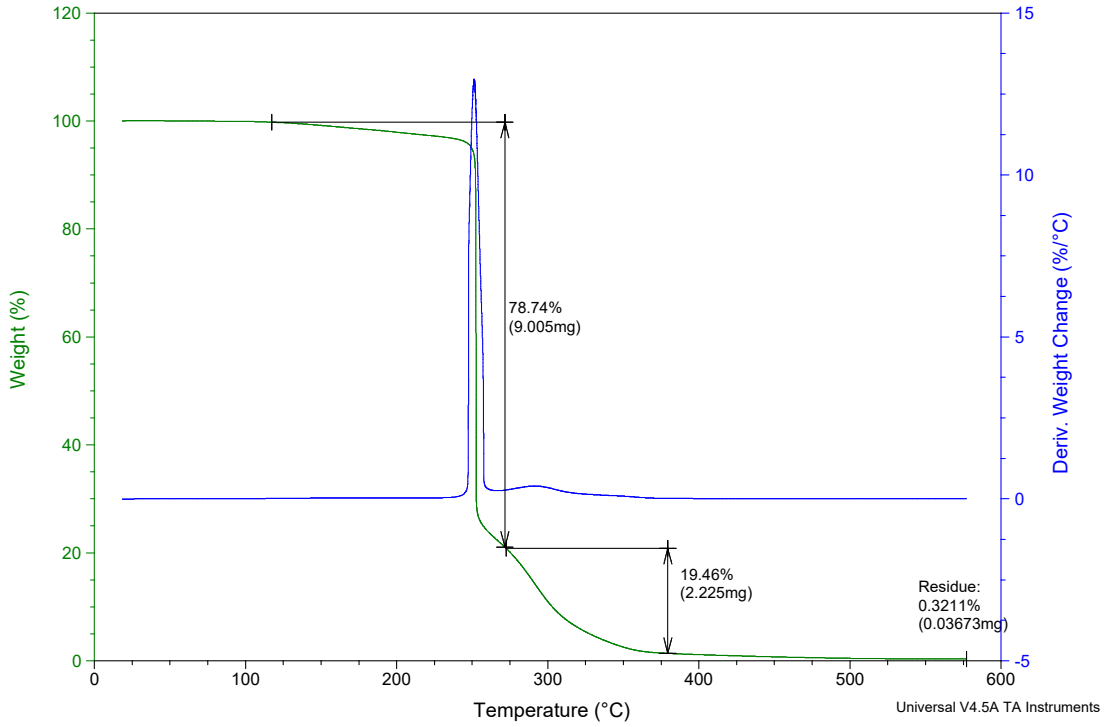

Fig. 2.6: Thermogravimetric analysis of purified CHO poly(ether-*co*-carbonate) from the reaction described in

Table **2.2**, entry 3.

2.4. General methods

All reagents were purchased from Sigma-Aldrich, Alfa-Aesar, or Caledon. All epoxides were distilled under reduced pressure. Unless otherwise stated, all reactions were performed under inert atmosphere. ^{1}H NMR spectra were recorded at 300 on a Bruker Avance III spectrometer with BBO probe and ^{13}C at 75.0 MHz on a Bruker Avance I spectrometer with TCI inverse gradient probe. *In situ* FTIR monitoring was performed using a 100 mL Parr Instruments 4560 stainless steel mini reactor vessel with motorized mechanical stirrer and a heating mantle. The vessel was modified with a bottom-mounted Mettler Toledo SiComp Sentinel ATR sensor, which was connected to a ReactIR 15 base unit through a silver-halide Fiber-to-Sentinel conduit. Profiles of the absorbance height at 1089 cm^{-1}, 1646 cm^{-1}, 1750 cm^{-1} and 1810 cm^{-1} were measured every 60 – 120 s. Similar methods for reaction monitoring via *in situ* IR have been reported elsewhere.[23,49-50] Molecular weight determination of polymer was performed by gel permeation chromatography on an Agilent Infinity HPLC instrument connected to a Wyatt Technologies triple detector system (light scattering, viscometry, and refractive index) equipped with Phenogel 10^3 Å and 10^4 Å 300 × 4.60 mm columns (covering mass ranges of 1,000 – 75,000 and 5,000 – 500,000 g mol^{-1}, respectively) with THF as eluent. Polymer samples were prepared in THF at a concentration of 4 mg mL^{-1} and filtered through 0.2 μm syringe filters. The sample solution was then eluted at a flow rate of 0.30 mL·min^{-1}. The values of dn/dc were calculated online (columns detached) assuming 100% mass recovery using the Astra 6 software package

(Wyatt Technologies), for PCHO dn/dc = 0.0960 mL g^{-1} and for PCHC dn/dc = 0.0701 mL g^{-1}. MALDI-TOF mass spectrometry was conducted at Bruker Daltonics (Billerica, MA, USA) on an UltrafleXtreme MALDI−TOF/TOF MS running in reflectron mode. Polymers were mixed in a 4:1(matrix:polymer) ratio in THF with 2,5-dihydroxybenzoic acid as the matrix with sodium trifluoroacetate as cationizing agent.

2.5. Polymerization methods

Homopolymerization: CHO and BnOH stock solution (1.00 g, 10.2 mmol CHO, 0.102 mmol BnOH) added to **2.1** (38.5 mg, 0.051 mmol) in a 20 mL scintillation vial and stirred under N_2 for 2 h, heating if necessary. An aliquot for ^{1}H and ^{13}C NMR spectroscopy was taken for the determination of conversion. The remaining material was extracted into dichloromethane and precipitated using cold acidified methanol. The solvent was decanted and the product dried at 60 °C in a vacuum oven overnight.

Copolymerization: CHO (3.00 g, 30.6 mmol) and BnOH (33.1 mg, 0.306 mmol) were combined and added to **2.1** (115.4 mg, 1.53×10^{-4} mol) and mixed until homogeneous. The mixture was added via syringe to a 100 mL stainless steel Parr autoclave at 25 °C, which was pre-dried by heating to 100 °C under vacuum overnight. The autoclave was heated to 80 °C, then charged with 20 bar of CO_2 and stirred. After 18 h, the autoclave was cooled to room temperature and vented in a fumehood. An aliquot for ^{1}H and ^{13}C NMR spectroscopy was taken immediately after opening for the determination of conversion. The copolymer was

extracted into dichloromethane and precipitated using cold acidified methanol. The solvent was decanted and the product dried at 60 °C in a vacuum oven overnight.

2.6. Conclusions

An amino-phenolate zinc complex **2.1** with BnOH was able to catalyze the synthesis of poly(ether) and poly(ether-*co*-carbonate) from CHO over a wide range of pressures and temperatures including 1 bar CO_2 with a moderate TOF of 4.4 h^{-1}. The carbonate content of this polymer is low (23%), but I believe that altering the ligand design to favour poly(carbonate) formation at lower pressures would lead to improvement in both TON and carbonate content. Increases in Lewis acidity at the metal typically results in increased carbonate content, therefore introducing electron withdrawing groups in place of one or more of the Ar-^{t}Bu groups of **H_2L2.1** may accomplish this goal. Similarly, rather than altering the ligand design, replacing one zinc centre with a highly electron deficient metal (i.e. lanthanide metal) is concurrent with recent trends in CO_2 and epoxide copolymerization catalysts that incorporate other metals into dinuclear systems and is worthy of study. Moderately disperse poly(ether-*co*-carbonates) of CHO could be synthesized with varied carbonate content by delaying CO_2 pressurization. Poly(ether-*co*-carbonates) containing multiple epoxides were also synthesized when CHO was mixed with either PO or LO, the latter providing much higher conversion and incorporation of epoxide. Studies considering LO are ongoing.

2.7. References

1. Liu, Y.; Dawe, L. N.; Kozak, C. M., Bimetallic and trimetallic zinc amino-bis(phenolate) complexes for ring-opening polymerization of rac-lactide. *Dalton Trans.* **2019**, *48*, pp 13699-13710.

2. Inoue, S.; Koinuma, H.; Tsuruta, T., Copolymerization of carbon dioxide and epoxide. *J. Polym. Sci. B.* **1969**, *7*, pp 287-292.

3. Kozak, C. M.; Ambrose, K.; Anderson, T. S., Copolymerization of carbon dioxide and epoxides by metal coordination complexes. *Coord. Chem. Rev.* **2018**, *376*, pp 565-587.

4. Liu, Q.; Wu, L.; Jackstell, R.; Beller, M., Using carbon dioxide as a building block in organic synthesis. *Nat. Commun.* **2015**, *6*, p 5933.

5. North, M.; Pasquale, R.; Young, C., Synthesis of cyclic carbonates from epoxides and CO_2. *Green Chem.* **2010**, *12*, pp 1514-1539.

6. Paul, S.; Zhu, Y.; Romain, C.; Brooks, R.; Saini, P. K.; Williams, C. K., Ring-opening copolymerization (ROCOP): synthesis and properties of polyesters and polycarbonates. *Chem. Commun.* **2015**, *51*, pp 6459-79.

7. Poland, S. J.; Darensbourg, D. J., A quest for polycarbonates provided via sustainable epoxide/CO_2 copolymerization processes. *Green Chem.* **2017**, *19*, pp 4990-5011.

8. Coates, G. W.; Moore, D. R., Discrete metal-based catalysts for the copolymerization of CO_2 and epoxides: discovery, reactivity, optimization, and mechanism. *Angew. Chem. Int. Ed.* **2004**, *43*, pp 6618-39.

9. Wang, Y. Y.; Darensbourg, D. J., Carbon dioxide-based functional polycarbonates: Metal catalyzed copolymerization of CO_2 and epoxides. *Coord. Chem. Rev.* **2018**, *372*, pp 85-100.

10. Jutz, F.; Buchard, A.; Kember, M. R.; Fredriksen, S. B.; Williams, C. K., Mechanistic investigation and reaction kinetics of the low-pressure copolymerization of cyclohexene oxide and carbon dioxide catalyzed by a dizinc complex. *J. Am. Chem. Soc.* **2011**, *133*, pp 17395-405.

11. Kember, M. R.; Knight, P. D.; Reung, P. T.; Williams, C. K., Highly active dizinc catalyst for the copolymerization of carbon dioxide and cyclohexene oxide at one atmosphere pressure. *Angew. Chem. Int. Ed.* **2009**, *48*, pp 931-3.

12. Bailer, J.; Feth, S.; Bretschneider, F.; Rosenfeldt, S.; Drechsler, M.; Abetz, V.; Schmalz, H.; Greiner, A., Synthesis and self-assembly of biobased poly(limonene carbonate)-block-poly(cyclohexene carbonate) diblock copolymers prepared by sequential ring-opening copolymerization. *Green Chem.* **2019**, *21*, pp 2266-2272.

13. Parrino, F.; Fidalgo, A.; Palmisano, L.; Ilharco, L. M.; Pagliaro, M.; Ciriminna, R., Polymers of limonene oxide and carbon dioxide: polycarbonates of the solar economy. *ACS Omega* **2018**, *3*, pp 4884-4890.

14. Zhu, Y.; Romain, C.; Williams, C. K., Sustainable polymers from renewable resources. *Nature* **2016**, *540*, pp 354-362.

15. Hauenstein, O.; Agarwal, S.; Greiner, A., Bio-based polycarbonate as synthetic toolbox. *Nat. Commun.* **2016**, *7*, p 11862.

16. Romain, C.; Zhu, Y.; Dingwall, P.; Paul, S.; Rzepa, H. S.; Buchard, A.; Williams, C. K., Chemoselective polymerizations from mixtures of epoxide, lactone, anhydride, and carbon dioxide. *J. Am. Chem. Soc.* **2016**, *138*, pp 4120-31.

17. Kernbichl, S.; Reiter, M.; Adams, F.; Vagin, S.; Rieger, B., CO_2-controlled one-pot synthesis of AB, ABA block, and statistical terpolymers from beta-butyrolactone, epoxides, and CO_2. *J. Am. Chem. Soc.* **2017**, *139*, pp 6787-6790.

18. Martín, C.; Kleij, A. W., Terpolymers derived from limonene oxide and carbon dioxide: access to cross-linked polycarbonates with improved thermal properties. *Macromolecules* **2016**, *49*, pp 6285-6295.

19. Childers, M. I.; Longo, J. M.; Van Zee, N. J.; LaPointe, A. M.; Coates, G. W., Stereoselective epoxide polymerization and copolymerization. *Chem. Rev.* **2014**, *114*, pp 8129-52.

20. Lehenmeier, M. W.; Kissling, S.; Altenbuchner, P. T.; Bruckmeier, C.; Deglmann, P.; Brym, A. K.; Rieger, B., Flexibly tethered dinuclear zinc complexes: a solution to the entropy problem in CO_2/epoxide copolymerization catalysis? *Angew. Chem. Int. Ed.* **2013**, *52*, pp 9821-9826.

21. Ambrose, K.; Robertson, K. N.; Kozak, C. M., Cobalt amino-bis(phenolate) complexes for coupling and copolymerization of epoxides with carbon dioxide. *Dalton Trans.* **2019**, *48*, pp 6248-6260.

22. Andrea, K. A.; Brown, T. R.; Murphy, J. N.; Jagota, D.; McKearney, D.; Kozak, C. M.; Kerton, F. M., Characterization of oxo-bridged iron amino-bis(phenolate) complexes formed intentionally or in situ: mechanistic insight into epoxide deoxygenation during the coupling of CO_2 and epoxides. *Inorg. Chem.* **2018**, *57*, pp 13494-13504.

23. Ni, K.; Paniez-Grave, V.; Kozak, C. M., Effect of azide and chloride binding to diamino-bis(phenolate) chromium complexes on CO_2/cyclohexene oxide copolymerization. *Organometallics* **2018**, *37*, pp 2507-2518.

24. Wichmann, O.; Sillanpää, R.; Lehtonen, A., Structural properties and applications of multidentate [O,N,O,X'] aminobisphenolate metal complexes. *Coord. Chem. Rev.* **2012**, *256*, pp 371-392.

25. Ren, W.-M.; Zhang, X.; Liu, Y.; Li, J.-F.; Wang, H.; Lu, X.-B., Highly active, bifunctional Co(III)-salen catalyst for alternating copolymerization of CO_2 with cyclohexene oxide and terpolymerization with aliphatic epoxides. *Macromolecules* **2010**, *43*, pp 1396-1402.

26. Trott, G.; Saini, P. K.; Williams, C. K., Catalysts for CO_2/epoxide ring-opening copolymerization. *Philos. Trans. Royal Soc. A* **2016**, *374*.

27. Trott, G.; Garden, J. A.; Williams, C. K., Heterodinuclear zinc and magnesium catalysts for epoxide/CO_2 ring opening copolymerizations. *Chem. Sci.* **2019**, *10*, pp 4618-4627.

28. Reiter, M.; Vagin, S.; Kronast, A.; Jandl, C.; Rieger, B., A Lewis acid beta-diiminato-zinc-complex as all-rounder for co- and terpolymerisation of various epoxides with carbon dioxide. *Chem. Sci.* **2017**, *8*, pp 1876-1882.

29. Cheng, M.; Moore, D. R.; Reczek, J. J.; Chamberlain, B. M.; Lobkovsky, E. B.; Coates, G. W., Single-Site Beta-Diiminate Zinc Catalysts for the Alternating Copolymerization of CO_2 and Epoxides: Catalyst Synthesis and Unprecedented Polymerization Activity. *J. Am. Chem. Soc.* **2001**, *123*, pp 8738-8749.

30. Qian, X.; Dawe, L. N.; Kozak, C. M., Catalytic alkylation of aryl Grignard reagents by iron(III) amine-bis(phenolate) complexes. *Dalton Trans.* **2011**, *40*, pp 933-43.

31. Liu, Y.; Dawe, L. N.; Kozak, C. K., Bimetallic and trimetallic zinc amine-bis(phenolato) complexes for ring-opening polymerization of rac-lactide. *Dalton Trans.* **2019**, *Accepted, in press.*

32. Daneshmand, P.; Michalsky, I.; Aguiar, P. M.; Schaper, F., Configurationally flexible zinc complexes as catalysts for rac-lactide polymerisation. *Dalton Trans.* **2018**, *47*, pp 16279-16291.

33. Drouin, F.; Oguadinma, P. O.; Whitehorne, T. J. J.; Prud'homme, R. E.; Schaper, F., Lactide Polymerization with Chiral β-Diketiminate Zinc Complexes. *Organometallics* **2010**, *29*, pp 2139-2147.

34. Williams, C. K.; Breyfogle, L. E.; Choi, S. K.; Nam, W.; Young, V. G., Jr.; Hillmyer, M. A.; Tolman, W. B., A highly active zinc catalyst for the controlled polymerization of lactide. *J. Am. Chem. Soc.* **2003**, *125*, pp 11350-9.

35. Plommer, H.; Reim, I.; Kerton, F. M., Ring-opening polymerization of cyclohexene oxide using aluminum amine-phenolate complexes. *Dalton Trans.* **2015**, *44*, pp 12098-102.

36. Ambrose, K.; Murphy, J. N.; Kozak, C. M., Chromium diamino-bis(phenolate) complexes as catalysts for the ring-opening copolymerization of cyclohexene oxide and carbon dioxide. *Inorg. Chem.* **2020**, *59*, pp 15375-15383.

37. Merle, N.; Tornroos, K. W.; Jensen, V. R.; Le Roux, E., Influence of multidentate N-donor ligands on highly electrophilic zinc initiator for the ring-opening polymerization of epoxides. *J. Organomet. Chem.* **2011**, *696*, pp 1691-1697.

38. Isnard, F.; Lamberti, M.; Lettieri, L.; D'Auria, I.; Press, K.; Troiano, R.; Mazzeo, M., Bimetallic salen aluminum complexes: cooperation between reactive centers in the ring-opening polymerization of lactides and epoxides. *Dalton Trans.* **2016**, *45*, pp 16001-16010.

39. Li, W.; Ouyang, H.; Chen, L.; Yuan, D.; Zhang, Y.; Yao, Y., A comparative study on dinuclear and mononuclear aluminum methyl complexes bearing piperidyl-phenolato ligands in ROP of epoxides. *Inorg. Chem.* **2016**, *55*, pp 6520-4.

40. Jessop, P. G.; Subramaniam, B., Gas-expanded liquids. *Chem. Rev.* **2007**, *107*, pp 2666-94.

41. Brown, N. J.; Harris, J. E.; Yin, X.; Silverwood, I.; White, A. J.; Kazarian, S. G.; Hellgardt, K.; Shaffer, M. S.; Williams, C. K., Mononuclear Phenolate Diamine Zinc Hydride Complexes and Their Reactions With CO_2. *Organometallics* **2014**, *33*, pp 1112-1119.

42. Hauenstein, O.; Reiter, M.; Agarwal, S.; Rieger, B.; Greiner, A., Bio-based polycarbonate from limonene oxide and CO_2 with high molecular weight, excellent thermal resistance, hardness and transparency. *Green Chem.* **2016**, *18*, pp 760-770.

43. Li, H.; Luo, H.; Zhao, J.; Zhang, G., Well-defined and structurally diverse aromatic alternating polyesters synthesized by simple phosphazene catalysis. *Macromolecules* **2018**, *51*, pp 2247-2257.

44. Rahman, M.; Brazel, C. S., The plasticizer market: an assessment of traditional plasticizers and research trends to meet new challenges. *Prog. Polym. Sci.* **2004**, *29*, pp 1223-1248.

45. Martin, C.; Kleij, A. W., Terpolymers Derived from Limonene Oxide and Carbon Dioxide: Access to Cross-Linked Polycarbonates with Improved Thermal Properties. *Macromolecules* **2016**, *49*, pp 6285-6295.

46. Kindermann, N.; Cristofol, A.; Kleij, A. W., Access to Biorenewable Polycarbonates with Unusual Glass Transition Temperature (Tg) Modulation. *ACS Catal.* **2017**, *7*, pp 3860-3863.

47. Pavlov, G.; Frenkel, S., Sedimentation parameter of linear polymers. In *Progress in Colloid & Polymer Science: Analytical Ultracentrifugation*, Behlke, J., Ed. Steinkopff: 1995; Vol. 99, pp 101-108.

48. Wu, G. P.; Darensbourg, D. J., Mechanistic Insights into Water-Mediated Tandem Catalysis of Metal-Coordination CO_2/Epoxide Copolymerization and Organocatalytic Ring-Opening Polymerization: One-Pot, Two Steps, and Three Catalysis Cycles for Triblock Copolymers Synthesis. *Macromolecules* **2016**, *49*, pp 807-814.

49. Andrea, K. A.; Kerton, F. M., Triarylborane-catalyzed formation of cyclic organic carbonates and polycarbonates. *ACS Catal.* **2019**, *9*, pp 1799-1809.

50. Darensbourg, D. J.; Yarbrough, J. C.; Ortiz, C.; Fang, C. C., Comparative kinetic studies of the copolymerization of cyclohexene oxide and propylene oxide with carbon dioxide in the presence of chromium salen derivatives. In situ FTIR measurements of copolymer vs cyclic carbonate production. *J. Am. Chem. Soc.* **2003**, *125*, pp 7586-7591.

2.8. Appendix

Table A2.1: ROP of epoxides catalyzed by **2.1** with BnOH (2 equiv). All reactions performed at 20 °C for 2 h.

Epoxide	Propylene oxide	Limonene oxide	Glycidol	Epichlorohydrin
Conversion (%)	0	0	0	20

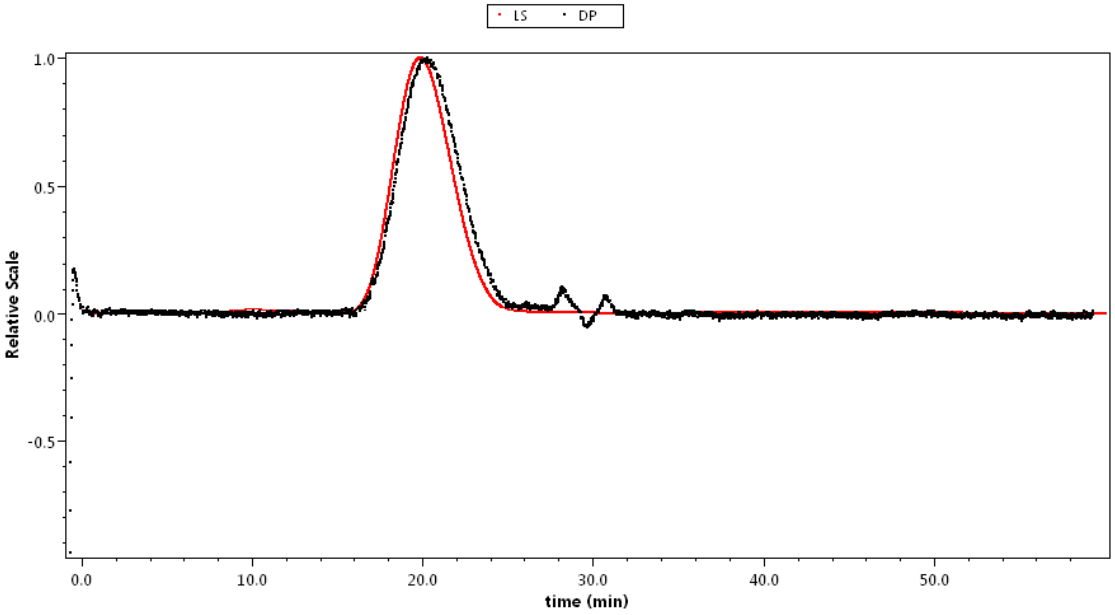

Fig. A2.1: Representative GPC for ROP of CHO with **2.1** and BnOH (Table 2.1, entry 5).

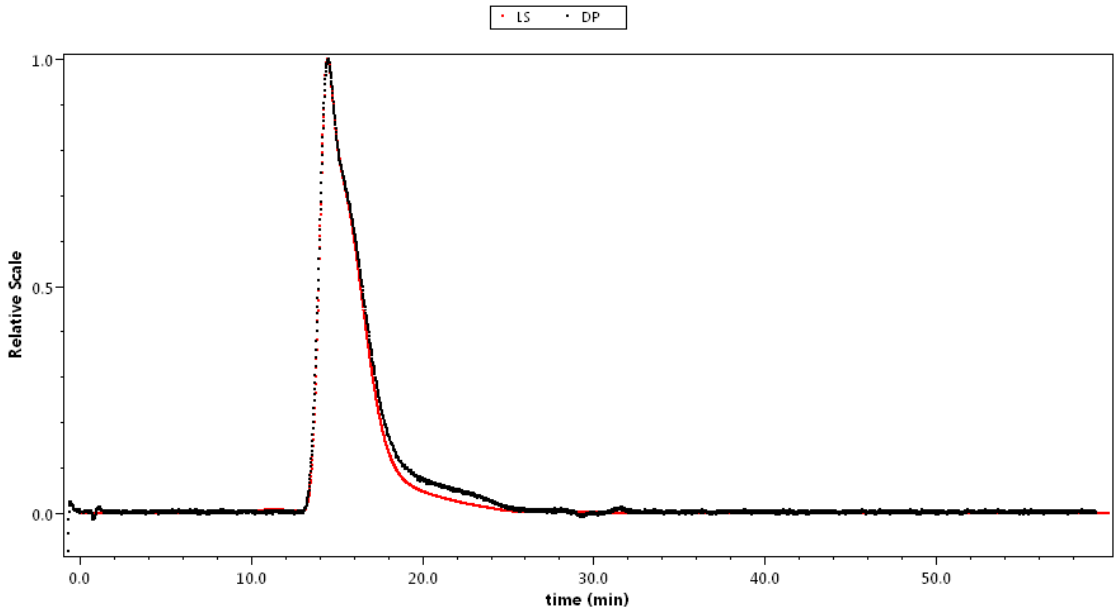

Fig. A2.2: Representative GPC trace for PCHC obtained by **2.1** and BnOH (

Table **2.2**, entry 3).

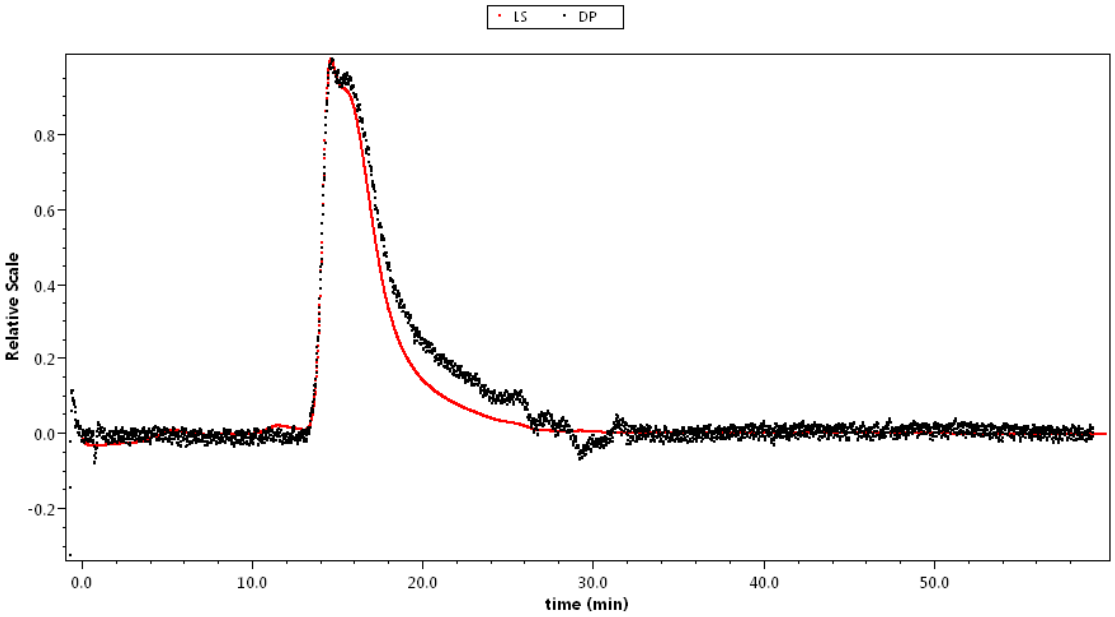

Fig. A2.3: GPC trace of LO/CHO copolymer obtained by **2.1** and BnOH.

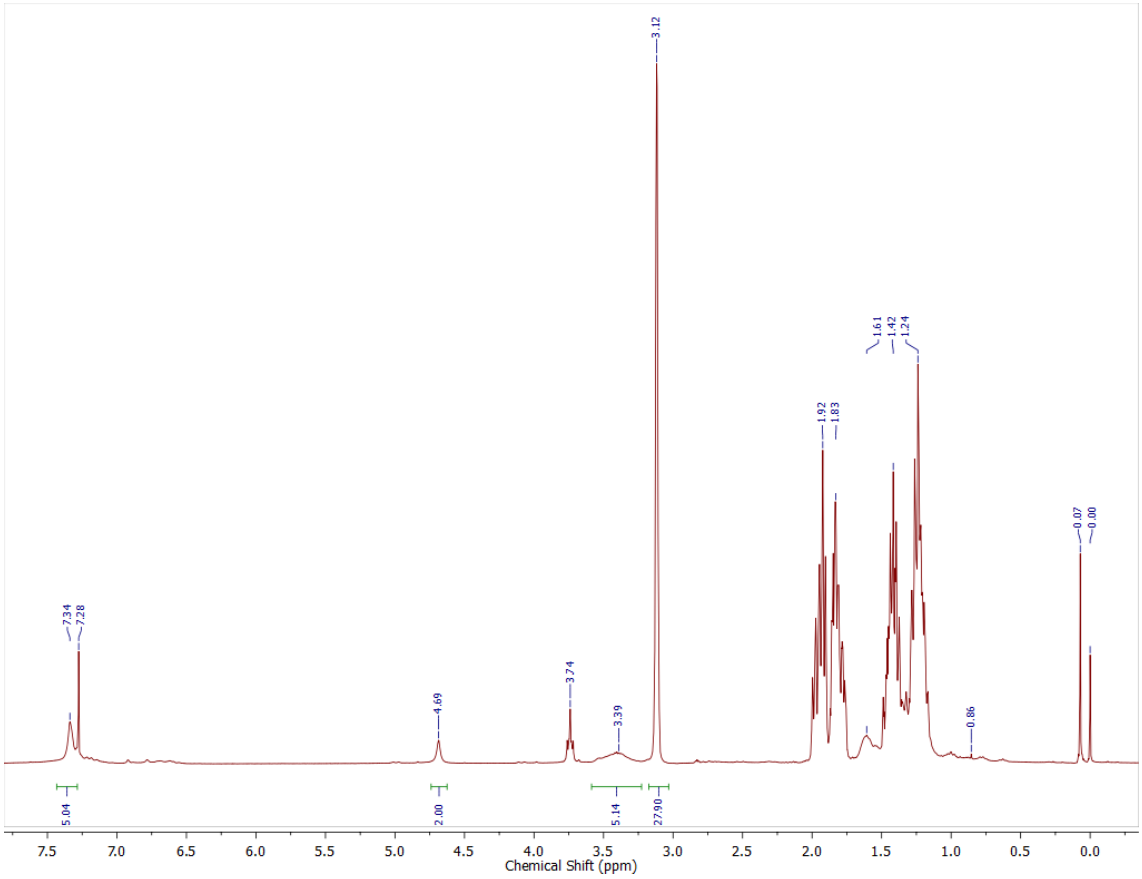

Fig. A2.4: ^{1}H NMR spectrum of low molecular weight PCHO in $CDCl_3$. BnOH end groups (δ 4.69, CH_2, δ 7.34 Ar*H*) poly(cyclohexene oxide) (δ 3.39, *H*C–C*H*), ethane (δ 0.86, C_2H_6) (300 MHz, $CDCl_3$, 298K)

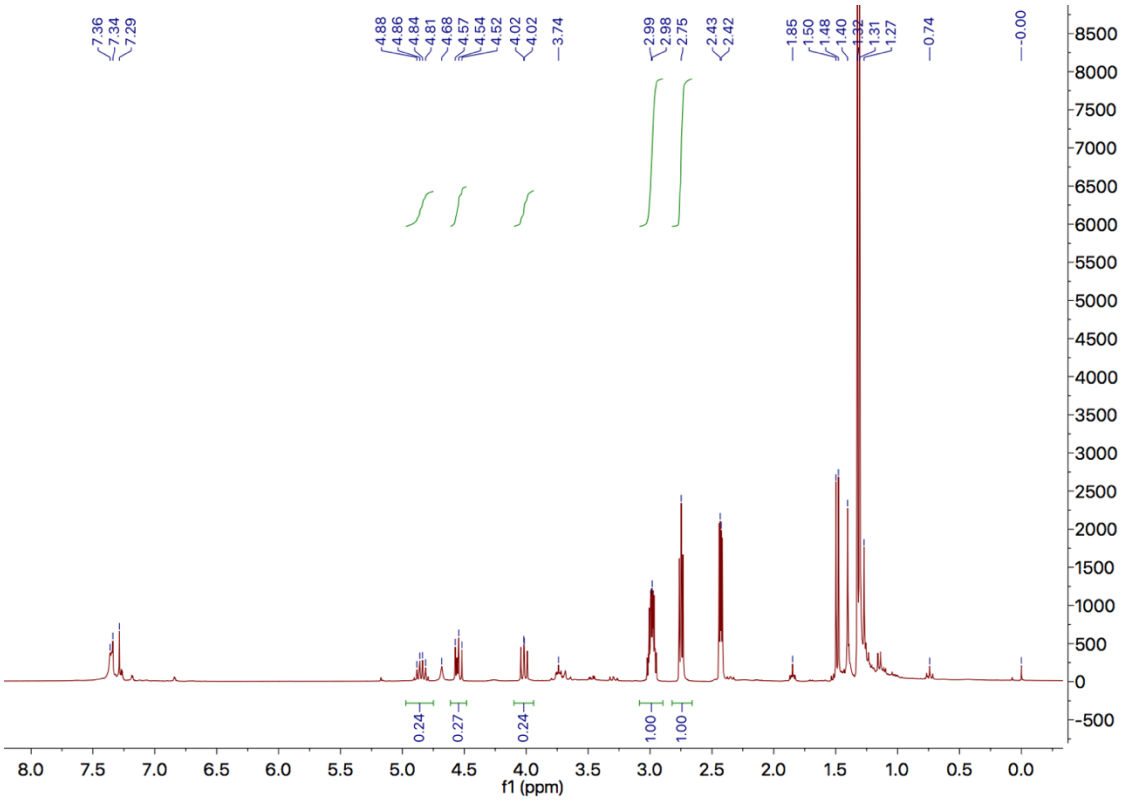

Fig. A2.5: ^{1}H NMR spectrum of crude reaction mixture of PO and CO_2 coupling products. Cyclic propylene carbonate (δ 4.02, 4.53 and 4.85), and PO (δ 2.43, 2.75, 2.99). Other resonances are from presence of **2.1**. (300 MHz, $CDCl_3$, 298K)

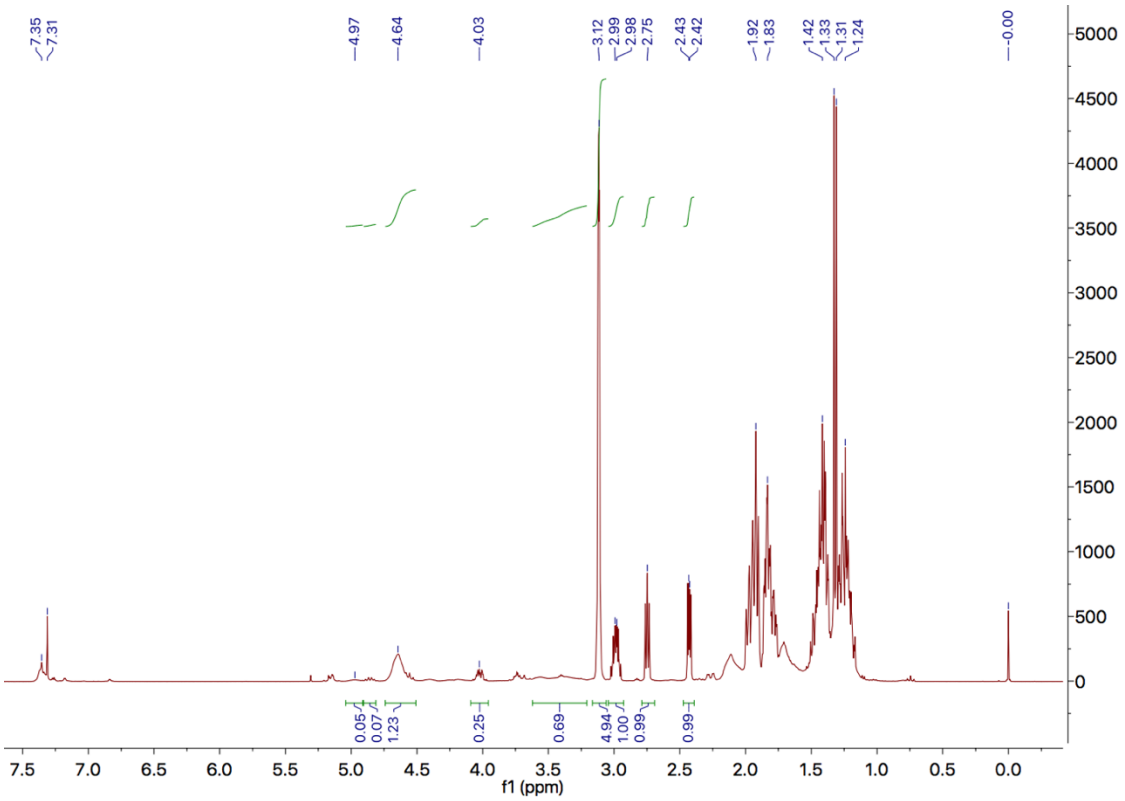

Fig. A2.6: ^{1}H NMR spectrum of crude polymer product from reaction containing a 1:1 mixture of CHO and PO. Poly(propylene carbonate) (δ 4.97), poly(cyclohexene carbonate) (δ 4.64), cyclic propylene carbonate (δ 4.03), poly(cyclohexene oxide) and poly(propylene oxide) (δ 3.20 – 3.60), (300 MHz, $CDCl_3$, 298K)

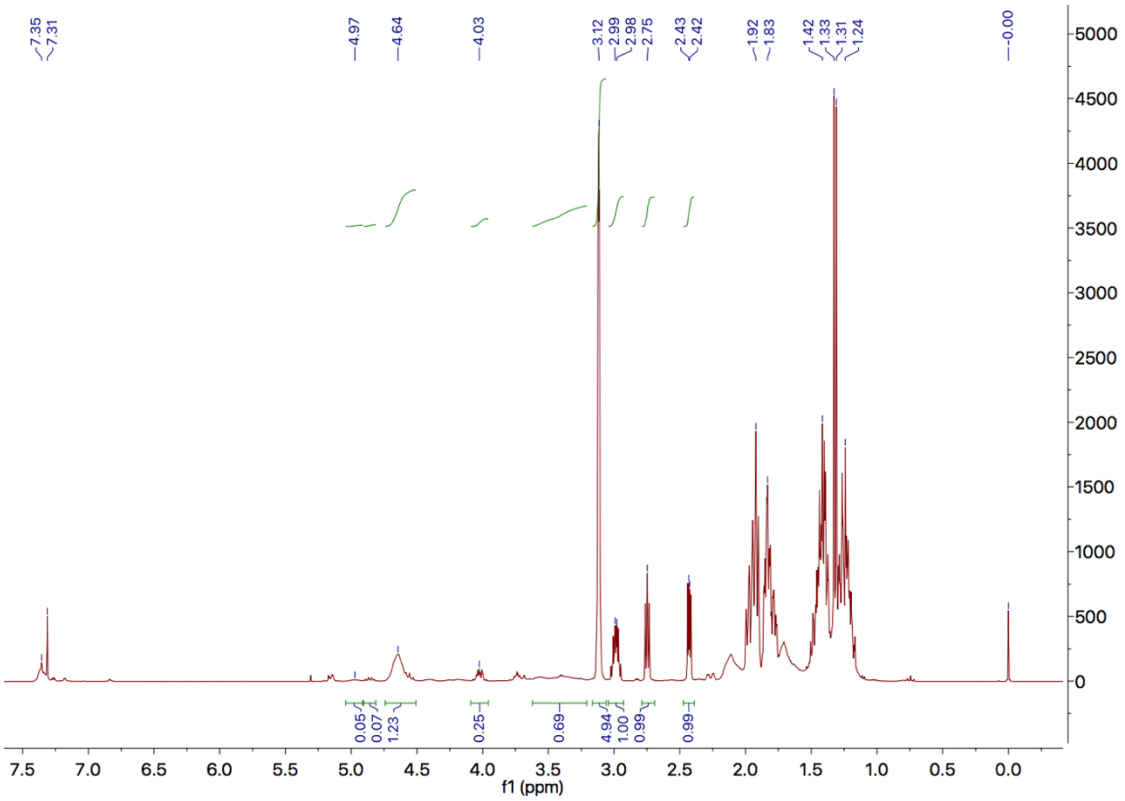

Fig. A2.7: ^{1}H NMR spectrum of purified LO/CHO polymer product. Poly(limonene carbonate) (stereo-irregular) and poly(cyclohexene carbonate) (δ 4.63 – 4.73), poly(cyclohexene oxide) (δ 3.25 – 3.70). (300 MHz, $CDCl_3$, 298K)

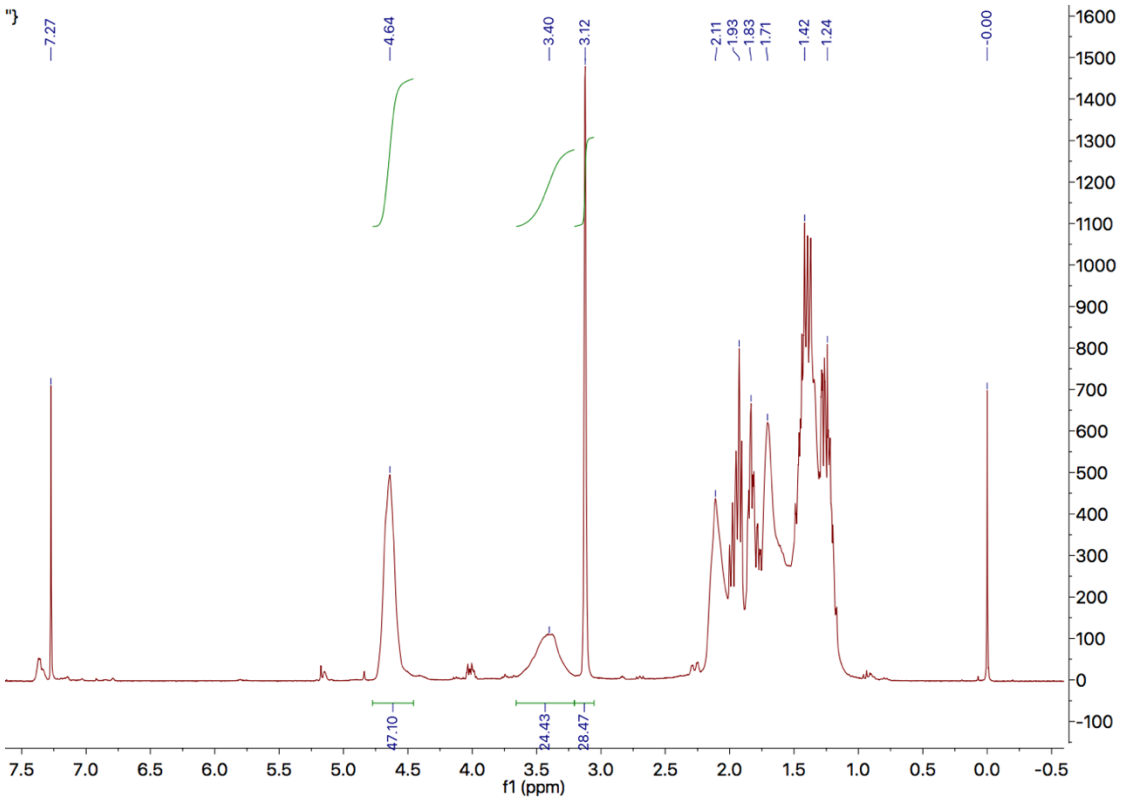

Fig. A2.8: Representative ^{1}H NMR spectrum of crude polymer product (Table 2.2, entry 3, 20 bar, 80 °C). Poly(cyclohexene carbonate) (δ 4.64), poly(cyclohexene oxide) (δ 3.40), CHO (δ 3.12) (300 MHz, $CDCl_3$, 298K)

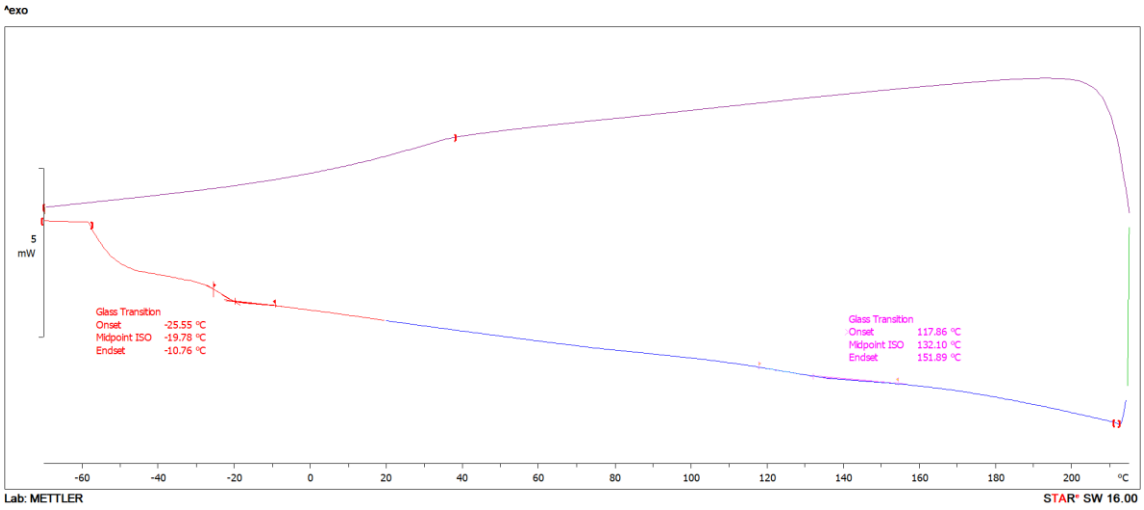

Fig. A2.9: Differential scanning calorimetric thermogram of CHO/LO copolymer. T_g at -19.78 and 132.10 °C.

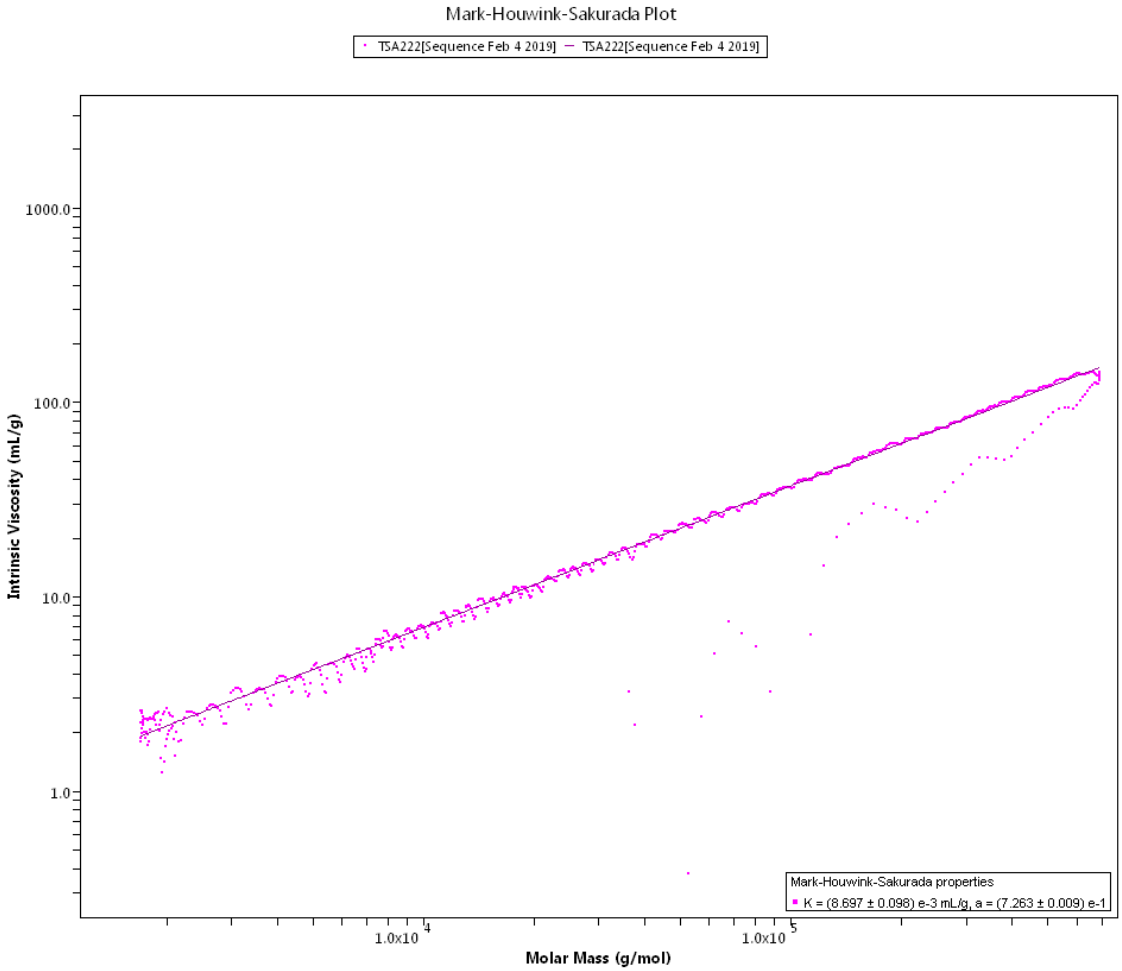

Fig. A2.10: Mark-Houwink-Sakurada plot for CHO/LO copolymer showing linearity in the sample.

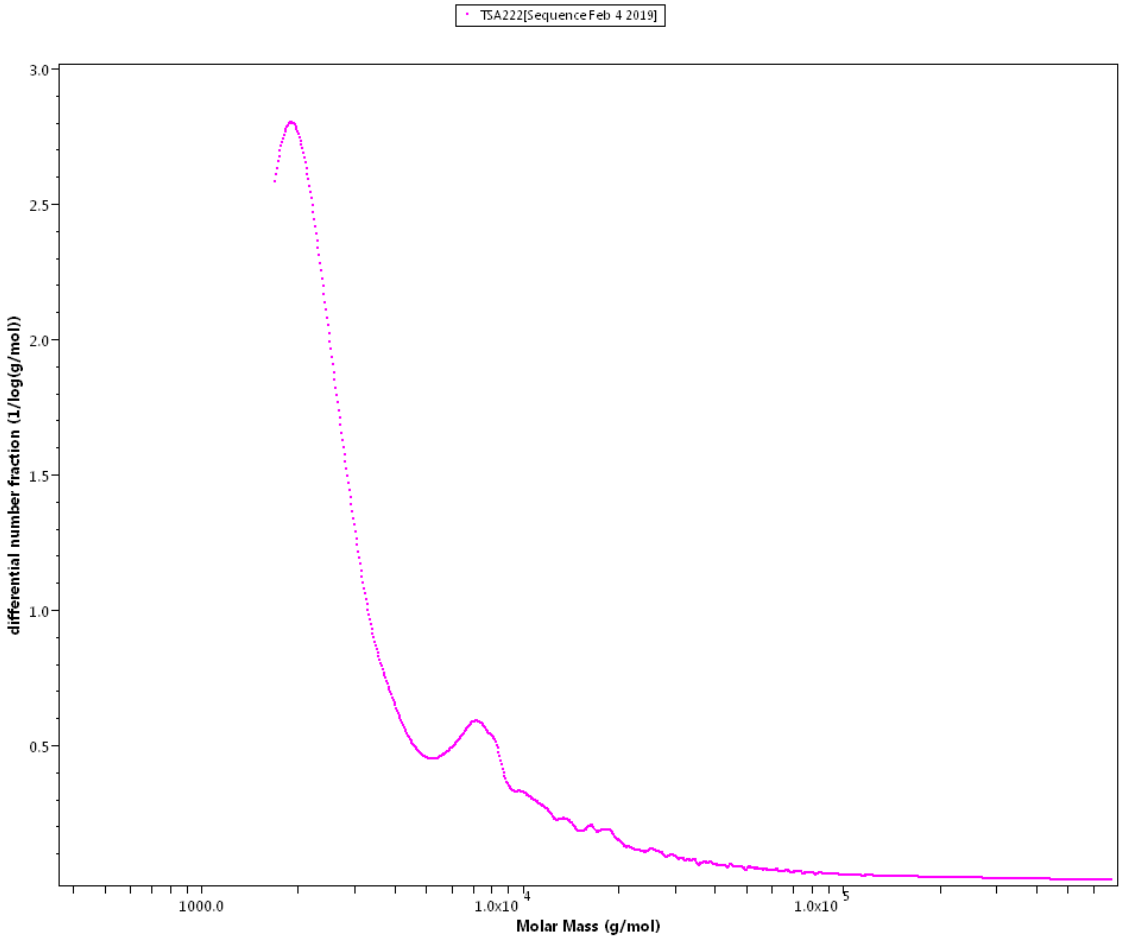

Fig. A2.11: Differential number fraction vs. molar mass plot of CHO/LO copolymer.

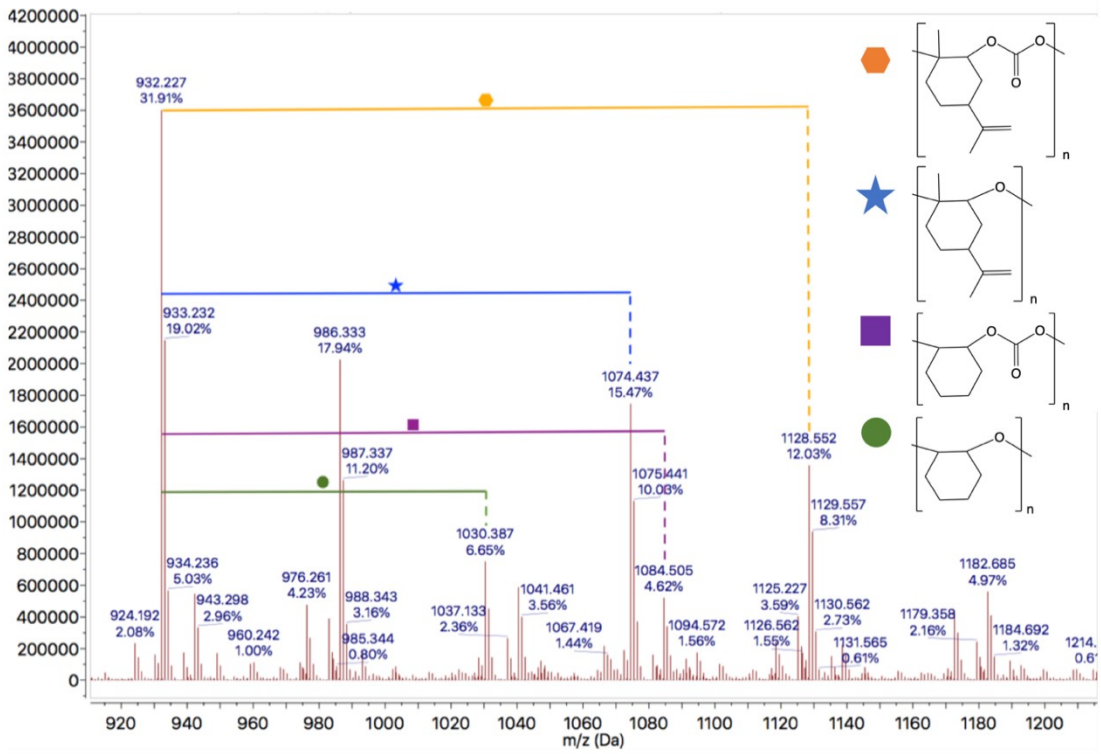

Fig. A2.12: MALDI-TOF mass spectrum of CHO/LO/CO_2 terpolymer showing presence of different comonomer incorporation.

Chapter 3

Synthesis of an alkylperoxo zinc complex and its application in the oxidation of alkenes

3.1. Introduction

Oxidation of unsaturated bonds has been a valuable tool for organic synthesis but is often limited by poor selectivity and harsh reagents. Oxidation of Grignard reagents by O_2 to form alcohols has been known for nearly as long as Grignard reagents themselves. Also, metal-peroxo intermediates are one of the species that form on metal surfaces during oxidation by O_2. This has been proposed to proceed via a σ-bond metathesis reaction between the metal-peroxo complex and an unreacted starting material (Scheme 3.1).[1-2] Alcohols are produced through this method via hydrolysis of the metal alkoxide complex. Structural characterization of metal complexes containing peroxide ligands is rare; the first report of such a species was published in 2003.[3]

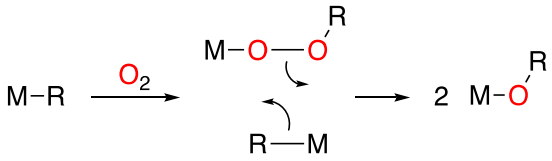

Scheme 3.1: Mechanism proposed by Bailey et al. for O_2 insertion and σ-bond metathesis to form metal alkoxides.[3]

Herein the formation and structural characterization of a new peroxo alkylzinc complex (**3.1**) is reported and the application of this, as well as a recently reported alkylperoxo zinc complex (**1.41**), toward oxidation and polymerization reactions (Scheme 3.3) is investigated. Based on the work of Lewiński, I theorized that it may be possible to achieve epoxidation of an alkene and subsequent copolymerization with CO_2 by using a single ligand-alkylperoxozinc catalytic system (Fig. 3.1). This would provide a one-pot synthesis of poly(carbonate) from potentially renewable substrates such as carvone and limonene. Preliminary findings of these efforts are described herein.

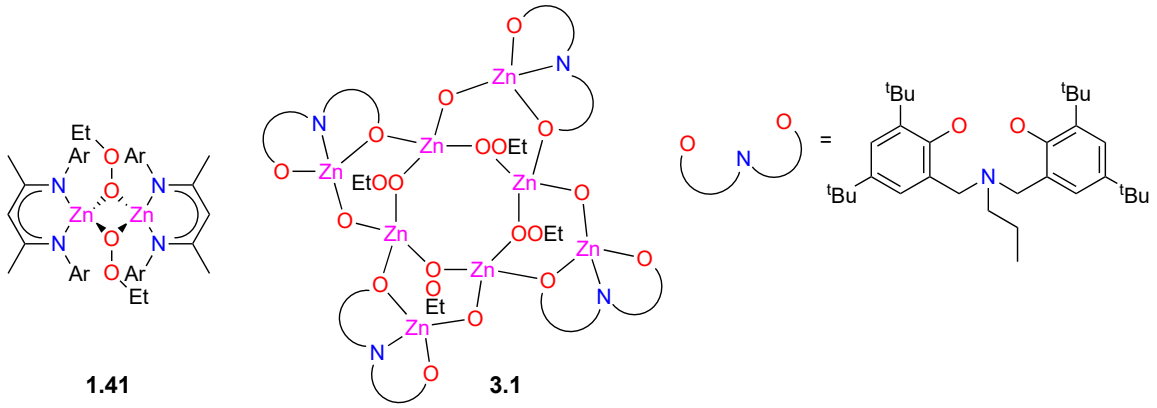

Fig. 3.1: Zinc peroxide species discussed in Chapter 3.

3.2. Metal peroxo complexes

Bailey and coworkers reported the first structurally characterized group 2 metal peroxide complex in 2003.[3] Dibenzylmagnesium was reacted with four amine-containing ligands: tetramethylethylenediamine (TMEDA), tetraethylethylenediamine (TEEDA), pentamethyldiethylenetriamine (PMDETA), and a *ß*-diketiminate ligand (Scheme 3.3), and

each reaction mixture was exposed to O_2 gas. Isolation of the alkylperoxo- and alkoxo intermediates is possible by isolating the intermediate formed in Scheme 3.1. Notably, the dimeric magnesium alkoxide product (**3.2**) could be isolated and structurally characterized using the *β*-diketiminate species in Scheme 3.2.

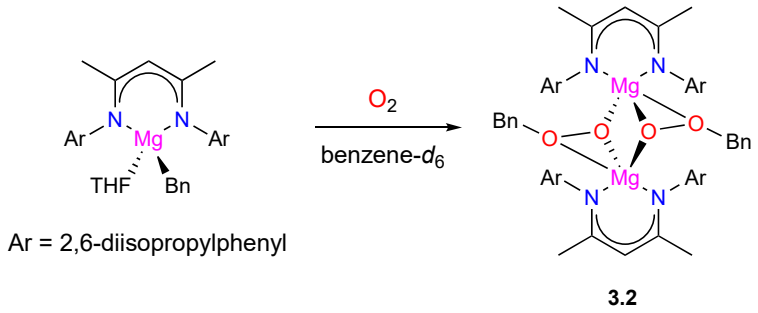

Scheme 3.2: Benzylperoxo-magnesium complex prepared by Bailey and coworkers.[3]

The report above was strictly on the structural identification of the species, but just a week later, Lewiński and coworkers reported the first structurally characterized zinc alkylperoxo complex and applied it toward the oxidation of enones.[4] The same *β*-diketiminate ligand was used here as well, and the conditions for peroxo complex formation can be seen in Scheme 3.3. Lewiński was interested in the epoxidation of electron-deficient olefins and believed zinc alkylperoxo complexes to be strong candidates as catalysts for the transformation as was reported by K. Yamamoto and N. Yamamoto.[5] For this, *trans*-chalcone and artemisia ketone were selected to probe steric influence and regioselectivity of the substrates (Scheme 3.4).

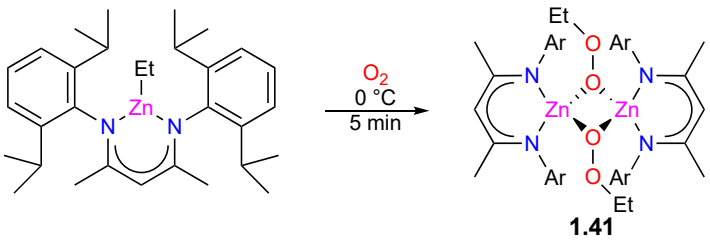

Scheme 3.3: Zinc alkylperoxide synthesis reported by Lewiński and coworkers.[4]

Over several minutes in toluene at 0 °C, 97% conversion of *trans*-chalcone was observed. For artemisia ketone, 96% conversion was observed and was completely selective for the enone moiety (Scheme 3.4). The selectivity and speed toward this functionality suggest that other enones would be suitable epoxidation candidates as well, but also that the presence of the ketone would be required for this particular type of catalytic system.

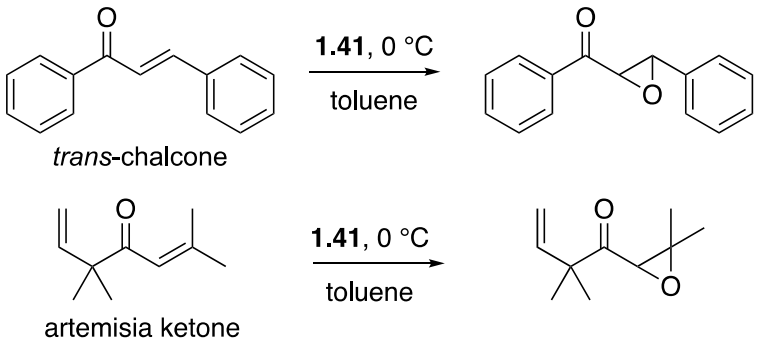

Scheme 3.4: Epoxidation reactions reported by Lewiński.[4]

In an effort to elucidate the mechanism of O_2 insertion into alkyl-zinc bonds, Lewiński utilized simple dialkylzinc structures to observe formation of the alkylperoxozinc bond via IR and NMR spectroscopy.[6] With Zn^{t}Bu$_2$, the solvated complex of THF was exposed to 1 bar of dioxygen at –78 °C (1 min), and with 4-methylpyridine (MePy, 1 or 2

equiv per zinc) at –78 and –45 °C (2 h). With THF, a dimeric alkoxy-zinc species was isolated, and the molecular structure determined by single crystal X-ray crystallography, while MePy led to isolation of a dimeric alkylperoxozinc species (**3.3**), also structurally characterized by single crystal X-ray diffraction. (Scheme 3.5). Performing the reactions with MePy at –78 °C resulted in no conversion of the alkyl-zinc moieties. Evidently, the simple monodentate Lewis basic ligand has an impact over the reactivity of the alkylperoxozinc species, stabilizing the resulting complex through ligand dissociation resulting in a 3-coordinate species which is apt to react with O_2 (Scheme 3.6). They suspected the dissociation of MePy is slow at –78 °C thus no oxygenation was observed, but at –45 °C, the reaction was much slower than with THF alone, supporting the dissociation hypothesis. Although it is believed to proceed through a radical mechanism, the introduction of TEMPO (2,2,6,6-tetramethylpiperidine *N*-oxide, 0.1 mol%) had no effect on the oxygenation reaction.

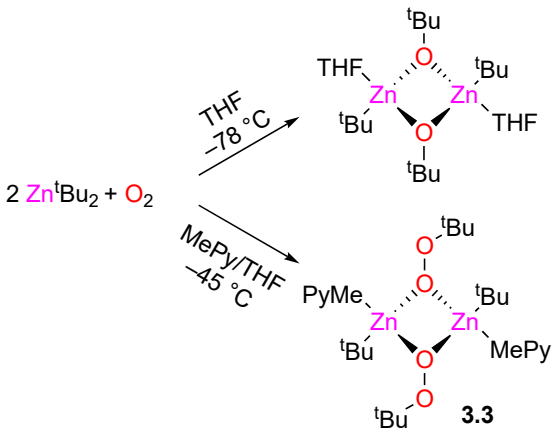

Scheme 3.5: Selectivity toward alkoxo- or alkylperoxozinc species dependent upon ligand reported by Lewiński.[6]

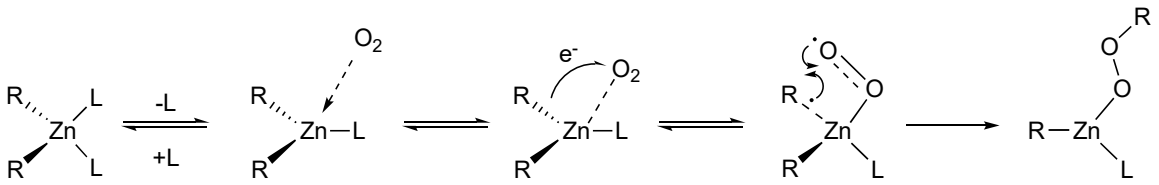

Scheme 3.6: Mechanism proposed by Lewiński for O_2 insertion into alkylzinc bonds.[6]

The isolation of **3.3** prompted the Lewiński group to continue using *tert*-butylperoxozinc complexes for epoxidation reactions. Substituting $ZnEt_2$ in the synthesis of **1.41** with Zn^tBu_2, the analogous complex could be obtained (Fig. 3.2).[7] They also examined other *N*,*N*-bidentate ligands (Fig. 3.2). Again, the epoxidation of *trans*-chalcone was probed, but rather than a stoichiometric reaction reported earlier, 10 equiv of *trans*-chalcone and 20 equiv of ^{t}BuOOH in toluene were used in an attempt at catalysis. After the epoxidation of the enone, the zinc complex is left as the alkoxozinc analogue and the alkylperoxozinc can be regenerated in the presence of a peroxide source – ^{t}BuOOH in this case. There was no comment on the ability of ^{t}BuOOH to epoxidize *trans*-chalcone.

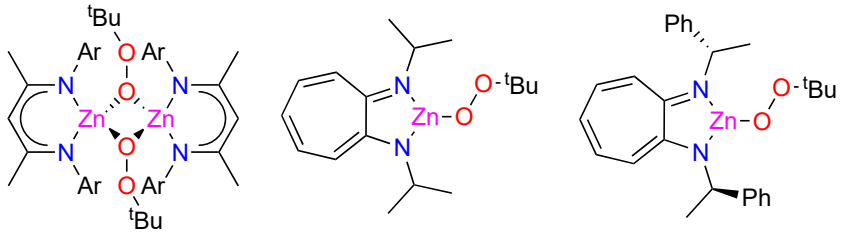

1.41-^{t}Bu **3.4** **3.5**

Fig. 3.2: Alkylperoxozinc complexes reported by Lewiński for catalyst epoxidation of *trans*-chalcone.[7]

Among the three catalysts, **1.41**-^{t}Bu was the most effective towards *trans*-chalcone conversion reaching 96% in 3 h at 0 °C with no enantiocontrol. Compound **3.4** was the slowest at 99% conversion in 8 h, again with no enantioselectivity, while compound **3.5** reached 98% conversion in 4 h with a 29% enantiomeric excess. This shows that the addition of the highly reactive ^{t}BuOOH does not deactivate the catalyst toward the enone substrate. This provides an avenue for swift epoxidation of bulk enone. They propose that π-π interactions between the substrate and the catalysts are the cause of differing reaction times, so it stands to reason that substrates devoid of aromatic functionality may exhibit reduced reactivity. The proposed mechanism for epoxidation does not explain the near complete conversion to epoxidized *trans*-chalcone as there are substoichiometric amounts of peroxo complexes able to be generated. Therefore, there must be another process that forms peroxides *in situ*. The reactions were run in air, and the reaction mixture was saturated with O_2 prior to the addition of the substrate solution. Although no comment was made regarding this discrepancy, it is possible that the peroxo-metal intermediates formed during metal oxidation by O_2 as discussed at the beginning of the chapter may account for the higher conversions.

3.3. Results and discussion

It was mentioned in Section 1.5 that the isolation of the alkylperoxozinc species **1.41** (Fig. 3.1) was the first to be structurally characterized by single crystal X-ray diffraction, and the enhanced stability of the material compared to other metal-peroxides was attributed to the properties afforded by the *ß*-diketiminate ligand of the precursor inhibiting the σ-bond

metathesis process that leads to alkoxide formation. Compound **1.41** is a variant of the famous Coates (BDI)ZnEt species commonly seen in CO_2 / epoxide copolymerization chemistry and as such I thought it to be an excellent candidate for these reactions. Additionally, synthesis of a novel zinc peroxide species based on the zinc compound **2.1** (described in Chapter 2) was also of interest. As the stability of the peroxo zinc complexes appear to be heavily dependent on the ligand framework, compound **2.1**, with its well-defined dimetallic core, may be able to stabilize the reactive peroxide species through dinuclear interaction much like the magnesium peroxo complexes discussed earlier in this Chapter. Interestingly, while the isolation of a zinc-peroxo complex was possible (similar reaction to that in Scheme 3.3 with 30 min reaction length), characterization via single crystal X-ray diffraction shows a clustered tetramer. Fig. 3.3 shows the core of the crystal structure with carbon atoms omitted for clarity. A complete representation can be found in Fig. 3.1. There are four ligands surrounding the species, four Zn–O–Zn hydroxide bridges, and four ethylperoxozinc units. Interestingly, of the two ethyl-zinc fragments present per unit of **2.1**, one is transformed into the ethylperoxozinc while the other appears to have been removed entirely, replaced with bridging hydroxo ligands. In other examples of alkylperoxozinc complexes, the alkyl-zinc functionality is either unaffected by the presence of O_2 or forms a peroxo or an alkoxo ligand.[6,8] Although the quality of the data is less than ideal, the central core illustrated below is relatively well defined. Comparing bond lengths of the alkylperoxozinc interactions suggest that Zn–O bonds (Zn5–O13 of 2.008(14) Å) are within the range of other alkylperoxozinc bonds, e.g. 2.068(6), 1.877(1) Å.[9-10] Peroxide bond lengths (O13–O14 of 1.492(19) Å) appear to be within typical ranges as well, e.g. 1.477(8), 1.491(4)

Å.[9-10] Efforts to grow higher quality crystals to access improved structural data have so far been unfruitful.

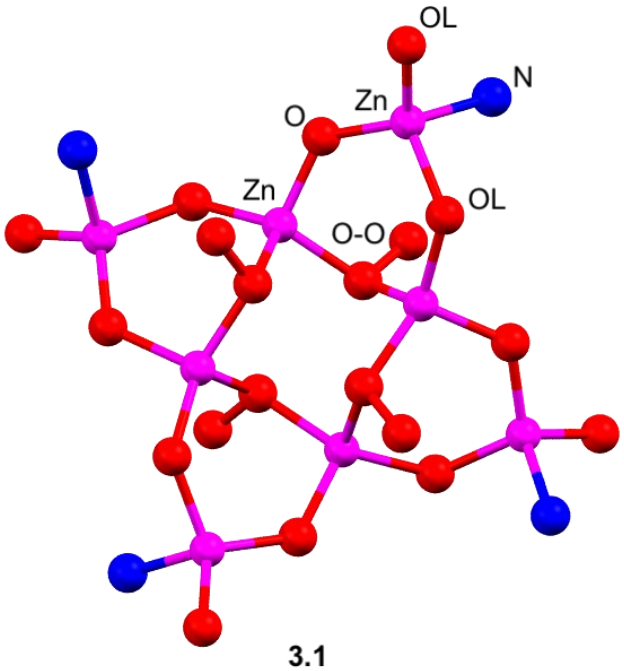

3.1

Fig. 3.3: Core structure of the alkylperoxozinc species **3.1** synthesized from **2.1** under dry O_2. "O-O" refers to the peroxide functionality omitting the ethyl group, "O" refers to the bridging hydroxide and "OL" and "N" are from the ligand shown in Fig. 3.1. Crystallographic data can be found in Table A3.1. Selected bond lengths (Table A3.2) and angles (Table A3.3) can be found in the appendix along with an image including all carbon atoms (Fig. A3.9).

The new complex **3.1** was studied alongside the previously characterized **1.41** reported by Lewiński and co-workers. The one-pot synthesis of poly(carbonate) via the route shown in Scheme 3.7 could be attempted with different substrates. Lewiński had reported 97% conversion of *trans*-chalcone to the corresponding epoxide by **1.41** over "several minutes" at 0 °C so using a similar procedure to first epoxidize the substrate via zinc-peroxide regeneration, followed by CO_2 pressurization, could lead to the formation of carbonate containing products. Ensuring appropriate stoichiometry would likely be crucial as the zinc-peroxides (rather than zinc-alkoxides) may be inactive toward CO_2 and epoxide coupling.

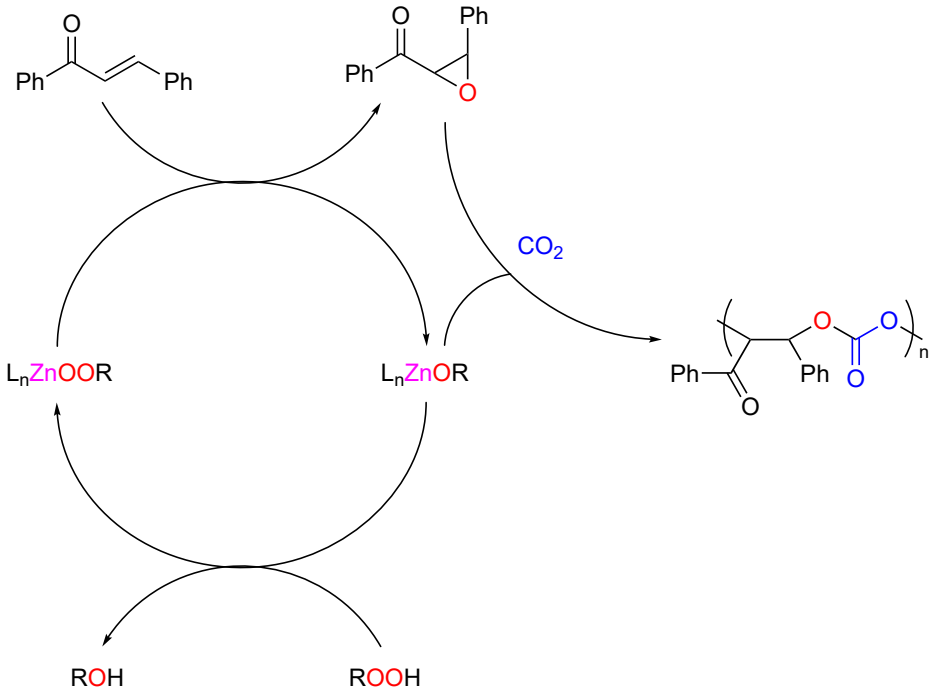

Scheme 3.7: Proposed catalytic cycle for epoxidation of *trans*-chalcone, copolymerization with CO_2, and regeneration of the alkylperoxozinc species.[7]

3.4. Other alkene-containing substrates

Beyond the *trans*-chalcone investigated by Lewiński, other unsaturated compounds were investigated that, once epoxidized, would yield materials that may be useful toward copolymerization with CO_2, providing a new method of synthesizing these oxidized compounds from their naturally sourced starting materials. It has been proposed that an *a,ß*-unsaturated ketone was required for epoxidation but the common epoxides in CO_2 and epoxide copolymerization do not contain this functionality yet remain of interest. Limonene and *R*-(–)-carvone (abbreviated as "carvone" henceforth) were chosen as each are naturally occurring terpenes that can be obtained from renewable sources; limonene from citrus zests and oak or pine trees, and carvone from spearmint (*R*-isomer) caraway seeds and dill (*S*-isomer), and can be derived from limonene itself.[11-12] Limonene is devoid of an *a,ß*-unsaturated ketone but limonene oxide is of particular interest in renewable CO_2 and epoxide copolymerization due to the desirable properties of poly(limonene carbonate) discussed in Chapter 2. Carvone does contain an *a,ß*-unsaturated ketone so is more akin to *trans*-chalcone but is unstudied in the field of CO_2 and epoxide copolymerization.

3.5. Oxidation reactions

Due to the difficulty of maintaining a constant temperature for these reactions in a stepwise manner, the stability of **3.1** with respect to temperature was tested first. Lewiński had observed that alkylperoxozinc species could be stabilized at ambient temperature when complexed with sufficient donor ligands. To examine this with the zinc complexes used here,

20 mg of **2.1** was dissolved in ~700 μL of toluene-d_8 in an LPV NMR tube. The solution was placed under vacuum and exposed to dry O_2 at 25 °C. ^{1}H NMR spectroscopy (Fig. A3.2) was performed at 20, 0, –20 and –40 °C. Spectroscopic analysis shows evolution of ethane gas (∂ 0.82), expected as the crystal structure shows that only one of the ethylzinc units of **2.1** is converted to a ethylperoxo zinc while the other is removed entirely. Several peaks emerge across the spectrum and, as shown in Fig. 3.1 and by single-crystal X-ray diffraction, four ligands are present per alkylperoxozinc complex with no clear symmetry thus the presence of many new signals is not surprising but difficult to assign accurately. As the ^{1}H NMR spectrum was relatively consistent with that obtained at reduced temperature, (the signals at reduced temperatures sharpen, particularly in the alkyl region corresponding to the aryl-*tert*-butyl functionality of the ligand, suggesting fluxional behavior in the complex thereby explaining the complicated spectra, Fig. A3.3) compound **3.1** appears stable in solution at room temperature. The complicated spectra may also arise from the presence of aggregates with polynuclearity that exist in equilibria in solution, as di and trimetallic analogues of **2.1** have been seen previously.[13]

DOSY analysis (at 20 °C, Fig. A3.4) suggests that the mass of the dominant species in solution is approximately half of the mass for the tetrameric complex observed in the solid state, so perhaps in solution the dominant species adopts a dimeric structure at 20 °C. Furthermore, the analysis shows diffusivity values for the complex within 1 order of magnitude (–4.4 and –5.1 log(cm^2 s^{-1})), suggesting only one species is present in solution. Given I was unable to observe solid-state material at elevated temperatures, and the results of the NMR spectroscopy studies, it is possible that the recrystallized tetrameric material is

sensitive to temperature. Screening reactions for epoxidation were therefore performed at ambient temperature to allow for consistency with reactions performed in the pressure vessel where temperature control below ambient is difficult.

3.6. One-pot synthesis of poly(carbonate)

As the catalysts were likely moisture sensitive, all reactions were performed in low pressure/vacuum NMR tubes allowing for control over the internal atmosphere as the reaction was monitored over time and **1.41** and **3.1** were generated *in situ* for each reaction. If epoxidation was observed for the substrates on NMR scale, CO_2 could be introduced to the sample to screen for low pressure (1 bar) activity toward polymerization or coupling. Using **1.41** equimolar with *trans*-chalcone at 25 °C in toluene-d_8, resonances corresponding to starting material and epoxidized product could be identified via ^{1}H NMR spectroscopy by comparing resonances at ∂ 3.82 for chalcone oxide to 7.78 for *trans*-chalcone and indicates 60% conversion to chalcone oxide over 4 h (Fig. A3.5), as per the initial report by Lewiński.[4] Subsequent addition of CO_2 resulted in 50% conversion to poly(ether) and no conversion to carbonate over 18 h. Repeating this procedure with **3.1** (generated *in situ*) resulted in conversion of 59% to chalcone oxide. No polymerization was observed after CO_2 introduction over 18 h. However, this is not unexpected as only the most exceptional zinc catalysts have demonstrated activity toward ROCOP or coupling of CO_2 at 1 bar CO_2.

As these reactions showed conversion to the epoxide in significant quantities and poly(ether) formation for **1.41**, a similar procedure to above was followed but the solution

was inserted into the pressure vessel and charged to 7 bar of CO_2 and heated to 50 °C for 1 h. These conditions are emulating those reported by Coates for the copolymerization of LO and CO_2 and increased pressure and temperature may induce poly(carbonate) production.[14] There was minimal evidence of poly(carbonate) or poly(ether) formation by IR spectroscopy, likely overlapping with other peaks in the spectrum. The solvent was removed under reduced pressure and the remaining solid dried at 60 °C in a vacuum oven. MALDI-TOF MS of the product indicates oligomeric formation of primarily poly(*trans*-chalcone oxide) and lesser amounts of poly(chalcone carbonate) (Fig. A3.6). While this was an exciting result, there was not enough material to isolate for further study.

Lewiński reported the use of *tert*-butyl hydroperoxide to regenerate the alkylperoxozinc species.[7] Due to the exploratory nature of this project, *meta*-chloroperoxybenzoate (*m*CPBA) was used as it was available in the laboratory having previously been used by C. Laprise.[15] As the conversion to polymer observed above were low for near stoichiometric reactions, the presence of the regenerating species may lead to improved polymeric yields as well. A reaction with **1.41** (0.240 mmol), 10 equiv of mCPBA and 20 equiv of *trans*-chalcone was performed at 10 bar CO_2 and 50 °C over 1 h in 4 mL toluene. No conversion to polymer or epoxide was observed by ^{1}H NMR spectroscopy. It is likely that the *m*CPBA is deactivating the catalyst and was not examined further. Due to time constraints and COVID-19 interruptions, screening of other peroxide reagents could not be performed.

With evidence for the concept of epoxidation–ROP in one pot, the focus was then shifted to the renewable, less sterically hindered monomers – limonene, a common reagent in CO_2 and epoxide copolymerization, and carvone, analogous to limonene but unexplored (Fig. 3.4). Reactions were performed at 70 °C and 20 bar CO_2 for 18 h. For these systems, reactions were performed in a Parr pressure vessel fitted with infrared ATR sensor for monitoring of reactions in real-time by IR spectroscopy as the ^{1}H NMR spectra of these products is complicated by stereoisomers and the oxidation products are not easily identifiable. Furthermore, information related to the chemical processes could be gleaned by monitoring signals corresponding to each product, and reaction progression by monitoring of those signals. Reactions were performed as described above using **1.41**. As anticipated, limonene was inactive toward oxidation, lacking the enone functionality that is likely required for epoxidation and indeed MALDI-TOF MS did not indicate the formation of polymeric material. Carvone oxide was detected by ^{1}H NMR in the crude reaction mixture described earlier and could be observed by IR spectroscopy *in situ* (Fig. 3.5). The stretching frequency at 694 cm^{-1} corresponds to the terminal alkene of carvone starting material (the carbonyl and cyclic alkene peaks overlap with other signals in the spectrum) while 1681 cm^{-1} arises from the carbonyl stretch of carvone oxide.[16-17] The reported value for C=O stretching in carvone oxide is 1710 cm^{-1} suggesting metal coordination causes a red-shift in the frequency. As the reaction continues, a diagnostic peak at 1552 cm^{-1} emerges that cannot be attributed to another compound. As the growth of this signal corresponds with production and subsequent consumption of carvone oxide, it is possible that it arises from poly(carvone carbonate) or cyclic carvone carbonate. No other clear signals could be identified in the crude mixture. ^{1}H NMR spectroscopy of the crude reaction mixture also suggests that

polymer material is forming with 22% conversion to poly(carbonate) (∂ 4.64) and 41% conversion to poly(ether) (∂ 3.38) compared against ∂ 4.80 and 4.76 of carvone (Fig. A3.7). No evidence of carvone oxide was observed, suggesting that it had been entirely consumed. MALDI-TOF MS was employed on the purified material and suggests that the dominant product is tris(carvone carbonate) initiated by ethoxide and terminated by hydroxy-carvone (Fig. A3.8) but polymers with 5, 7, 9 and 11 repeating units could be observed as well. While these are small oligomers, this was not unexpected as the lack of peroxide regeneration source for the zinc catalyst should limit the formation of carvone oxide. Furthermore, the red-shifted stretching frequency corresponding to carvone oxide in the IR spectrum may indicate a strong interaction with the catalytic species and hampering dissociation of epoxide, thereby limiting propagation. The ethoxide initiating group agrees with the proposed reaction mechanism in Scheme 3.7. The MS results also indicate lesser formation of mixtures of poly(carbonate) and poly(ether), but no poly(ether) formation could be observed by other means. To my knowledge, this is the first example of poly(chalcone carbonate) and poly(carvone carbonate-*co*-ether) formation and the first example of poly(carbonate) formation from epoxide deficient starting materials in one-pot.

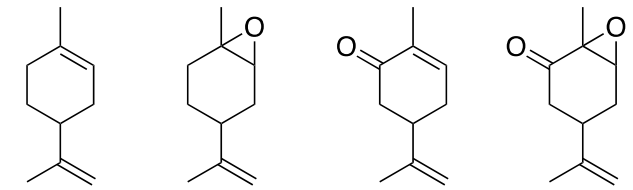

Fig. 3.4: Alkenes and corresponding epoxides studied for epoxidation activity by **1.24** and **3.1**.

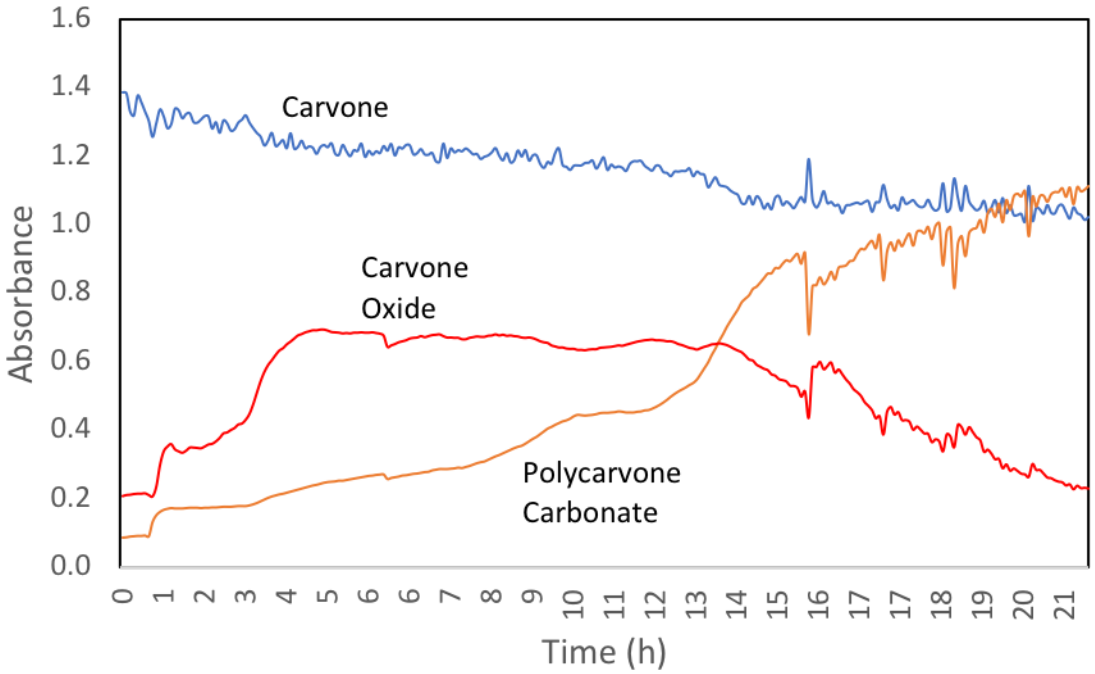

Fig. 3.5: IR trace of reaction of **1.41** with carvone and subsequent polymerization in neat carvone. Carvone was monitored at 694 cm^{-1} (terminal C=C), carvone oxide at 1681 cm^{-1} (C=O), and polycarvone carbonate at 1551 cm^{-1} (C=O). CO_2 pressurization at 30 min then heated to 70 °C, reaching temperature at approximately 1 h.

3.7. Conclusions and future considerations

Although the isolation of any significant polymer material was unsuccessful, the evidence of formation of even small amounts demonstrates that the potential for reaction optimization and polymer purification is high. Notably, it appears that ^{t}BuOOH or another alkyl peroxide is essential for rapid regeneration of the alkylperoxozinc species and would improve epoxidation and polymer yields significantly. Additionally, as mentioned earlier,

performing the reactions at stoichiometric ratios or with slight excess of epoxidation substrate may be prudent to reduce variables throughout the optimization process, and to ensure the zinc-alkoxide species is present after epoxidation. It is unlikely that this is truly catalytic due to the inability to recycle **3.1** as the polymer purification process will destroy the complex, and the precursor, **2.1**, has exhibited limited activity toward copolymerization at reduced catalyst loading.[18] Thus far, epoxidation via alkylperoxozinc species has been limited to enone substrates, but with the emergence of heterobimetallic catalytic systems in other fields of polymerization, similar design choices may lead to epoxidation of other unsaturated functionality via alkylperoxozinc or -magnesium heterobimetallic catalysts as well.

3.8. Experimental

General Methods: All reagents were purchased from Sigma-Aldrich, Alfa-Aesar, or Caledon. All epoxides were distilled. Unless otherwise stated, all reactions were performed under inert atmosphere of N_2. ^{1}H NMR spectra were recorded at 300 MHz on a Bruker Avance I spectrometer with BBO probe and ^{13}C at 75.0 MHz on a Bruker Avance I spectrometer with TCI inverse gradient probe. *In situ* FTIR monitoring was performed using a 100 mL Parr Instruments 4560 stainless steel mini reactor vessel with motorized mechanical stirrer and a heating mantle. The vessel was modified with a bottom-mounted Mettler Toledo SiComp Sentinel ATR sensor, which was connected to a ReactIR 15 base unit through a silver-halide Fiber-to-Sentinel conduit. Profiles of the absorbance height at 1089 cm^{-1}, 1646 cm^{-1}, 1750 cm^{-1} and 1810 cm^{-1} were measured every 60 – 120 s. Similar methods for reaction monitoring via *in situ* IR have been reported elsewhere.[19-21] MALDI-

TOF MS was performed using a Bruker ultrafleXtreme TOF/TOF MALDI Time-of-Flight Mass Spectrometer System equipped with a reflectron and BRUKER smartbeam™-II laser (355 nm). Samples were prepared on the benchtop. 2,3-Dihydroxybenzoic acid (DHBA) was used as the matrix for the polymers with sodium trifluoroacetate (NaTFA) as cationizing agent. Preparation of the samples and data collection was performed by Dr. Stefana Egli by dissolving matrix in THF (5 mg/mL), polymer in THF (1 mg/mL), and cationizing agent in THF (1 mg/mL), combining the solutions in 20:1:3 ratio and spotting 1 μL on the plate to dry. Data processing was performed using Polymerix© software.

Synthesis of 3.1: 2.1 (1.00 g) was dissolved in 20 mL of toluene under N_2 and cooled –20 °C using an ethylene glycol circulating bath. The solution was then exposed to O_2 gas that was dried over a $MgCl_2$ column for 20 min, sealed and cooled to –35 °C overnight. ^{1}H NMR (500 MHz, toluene-d_8, 298 K, compared against **2.1**, Fig. A3.1): ∂ 7.55 – 6.55 (m, 4H, Ar*H*), ∂ 5.11 (d, 2H, ArCH_2N), ∂ 4.77 (m, 2H, ArCH_2N), ∂ 4.43 (m, 2H, ArCH_2N), ∂ 4.11 (m, 2H, ArCH_2N), ∂ 4.03 (m, 2H, OCH_2CH$_3$), ∂ 3.72 (m, 2H, ArCH_2N), ∂ 3.13 (m, 2H, ArCH_2N), ∂ 1.68 (m, 9H, C(CH$_3$)$_3$), ∂ 1.45, 1.40 (m, 9H, C(CH$_3$)$_3$), ∂ 0.98 (m, 3H, OCH$_2$CH_3) ∂ 0.91 – 0.26 (m, 7H, NCH_2CH_2CH_3). DOSY analysis shows diffusivity values for the complex within 1 order of magnitude (–4.4 and –5.1 log(cm^2 s^{-1})) suggesting a single species. Colourless crystals suitable for X-ray diffraction were obtained from the solution. The structure was solved by Dr. Louise Dawe at Wilfred Laurier University. The crystals were unstable at elevated temperatures and were stored in toluene at –35 °C under inert atmosphere.

Oxidation of *α,ß*-unsaturated ketones, alkenes and terpenes: Due to the difficulty of isolating and storing of **1.41** and **3.1**, they were generated *in situ* for each reaction. 0.034 mmol of the pre-catalyst and 0.068 mmol of the reactant were dissolved in ~700 μL of toluene-d_8 or C_6D_6 in a Low Pressure/Vacuum (LPV) NMR tube. The solution was then exposed to dry O_2 gas for 30 min while agitating periodically. An aliquot of the crude reaction mixture was taken for ^{1}H NMR spectroscopy and used to determine conversion to product. Where appropriate, the remaining material was extracted into dichloromethane and precipitated using cold acidified methanol. The solvent was decanted and the product dried at 60 °C in a vacuum oven overnight.

One-pot epoxidation-polymerization: Pre-catalyst (0.067 mmol) and reactant (0.134 mmol) were dissolved in 5 mL toluene. The mixture was added via syringe to a 100 mL stainless steel Parr autoclave at 25 °C, which was pre-dried by heating to 100 °C under vacuum overnight. A description of the instrument can be found in Section 2.3.1. The solution was stirred and exposed to O_2 that was passed over a $MgCl_2$ drying column. After 30 min the autoclave was charged to the appropriated pressure and heated to the specified temperature. After the allotted time, the autoclave was cooled to room temperature and vented in the fumehood. An aliquot for ^{1}H and ^{13}C NMR spectroscopy was taken immediately after opening for the determination of conversion. The mixture was then extracted into dichloromethane and precipitated using cold acidified methanol. The solvent was decanted and removed under reduced pressure. The precipitated product was dried at 60 °C in a vacuum oven overnight.

***trans*-Chalcone epoxidation:** Following the procedure above at 7 bar and 50 °C, epoxidation of *trans*-chalcone oxide and subsequent polymerization was observed via ^{1}H NMR (300 MHz, toluene-d_8, 298 K): ∂ 7.65 – 7.37 (m, 2H, Ar*H*C=C*H*C, substrate), ∂ 3.82 (d, 1H, ArCH(O)C*H*C, *a*-H epoxide), ∂ 3.28 (d, 1H, *ß*-H epoxide), ∂ 3.36 (m, 2H, Ar*H*C(O)C*H*(=O), poly(ether)) (Fig. A3.5).

(*R*)-(–)-carvone epoxidation: Following the procedure above at 20 bar and 70 °C, epoxidation of carvone by **1.41** was confirmed via ^{1}H NMR (500 MHz, toluene-d_8, 298 K): ∂ 6.75 (m, 1H, *ß*-H, carvone), ∂ 4.80 (d, 1H, C(CH_3)CH_2, carvone), ∂ 4.76 (d, 1H, C(CH_3)CH_2, carvone), ∂ 4.64 (m, 1H, poly(carbonate)), ∂ 3.38 (m, 1H, poly(ether)) (Fig. A3.7). MALDI-TOF mass spectrometry indicates the formation of polymeric units of formula $C_{12}H_{20}O_2(C_{11}H_{15}O_4)_nH$ where n = 3, 5, 7, 9, and 11.

3.9. References

1. Bouveault, L., *Bull. Soc. Chim.* **1903**, *29*, p 1051.

2. Porter, C. W.; Steel, C., Oxidation of the Grignard Reagent. *J. Am. Chem. Soc.* **1920**, *42*, pp 2650-2654.

3. Bailey, P. J.; Coxall, R. A.; Dick, C. M.; Fabre, S.; Henderson, L. C.; Herber, C.; Liddle, S. T.; Loroño-González, D.; Parkin, A.; Parsons, S., The First Structural Characterisation of a Group 2 Metal Alkylperoxide Complex: Comments on the Cleavage of Dioxygen by Magnesium Alkyl Complexes. *Chem. Eur. J.* **2003**, *9*, pp 4820-4828.

4. Lewiński, J.; Ochal, Z.; Bojarski, E.; Tratkiewicz, E.; Justyniak, I.; Lipkowski, J., First Structurally Authenticated Zinc Alkylperoxide: A Model System for the Epoxidation of Enones. *Angew. Chem. Int. Ed.* **2003**, *42*, pp 4643-4646.

5. Yamamoto, K.; Yamamoto, N., Epoxidation of α,β-Unsaturated Ketones Using Dialkylzinc-Oxygen Reagents. *Chem. Lett.* **1989**, *18*, pp 1149-1152.

6. Lewiński, J.; Śliwiński, W.; Dranka, M.; Justyniak, I.; Lipkowski, J., Reactions of $[ZnR_2(L)]$ Complexes with Dioxygen: A New Look at an Old Problem. *Angew. Chem. Int. Ed.* **2006**, *45*, pp 4826-4829.

7. Kubisiak, M.; Zelga, K.; Justyniak, I.; Tratkiewicz, E.; Pietrzak, T.; Keeri, A. R.; Ochal, Z.; Hartenstein, L.; Roesky, P. W.; Lewiński, J., Catalytic Epoxidation of Enones Mediated by Zinc Alkylperoxide/tert-BuOOH Systems. *Organometallics* **2013**, *32*, pp 5263-5265.

8. Leszczyński, M. K.; Justyniak, I.; Lewiński, J., Toward Factors Affecting the Degree of Zinc Alkyls Oxygenation: A Case of Organozinc Guanidinate Complexes. *Organometallics* **2017**, *36*, pp 2377-2380.

9. Lewiński, J.; Suwała, K.; Kaczorowski, T.; Gałęzowski, M.; Gryko, D. T.; Justyniak, I.; Lipkowski, J., Oxygenation of alkylzinc complexes with pyrrolylketiminate ligand: access to alkylperoxide versusoxo-encapsulated complexes. *Chem. Commun.* **2009**, pp 215-217.

10. Mukherjee, D.; Ellern, A.; Sadow, A. D., Remarkably Robust Monomeric Alkylperoxyzinc Compounds from Tris(oxazolinyl)boratozinc Alkyls and O_2. *J. Am. Chem. Soc.* **2012**, *134*, pp 13018-13026.

11. Ciriminna, R.; Lomeli-Rodriguez, M.; Demma Carà, P.; Lopez-Sanchez, J. A.; Pagliaro, M., Limonene: a versatile chemical of the bioeconomy. *Chem. Commun.* **2014**, *50*, pp 15288-15296.

12. de Carvalho, C. C. C. R.; da Fonseca, M. M. R., Carvone: Why and how should one bother to produce this terpene. *Food Chem.* **2006**, *95*, pp 413-422.

13. Liu, Y.; Dawe, L. N.; Kozak, C. M., Bimetallic and trimetallic zinc amino-bis(phenolate) complexes for ring-opening polymerization of rac-lactide. *Dalton Trans.* **2019**, *48*, pp 13699-13710.

14. Byrne, C. M.; Allen, S. D.; Lobkovsky, E. B.; Coates, G. W., Alternating copolymerization of limonene oxide and carbon dioxide. *J. Am. Chem. Soc.* **2004**, *126*, pp 11404-5.

15. Laprise, C. M. Synthesis of non-isocyanate polyurethanes from waste-derived fish oil. Master's thesis, Memorial University of Newfoundland, St. John's, CA, 2019.

16. 1,6-epoxycarvone IR and NMR spectra. *Spectral Database of Organic Compounds (SDBS) No. 53221*.

17. (R)-(–)-6,8-p-methandien-2-one IR and NMR spectra. *Spectral Database of Organic Compounds (SDBS) No. 2349*.

18. Anderson, T. S.; Kozak, C. M., Ring-opening polymerization of epoxides and ring-opening copolymerization of CO_2 with epoxides by a zinc amino-bis(phenolate) catalyst. *Eur. Polym. J.* **2019**, *120*, p 109237.

19. Ni, K.; Paniez-Grave, V.; Kozak, C. M., Effect of azide and chloride binding to diamino-bis(phenolate) chromium complexes on CO_2/cyclohexene oxide copolymerization. *Organometallics* **2018**, *37*, pp 2507-2518.

20. Andrea, K. A.; Kerton, F. M., Triarylborane-catalyzed formation of cyclic organic carbonates and polycarbonates. *ACS Catal.* **2019**, *9*, pp 1799-1809.

21. Darensbourg, D. J.; Yarbrough, J. C.; Ortiz, C.; Fang, C. C., Comparative kinetic studies of the copolymerization of cyclohexene oxide and propylene oxide with carbon dioxide in the presence of chromium salen derivatives. In situ FTIR measurements of copolymer vs cyclic carbonate production. *J. Am. Chem. Soc.* **2003**, *125*, pp 7586-7591.

3.10. Appendix

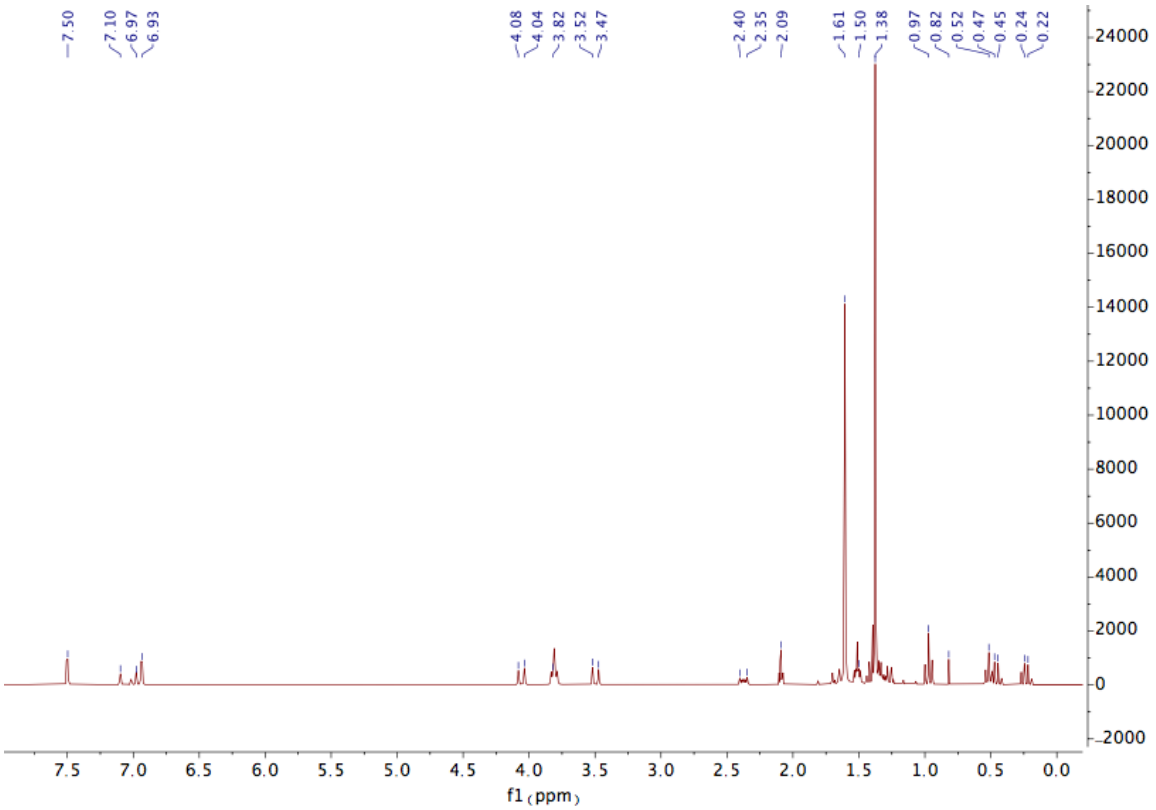

Fig. A3.1: Compound **2.1** in toluene-d_8. Presence of ethane (∂ 0.82) suggests adventitious water is present in the solvent, causing the appearance of peaks corresponding to the decomposition product. (500 MHz, 298 K)

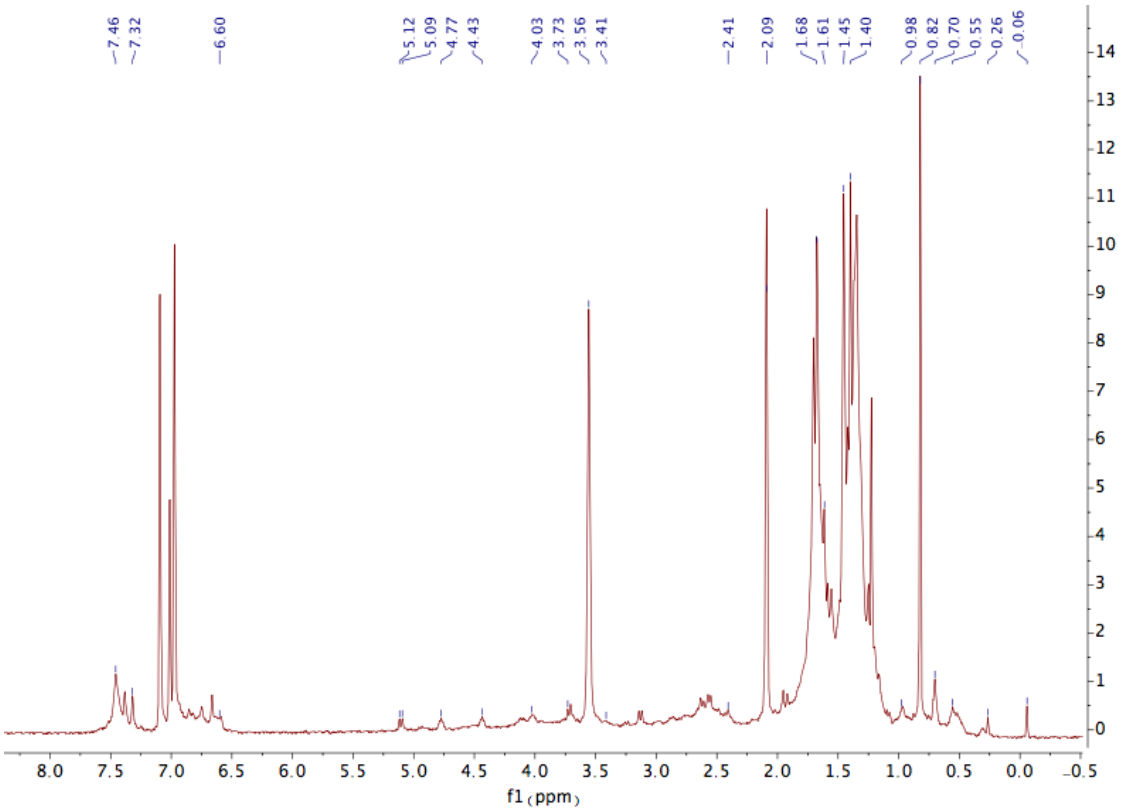

Fig. A3.2: Compound **2.1** and O_2 to form **3.1** in toluene-d_8. (500 MHz, 298 K)

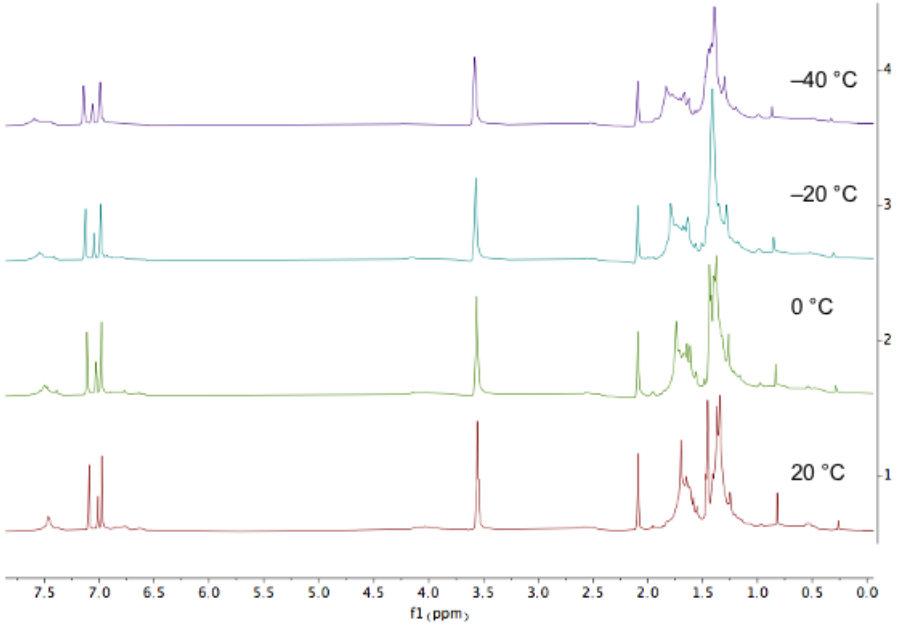

Fig. A3.3: Compound **3.1** at -20, 0, 20 and 40 °C in toluene-d_8. (500 MHz)

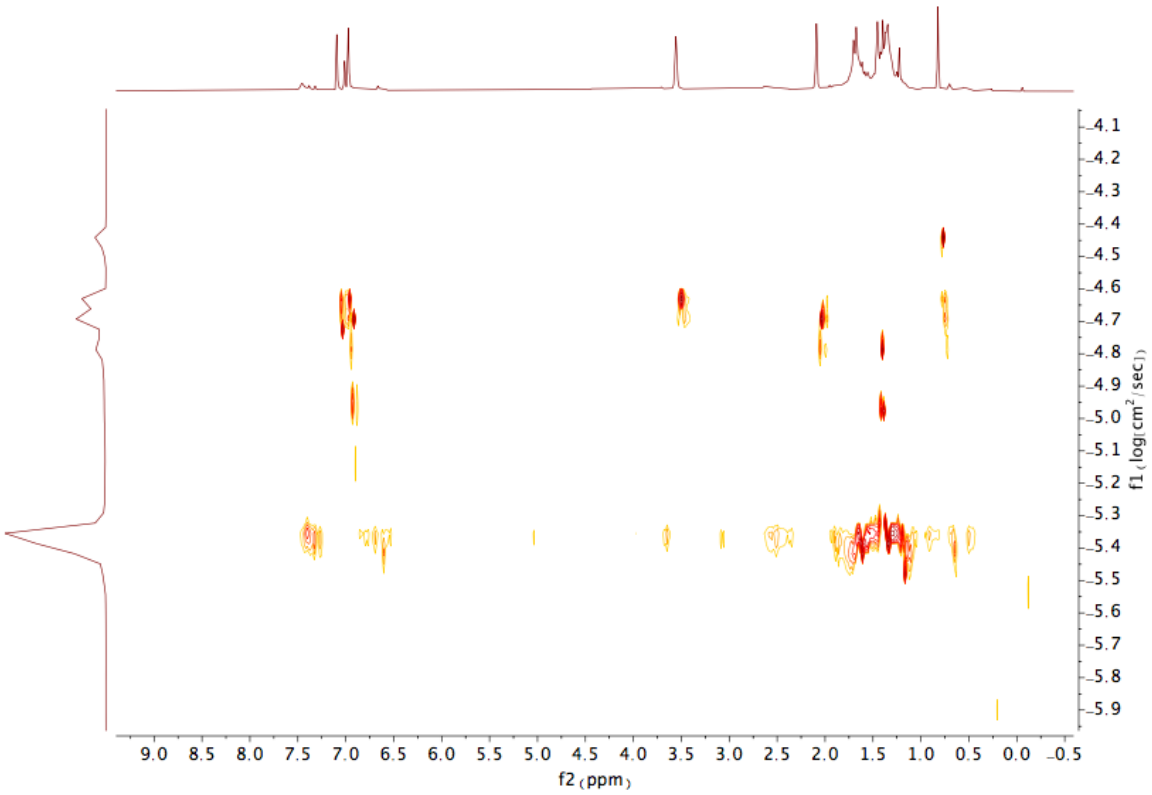

Fig. A3.4: DOSY spectrum of compound **3.1**, with solvent diffusion occurring between -4.4 and -5.1 log(cm^2 s^{-1}) (toluene and THF) and the remaining signals correspond to a single species that can be attributed to the reaction product of **2.1** and O_2 as a dimer. (toluene-*d*$_8$, 500 MHz, 298 K)

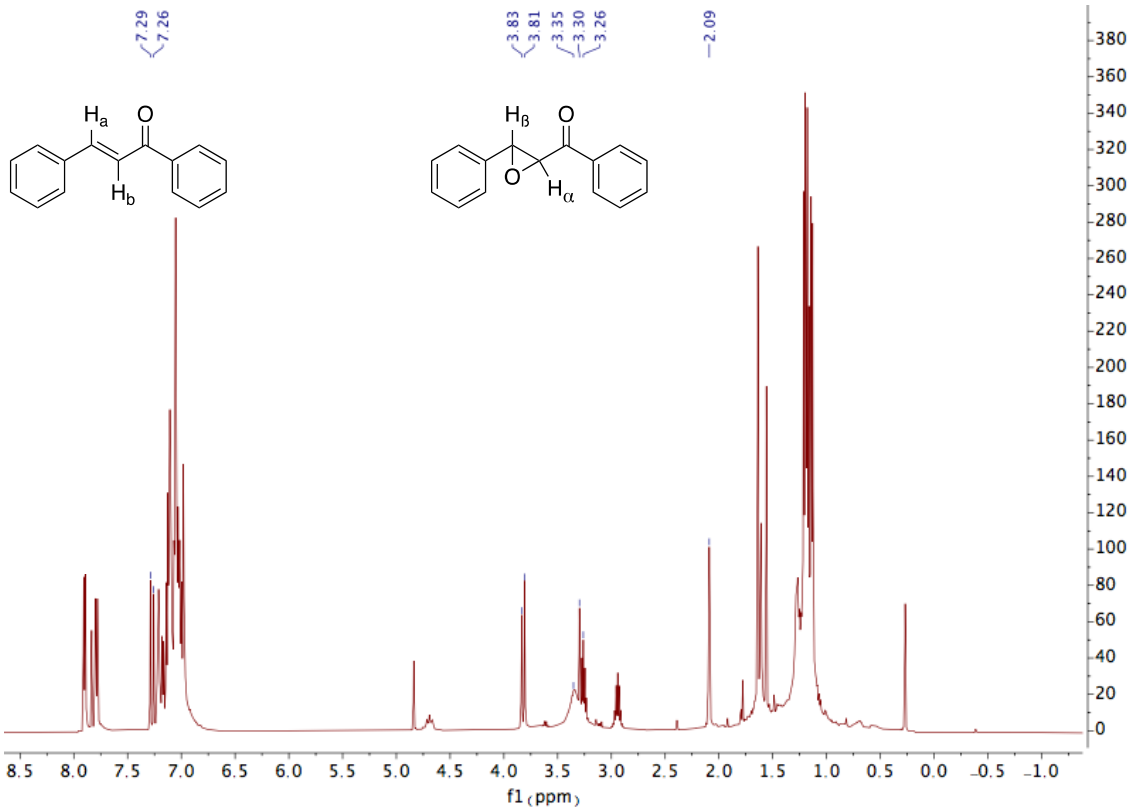

Fig. A3.5: Epoxidation of *trans*-chalcone by **1.41** in toluene-d_8. ∂ 3.36 corresponds to poly(ether), ∂ 3.82 ($H_ß$) and 3.28 ($H_α$) to the epoxide and ∂ 7.80 (H_a) and 7.29 (H_b) to the substrate. (300 MHz, 298 K)

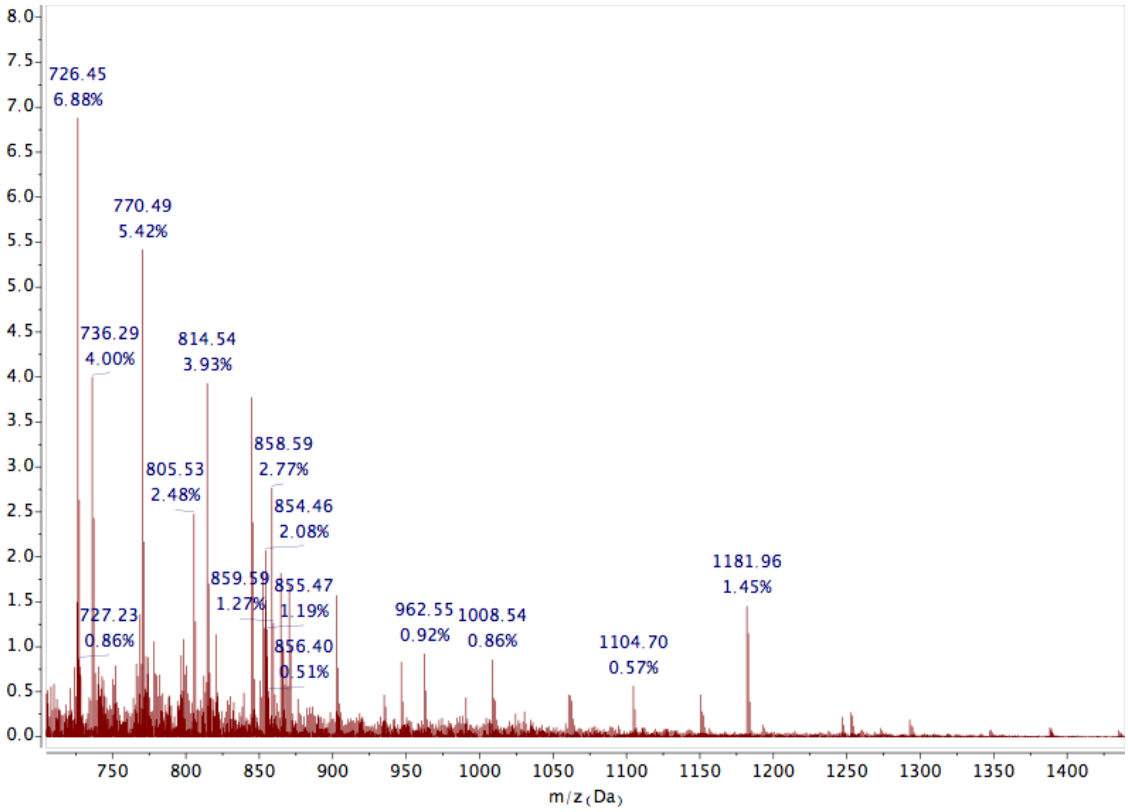

Fig. A3.6: MALDI-TOF MS of poly(*trans*-chalcone oxide). The predominant peak at m/z 726.45 represents tri(*trans*-chalcone oxide, M) initiated by an ethoxy group and terminated by a proton with lithium cation. m/z 962.55 and 1181.96 represent the subsequent M+1 and M+2 chalcone oxide units respectively. These peaks represent a very low percentage of the spectrum but the dominant material could not be identified.

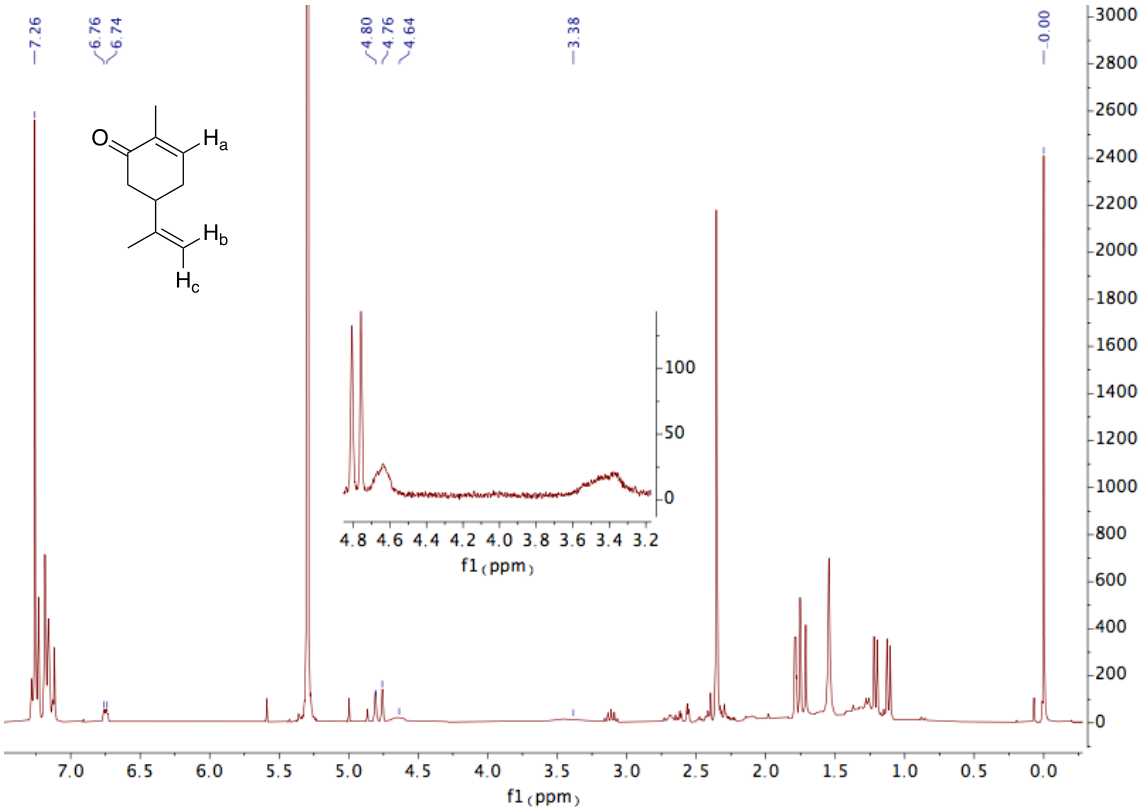

Fig. A3.7: One-pot epoxidation-polymerization of (R)-carvone by **1.41**. ∂ 6.75 (H_a), 4.80 (H_b) and 4.76 (H_c) correspond to carvone, ∂ 4.64 to poly(carvone carbonate) and ∂ 3.38 to poly(carvone ether). (toluene-d_8, 300 MHz, 298 K)

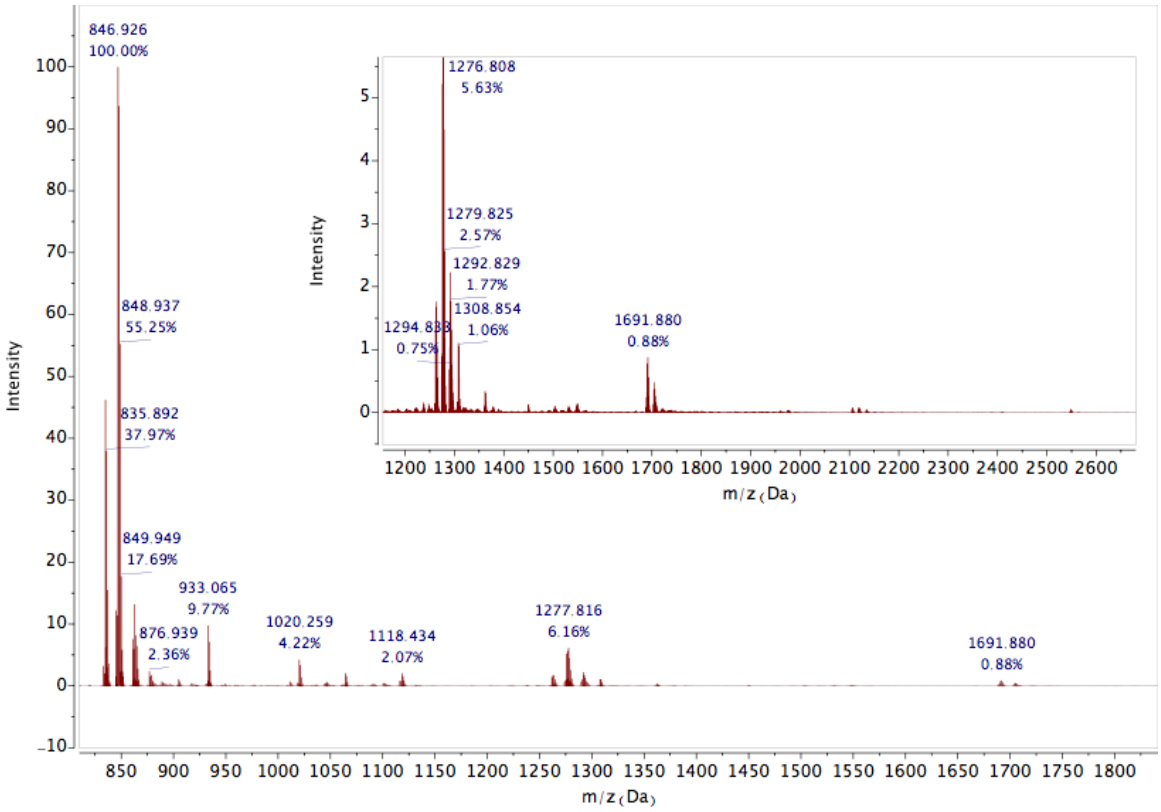

Fig. A3.8: MALDI-TOF MS of poly(carvone carbonate). The predominant peak at m/z 846.93 represents tri(carvone carbonate, M) initiated by an ethoxy group and terminated by a proton. m/z 1291.83 and 1691.88 represent the subsequent M+2 and M+4 carvone carbonate units respectively. Other regular polymer products, M+6 and M+8, can be identified as well.

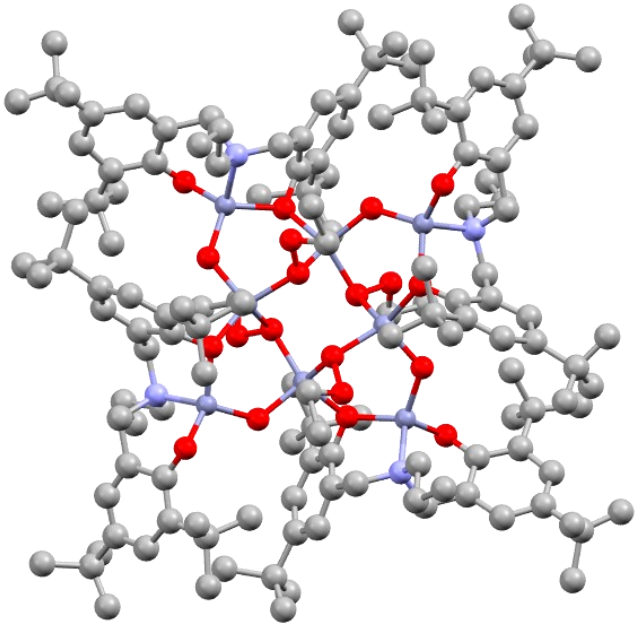

Fig. A3.9: Structure of **3.1** as determined via single crystal X-ray diffraction with hydrogen atoms omitted for clarity.

Table A3.1: Crystal data and structure refinement of compound **3.1**.

	3.1
Empirical formula	$C_{140}H_{225}N_4O_{20}Zn_8$
Crystal colour	Colourless
Formula weight	2807.19
Temperature/K	100
Crystal system	Triclinic
Space group	P -1
a/Å	22.087(2)
b/Å	22.1272(19)
c/Å	24.358(2)
α/°	67.739(8)
ß/°	81.662(8)
γ/°	89.736(7)
Volume/Å^3	10884.5(18)
Z	2
ϱ_{calc}g/cm^3	0.857
μ/mm^{-1}	0.907
F(000)	2986
Crystal size/mm^3	0.1 × 0.1 × 0.1
Radiation	MoKα (λ = 0.71073
2 θ range for data collection/°	3.196 to 41.632
Index ranges	–22 ≤ h ≤ 22, –22 ≤ k ≤ 22, –24 ≤ l ≤ 24
Reflections collected	90077
Independent reflections	22787 [R_{int} = 0.2331, R_{sigma} = 0.2079]
Data/restraints/parameters	22787/1608/1549
Goodness-of-fit on F^2	1.354
Final R indexes [I>=2σ(I)]	R_1 = 0.1687, wR_2 = 0.4220
Final R indexes [all data]	R_1 = 0.2395, wR_2 = 0.4739
Largest diff. peak/hole / e Å^{-3}	1.485/–1.480

Table A3.2: Selected bond lengths from structural data of **3.1**.

Atom	Atom	Length/Å	Atom	Atom	Length/Å
Zn1	O2	2.035(13)	Zn7	O17	2.049(13)
Zn1	O12	1.968(14)	Zn7	O19	1.996(13)
Zn2	O4	2.047(14)	Zn8	O8	2.087(13)
Zn2	O9	1.982(14)	Zn8	O12	1.973(14)
Zn3	O6	2.077(14)	Zn8	O13	2.020(14)
Zn3	O10	1.951(14)	Zn8	O19	2.046(13)
Zn4	O8	2.005(13)	O13	O14	1.492(19)
Zn4	O11	1.994(13)	O14	C133	1.49(3)
Zn5	O2	2.010(14)	C133	C134	1.58(3)
Zn5	O9	1.995(14)	O15	O16	1.469(17)
Zn5	O13	2.008(14)	O16	C135	1.52(3)
Zn5	O15	2.010(13)	C135	C136	1.69(3)
Zn6	O4	2.034(13)	O17	O18	1.488(17)
Zn6	O10	1.972(14)	O18	C137	1.48(2)
Zn6	O15	2.039(13)	C137	C138	1.55(3)
Zn6	O17	2.001(13)	O19	O20	1.575(18)
Zn7	O6	2.047(13)	O20	C139	1.45(2)
Zn7	O11	1.971(13)	C139	C140	1.67(3)

This data represents only the core structure shown in Fig. 3.3 as the quality of data decreases greatly further from the centre.

Table A3.3: Selected bond angles from structural data of **3.1**.

Atom	Atom	Atom	Angle/°	Atom	Atom	Atom	Angle/°
O12	Zn1	O2	109.0(6)	Zn5	O2	Zn1	122.0(7)
O9	Zn2	O4	111.8(6)	Zn6	O4	Zn2	120.3(6)
O10	Zn3	O6	109.7(6)	Zn7	O6	Zn3	119.3(7)
O11	Zn4	O8	112.4(5)	Zn4	O8	Zn8	120.4(6)
O2	Zn5	O15	135.2(6)	Zn2	O9	Zn5	123.7(8)
O9	Zn5	O2	104.4(6)	Zn3	O10	Zn6	127.6(8)
O9	Zn5	O13	113.5(6)	Zn7	O11	Zn4	124.7(6)
O9	Zn5	O13	101.8(6)	Zn1	O12	Zn8	127.6(7)
O13	Zn5	O2	107.0(6)	Zn5	O13	Zn8	115.1(7)
O13	Zn5	O15	94.6(6)	O14	O13	Zn5	106.6(10)
O4	Zn6	O15	107.7(6)	O14	O13	Zn8	111.6(9)
O10	Zn6	O4	106.4(6)	O13	O14	C133	106.9(14)
O10	Zn6	O15	112.9(5)	Zn5	O15	Zn6	113.6(6)
O10	Zn6	O17	101.6(6)	O16	O15	Zn5	113.6(10)
O17	Zn6	O4	132.6(5)	O16	O15	Zn6	104.3(8)
O17	Zn6	O15	95.1(5)	O15	O16	C135	105.3(14)
O6	Zn7	O17	109.6(6)	Zn6	O17	Zn7	111.9(6)
O11	Zn7	O6	104.5(5)	O18	O17	Zn6	110.4(9)
O11	Zn7	O17	110.5(5)	O18	O17	Zn7	106.4(8)
O11	Zn7	O19	103.8(5)	C137	O18	O17	103.6(13)
O19	Zn7	O6	134.7(5)	Zn7	O19	Zn8	116.0(6)
O19	Zn7	O17	92.3(5)	O20	O19	Zn7	110.3(8)
O12	Zn8	O8	107.7(6)	O20	O19	Zn8	106.1(8)
O12	Zn8	O13	100.2(6)	C139	O20	O19	104.0(13)
O12	Zn8	O19	113.3(5)	O14	C133	C134	104.9(18)
O13	Zn8	O8	136.5(6)	O16	C135	C136	99.1(18)
O13	Zn8	O19	91.3(5)	O18	C137	C138	103.6(16)
O19	Zn8	O8	106.9(5)	O20	C139	C140	101.0(16)

This data represents only the core structure shown in Fig. 3.3 as the quality of data decreases greatly further from the centre.

Chapter 4

Iron catalyzed synthesis of poly(carbonate), poly(ester), and complex terpolymers

Statement of Co-Authorship

Part of this chapter has been published under the title "*Iron Complexes for Cyclic Carbonate and Polycarbonate Formation: Selectivity Control from Ligand Design and Metal-Center Geometry*" in *Inorganic Chemistry*, **2019**, *58*, 16, 11231 – 11240.

Authors: Kori A. Andrea, Erika D. Butler, Tyler, R. Brown, Timothy S. Anderson, Dakshita Jagota, Cassidy Rose, Emily M. Lee, Sarah D. Goulding, Jennifer N. Murphy, Francesca M. Kerton and Christopher, M. Kozak.

This article was a group effort combining the work of several graduate and undergraduate student co-authors from the research groups of Professors Kozak and Kerton.

My contribution (listed in the paper as 4th co-author) was the thorough screening of reactions catalyzed by compounds **4.8** – **4.10** for cyclic products and fully characterizing them, including crystallography for compounds **4.8** and **4.10**, and other instances involving other catalysts listed below that will be highlighted in the text as necessary.

Kori A. Andrea took the role of project leader and coordinated the efforts of all the co-authors. She contributed to all aspects of the project including experiment design and

conducting polymerization and kinetics studies, literature review, data collection and analysis, manuscript preparation and the addressing the peer-review comments.

Erika D. Butler synthesized compounds **4.1a**, **4.2**, **4.5** and **4.6** and performed initial screening reactions.

Tyler R. Brown synthesized compounds **4.8 – 4.10** and performed initial screening reactions.

Dakshita Jagota assisted Kori Andrea with compound synthesis and characterization of iron compounds and reaction products.

Cassidy Rose assisted Timothy Anderson with iron compound synthesis and reactions.

Emily M. Lee and Sarah D. Goulding were WISE-SSEP students who assisted Kori Andrea with compound synthesis and characterization of iron compounds and reaction products.

Jennifer N. Murphy performed the crystallography for compounds **4.1b**, **4.2**, **4.11** and **4.14b**.

Francesca M. Kerton and Christopher M. Kozak are the principal investigators and provided the initial idea of the project. Drs. Kerton and Kozak oversaw data analysis, experimental design and approach, manuscript preparation and submission and co-author supervision.

Introduction

4.1. Iron catalysts

The use of carbon dioxide as a C1 feedstock was discussed in earlier Chapters. Similar to the zinc-catalyzed transformations highlighted in Chapter 2, first row transition metal catalysts have demonstrated excellent ability to incorporate carbon dioxide into polymers or smaller molecules such as cyclic carbonate. Among the more attractive metals for these processes in recent years is iron. Iron is typically benign both environmentally and biologically and is among the most abundant metals on earth. Control of the Lewis acidity of the metal(s) is essential toward catalytic activity and careful ligand design can manipulate these properties significantly to create favourable conditions for controlled polymer synthesis.[1] In ring-opening polymerization reactions, the catalytic ring-opening process is dependent upon the energy required to exploit the ring-strain of the compound. Temperature is sometimes a viable switch in polymer synthesis; however, this also limits the segmentation to first consuming the monomer with a lower activation energy and typically results in gradient copolymers. More recent reports have detailed catalytic systems that can achieve this control through other means such as redox activation and electrochemical switching and will be discussed below. Ultimately the goal of the project discussed here was to utilize complexes **4.8** and **4.9** (Fig. 4.1) from among several that were reported by the Kerton and Kozak groups for the synthesis of simple poly(ether)s and poly(ester)s, and to use these findings to synthesize more complex copolymers containing segments of each.[2] As

oxidation switching with these systems was likely not viable, more conventional variables for co- and terpolymer control were investigated.

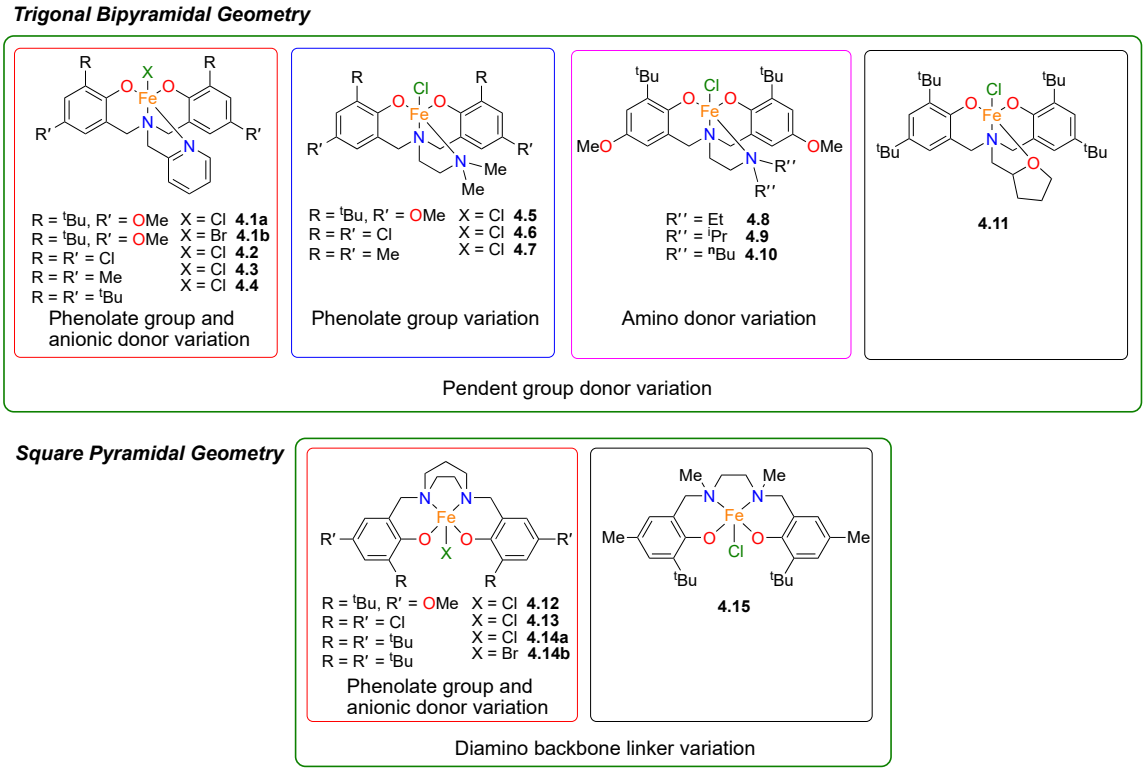

Fig. 4.1: Iron complexes reported by Kerton and Kozak. Compounds **4.8** and **4.9** will be discussed in this chapter. Reprinted with permission from Kori A. Andrea et al., *Inorg. Chem.*, **2019**, *58* (16), 11231 – 11240. Copyright © 2019 American Chemical Society.

4.2. Iron catalyzed ROP reactions

Poly(lactic acid) (PLA) has been produced commercially since 1881 but ring-opening polymerization was not reported until 1932 by Carothers.[3] Some of the earlier metal-based catalysts involved simple metal salts and oxides and found that the more nucleophilic anions

like alkoxides and carbanions were most effective at ring-opening the lactide, but with poor control, while the others were either slow or ineffective.[4-6] Over the past 30 years there has been an extensive study of PLA production catalyzed by metal-based catalysts using nearly every metal on the periodic table and these efforts have been reviewed extensively.[7-10] Commercial production of PLA is primarily catalyzed by tin octoate, tin(II) 2-ethylhexanoate ($Sn(Oct)_2$) due to ability of the catalyst to produce polymers with molecular weights up to 10^5 g mol^{-1}.[9] Although this particular compound has been deemed a safe food additive by the FDA, the toxicity of tin compounds prevents PLA produced by $Sn(Oct)_2$ from being used for biomedical applications. In order to diversify the potential uses of PLA, more benign catalysts have been developed to reduce or eliminate the downsides of heavy metal-based catalysis. Complexes of iron will be the focus of this Chapter.

In 2013 the Byers group reported iron bis(imino)pyridine complexes for ROP of lactide (Fig. 4.2).[11] Complexes of similar design were effective for many other types of polymerization like ethylene polymerization, hydrogenation/hydrosilylation of alkenes and intermolecular cycloadditions and thus were a candidate for lactide polymerization as well. In fact, this report was the first to utilize a bis(imino)pyridine transition metal complex for lactide ROP. Furthermore, bis(imino)pyridine complexes are suitable for both stabilizing both Fe(II) and Fe(III) oxidation states, allowing for studying the effect of metal oxidation state on ROP catalysis. Iron(II) complex **4.16** demonstrated living polymerization activity at 0.2 mol% catalyst loading (lactide at 0.25 M in CH_2Cl_2) with 88% conversion after 3 h at 25 °C, but polymer molecular weight dispersities of $Đ$ = 1.18 were slightly higher than expected for typical living polymerization activity. Up to 15 sequential additions resulted in linear

increase of molecular weight, consistent with a living polymerization process, reaching molecular weights up to 75,000 g mol^{-1}. Molecular weight was in good agreement with the theoretical values for single alkoxide initiation with the exception of **4.18**, which suggested dual initiation and is likely a result of similar electronic influence of the propagating polymer (lactic acid conjugate base pK_a = 18) and neopentyl alcohol (pK_a = 16) whereas the 4--methoxyphenol is much more acidic with pK_a of 10.2.[11] Dispersities for all other catalytic systems were from 1.21 – 1.33 and attributed to either slow initiation processes or chain transfer encouraged by impurities in the lactide.

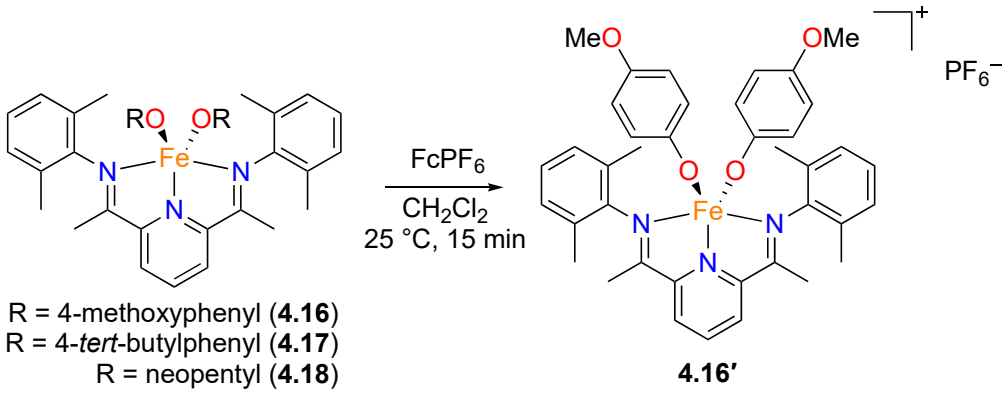

Fig. 4.2: Iron bis(imino)pyridine complexes for lactide ROP[11].

Isolation of crystals suitable for XRD was only possible with **4.16′** so this was utilized to see if the oxidation of the species *in situ* would allow for control of the polymerization. Although there are examples of bimetallic catalysts that demonstrate oxidative switches (discussed below) there were, until this point, few examples where the active site was responsible for the redox switch as well. **4.16′** was entirely inactive toward lactide ROP under the above conditions over 24 h presenting the first redox switchable iron complex for lactide polymerization. The switch was demonstrated by allowing **4.16** to polymerize lactide until

approximately 25% conversion was reached, then adding $FcPF_6$ to oxidize to the catalyst to compound **4.16′** where upon polymerization halted. Reducing **4.16′** back to **4.16** with $CoCp_2$ resulted in reactivation of polymerization. This process could be repeated multiple times with minimal effect on the physical properties of the polymers produced. As there has been a move to use more environmentally and biologically benign metals for catalysis, these iron systems represent an important step toward this goal.

In 2017, air-stable iron(III) salen complexes were reported by Duan et al. for the ROP of cyclic esters (Fig. 4.3).[12] Salen type ligands have been highlighted in earlier chapters for CO_2 and epoxide copolymerization. This report described the first polymerization of lactones by air-stable iron-salen complexes. The design was such that the backbone, E, could be altered to observe the effect of backbone flexibility on the polymerization activity. The electronic effect of the substituents on the phenolate groups was considered with a narrower scope. Throughout the screening reactions, propylene oxide (PO) was noted to be a necessary component for initiation as the nucleophilicity of the chloride anion was insufficient toward lactide. It was postulated that the alkoxide generated through PO ring-opening was the initiator for polymerization and the corresponding end-group could be identified via ^{1}H and ^{13}C NMR spectroscopy. Reactions involving less than 50% PO (v/v in toluene) were slower than any concentration above 50%, at which point reactivity plateaus. At 0.1 mol% catalyst loading, 0.4 g LA in 2 mL PO, **4.17** and **4.18** showed similar activity at 60 °C while **4.19** proved the most effective even at 25 °C. The increased activity was attributed to the flexible backbone of **4.19**. Among these three, the products were primarily isotactic PLA (P_m, the probability of finding *meso* diads, of 0.78, 0.77 and 0.70 for **4.17**, **4.18**

and **4.19** respectively) suggesting that the stereocentres of **4.18** are relatively inconsequential. Instead, elevated temperatures reduced the stereoregularity, suggesting a chain-end mechanism. The activity of the complexes was primarily affected by the aryl substituents, with **4.20** showing 80% conversion over 15 h, **4.22** the highest at 90% conversion within 2 h, and the unsubstituted **4.24** being inactive in 6 h. The methylated bridged compounds **4.21** and **4.23** showed no difference in activity compared to their ethylene bridged analogues. Molecular weights were inconsistent with theoretical values, **4.20** – **4.23** showed lower than expected, suggesting chain transfer or premature termination processes are common, while compounds **4.17** – **4.24** and **4.24** (extended reaction time of 18 h) exhibited higher than expected molecular weights, likely a result of slow initiation or reaction with PO. Dispersities in all cases were fairly broad, 1.38 – 3.46, with the exception of **4.21**, giving dispersity of 1.13 at 49% conversion with low molecular weight (4,900 g mol^{-1}).

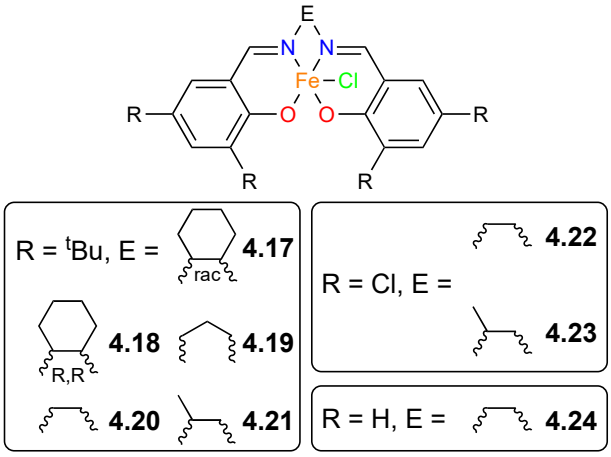

Fig. 4.3: Iron salen complexes reported by Duan for ROP of cyclic esters.[12]

In 2019, Jones and coworkers reported air-stable iron(III) acetate compounds, the first examples of iron(III) acetate catalyzed polymerization and CO_2/epoxide coupling

catalysts.[13] Similar to the report by Duan above, the ligand effect was investigated but also included variation of the amine/imine donor. Salalen, salen and salan ligands were studied to investigate the structure-activity relationship of these classes (Fig. 4.4). As Kerton had reported that the flexibility of the amino-bis(phenolate) ligand was crucial to high activity toward CO_2/epoxide chemistry, Jones believed that an extensive study on ligands applicable for this type of reaction with other metals was prudent.[2]

rac-Lactide ROP reactions were conducted at 100 °C for 24 h with 1 mol% catalyst loading and requiring 1 mol% of each BnOH and NEt_3. They proposed that the OAc anion is inactive for initiation but addition of NEt_3 to deprotonate BnOH to form $HNEt_3^+$ cation abstracts the $^-$OAc anion, generating the metal alkoxide species from the $^-$OBn anion. Generally, the salalen species exhibited low activity and no selectivity. Extension of the diamine backbone to propylene (**4.29**) decreased conversions. Increasing the bulk at the aryl positions of the ethylene diamine derivatives, however, did improve activity slightly, 26% conversion (**4.25**) increasing to 57 and 60% (**4.26** and **4.27** respectively). **4.28** was nearly inactive, converting at 5%. Molecular weights were lower than anticipated for all polymers but dispersities were fairly narrow (1.10 – 1.26).

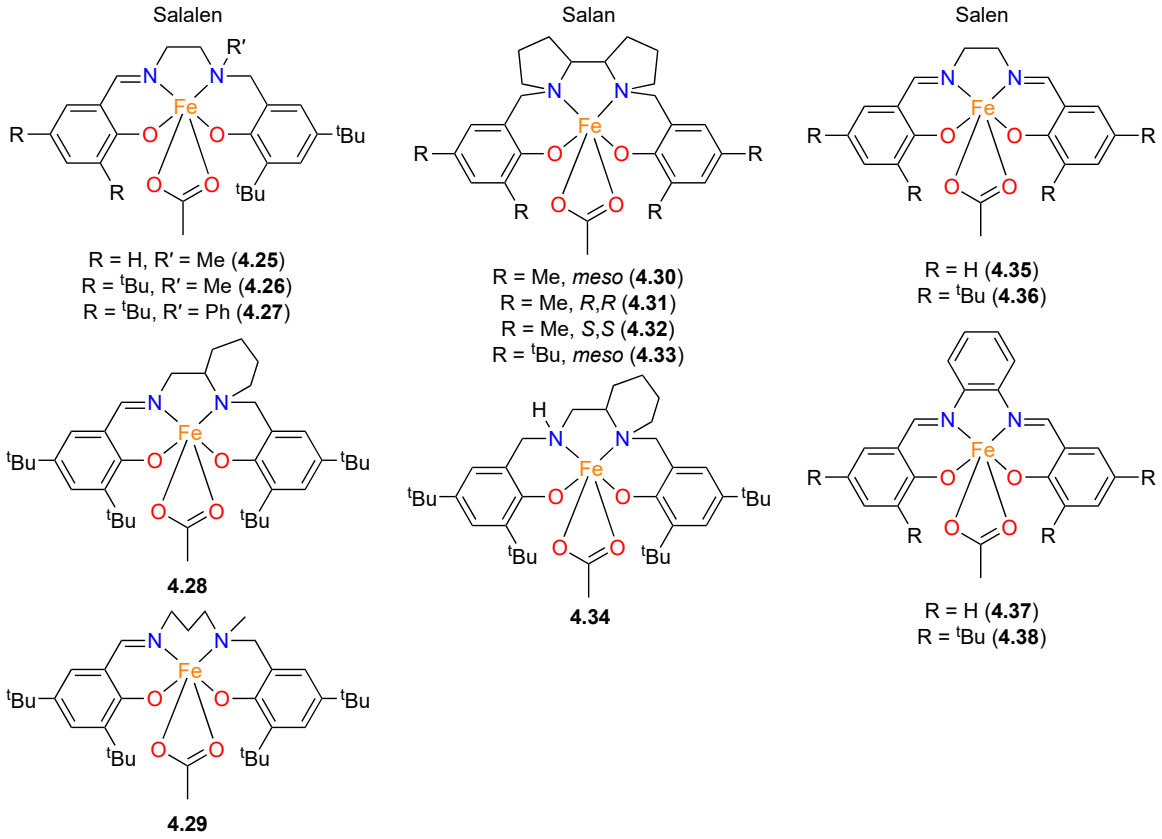

Fig. 4.4: Salalen, salan and salen iron acetate complexes reported by Jones.[13]

The salan complexes generally exhibited enhanced reactivity compared to the salalen derivatives. Reduced steric bulk at the aryl positions improved reactivity, **4.30** converting 92% and **4.33** just 52%. Enantiopure analogues of the salan (**4.31** and **4.32**) were less active than the *meso* species at 21 and 32% conversion respectively, which they attribute to differences in the solid-state structure. The dispersities **4.30** – **4.33** were between 1.20 – 1.30. The most active species was **4.34**, a reduced analogue of **4.38**, reaching 93% conversion. Slight preference for isotactic poly(ester) (P_m = 0.66) was observed for **4.34**. Complexes **4.33** and **4.34** exhibited the narrowest dispersities of all complexes at 1.09. The salen complexes exhibited the highest activities overall, with **4.35**, **4.37** and **4.38** converting at 95%, 94% and

89% respectively, but moderate dispersities of 1.49, 1.65 and 1.46. All salen species also exhibited slight isotactic preference (P_m 0.56 – 0.71) with **4.36** and **4.38** producing the highest. Complex **4.36** was significantly less active at 67% conversion but gave a narrow dispersity of 1.16. With the exception of **4.30**, all molecular weights were lower than the theoretical calculations, and this was explained by ethoxide initiated polymerization from ethanol impurity in the catalytic species and transesterification reactions. The most active species (**4.30**, **4.34**, **4.37**, **4.38**) were also investigated at 80 °C maintaining high conversions (82 – 96%) and narrowing of dispersities slightly in all cases. Here, molecular weights were all lower than anticipated and again attributed to ethanol impurity while transesterification could not be observed via MALDI-TOF MS analysis.

The reactivity of these species toward CO_2 and epoxide coupling was also investigated. All reactions were performed neat at 0.08 mol% catalyst loading, 0.64 mol% tetrabutylammonium chloride (Bu_4NCl), 10 bar CO_2 and 80 °C for 24 h. Initially, CHO was used as the epoxide and in all cases where conversion was observed, the primary product was *cis*-CHC with small amounts (0 – 6%) *trans*-CHC and occasionally poly(ether) (14 – 37%). No poly(carbonate) was observed. Again, a co-catalyst was necessary to initiate the ring-opening of the monomer. While Bu_4NCl alone was an active catalyst (43% conversion) the selectivity for *cis*-CHC was lower at 83% with 17% PCHO. Similarly, using $Fe(OAc)_2$ as the catalyst led to a conversion of 48% but just 76% selectivity and 23% PCHO. Among the iron-salalen complexes (**4.25** – **4.29**) the highest activities were achieved with those with the most flexible backbones, namely **4.29** at 53%, and the bulky phenolate-substituted **4.26** just behind at 52%. All of these species were able to achieve near complete selectivity for *cis*-CHC. The

iron-salan complexes (**4.30** – **4.34**) were generally better catalysts for this reaction. Species **4.30** was a poor catalyst converting just 30% with 57% selectivity for *cis*-CHC and 37% conversion to PCHO. The poor selectivity was attributed to impurities in the species. The *R,R* stereoisomer **4.31** was highly active relative to the other species reaching 60% conversion with complete selectivity, while the *S,S* isomer **4.32** reached 47%, again selective for *cis*-CHC. Species **4.33** was selective toward *cis*-CHC and converted at 45% while **4.34** proved the most effective catalyst in the study converting 66% selectively for *cis*-CHC. They speculated that H-bonding in the backbone is responsible for encouraging reactivity by interacting with the incoming epoxide/CO_2. Lastly, the iron-salen species were investigated and it was found that the planar **4.37** and **4.38** were more active than their less planar analogues (**4.35** and **4.36** respectively). While **4.35** and **4.36** were highly selective for *cis*-CHC, their conversions were lower than the salan species at 28% and 43%. Species **4.37** converted 52% selectively and **4.38** at 59%, the third highest in the study, but with reduced selectivity at just 84%, the remaining 16% identified as PCHO.

As **4.34** was identified as the most effective species toward CO_2 and epoxide coupling, other co-catalysts were screened but found to be less active when using Bu_4NBr, PPNCl, or tetrabutylammonium acetate (TBAOAc), although the former two retained selectivity for *cis*-CHC. From here, the substrate scope was expanded by using PO, styrene oxide (SO), epichlorohydrin (ECH), phenylglycidyl ether (PGE) and allylglycidyl ether (AGE). Under the same conditions as above, all epoxides demonstrated complete selectivity for the *cis*-carbonate products. PO resulted in a conversion of 79%, an anticipated result as it is less sterically hindered than CHO. Using SO led to a conversion of 66%, more in line with

CHO and attributed again the steric influence of the epoxides. The epoxides containing electron-withdrawing groups were also quite active, ECH at 75% while PGE and AGE reached 97% and 93% respectively.

4.3. Iron catalyzed CO_2 and epoxide copolymerization

While there are some examples of iron catalysts for CHO and CO_2 copolymerization (see Chapter 1), and coupling of different epoxides with CO_2 to form cyclic carbonate shown above, it was not until recently that catalysts capable of coupling different epoxides for polymer formation were reported. To date, these are iron-corrole catalysts reported by Nozaki in 2013.[14] The trianionic corrole ligand framework was paired with either anionic or neutral axial ligands to afford iron complexes of +4 and +3 oxidation state respectively (Fig. 4.5). These catalysts were applied to copolymerization of epoxides (CHO, PO, and GPE) and CO_2. Using **4.39** (0.05 mol% per iron) and 0.025 mol% PPNCl in neat PO, 20 bar CO_2 at 60 °C, polymer could be formed selectively in 1 h at 51% conversion. While carbonate selectivity was low (17%), the molecular weight of the polymer was 29,000 g mol^{-1} with a moderate dispersity of 1.26. The complex was inactive without PPNCl co-catalyst and increases in co-catalyst loading increased carbonate selectivity while decreasing selectivity for polymer formation. Decreasing the temperature to 40 °C improved carbonate content (23%) but reduced activity significantly showing 7% conversion. Increasing the temperature to 80 °C resulted in modest increase in conversion (65%) and a decrease in carbonate selectivity (11%). At 60 °C, decreasing CO_2 pressure to 5 bar resulted in 59% conversion to polymer but greatly reduced carbonate incorporation (6%). Increasing pressure to 50 bar greatly

reduced activity (11%) with a modest increase in carbonate selectivity of 29%. Compound **4.41**, containing the chloride ligand, was less active than **4.39** under the initial conditions while **4.42**, the Fe(III) species, was slightly more active. Carbonate incorporation and dependency on reaction conditions were consistent for each. Compound **4.40** use was limited, but at 5 bar, 60 °C, 0.05 mol% per iron and 0.025 mol% PPNCl produced 19% polymer at 60% carbonate incorporation over 12 h with only 47% selectivity for polymer over propylene carbonate. While selectivity for carbonate linkages was generally low, these present the first examples of iron-catalyzed PO and CO_2 copolymerization.

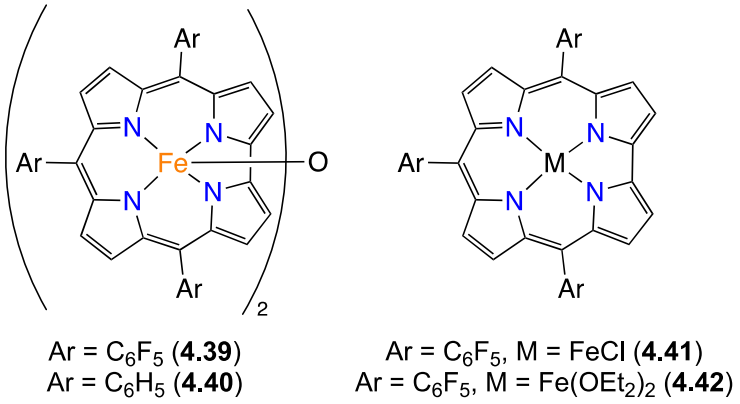

Fig. 4.5: Iron(IV) and iron(III)-corrole complexes reported by Nozaki for epoxide and CO_2 copolymerization.[14]

Glycidyl phenyl ether was also examined with **4.39**. Under the initial conditions above, 20% of the monomer could be converted to polymer (9% carbonate) in 1 h with no evidence of cyclic carbonate formation. Increasing the reaction time to 49 h resulted in complete conversion to polymer (11% carbonate) with moderate molecular weight (13,700 g mol^{-1}) and very high dispersity of 7.01. Increasing the pressure to 50 bar CO_2 improved

carbonate content (22%) but reduced molecular weight to 5,100 g mol^{-1} and doubled the dispersity to 14.4. While these results are limited in control, they demonstrate an increased scope of epoxide that had to this point been elusive for iron catalyzed copolymerization with CO_2. Although this report remains the sole example of the incorporation of these epoxides in CO_2 and epoxide copolymerization, it is an important step in polymer synthesis and their use in other polymerization reactions, such as coupling with cyclic esters, will be discussed below.

4.4. Copolymerization and terpolymerization reactions

In the area of multimer polymerization processes (polymers formed from more than one reagent e.g. the poly(carbonate) comprised of epoxides and CO_2 discussed above) there has been a desire to develop systems that can selectively control the propagation of each monomer, ideally in one pot, from different branches of polymer synthesis. While there are several examples in nature of highly efficient catalysts for these processes, allosteric control, the synthetic chemists approach is primarily through metal-based catalysis.[1] Among the control processes are mechanochemical and photochemical but the focus here will be on chemical control and electrochemical systems. In 2006, the first report of redox-facilitated polymerization was reported by Gibson and Long. The catalyst, **4.43**, was a titanium-salen species with two tethered ferrocene moieties[15] (Fig. 4.6). The neutral complex was able to polymerize *rac*-lactide 30 times faster than its oxidized analogue. Although both were slow (the neutral species converting 50% in 50 h) each species produced atactic polymer with fairly narrow dispersities of 1.2. The rate change was also reversible *in situ* through oxidation

of the species by AgOTf or reduction using the one-electron reductant Cp^*_2Fe. Notably, neither AgOTf nor Cp^*_2FeOTf were active toward polymerization, suggesting that the ferrocene moieties were not directly participating in the polymerization. As the switch is reversible and the rate of polymerization is comparable almost immediately after a switching cycle, they propose that it is in fact the influence of the iron oxidation state on the electronic nature of the titanium centre that dictates the rate of polymerization, rather than inhibition by the triflate counterion. This may be due to the mechanism of polymerization relying upon polymer-chain dissociation which is inhibited with increased Lewis acidity. Despite the fact that lactide polymerization could not be completely halted through this process, it proved a key finding for redox active catalysts in other systems.

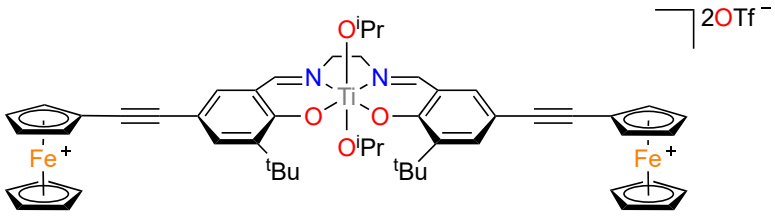

4.43

Fig. 4.6: Oxidized titanium-ferrocene bifunctional catalyst utilized by Gibson and Long for lactide polymerization.[15]

In 2011, the Diaconescu group first published yttrium and indium 10-di(2-*t*-butyl-6-diphenyl-phosphiniminophenoxy)ferrocene (phosfen) complexes.[16] The interchange between the neutral and ionic structures were reversible (Fig. 4.7) via oxidation and reduction by ferrocene tetra(pentafluorophenyl)borane ($FcBAr^F$) and cobaltocene ($CoCp_2$) respectively. These complexes were catalysts for ROP of cyclic esters and trimethylene carbonate. Notably, **4.44** with 100 equiv. L-lactide resulted in 74% conversion

after 3 h at 25 °C in THF while the ionic species **4.44′** was completely inactive under these conditions. Switching of the catalysts *in situ* from **4.44** to **4.44′** resulted in very clear halting of conversion (Fig. 4.8), which could be re-initiated by reduction to **4.44**. This is consistent with the report by Gibson and Long above. All polymers produced were of narrow dispersities between 1.03 and 1.08. Complexes **4.45** and **4.45′** were mostly inactive toward cyclic ester ROP, therefore, trimethylene carbonate (TMC) was investigated instead. **4.45** with 100 equiv. TMC at 25 °C over 24 h in benzene-d_6 resulted in only 2% conversion while **4.45′** under the same conditions led to 49% conversion to polymer. Unlike the yttrium species and the titanium compounds (**4.43** and **4.43′**) the selectivity for polymer propagation improves with the ferrocenium analogue. The products were not characterized. For comparison, **4.44** and **4.44′** were utilized under these conditions but resulted in complete conversion in minutes. Reducing the temperature to –78 °C in THF was consistent with the L-lactide results above, with **4.44** having 29% conversion and **4.44′** just 4%.

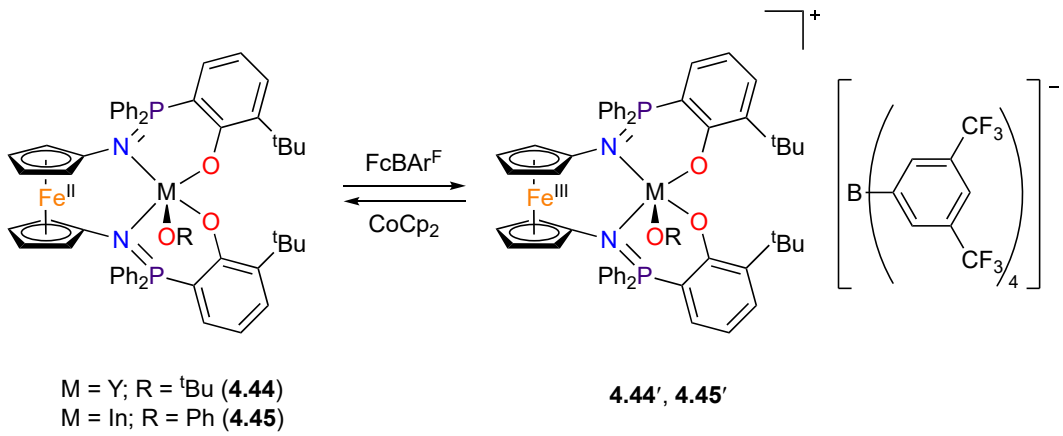

M = Y; R = ^{t}Bu (**4.44**)
M = In; R = Ph (**4.45**)

4.44′, **4.45′**

Fig. 4.7: Yttrium and indium phosfen complexes for ROP reactions.[16]

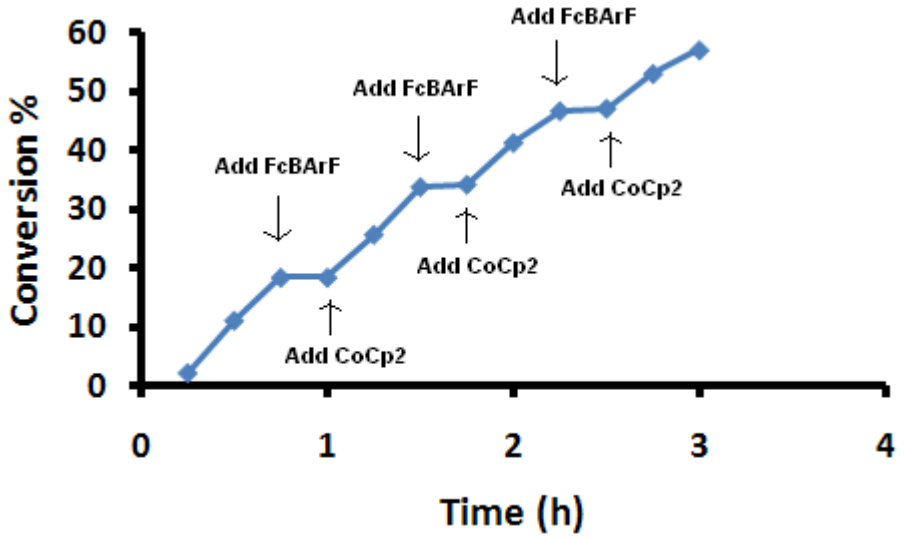

Fig. 4.8: L-lactide (100 equiv) ROP by **4.44** demonstrating switchable nature through oxidation to **4.44′** with $FcBAr^F$. Reduction to **4.44** occurs where $CoCp_2$ is added. Reprinted with permission from Broderick et al., *J. Am. Chem. Soc.* **2011**, *133* (24), 9278-9281. Copyright © 2011 American Chemical Society.

This study was followed the same year utilizing a cerium metal centre with the same ligand framework.[17] Here, rather than ferrocene oxidation, the cerium was oxidized instead (Fig. 4.9). Here, **4.46** with 100 equiv. L-lactide at 25 °C over 30 min resulted in 96% conversion to polylactide. The polymer dispersities ranged from 1.07 – 1.34. Under these conditions, compound **4.46′** was completely inactive. Similarly, *in situ* switching resulted in the same halting and continuation observed for **4.46** and **4.46′**. The results from these studies and that by Gibson and Long suggest that there is a strong relationship between the iron and other metal present that greatly influences catalytic activity although iron is not directly participating in catalysis with these systems.

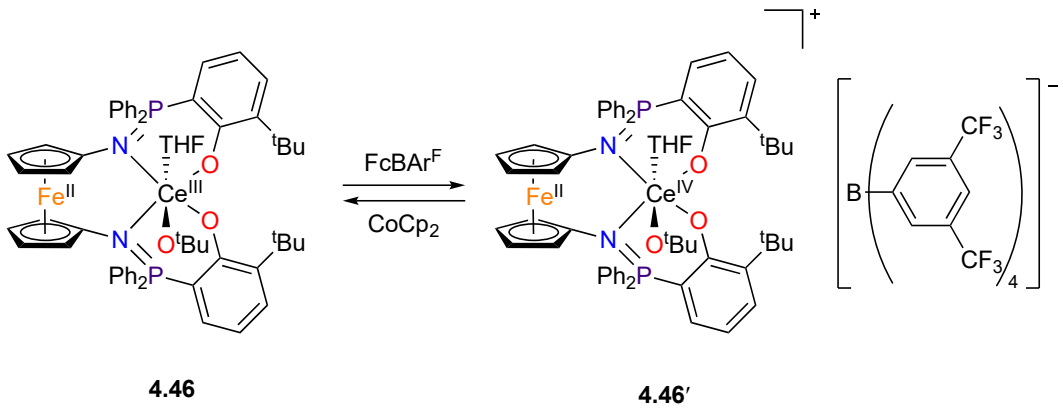

4.46 **4.46′**

Fig. 4.9: Cerium complexes for ROP reactions.[17]

In 2016, the Byers group reported the first switchable iron catalysts for the block copolymerization of lactide and CHO.[18] These are referred to simply as iron alkoxides and the nature of the alkoxide is not specified. However, in the previous report only one of these complexes was oxidized thus it can be surmised that the 4-methoxyphenyl alkoxide containing complex **4.16** is the species in question (Fig. 4.2). Contrasting to the efficacy of the neutral iron(II) species **4.16** toward ROP of lactide (vide supra) the cationic iron(III) complex **4.16′** was an effective catalyst for the ROP of many epoxides, most notably CHO in chlorobenzene to mitigate heat generation, but was entirely inactive toward ROP of lactide. Furthermore, **4.16** was entirely inactive toward CHO ROP. This gave access to a readily switchable ROP catalyst for block copolymer synthesis. This was demonstrated by a 1:1 mixture of LA:CHO in chlorobenzene with 2 mol% catalyst loading and first polymerizing LA with **4.16** to near complete conversion, oxidizing to **4.16′** with ferrocenium hexafluorophosphate ($FcPF_6$), and allowing CHO ROP to continue. Although evidence of CHO homopolymerization was present, these materials were discrete and could be separated

from the block copolymers which were found to have molecular weights from 20,100 – 37,500 g mol^{-1} and dispersities of 1.4 – 1.5. Selectivity for copolymer was 65 – 67%. Similarly, reverse order reactions beginning with ROP of CHO resulted in similar molecular weight polymers and dispersities but with a much higher selectivity for copolymerization of 98%.

The downside to the aforementioned redox-switchable systems is of course the addition of stoichiometric amounts of reagents that may require removal from the polymer products, particularly if they are to be scaled up to for industrial application. In an effort to mitigate this effect, the Byers group reported the same complex **4.16** as was used in 2016 to selectively polymerize lactide and CHO. Rather than using the redox reagents in stoichiometric quantities, the "switch" between **4.16** and **4.16′** was facilitated electrochemically by applying the appropriate potential to oxidize or reduce the lithium counter electrode; lithium salts exhibit no activity toward polymerization of lactide or epoxides.[19] Precautions were taken to separate the counter electrode from the carbon working electrode via a poly(vinylidene fluoride) coated glass frit, preventing unwanted redox events during polymerization. For lactide polymerization, 1 mol% **4.16′** was combined in 3 mL of 0.1 mol% $^{n}Bu_4NPF_6$ in dichloromethane with *rac*-lactide in 2 mL of the same solution. A reductive potential of 2.3 V was applied to generate **4.16** over 35 min. 75% conversion was achieved over 8 h and is consistent with results from chemical reduction seen above. The ability to sequentially reduce and oxidize the species was also demonstrated by first reducing to **4.16** and polymerizing until approximately 30% conversion of the lactide, and oxidizing to **4.16′**, resulting in complete deactivation of the catalyst. Reducing back to **4.16** continued the polymerization process. With this method molecular weights are slightly higher than the

theoretical weights, but the rate of polymerization remained consistent, suggesting complete reactivation of the catalytic species. There is, however, an increase in dispersities for each subsequent oxidation-reduction cycle; beginning at 1.3 and increasing to 1.5 after the first cycle, and 1.9 after the second. They propose this occurs due to the time required to complete the electrolysis reactions, effectively temporarily lowering catalyst concentrations. Epoxide selectivity was again demonstrated toward CHO by adding the inactive **4.16**, oxidizing to **4.16′** and observing polymerization. This too could be halted and restarted in reverse order to the LA above. Control over poly(ether) formation was lower than seen for poly(ester) and was consistent with the 2016 report, suggesting that the polymerization process is based entirely upon the catalytic species and unaffected by redox method. Lastly, the ability to form block-copolymers was demonstrated when beginning with either catalytic species. Reactions were performed at 0.5 mol% catalyst loading and 5:1 ratio of CHO to LA. When beginning with **4.16**, LA polymerization occurs exclusively until at 50% conversion the process is slowed by oxidation to **4.16′**, at which point a small increase in LA conversion (~5%) is observed alongside the CHO ROP initiation during the redox event. Once complete, CHO polymerization is observed with no further consumption of LA. Similarly, beginning with **4.16′** results in CHO consumption until the reduction to **4.16**, where no further CHO consumption is observed, and LA consumption commences. In each case, the formation of distinct block-copolymers can be verified via ^{13}C NMR spectroscopy. 88% selectivity for copolymer was obtained, with the remaining 12% attributed to poly(ether), a consequence of the non-living character of the epoxide polymerization.

Kleij reported an iron triphenolate catalyst (**4.47**) for terpolymerization reactions of terpene oxides (limonene oxide, limonene dioxide, 3-carene oxide and menthene oxide) and aromatic cyclic anhydrides (phthlalic anhydride and 1,8-naphthalic anhydride).[20] Each of the phenolate moieties of the ligand are tethered by a single amine and are structurally similar to compounds **4.8** and **4.9** (Fig. 4.10). Notably, in the presence of 1 equiv PPNCl as a co-catalyst at 65 °C, PA was able to couple with all epoxides other than limonene dioxide at high conversions (>75%) with excellent chemoselectivities and glass transition temperatures between 130 to 165 °C, to date the highest reported temperatures for semi-renewable PA-based copolymers. The reactions each took at least 24 h, with carene oxide reactions taking 100 h to reach 76% conversion, or elevated temperatures (95 °C) to achieve complete conversion in 24 h. Reactions with limonene dioxide (LDO) had to be performed at reduced temperatures of 45 °C as higher temperatures led to the production of insoluble material that they attribute to cross-linking of the monomer. Conversion did not top 52% and the resulting polymer was disperse (2.52) with a low glass transition temperature of 53 °C.

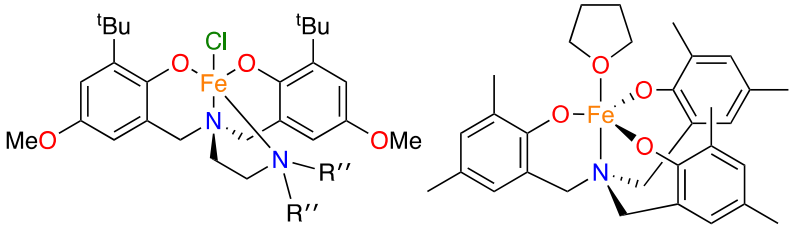

Fig. 4.10: Complexes **4.8** and **4.9** compared to complex **4.47** used by Kleij for selective terpolymerization of terpene oxides and aromatic anhydrides.[20]

Naphthalic anhydride (NA) copolymerization with CHO and LO was also tested to add more rigidity and improve glass transition temperatures compared to PA. For CHO and NA, **4.47** with 1 equiv. PPNCl over 72 h led to the production of polymers with varying molecular weights (2,300 – 11,400 g mol^{-1}) depending on the choice of solvent as NA exhibits limited solubility in epoxides. Despite the lower molecular weights and moderate dispersities (1.25 – 2.35), glass transition temperatures spanning 182 – 208 °C were obtainable. The higher values correlate approximately with increasing molecular weight. LO and NA under the same conditions produced very low molecular weight polymers (1.6 – 2.2 kg mol^{-1}) with dispersities from 1.36 – 1.52 but exhibit remarkably high glass transition temperatures of 227 – 243 °C. Greater molecular weight and control were observed in solution phase (THF) polymerization. The wide range of glass transition temperatures achievable by altering monomers to similarly active analogues could have strong implications for polymer design from more renewable sources in the future.

These works demonstrate the epoxide scope and activity toward different polymerization reactions available to iron complexes that can vary structurally and electronically, and the robust nature of similar catalytic species with respect to functional group tolerance and co-catalyst sources.

4.5. Catalyst synthesis

The syntheses of compounds **4.8** and **4.9** were initially performed by Tyler Brown, and subsequent syntheses were performed as described in the supporting information of the report by Kerton, Kozak and co-workers.[2]

4.6. Copolymerization of cyclohexene oxide and CO_2

All iron complexes in Fig. 4.1 (shown again below) were assessed as catalysts for the copolymerization of CO_2 and cyclohexene oxide (CHO). In general, all trigonal bipyramidal complexes, except complexes **4.8**, **4.9** and **4.10**, were active exclusively for poly(carbonate) formation giving polymers with >99% carbonate linkages (Table 4.1, entries 1–12). For **4.8**, **4.9** and **4.10**, I found modest yields of *cis*-cyclohexene carbonate were produced instead, whereas catalysts giving poly(carbonate) showed no cyclic carbonate formation. K. Andrea found the square pyramidal complexes **4.12 – 4.14b** bearing a homopiperazine backbone showed no conversion of CHO (entries 13 – 16), while complex **4.15** with a salan backbone gave a conversion of 34% to *cis*-cyclohexene carbonate (entry 17). Discussed in the full report, complexes **4.12 – 4.14b** can undergo epoxide deoxygenation with the substrate and it is possible that complex **4.15** behaves similarly. When **4.15** was combined with CHO the immediate formation of a brick red precipitate was observed, suggestive of μ-oxo complex formation, which we and others have previously reported.[21-22] Characterization of this red complex by UV-vis and MALDI-TOF MS was consistent with these earlier reports of μ-oxo complex formation. Therefore, we propose that the μ-oxo complex formation by iron

chloride complexes may be indicative of no activity toward ROCOP (i.e. it shuts down this reaction manifold).

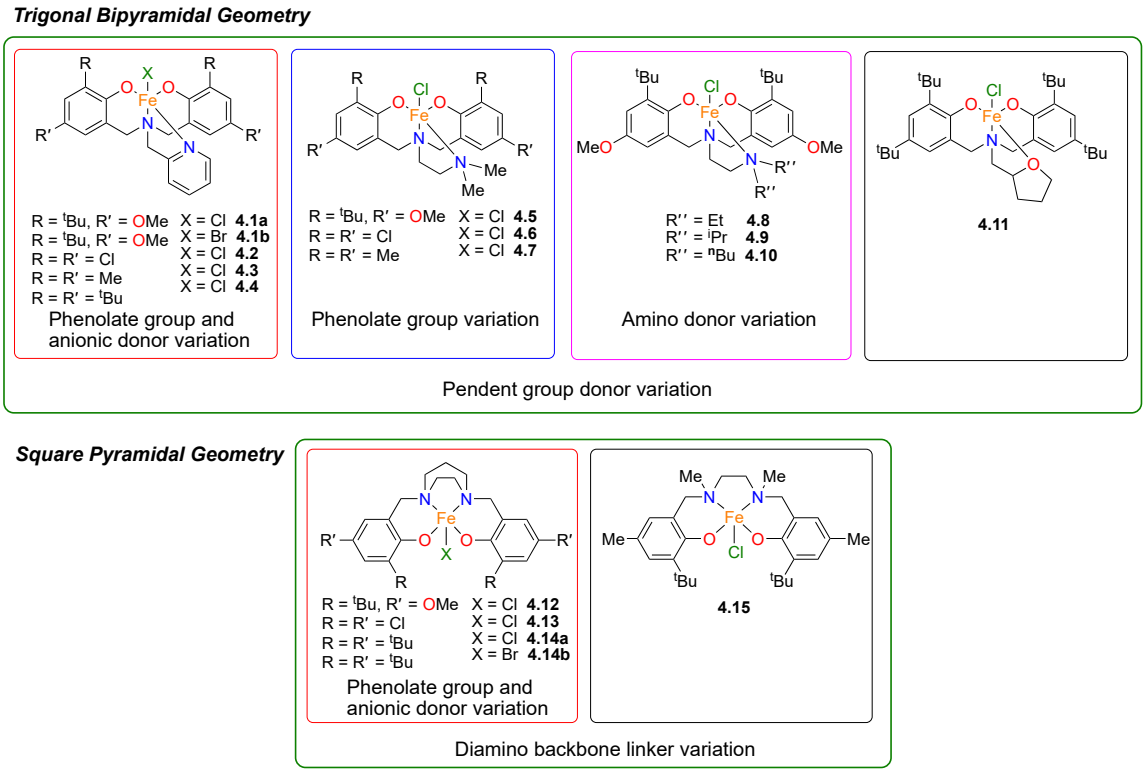

Fig. 4.11: Iron complexes reported by Kerton and Kozak. Compounds **4.8** and **4.9** will be discussed in this chapter. Reprinted with permission from Kori A. Andrea et al., *Inorg. Chem.*, **2019**, *58* (16), 11231 – 11240. Copyright © 2019 American Chemical Society.

In terms of complexes that are active for the copolymerization of CHO and CO_2, the overall reactivity was highly dependent on the nature of the pendent donor, the electronics and sterics of the phenolate donor, and the halide ligand at the iron center. K. Andrea found that the iron chloride complexes gave a higher overall conversion than the corresponding

iron bromides (entries 2–3). For complexes possessing pyridyl pendent groups, K. Andrea and I noted that electron-rich phenolate rings resulted in slightly improved conversions over those with electron withdrawing groups (entries 1 and 2). K. Andrea found the sterics of the phenolate groups were inconsequential on the reactivity (entries 4 – 5).

When the hybridization of the pendent donor is changed from an sp^2 nitrogen of a pyridyl group (complex **4.1a**) to an sp^3 amine (complex **4.5**), the influence of the electronic nature of the phenolate groups was reversed. That is, instead of electron donating groups giving the highest reactivity, electron withdrawing substituents paired with the sp^3 nitrogen-containing pendent donor were most active (entries 2 and 7). I found as the steric bulk of the sp^3-N pendent donor increased, selectivity of the product switched from perfectly alternating poly(carbonate) to *cis*-cyclohexene carbonate (entries 6 and 9 – 11). K. Andrea used compound **4.11**, bearing an oxygen pendent donor, which gave modest conversions to cyclohexene carbonate (entry 12), and square pyramidal complexes were inactive for poly(carbonate) formation (entries 13 – 17). These results show that not only the geometry of the metal center, but also a careful pairing of the pendent donor and the electronics of the phenolate rings is crucial for product selectivity and activity. Our study demonstrates that the highly modifiable amino-phenolate ligands can be tailored to yield iron complexes for ROCOP activity in a similar way to titanium and zirconium systems for ethylene and α-olefin polymerization.[23-25] Reactivity control using these ligands has also been shown for cyclic ester ROP using group 3 and lanthanide centers.[26-30]

Compound **4.1a** showed the best activity for poly(carbonate) formation and so K. Andrea and I studied its reactions in more detail. At 0.5 mol% Fe, K. Andrea observed 99% conversion to perfectly alternating poly(cyclohexene carbonate) with narrow dispersity (entry 2). However, when she decreased the catalyst loading to 0.2 mol% conversions decreased (entry 18). Lowering the temperature from 60 °C to 40 °C showed only a small decrease in conversion but decreasing the temperature further to 25 °C resulted in no conversion (entries 2 and 19-20). Lower conversions were observed with decreasing CO_2 pressure. We were pleased to observe a conversion of 56% CHO to PCHC at 7 bar CO_2 but decreasing pressure to 1 bar afforded only 5% conversion to PCHC (entries 2 and 21-24, K. Andrea, and 25, T. Anderson). It was also found that as CO_2 pressure decreased, the polymer molecular weights and dispersities remained constant. While overall conversions declined with decreasing CO_2 pressure, strictly alternating copolymers were always produced. An [OSSO]-iron(III) system has also been shown to provide completely alternating poly(carbonate) at CO_2 pressures as low as 1 bar, but also with decreased conversions.[31] Related catalysts, however, typically give a lower carbonate content in the polymer product when CO_2 pressure is decreased.[14,32]

K. Andrea continued by varying reaction time showing copolymerization occurred with 41% conversion obtained in 1 h (entry 26), corresponding to a TOF of 82 h^{-1}, which was not further optimized. Allowing reactions to continue for 8 h gave 66% conversion while after 22 h 99% conversion to poly(carbonate)s was obtained (entries 2 and 27). I then sought to test the influence of the co-catalysts and anionic co-catalysts (PPNCl and Bu_4NBr)

gave the best results, with PPNCl slightly out-performing Bu_4NBr which we attributed to the enhanced ability of Cl^- to ring-open the coordinated epoxide because of its smaller size in comparison to Br^-. I found that no reactivity was observed when the neutral co-catalyst DMAP was used. We believe the stronger binding of DMAP to the iron center hinders coordination of the incoming epoxide for activation (as mentioned above, Fe-DMAP adduct formation was observed via MALDI-TOF MS). This potentially leads to less active systems for propylene carbonate formation and inhibits poly(carbonate) formation. K. Andrea and I noted that when PPNCl was used in excess relative to iron, product selectivity switched from perfectly alternating poly(carbonate) to *cis*-CHC (entries 2 and 30) This switching of selectivity for polymeric vs cyclic carbonate formation has been previously reported for iron catalysts by Williams,[32] and by Kleij and Pescarmona.[33-34] End-group analysis of the poly(carbonate)s obtained was performed using MALDI-TOF MS and showed both chloride and hydroxide end-groups (Fig. A4.1). These are expected as the nucleophilic chloride initiates ring-opening of the coordinated epoxide, while termination of the growing chain occurs when reactions are quenched with acidified methanol.

Table 4.1: Copolymerization of CHO and CO_2 catalyzed by **4.1** – **4.15**.

Entry[a]	Complex	[CHO]:[Cocat]:[Fe]	Cocat.	PCO_2 (bar)	Conv. (%)[b,c]	M_n (g mol^{-1})[d]	$Đ$ [d]
1	**4.2**	200:1:1	PPNCl	60	89	8,100	1.09
2	**4.1a**	200:1:1	PPNCl	60	99	9,200	1.14
3	**4.1b**	200:1:1	PPNCl	60	76	4,300	1.07
4	**4.3**	200:1:1	PPNCl	60	89	5,800	1.07
5	**4.4**	200:1:1	PPNCl	60	88	7,500	1.10
6	**4.5**	200:1:1	PPNCl	60	48	3,600	1.02
7	**4.6**	200:1:1	PPNCl	60	90	7,500	1.09
8	**4.7**	200:1:1	PPNCl	60	78	4,500	1.07
9	**4.8**	200:1:1	PPNCl	60	20 (*cis*)	-	-
10	**4.9**	200:1:1	PPNCl	60	12 (*cis*)	-	-
11	**4.10**	200:1:1	PPNCl	60	7 (*cis*)	-	-
12	**4.11**	200:1:1	PPNCl	60	48	3,500	1.04
13	**4.12**	200:1:1	PPNCl	60	0	-	-
14	**4.13**	200:1:1	PPNCl	60	0	-	-
15	**4.14a**	200:1:1	PPNCl	60	0	-	-
16	**4.14b**	200:1:1	PPNCl	60	0	-	-
17	**4.15**	200:1:1	PPNCl	60	34 (*cis*)	-	-
18	**4.1a**	500:1:1	PPNCl	60	39	4,700	1.02
19[e]	**4.1a**	200:1:1	PPNCl	60	0	-	-
20[f]	**4.1a**	200:1:1	PPNCl	60	89	5,700	1.06
21	**4.1a**	200:1:1	PPNCl	40	88	5,400	1.05
22	**4.1a**	200:1:1	PPNCl	20	77	6,400	1.13
23	**4.1a**	200:1:1	PPNCl	10	63	5,000	1.04
24	**4.1a**	200:1:1	PPNCl	7	56	5,200	1.09
25	**4.1a**	200:1:1	PPNCl	1	5	-	-
26[g]	**4.1a**	200:1:1	PPNCl	60	41	3,600	1.03
27[h]	**4.1a**	200:1:1	PPNCl	60	66	4,900	1.01
28	**4.1a**	200:1:1	Bu_4NBr	60	81	5,700	1.09
29	**4.1a**	200:1:1	DMAP	60	0	-	-
30	**4.1a**	200:4:1	PPNCl	60	99 (*cis*)	-	-

[a] Reaction conditions unless otherwise stated: Neat cyclohexene oxide (30.6 mmol), Fe catalyst (0.152 mmol), PPNCl (0.152 mmol), 60 °C, 22 h. [b] Conversion determined using ^{1}H NMR spectroscopy by comparing the integral resonances for PCHC (4.60 – 4.65 ppm), CHC (3.90 – 4.07 ppm (*trans*) or 4.63 – 4.70 ppm (*cis*)) and resonances for residual epoxide. No mixtures of poly(carbonate) and cyclic carbonate were observed by NMR. [c] Values describe conversion to poly(carbonate) unless followed by (*cis*), which denotes *cis*-cyclic cyclohexene carbonate formation. No *trans*-cyclic carbonate was observed. [d] Determined in THF by GPC equipped with a multi-angle light scattering detector. [e] Reaction temperature: 25 °C [f] Reaction temperature: 40 °C [g] Reaction time: 1 h. [h] Reaction time: 8 h.

4.7. Lactide ring-opening polymerization

As discussed above, compounds **4.8** and **4.9** (Scheme 4.1) were able to couple epoxides and CO_2 to form cyclic carbonate. The synthesis of poly(ester)s and multicomponent polymers containing ester, ether and carbonate functionality were of interest and thus epoxide and lactide ROP and alternating copolymerization of epoxides with phthalic anhydride (PA) was explored. Although **4.8** and **4.9** were inactive to polymerization under the conditions described above even at 60 °C (cyclic carbonate is the thermodynamic product), the formation of cyclic carbonate shows that ring-opening of epoxides is feasible and so alkoxide formation as the initiator for other monomers is a possibility. Furthermore, intermediates from those processes may be active toward ROP of epoxides themselves. First, the activity of compounds **4.8** and **4.9** toward ROP of lactide (LA) was investigated. Compound **4.8** produces narrowly disperse poly(carbonate) at moderate conversions and could be a strong candidate for well controlled polymerizations, while compound **4.9** demonstrates poor activity for poly(carbonate) synthesis but contains an extended Fe-N^{i}Pr$_2$ bond compared to **4.8**. This may facilitate active site generation via steric influence[35] or by encouraging Cl^- dissociation via steric repulsion leading to faster monomer activation, although no significant change in activity was observed for PO and CO_2 coupling with steric changes at the amine pendent donor between compounds **4.5**, **4.8** and **4.9**. Table 4.2 shows the results of the LA ROP studies. The generation of an alkoxide initiator from the ring-opening of the epoxide solvents was likely required to achieve LA conversion (Scheme 4.1). A recent report by Capacchione proposes a similar process to that in Scheme 4.1 with iron-catalyzed ROP of cyclic esters.[36] Compound **4.8** in PO was completely inactive without the

presence of PPNCl co-catalyst (entries 1 – 4) and modestly active in CHO reaching 45% conversion of LA after 1 h (entry 5) with molecular weight (3,700 g mol^{-1}) at half of the expected value (7,200 g mol^{-1}) suggesting two polymer chains growing per iron centre. In the presence of PPNCl co-catalyst in PO at 60 °C, 8% conversion of LA was observed after 1 h (entry 6). An increase in temperature to 80 °C (entry 7) and increased reaction time of 4 h resulted in complete conversion of LA with no evidence of poly(ether) formation and molecular weight (10,700 g mol^{-1}) slightly lower than the expected mass of 14,400 g mol^{-1}. As compounds **4.8** and **4.9** were active toward CO_2 and epoxide coupling to form cyclic carbonate, carbonate enchainment may be possible with a different polymer chain end or may inhibit poly(ester) formation. Thus, entry 8 depicts a reaction performed at 80 °C and charged to 20 bar CO_2 after 1 h. No poly(carbonate) was observed with 99% poly(ester) formation at extended reaction time of 18 h. Notably, the molecular weight is lower (6,200 g mol^{-1}) than the corresponding reaction in the absence of CO_2 (entry 7) suggesting the presence of CO_2 is inhibiting LA enchainment. Compound **4.8** was inactive in toluene (entry 9). Using compound **4.9** in PO with PPNCl co-catalyst at 80 °C, complete conversion could be achieved in 4 h (entry 10) but with 60% conversion to homopolymer as well. Complete or high conversion was also achieved at these conditions without the presence of external additive in both PO and CHO (entry 11, 12) but again molecular weights are lower than would be expected with single-site polymerization. In toluene, compound **4.9** with PPNCl was also inactive (entry 13).

Table 4.2: Results of lactide ROP catalyzed by compounds **4.8** and **4.9**.

Entry[a]	Cat.	Cocat.	Solvent	Temp. (°C)	Time (h)	Conv. LA (%)[b]	M_n (g mol^{-1})[c]
1	**4.8**	BnOH	Toluene	80	18	0	-
2	**4.8**	-	PO	80	1	0	-
3	**4.8**	-	PO	60	1	0	-
4	**4.8**	-	PO	100	1	0	-
5	**4.8**	-	CHO	80	1	45	3,700
6	**4.8**	PPNCl	PO	60	1	8	-
7	**4.8**	PPNCl	PO	80	4	99	10,700
8[d]	**4.8**	PPNCl	PO	80	18	99	6,200
9	**4.8**	PPNCl	Toluene	80	4	0	-
10	**4.9**	PPNCl	PO	80	4	99	N/A[e]
11	**4.9**	-	PO	80	18	99	6,700
12	**4.9**	-	CHO	80	1	85	9,400
13	**4.9**	PPNCl	Toluene	80	18	0	-

[a] All reactions were performed with catalyst and co-catalyst loadings of 1 mol% in 2 mL of solvent. M_n theoretical = 14,500 g mol^{-1}. [b] Determined via integration of the methine resonances of *rac*-lactide and PLA of crude reaction mixture [c] Determined via integration of the resonances of Cl-PO (∂ 1.10 or 3.74) or Cl-CHO initiator (∂ 3.73) and PLA (∂ 1.61 – 1.43 or 5.30 – 5.05). [d] Reaction performed in pressure vessel, charged to 20 bar CO_2 after 1 h. [e] Significant homopolymerization obscured signals in the ^{1}H NMR spectrum used to calculate molecular weight.

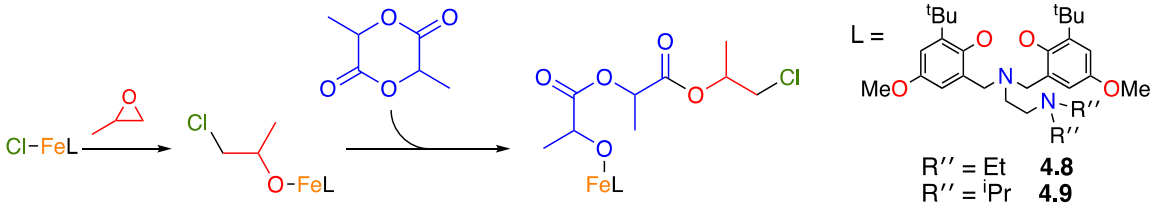

Scheme 4.1: Proposed method of activation by compounds **4.8** and **4.9** toward the ROP of LA. Similar activation models have been reported elsewhere.[10,36-37]

4.8. Multicomponent polymerization reactions

Multicomponent polymerization reactions involving lactones, anhydrides and epoxides were also of interest. Inspired by the work of Byers described above,[11,18-19] as well as the pressure-switchable system reported by Rieger[38] and discussed in Chapter 2, the synthesis of poly(ester-ether) and poly(ester-carbonate) block copolymers and terpolymers in one pot was investigated. As the results in Table 4.2 demonstrated that compound **4.9** was a more effective catalyst toward LA ROP, it was then applied toward reactions containing PA (Table 4.3). The ROP of PA is not possible sequentially and thus another monomer is required to obtain the poly(ester) fragments from this compound. A simple representation of this reaction is shown in Scheme 4.2.

Table 4.3: Results of PA, LA and epoxide terpolymerization reactions catalyzed by **4.9**.

Entry[a]	Cocat.	Ester Monomer[b]	Solvent	Time (h)	Conv. Ester Monomer (%)[c]	Conv. Epox. (%)[c]	Ester: Ether ratio	M_n (g mol^{-1}) [$Đ$][d]
1	-	PA	CHO	1	100	53	1:3	11,800 [1.19]
2	-	PA	PO	1	55	15	1:2	4,100 [1.03]
3	-	PA	PO	24	100	15[e]	2:1	12,900 [1.13]
4	-	PA/CO_2	PO	24	100	17[e]	2:1	8,200 [1.04]
5[f]	-	PA	PO	4	1	<1	-	-
6	-	PA	LO	1	0	0	-	-
7	-	PA:CHO	Tol.	1	0	-	-	-
8	-	PA:PO	Tol.	1	0	-	-	-
9	-	PA:LA	CHO	2	75:0	13	1:1	N/A[e]
10	-	PA:LA	Tol.	1	0	-	-	-
11	PPNCl	PA:LA	Tol.	1	0	-	-	-
12	CHO	PA:LA	Tol.	1	0	-	-	-
13	PPNCl	PA	PO	1	81	8	1:0	8,500 [1.03]
14	PPNCl	PA	LO	1	9	<1	-	-
15	PPNCl	PA	LO	24	100	10	1:0	6,000 [1.06]

[a] Compound **4.9**, co-catalyst, ester monomer, solvent (1:1:100:1000), 80 °C. [b] All ester monomer mixture ratios are 1:1 except CO_2. [c] Determined by ^{1}H NMR spectroscopy of crude reaction mixture. Conversion of solvent includes the corresponding amount required for anhydride ROCOP (10% at 100% conversion of anhydride). [d] Determined by triple detection GPC analysis of isolated material. [e] Includes conversion to cyclic carbonate. [f] PA:Fe ratio of 1000:1. [e] Product lost.

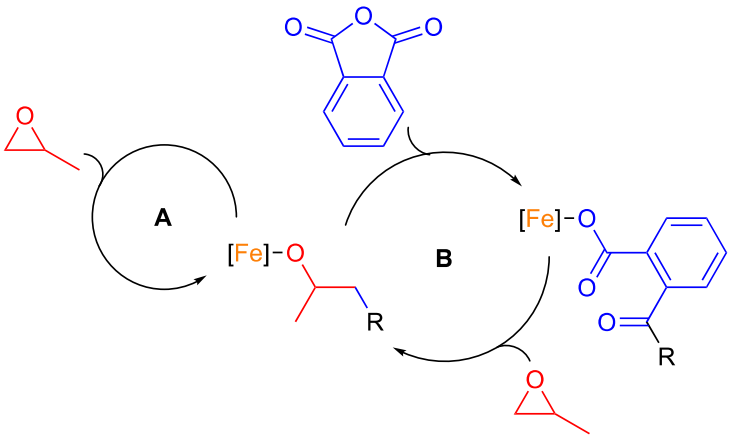

Scheme 4.2: Possible catalytic cycle for the reactions in Table 4.3 containing PA in an epoxide, shown as PO for clarity. Similar activation models have been reported elsewhere.[37,39] [40] R = nucleophile initiator as polymerization begins followed by growing polymer chain as epoxide/anhydride are enchained.

4.9. Discussion

As the results in Table 4.2 illustrate, both **4.8** and **4.9** are effective catalysts for ROP of *rac*-lactide, although **4.8** is most active in the presence of an external nucleophile. Ideally, lactide ROP could be achieved without the presence of external co-catalyst that may affect reactivity in the more complicated systems presented in Table 4.3. As **4.8** was unable to convert greater than 50% of the lactide in 1 h without PPNCl present, focus was shifted toward **4.9** which demonstrated this ability. As pure polylactide has been characterized extensively, detailed characterization of the compounds reported here (DSC, TGA) was excluded. Instead, focus was placed on copolymerization products.

In attempt to synthesize copolymers selectively, **4.9** was utilized as a catalyst toward epoxide and phthalic anhydride copolymerization. As mentioned above, PA cannot ring-open through reaction with another PA molecule but is susceptible to ring-opening from a suitable nucleophile such as the alkoxide intermediates generated from the ring-opening of epoxides and lactide. As such, if the activation energy required to ring-open the anhydride is lower than that of either the epoxide or lactide, it should be consumed preferentially, limiting poly(lactide) or poly(ether) formation and instead produce perfectly alternating copoly(ester). This behaviour has been demonstrated with PA and CHO by Williams and co-workers.[41] Reactions were performed at 1 mol% catalyst loading at 80 °C unless otherwise noted. Complete conversion of PA was observed when CHO was used as a solvent within 1 h (Table 4.3, entry 1). Molecular weights were significantly lower than the expected for strictly poly(ester) (11,800 g mol^{-1} compared to 24,600 g mol^{-1} theoretical) but the dispersity was relatively narrow at 1.19. This may be due to chain-transfer reactions facilitated by adventitious water, and low molecular weight poly(ether) remaining after the polymer purification phase. Fig. A4.3 shows a small shoulder in the plot of differential weight fraction vs. molecular weight, however it is of low relative concentration and of similar mass to the predominant peak. This is perhaps a result of non-uniform initiation processes. MALDI-TOF MS data for this polymer indicates that chloride is the predominant initiating species however there is significant evidence of chain-transfer as hydroxide initiation is nearly as prevalent, perhaps from adventitious water. For chloride-initiated polymerization, the polymer is primarily composed of 3:1 ratio of poly(ether) to poly(ester) with sodium counterion, while hydroxide-initiated polymer shows 1:1 ratio for each with no counterion. Both polymers appear to be terminated by cyclohexanol end-groups. The remainder of the

signal corresponding to polymer appears to be composed of chloride and hydroxide-initiated polymer with no counterion and sodium counterion, respectively. As the MALDI sample was prepared from crude material, the polymer comprises 51% of the signal, corresponding approximately with the total conversion of the reactants in the sample by ^{1}H NMR spectroscopy. The dominant peak in the spectrum appears to correspond to a CHO-**4.9** adduct. Using PO as the solvent reduced overall PA conversion (entry 2, 55%) within 1 h but with much greater control over polymer composition with just 5% conversion to poly(ether). The molecular weight was again lower than anticipated at 4,100 g mol^{-1} compared to the expected 11,400 g mol^{-1}, but the dispersity was very narrow at 1.03. Multimodal polymer molecular weight distributions can be observed in Fig. A4.4, with higher molecular weight material (~5,300 g mol^{-1}) separated from the dominant peak around 3,900 g mol^{-1}. A small peak appears at 4,300 g mol^{-1} as well. One of these may be attributed to the poly(ether) production (low overall conversion) while non-uniform initiation could give rise to the other, as above, while the copoly(ester) is the predominant product.

Next, CO_2 (20 bar) was introduced to a reaction in PO after 1.5 h of stirring in the pressure vessel at 80 °C to allow PA conversion without adding another reactant (entry 3). The total reaction time after CO_2 addition was 24 h. Here, there was no evidence of poly(ether) or poly(carbonate) formation but 5% conversion to cyclic carbonate alongside complete conversion of the PA to poly(ester) was observed by ^{1}H NMR spectroscopy. The low conversion to cyclic carbonate suggests that fine control over this particular system is likely plausible with tweaks to the conditions. Notably, isolation of the polymer was difficult and only 35 mg of material was obtained. The molecular weight of this was 12,900 g mol^{-1}

(theoretical 11,400 g mol^{-1} for -PA-PO- copolymer). Repeating this procedure with CO_2 pressurization immediately and 24 h reaction time resulted in similar results (entry 4). Again, the PA was completely consumed, and the only other observable product was cyclic carbonate at 7%. These reactions suggest that the presence of CO_2 is inhibiting homopolymerization seen in entry 2, although the cyclic carbonate production may compete somewhat with the consumption of PA. The molecular weight of 8,200 g mol^{-1} is once again lower than the anticipated 11,400 g mol^{-1} for strictly -PA-PO- polymer with a narrow dispersity of 1.04. There was no evidence of bimodality, perhaps due to the aforementioned inhibition of poly(ether) formation in the presence of CO_2 (Fig. A4.5). Reducing the catalyst loading to 0.1 mol% in PO resulted in no activity (entry 5). Using LO as the epoxide (1 mol%, entry 6) was similarly inactive. This is unsurprising as the steric influence at the epoxide moiety of LO limits its reactivity compared to CHO. Reactions with stoichiometric quantities (with respect to PA, entries 7 and 8) of the epoxides in toluene were inactive toward polymer formation.

Introduction of LA to the system with CHO (entry 9) reduced overall PA and CHO conversions compared to that in entry 1, but no LA was consumed, suggesting some type of inhibited interaction between the LA and the catalytic species in the presence of PA. Utilizing toluene as a solvent expectedly produced no conversion as there was no suitable monomer with which to form the alkoxide initiator believed necessary for initiation (entry 10). Using PPNCl as a co-catalyst in toluene under the same conditions resulted in no conversion of PA or LA (entry 11). Using CHO as a co-catalyst (1 mol%, entry 12) in toluene resulted in no conversion. The addition of a non-epoxide co-catalyst PPNCl (1

mol%) was used with PA in PO (entry 13) and produced poly(ester) at 81% conversion within 1 h with a molecular weight of 8,500 g mol^{-1}, again much lower than the theoretical value of 16,700 g mol^{-1}. The dispersity was very narrow at 1.03.

As the overarching goal was to develop terpolymerization catalysts with renewable or semi-renewable substrates, limonene oxide was investigated further as the epoxide solvent. As LO was inactive without a co-catalyst, using PPNCl to facilitate LO ring-opening over 1 h resulted in 9% conversion of the PA with no homopolymerization. The need of an external nucleophile was consistent with Kleij and coworkers findings.[20] The molecular weight suggests dimeric species or diols, but this may be due to a slow initiation process. Increasing reaction time to 24 h resulted in complete conversion of PA with no evidence of ether linkages. This is notable as there are few reports of iron catalyzed ROCOP involving LO. The molecular weight of the resulting polymer was low (6,000 g mol^{-1}, theoretical 30,000 g mol^{-1}) but with very narrow dispersity of 1.06. The GPC trace exhibits much clearer bimodality than those seen with other epoxides (Fig. A4.6) but the limited reactivity of LO is the likely source of slow initiation processes leading to small deviations in polymer uniformity.

The molecular weights were about half of the theoretical values for single-site polymerization in nearly every case, which suggests that multiple chains are growing from each catalyst. This behavior is not uncommon in metal salen-catalyzed polymerization reactions as the square-based pyramidal geometry results in each axial position potentially behaving as an active site, and a similar process may be occurring in this system. The crystal

structure of **4.9** shows a trigonal bipyramidal geometry and it is possible that multiple chains can be initiated per metal as illustrated in Fig. 4.12 as the pendent amine-iron bond is longer than analogous compounds with less bulky amine substituents and may dissociate more readily. Multiple chain growth would be dependent upon the presence of another initiating species, perhaps the chloride anion bound to iron, but even those reactions devoid of co-catalyst as a secondary source exhibit this behaviour. MALDI-TOF MS data suggests that no transesterification is occurring in the polymer.

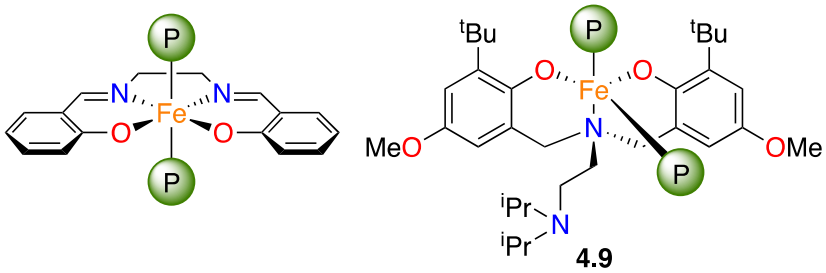

Fig. 4.12: Representative iron-salen compound with polymer chains growing at each axial position (left) and possible configuration for dual-site polymer propagation with **4.9**.

4.10. Conclusions

The work in this Chapter represents the beginning of a new project that has stemmed from the work presented in Section 4.6. The results presented here demonstrate the potential of amino-bis(phenolate) iron complexes as catalysts for complex mixtures of monomers, particularly for those containing limonene oxide, without using chemical or electronic redox switches. Although compound **4.9** has exhibited selectivity for perfectly alternating copolyester from limonene oxide and phthalic anhydride, this was likely a result of the

limited ability to ring-open the epoxide consecutively to form poly(limonene oxide). If fine control with these particular systems not be feasible for other epoxides or anhydrides, the tunability of amino-bis(phenolate) ligands presents an opportunity to design complexes that may take advantage of the switchable nature of other iron complexes. MALDI-TOF MS data on the remaining materials should allow for elucidation of the polymerization mechanism.

4.11. General Methods

All reagents were purchased from Sigma-Aldrich, Alfa-Aesar, or Caledon. All epoxides were distilled over CaH_2. Unless otherwise stated, all reactions were performed under inert atmosphere of N_2. ^1H NMR spectra were recorded at 300 MHz on a Bruker Avance III spectrometer with BBO probe and ^{13}C at 75.0 MHz on a Bruker Avance I spectrometer with TCI inverse gradient probe. *In situ* FTIR monitoring was performed using a 100 mL Parr Instruments 4560 stainless steel mini reactor vessel with motorized mechanical stirrer and a heating mantle. The vessel was modified with a bottom-mounted Mettler Toledo SiComp Sentinel ATR sensor, which was connected to a ReactIR 15 base unit through a silver-halide Fiber-to-Sentinel conduit. Profiles of the absorbance height at 1089 cm^{-1} (poly(ether)), 1750 cm^{-1} (poly(carbonate)), 1810 cm^{-1} (cyclic carbonate) and 1860 cm^{-1} (PA) were measured every 60 – 120 s. Similar methods for reaction monitoring via *in situ* IR have been reported elsewhere.[42-44] Molecular weight determination of copolymer was performed by gel permeation chromatography on an Agilent Infinity HPLC instrument connected to a Wyatt Technologies triple detector system (light scattering, viscometry and refractive index) equipped with Phenogel 10^3 Å and 10^4 Å 300 × 4.60 mm columns (covering

mass ranges of 1,000 – 75,000 and 5,000 – 500,000 g mol^{-1}, respectively) with THF as eluent. Polymer samples were prepared in THF at a concentration of 4 mg mL^{-1} and filtered through 0.2 μm syringe filters. The sample solution was then eluted at a flow rate of 0.30 mL min^{-1}. The values of d*n*/d*c* were calculated online (columns detached) assuming 100% mass recovery using the Astra 6 software package (Wyatt Technologies), for PCHO d*n*/d*c* = 0.0960 mL g^{-1} and for PCHC d*n*/d*c* = 0.0701 mL g^{-1}. MALDI-TOF MS was performed using a Bruker ultrafleXtreme TOF/TOF MALDI Time-of-Flight Mass Spectrometer System equipped with a reflectron and BRUKER smartbeam™-II laser (355 nm). Samples were prepared on the benchtop. 2,3-Dihydroxybenzoic acid (DHBA) was used as the matrix for the polymers with sodium trifluoroacetate (NaTFA) as cationizing agent. Preparation of the samples and data collection was performed by Dr. Stefana Egli by dissolving matrix in THF (5 mg mL^{-1}), polymer in THF (1 mg/mL), and cationizing agent in THF (1 mg/mL), combining the solutions in 20:1:3 ratio and spotting 1 μL on the plate to dry. Data processing was performed using Polymerix© software.

4.12. Polymerization Methods

Poly(ester) synthesis: Under inert atmosphere, LA (0.400 g, 2.78 mmol) was dissolved in 27.8 mmol of epoxide by mass (~2 mL of solvent). The reaction mixture was combined with 1 mol% catalyst and co-catalyst where applicable in a 20 mL scintillation vial or 5 mL microwave vial, stirred and heated at the specified temperatures. An aliquot for ^{1}H NMR spectroscopy (Fig. A4.7) was taken for the determination of conversion and molecular weights by comparing resonances corresponding to LA starting material (∂ 5.09, 1.66) and

PLA (∂ 4.87, 4.56, 4.03). The remaining solvent was then removed under reduced pressure and product dried at 60 °C in a vacuum oven.

Poly(ester-*co*-ether) synthesis: Under inert atmosphere, PA (0.41 g, 2.78 mmol) was dissolved in 27.8 mmol of epoxide by mass (~2 mL solvent). The reaction mixture was combined with 1 mol% catalyst and co-catalyst where applicable in a 20 mL scintillation vial, 5 mL microwave vial, or pressure vessel via syringe injection, heated and stirred at the specified temperatures. Reactions in the pressure vessel would be charged with CO_2 prior to heating. An aliquot for ^{1}H NMR spectroscopy (Fig. A4.8) was taken for the determination of conversion by comparing resonances corresponding to PA (∂ 7.98) and epoxide resonance with poly(ester) (∂ 7.69 – 7.48). The copolymer was extracted into minimal CH_2Cl_2 and precipitated with cold Et_2O. The solvent was decanted and the product dried at 60 °C in a vacuum oven.

4.13. References

1. Leibfarth, F. A.; Mattson, K. M.; Fors, B. P.; Collins, H. A.; Hawker, C. J., External Regulation of Controlled Polymerizations. *Angew. Chem. Int. Ed.* **2013**, *52*, pp 199-210.

2. Andrea, K. A.; Butler, E. D.; Brown, T. R.; Anderson, T. S.; Jagota, D.; Rose, C.; Lee, E. M.; Goulding, S. D.; Murphy, J. N.; Kerton, F. M.; Kozak, C. M., Iron Complexes for Cyclic Carbonate and Polycarbonate Formation: Selectivity Control from Ligand Design and Metal-Center Geometry. *Inorg. Chem.* **2019**, *58*, pp 11231-11240.

3. Carothers, W. H.; Dorough, G. L.; Natta, F. J. v., Studies of Polymerization and Ring Formation. X. The Reversible Polymerization of Six-Membered Cyclic Esters. *J. Am. Chem. Soc.* **1932**, *54*, pp 761-772.

4. Kricheldorf, H. R.; Kreiser-Saunders, I., Polylactones, 19. Anionic polymerization of L-lactide in solution. *Makromol. Chem.* **1990**, *191*, pp 1057-1066.

5. Kricheldorf, H. R.; Serra, A., Polylactones. *Polym. Bull. (Berlin)* **1985**, *14*, pp 497-502.

6. Kricheldorf, H.; Boettcher, C., Polylactones. XXV. Polymerizations of racemic- and meso-D,L-Lactide with Zn, Pb, Sb, and Bi Salts—Stereochemical Aspects. *Journal of Macromolecular Science* **1993**, *Part A: Pure and Applied Chemistry*, pp 441-448.

7. Garlotta, D., A Literature Review of Poly(Lactic Acid). *J. Polym. Environ.* **2001**, *9*, pp 63-84.

8. Kremer, A. B.; Mehrkhodavandi, P., Dinuclear catalysts for the ring opening polymerization of lactide. *Coord. Chem. Rev.* **2019**, *380*, pp 35-57.

9. Dechy-Cabaret, O.; Martin-Vaca, B.; Bourissou, D., Controlled Ring-Opening Polymerization of Lactide and Glycolide. *Chem. Rev.* **2004**, *104*, pp 6147-6176.

10. Wheaton, C. A.; Hayes, P. G.; Ireland, B. J., Complexes of Mg, Ca and Zn as homogeneous catalysts for lactide polymerization. *Dalton Trans.* **2009**, pp 4832-4846.

11. Biernesser, A. B.; Li, B.; Byers, J. A., Redox-Controlled Polymerization of Lactide Catalyzed by Bis(imino)pyridine Iron Bis(alkoxide) Complexes. *J. Am. Chem. Soc.* **2013**, *135*, pp 16553-16560.

12. Duan, R.; Hu, C.; Li, X.; Pang, X.; Sun, Z.; Chen, X.; Wang, X., Air-Stable Salen–Iron Complexes: Stereoselective Catalysts for Lactide and ε-Caprolactone Polymerization through in Situ Initiation. *Macromolecules* **2017**, *50*, pp 9188-9195.

13. Driscoll, O. J.; Hafford-Tear, C. H.; McKeown, P.; Stewart, J. A.; Kociok-Köhn, G.; Mahon, M. F.; Jones, M. D., The synthesis, characterisation and application of iron(iii)–acetate complexes for cyclic carbonate formation and the polymerisation of lactide. *Dalton Trans.* **2019**, *48*, pp 15049-15058.

14. Nakano, K.; Kobayashi, K.; Ohkawara, T.; Imoto, H.; Nozaki, K., Copolymerization of Epoxides with Carbon Dioxide Catalyzed by Iron–Corrole Complexes: Synthesis of a Crystalline Copolymer. *J. Am. Chem. Soc.* **2013**, *135*, pp 8456-8459.

15. Gregson, C. K. A.; Gibson, V. C.; Long, N. J.; Marshall, E. L.; Oxford, P. J.; White, A. J. P., Redox Control within Single-Site Polymerization Catalysts. *J. Am. Chem. Soc.* **2006**, *128*, pp 7410-7411.

16. Broderick, E. M.; Guo, N.; Vogel, C. S.; Xu, C.; Sutter, J.; Miller, J. T.; Meyer, K.; Mehrkhodavandi, P.; Diaconescu, P. L., Redox Control of a Ring-Opening Polymerization Catalyst. *J. Am. Chem. Soc.* **2011**, *133*, pp 9278-9281.

17. Broderick, E. M.; Guo, N.; Wu, T.; Vogel, C. S.; Xu, C.; Sutter, J.; Miller, J. T.; Meyer, K.; Cantat, T.; Diaconescu, P. L., Redox control of a polymerization catalyst by changing the oxidation state of the metal center. *Chem. Commun.* **2011**, *47*, pp 9897-9899.

18. Biernesser, A. B.; Delle Chiaie, K. R.; Curley, J. B.; Byers, J. A., Block Copolymerization of Lactide and an Epoxide Facilitated by a Redox Switchable Iron-Based Catalyst. *Angew. Chem. Int. Ed.* **2016**, *55*, pp 5251-5254.

19. Qi, M.; Dong, Q.; Wang, D.; Byers, J. A., Electrochemically Switchable Ring-Opening Polymerization of Lactide and Cyclohexene Oxide. *J. Am. Chem. Soc.* **2018**, *140*, pp 5686-5690.

20. Peña Carrodeguas, L.; Martín, C.; Kleij, A. W., Semiaromatic Polyesters Derived from Renewable Terpene Oxides with High Glass Transitions. *Macromolecules* **2017**, *50*, pp 5337-5345.

21. Andrea, K. A.; Brown, T. R.; Murphy, J. N.; Jagota, D.; McKearney, D.; Kozak, C. M.; Kerton, F. M., Characterization of oxo-bridged iron amino-bis(phenolate) complexes formed intentionally or in situ: mechanistic insight into epoxide deoxygenation during the coupling of CO_2 and epoxides. *Inorg. Chem.* **2018**, *57*, pp 13494-13504.

22. Whiteoak, C. J.; Torres Martin de Rosales, R.; White, A. J. P.; Britovsek, G. J. P., Iron(II) Complexes with Tetradentate Bis(aminophenolate) Ligands: Synthesis and Characterization, Solution Behavior, and Reactivity with O_2. *Inorg. Chem.* **2010**, *49*, pp 11106-11117.

23. Segal, S.; Goldberg, I.; Kol, M., Zirconium and Titanium Diamine Bis(phenolate) Catalysts for α-Olefin Polymerization: From Atactic Oligo(1-hexene) to Ultrahigh-Molecular-Weight Isotactic Poly(1-hexene). *Organometallics* **2005**, *24*, pp 200-202.

24. Tshuva, E. Y.; Goldberg, I.; Kol, M.; Goldschmidt, Z., Zirconium Complexes of Amine-Bis(phenolate) Ligands as Catalysts for 1-Hexene Polymerization: Peripheral Structural Parameters Strongly Affect Reactivity. *Organometallics* **2001**, *20*, pp 3017-3028.

25. Groysman, S.; Tshuva, E. Y.; Goldberg, I.; Kol, M.; Goldschmidt, Z.; Shuster, M., Diverse Structure−Activity Trends in Amine Bis(phenolate) Titanium Polymerization Catalysts. *Organometallics* **2004**, *23*, pp 5291-5299.

26. Kerton, F. M.; Whitwood, A. C.; Willans, C. E., A High-throughput Approach to Lanthanide Complexes and their Rapid Screening in the Ring Opening Polymerisation of Caprolactone. *Dalton Trans.* **2004**, pp 2237-2244.

27. Clark, L.; Cushion, M. G.; Dyer, H. E.; Schwarz, A. D.; Duchateau, R.; Mountford, P., Dicationic and Zwitterionic Catalysts for the Amine-initiated, Immortal Ring-opening Polymerisation of rac-Lactide: Facile Synthesis of Amine-terminated, Highly Heterotactic PLA. *Chem. Commun.* **2010**, *46*, pp 273-275.

28. Liu, B.; Roisnel, T.; Guégan, J.-P.; Carpentier, J.-F.; Sarazin, Y., Heteroleptic Silylamido Phenolate Complexes of Calcium and the Larger Alkaline Earth Metals: β-Agostic Ae···Si–H Stabilization and Activity in the Ring-Opening Polymerization of L-Lactide. *Chem. Eur. J.* **2012**, *18*, pp 6289-6301.

29. Dyer, H. E.; Huijser, S.; Susperregui, N.; Bonnet, F.; Schwarz, A. D.; Duchateau, R.; Maron, L.; Mountford, P., Ring-Opening Polymerization of rac-Lactide by Bis(phenolate)amine-Supported Samarium Borohydride Complexes: An Experimental and DFT Study. *Organometallics* **2010**, *29*, pp 3602-3621.

30. Ajellal, N.; Carpentier, J.-F.; Guillaume, C.; Guillaume, S. M.; Helou, M.; Poirier, V.; Sarazin, Y.; Trifonov, A., Metal-catalyzed Immortal Ring-opening Polymerization of Lactones, Lactides and Cyclic Carbonates. *Dalton Trans.* **2010**, *39*, pp 8363-8376.

31. Della Monica, F.; Maity, B.; Pehl, T.; Buonerba, A.; De Nisi, A.; Monari, M.; Grassi, A.; Rieger, B.; Cavallo, L.; Capacchione, C., [OSSO]-Type Iron(III) Complexes for the Low-Pressure Reaction of Carbon Dioxide with Epoxides: Catalytic Activity, Reaction Kinetics, and Computational Study. *ACS Catal.* **2018**, *8*, pp 6882-6893.

32. Buchard, A.; Kember, M. R.; Sandeman, K. G.; Williams, C. K., A Bimetallic Iron(III) Catalyst for CO_2/Epoxide Coupling. *Chem. Commun.* **2011**, *47*, pp 212-214.

33. Taherimehr, M.; Al-Amsyar, S. M.; Whiteoak, C. J.; Kleij, A. W.; Pescarmona, P. P., High Activity and Switchable Selectivity in the Synthesis of Cyclic and Polymeric Cyclohexene Carbonates with Iron Amino Triphenolate Catalysts. *Green Chem.* **2013**, *15*, pp 3083-3090.

34. Taherimehr, M.; Serta, J.; Kleij, A. W.; Whiteoak, C. J.; Pescarmona, P. P., New Iron Pyridylamino-Bis(Phenolate) Catalyst for Converting CO_2 into Cyclic Carbonates and Cross-Linked Polycarbonates. *ChemSusChem* **2015**, *8*, pp 1034-1042.

35. Yang, Y.; Wang, H.; Ma, H., Stereoselective Polymerization of rac-Lactide Catalyzed by Zinc Complexes with Tetradentate Aminophenolate Ligands in Different Coordination Patterns: Kinetics and Mechanism. *Inorg. Chem.* **2015**, *54*, pp 5839-5854.

36. Impemba, S.; Della Monica, F.; Grassi, A.; Capacchione, C.; Milione, S., Cyclic Polyester Formation with an [OSSO]-Type Iron(III) Catalyst. *ChemSusChem* **2020**, *13*, pp 141-145.

37. Andrea, K. A.; Kerton, F. M., Iron-catalyzed reactions of CO_2 and epoxides to yield cyclic and polycarbonates. *Polym. J. (Tokyo, Jpn.)* **2020**.

38. Kernbichl, S.; Reiter, M.; Adams, F.; Vagin, S.; Rieger, B., CO_2-controlled one-pot synthesis of AB, ABA block, and statistical terpolymers from beta-butyrolactone, epoxides, and CO_2. *J. Am. Chem. Soc.* **2017**, *139*, pp 6787-6790.

39. Paul, S.; Zhu, Y.; Romain, C.; Brooks, R.; Saini, P. K.; Williams, C. K., Ring-opening copolymerization (ROCOP): synthesis and properties of polyesters and polycarbonates. *Chem. Commun.* **2015**, *51*, pp 6459-79.

40. Andrea, K. A.; Kerton, F. M., Iron-catalyzed reactions of CO_2 and epoxides to yield cyclic and polycarbonates. *Polym. J. (Tokyo, Jpn.)* **2021**, *53*, pp 29-46.

41. Saini, P. K.; Romain, C.; Zhu, Y.; Williams, C. K., Di-magnesium and zinc catalysts for the copolymerization of phthalic anhydride and cyclohexene oxide. *Polym. Chem.* **2014**, *5*, pp 6068-6075.

42. Ni, K.; Paniez-Grave, V.; Kozak, C. M., Effect of azide and chloride binding to diamino-bis(phenolate) chromium complexes on CO_2/cyclohexene oxide copolymerization. *Organometallics* **2018**, *37*, pp 2507-2518.

43. Andrea, K. A.; Kerton, F. M., Triarylborane-catalyzed formation of cyclic organic carbonates and polycarbonates. *ACS Catal.* **2019**, *9*, pp 1799-1809.

44. Darensbourg, D. J.; Yarbrough, J. C.; Ortiz, C.; Fang, C. C., Comparative kinetic studies of the copolymerization of cyclohexene oxide and propylene oxide with carbon dioxide in the presence of chromium salen derivatives. In situ FTIR measurements of copolymer vs cyclic carbonate production. *J. Am. Chem. Soc.* **2003**, *125*, pp 7586-7591.

4.14. Appendix

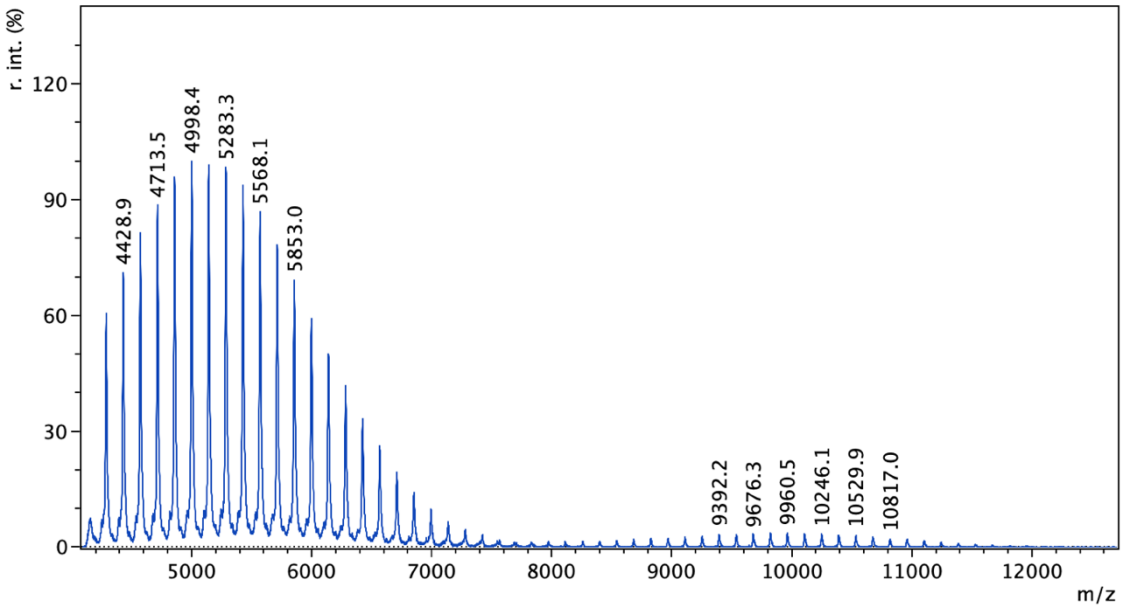

Fig. A4.1: Representative MALDI-TOF mass spectrum of polycyclohexene carbonate obtained using iron complex **4.2** and PPNCl (as in Table 4.1 entry 1). Polymer fragments identified as $Cl(C_6H_{10}CO_3)_n(C_6H_{10})OH]Na^+$. Reprinted with permission from Kori A. Andrea et al., *Inorg. Chem.*, **2019**, *58* (16), 11231 – 11240. Copyright © 2019 American Chemical Society.

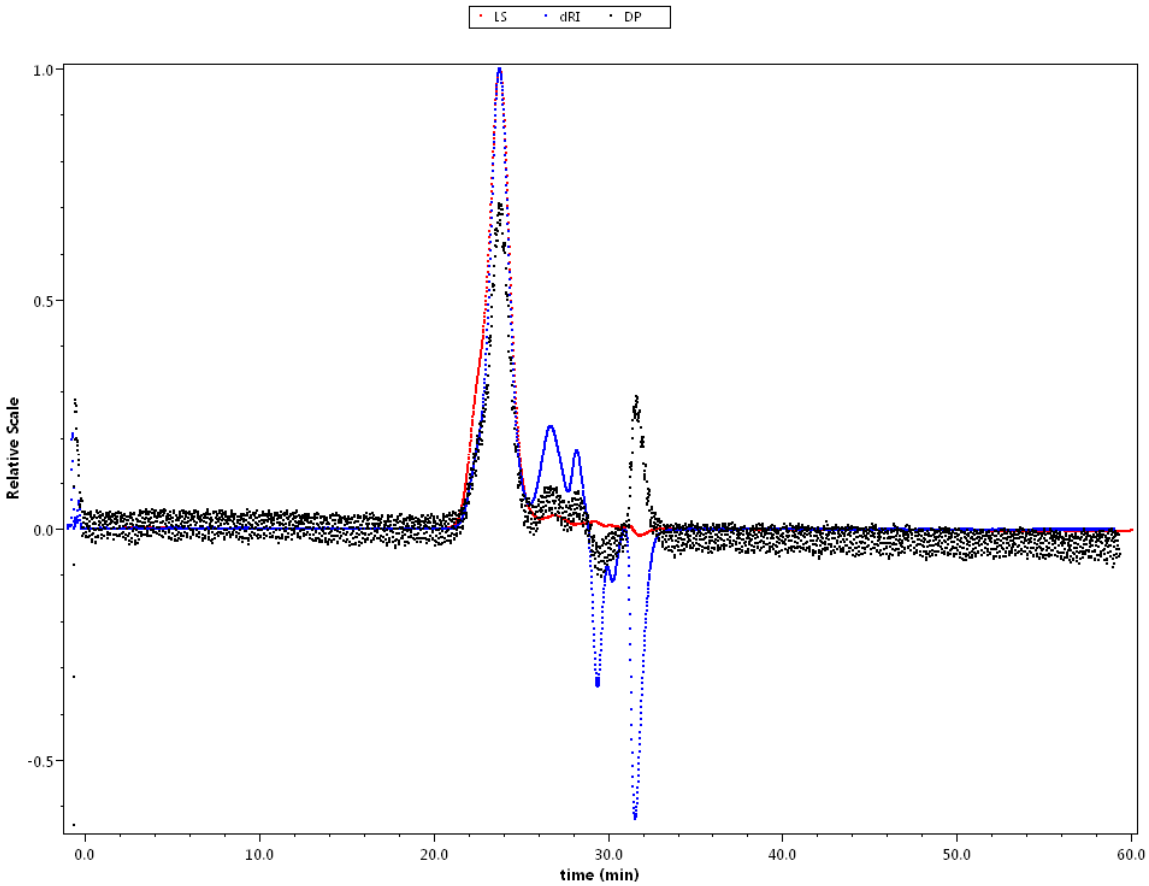

Fig. A4.2: Representative GPC trace for poly(ester)s described in this Chapter (Table 4.3, entry 13).

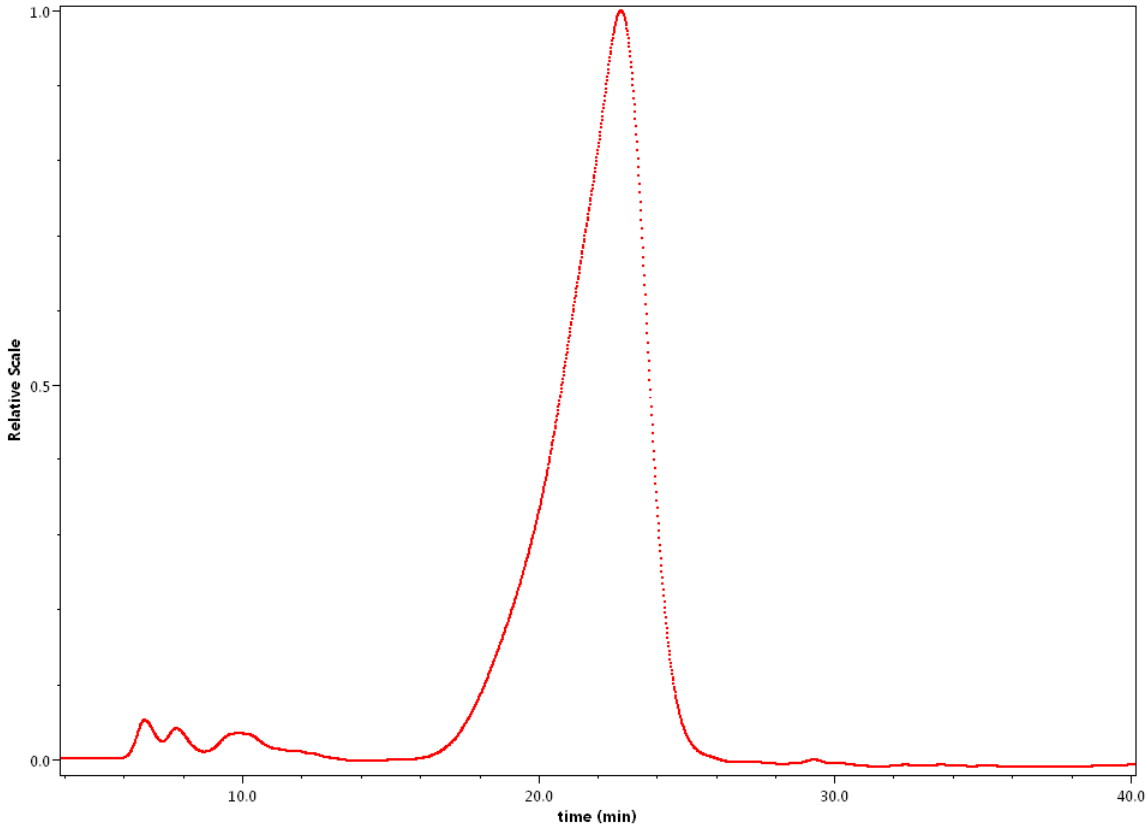

Fig. A4.3: Light scattering trace showing relative mass distribution for polymer in Table 4.3, entry 1.

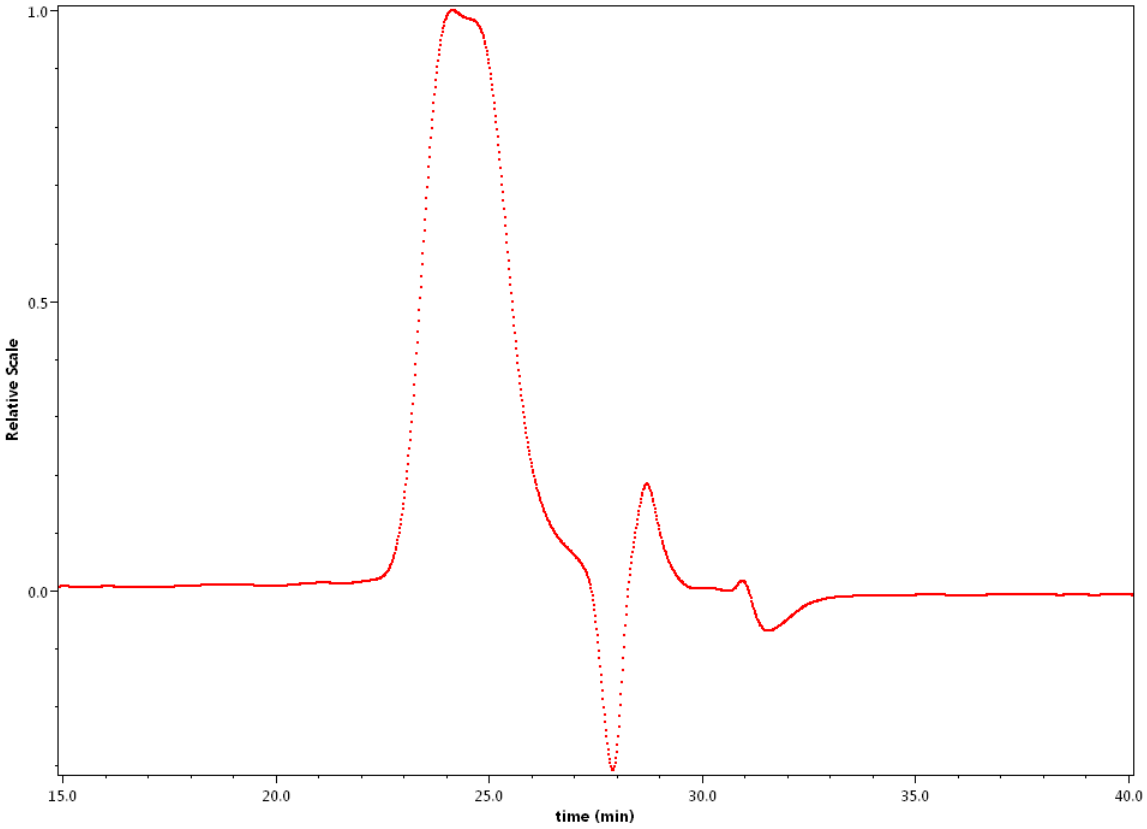

Fig. A4.4: Light scattering trace showing relative mass distribution for polymer in Table 4.3, entry 2.

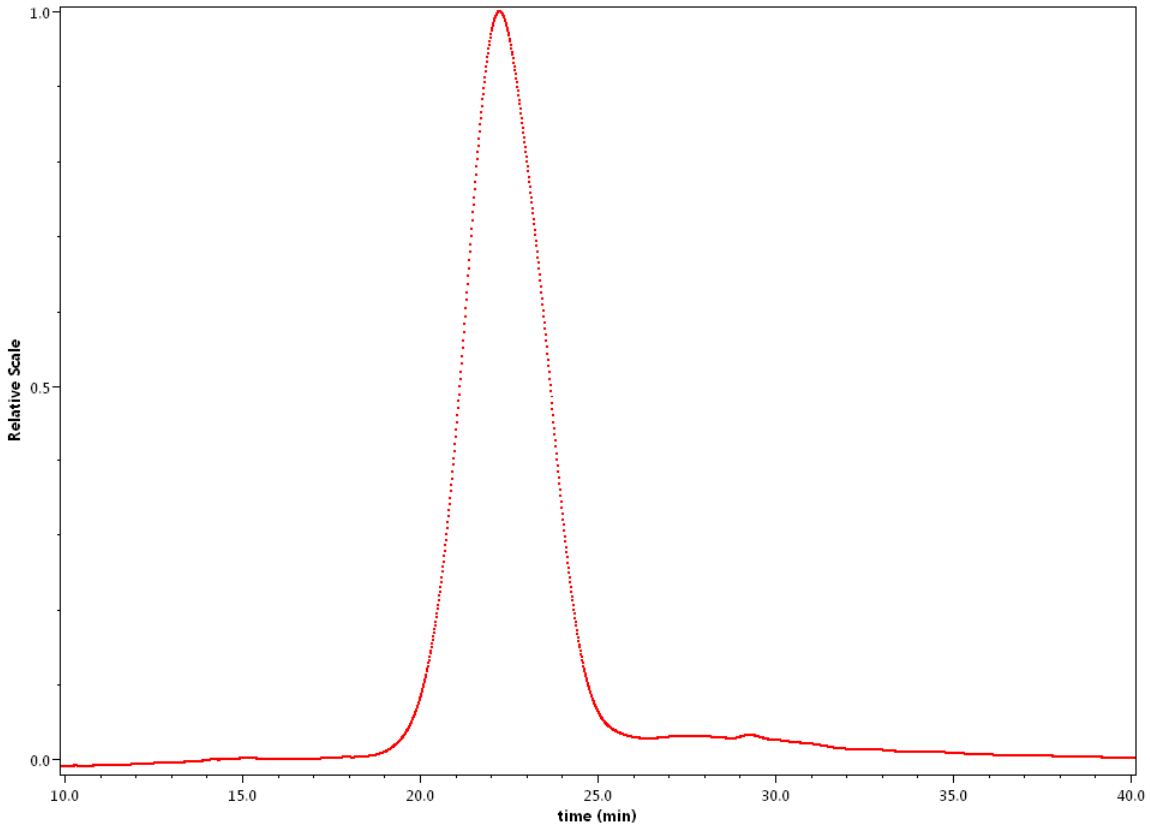

Fig. A4.5: Light scattering trace showing relative mass distribution for polymer in Table 4.3, entry 4.

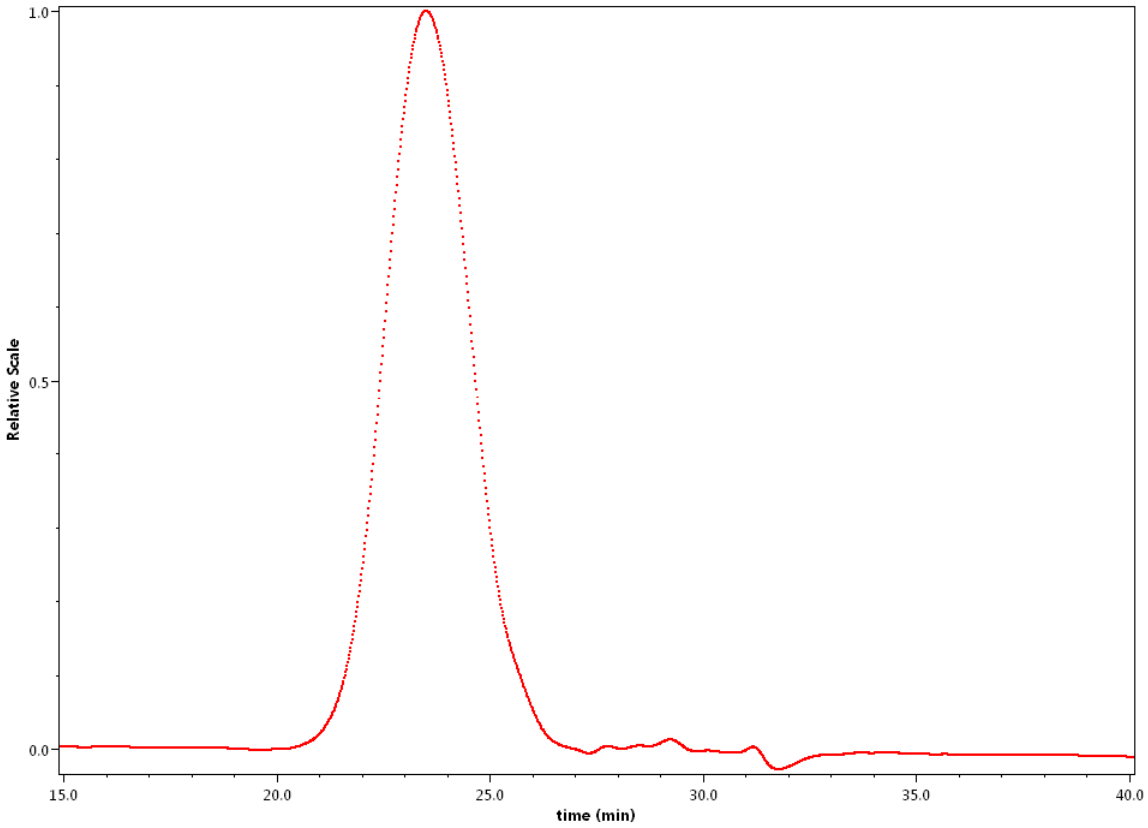

Fig. A4.6: Light scattering trace showing relative mass distribution for polymer in Table 4.3, entry 15.

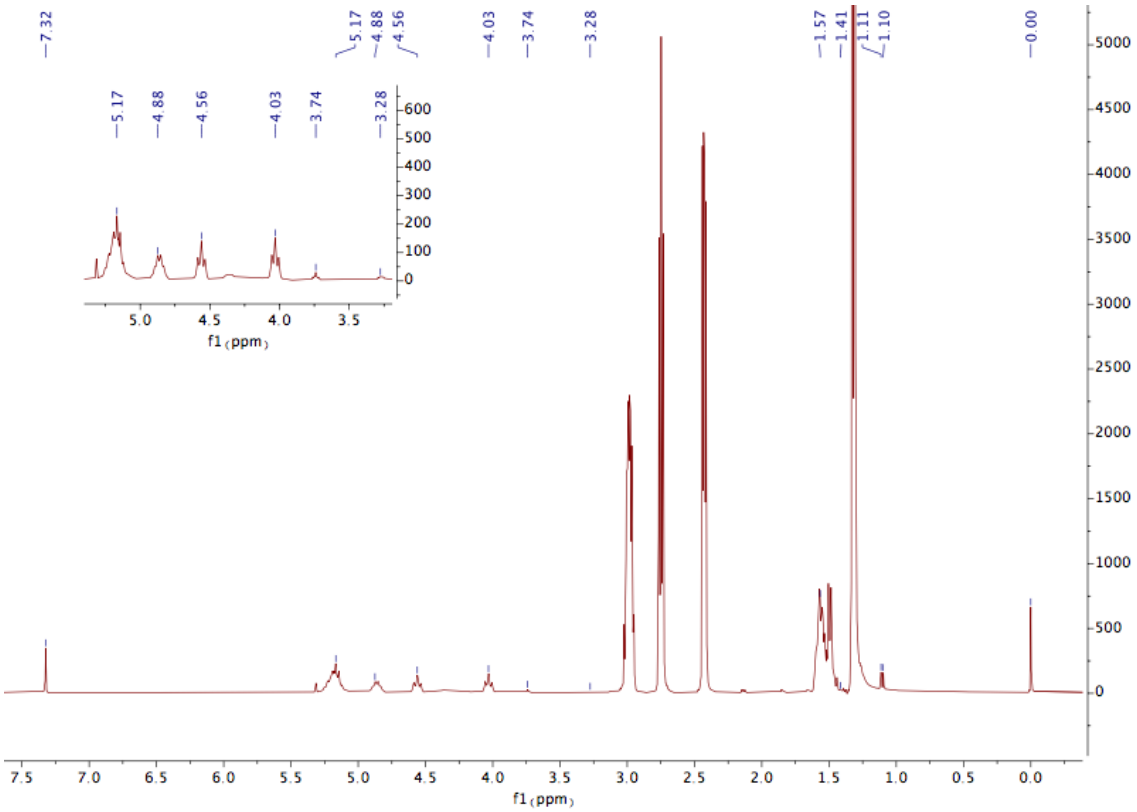

Fig. A4.7: ^{1}H NMR spectrum ($CDCl_3$) of crude PLA for

, entry 3. Propylene oxide end groups can be observed at δ 3.74, 3.27 and 1.10. δ 5.17 corresponds to PLA, 4.87, 4.56 and 4.03 correspond to cyclic propylene carbonate.

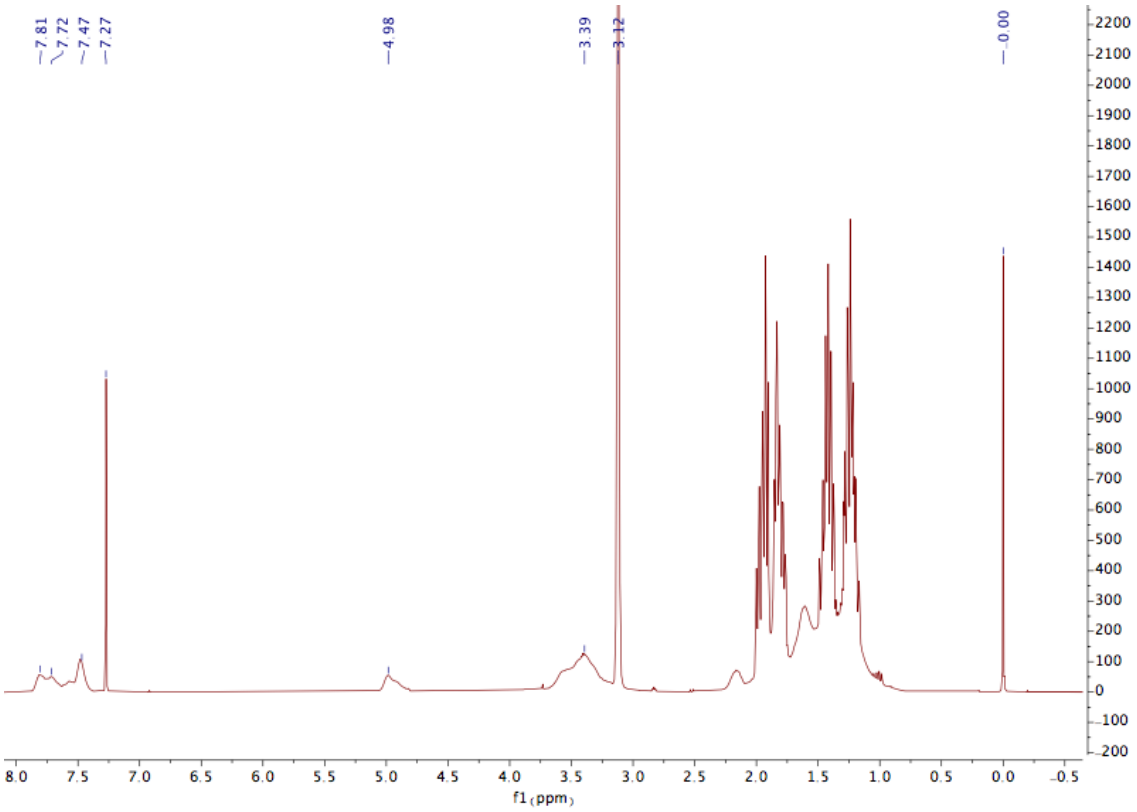

Fig. A4.8: ^{1}H NMR spectrum ($CDCl_3$) for Table 4.3, entry 2. δ 7.98 is unreacted PA. δ 4.39 and 5.41 correspond to PO segments of the poly(ester) while 7.69 – 7.48 represent the PA segment.

Chapter 5

Conclusions, Additional Experiments and Future Directions

This thesis has covered projects that had been completed or were near completion. In addition to the work previously described, there were other lines of investigation that were pursued that would benefit from deeper investigation. These will be discussed in this chapter.

5.1. Zinc catalysis for hydroamination and CO_2 and epoxide copolymerization

In addition to the aforementioned ethyl-zinc species described previously, the synthesis of zinc alkyls, amides and alkoxides were also investigated – specifically, $Zn(OBn)_2$, $Zn(N(SiMe_3)_2)_2$ and $Zn(CH_2SiMe_3)_2$ as starting materials for zinc complex synthesis. Zinc alkoxides were of particular interest as the initiator in Chapter 2 is theorized to be an alkoxide generated *in situ* and the Kozak group had previously synthesized an isopropoxide analogue of compound **2.1** that was isolated as a trinuclear, bis(ligand) species **5.1** (Fig. 5.1).[1] It is possible that bulkier alkoxide groups may prevent this behavior, and a well-defined dinuclear catalyst similar in structure to **2.1** may be obtained. This could provide insight into the mechanism as the identity of the active species in polymerization reactions involving **2.1** and BnOH remains unknown.

Zinc amides are a class of catalyst reported for polymerization reactions but are often sluggish compared to other catalysts due to the limited nucleophilicity of the amido groups.[2-3] As many other catalysts exhibit fine control in the presence of such initiators it is possible that the ligand design reported in Chapter 2 is suitable for such a system as well.

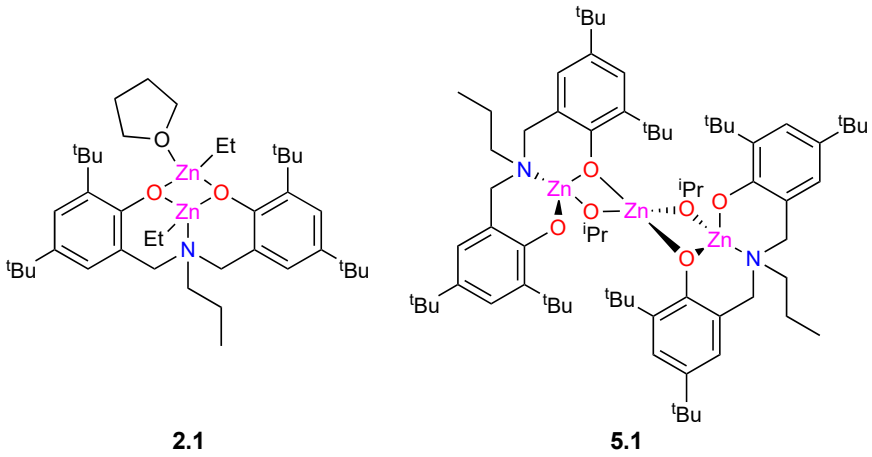

2.1 **5.1**

Fig. 5.1: Dizinc, mono(ligand) compound **2.1** and trizinc, bis(ligand) compound **5.1** reported by Kozak and coworkers.[1,4]

To date, my attempts to isolate benzyloxide derivatives of **2.1** have been unsuccessful. The attempted preparation of $Zn(OBn)_2$ from diethyl zinc instead resulted in $(Et)_xZn(OBn)_y$ clusters.[5] $Zn(N(SiMe_3)_2)_2$ is a useful starting material for synthesis of amido zinc complexes.[6] In the reaction with **H_2L2.1** in pursuit of (**L2.1**)$Zn(N(SiMe_3)_2)$, the product could not be identified. Kol and co-workers reported a salan-zinc tetrahedral complex devoid of $N(SiMe_3)_2$ ligands from the starting material.[7] It is possible a similar process is occurring here with a dimeric structure, or oligomeric coordination polymers, forming through bridging phenoxides similar to the isopropoxide trinuclear species **5.1** above but characterization of the product was unsuccessful. Similarly, $Zn(CH_2SiMe_3)_2$ was synthesized

as reported elsewhere[8] but attempts to synthesize complexes based on **L2.1** or **5.1** resulted in isolation of free ligand and insoluble, colourless powder. It is known that trace contamination of glassware surfaces with protons or hydronium ions can result in the decomposition of highly moisture sensitive metal complexes and thus glassware was "silanized" with trimethylsilyl chloride to ensure the SiO_2 surface was devoid of protic sites. Despite my best efforts the resulting complexes proved far too sensitive to isolate and for the purposes of polymerization, diol contamination ever-present in epoxides would likely deactivate any potential catalyst containing this ligand.

Sarazin and co-workers had previously demonstrated the efficacy of ligand **5.2** paired with ZnEt, $Zn(N(SiMe_3)_2)$, $Zn(N(SiMe_2H)$ and $Zn(OSiPh_3)$ toward ROP of cyclic esters. Given the remarkable activity of other zinc species toward CO_2 and epoxide copolymerization (Chapter 2) I thought the potential of this family of compound toward such reactions appeared high.[6] Compound **5.3** was synthesized and applied toward the copolymerization of CHO and CO_2 at 0.5 mol%, 40 bar and 60 °C for 18 h (Scheme 5.1). Without a co-catalyst, no activity was observed under these conditions for any polymerization or coupling reactions. Under the same conditions with 1 equiv BnOH co-catalyst, 35% conversion to PCHC was observed and 5% to poly(ether) with polymer molecular weight of 30,800 g mol^{-1} and dispersity of 2.88. As these results were suboptimal compared to those reported in Chapter 2 with compound **2.1**, no further CO_2 and epoxide copolymerization was studied with this complex.

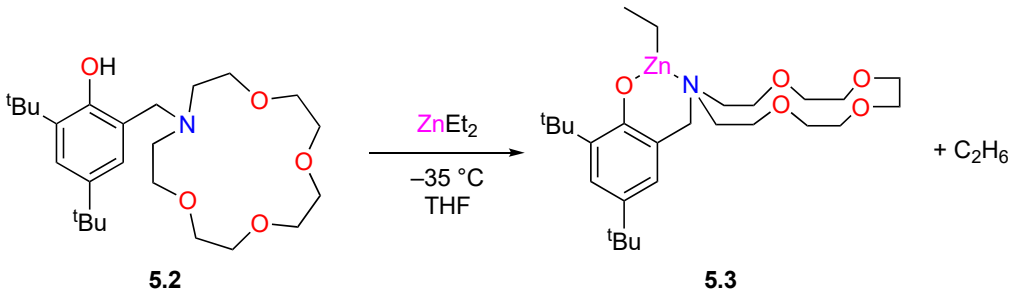

5.2 **5.3**

Scheme 5.1: Macrocyclic-aza-crown-ether-phenol compound **5.2** and corresponding zinc complex **5.3**.

Sarazin and co-workers had used the ligand framework above to synthesize cationic zinc complexes that could be stabilized through interactions of the metal with the crown-ether segment and a counterion. In order to release ethane a strong acid is required with a stabilizing counterion and bulky borate ions were found to be suitable for this purpose. Brookhart's acid, $[H(OEt_2)_2]^+[B((m\text{-}CF_3)_2C_6H_3)_4]^-$, was prepared according to literature procedure and combined with aza-crown-ether-phenol **5.2** in toluene to afford the diacid.[9] This was then combined with diethyl zinc in toluene to form the corresponding cationic zinc borate species **5.4** (Scheme 5.2), which could be isolated in high yield (81%). Crystals suitable for X-ray diffraction were grown from the reaction mixture (Fig. 5.2). As anticipated, the cationic metal centre was stabilized through interactions with the oxygen atoms of the aza-crown-ether fragment. The low activity of **5.3** toward copolymerization discouraged me from applying **5.4** for similar reactions, instead focusing on the essence of my Mitacs Globalink Research Award project – hydroelementation reactions. This grant aimed to develop transition metal complex catalysts for hydrophosphination and hydroamination reactions. Small molecules containing nitrogen and phosphorus are important in pharmaceuticals,

agrochemicals, materials, natural product synthesis and for ligand design in catalysis. Synthesis of nitrogen and phosphorus containing molecules with varied functionality is highly desirable and one-pot hydroelementation reactions could replace the current multi-step processes employed industrially.

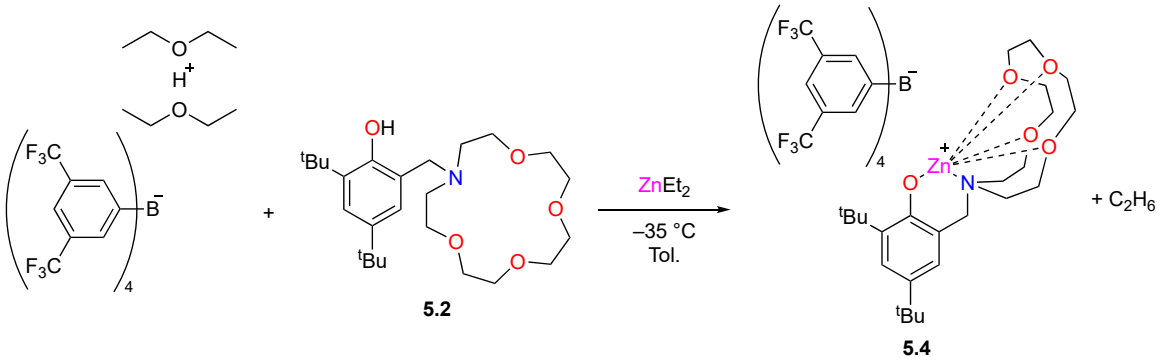

Scheme 5.2: Synthesis of ionic zinc borate **5.4**.

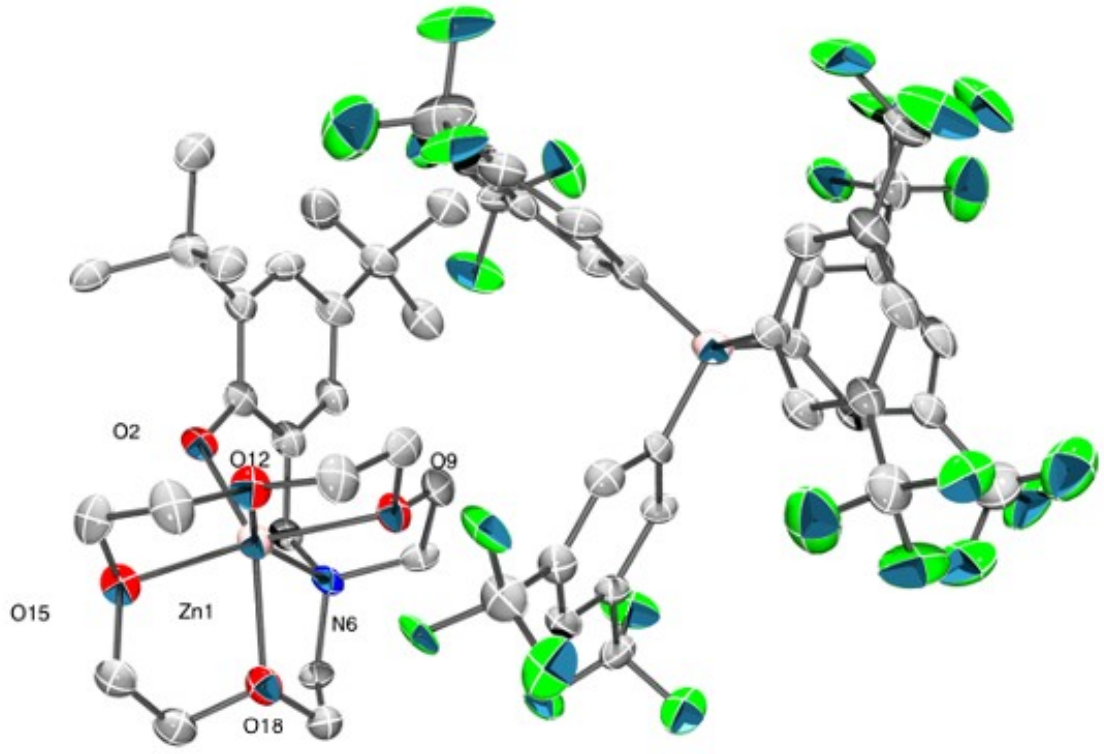

Fig. 5.2: Partially labelled ORTEP view of ionic zinc compound **5.4**. Thermal ellipsoids are drawn at 50% probability with hydrogen atoms omitted for clarity. Selected bond distances (Å) and angles (°): Zn(1) – O(2), 1.919(6); Zn(1) – O(9), 2.198(6); Zn(1) – O(12), 2.174(6); Zn(1) – O(15), 2.251(6); Zn(1) – O(18), 2.196(6); Zn(1) – N(6), 2.162(8); O(2) – Zn(1) – O(9), 112.8(2); O(2) – Zn(1) – O(12), 95.9(2); O(9) – Zn(1) – O(12), 73.2(2); O(2) – Zn(1) – O(15), 89.2(2); O(9) – Zn(1) – O(15), 142.4(2); O(12) – Zn(1) – O(15), 74.6(2); O(2) – Zn(1) – O(18), 150.0(2); O(9) – Zn(1) – O(18), 95.3(2); O(12) – Zn(1) – O(18), 102.4(2); O(15) – Zn(1) – O(18), 73.2(2); O(2) – Zn(1) – N(6), 95.4(3); O(9) – Zn(1) – N(6), 77.6(3); O(12) – Zn(1) – N(6), 150.8(3); O(15) – Zn(1) – N(6), 132.4(2); O(18) – Zn(1) – N(6), 80.1(3).

Screening for hydroamination activity was performed with compounds **2.1** and **5.4**. The aminoalkene, 2,2-diphenyl-4-penteneamine, **5.5** (Fig. 5.3) was chosen as the substrate as

intramolecular hydroamination is entropically neutral as opposed to intermolecular reactions, and substrates containing *gem*-disubstituted functionality favour cyclohydroamination. Under the conditions described in Table 5.1, cyclohydroamination of **5.5** was ineffective or very poor after 18 h. At elevated temperatures (40 and 80 °C) **2.1** was inactive toward hydroamination in $CDCl_3$. Changing the solvent to C_6D_6, hypothesizing that trace HCl present in $CDCl_3$ may impede reactivity or deactivate the catalyst, a low conversion of 5% could be observed. This result was much lower than other catalysts in the literature under the same conditions so no further hydroamination catalysis was pursued with this complex. Compound **5.4** was insoluble in C_6D_6 and so the polar aprotic CD_3CN was instead employed, but no conversion was observed at 25 °C. Attempts to isolate a CD_3CN adduct of **5.4** proved fruitless. As the activity toward hydroamination was low, and CO_2 and epoxide copolymerization studies were affording good results, further hydroelementation reactions were forgone in favour of the polymer research of Chapters 2 and 3.

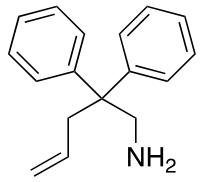

5.5

Fig. 5.3: Aminoalkene used to screen hydroamination activity.

Table 5.1: Hydroamination of **5.5** by zinc catalysts.

Entry[a]	Catalyst	Solvent[b]	Temp. (°C)	Conv. (%)[c]
1	**2.1**	$CDCl_3$	25	0
2	**2.1**	$CDCl_3$	40	0
3	**2.1**	$CDCl_3$	80	0
4	**2.1**	C_6D_6	25	5
5	**5.4**	CD_3CN	25	0
6	**5.7**	C_6D_6	80	0

[a]0.5 mol% catalyst loading, 18 h. [b]700 μL. [c]Determined via ^{1}H NMR of the reaction mixture.

In hindsight, **5.4** and other ionic complexes could be ideal candidates for copolymerization of CO_2 and epoxides as some other ionic species have previously demonstrated high activity for such chemistry. Specifically, Lu, Darensbourg and co-workers have reported several bifunctional chromium catalysts that contain onium salts tethered to the ligand framework, such as compound **5.6** (Fig. 5.4).[10] This particular species was highly active toward PO and CO_2 copolymerization. Later, Sarazin and co-workers reported that a cationic zinc borate species performed much better than the comparative alkaline earth metal analogues for ROP of lactide.[11] This information, and the successes of ionically tagged metal complex-catalyzed copolymerization of CO_2 and epoxides[10] may suggest that these ionic zinc species could be excellent candidates for poly(ester-*co*-carbonate) synthesis described in Chapter 4. If the low activity of **5.3** and **5.4** toward epoxides could be improved or controlled carefully, this could open up the potential for more complex terpolymerization reactions described in earlier Chapters.

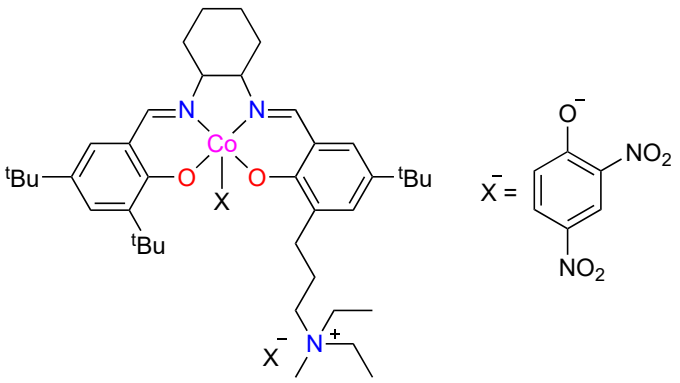

5.6

Fig. 5.4: Ionically tagged cobalt complex used for CO_2 and PO copolymerization.[10]

5.2. Group IV catalysts for hydroelementation reactions

A project started as part of a Mitacs Globalink Research Award consisted of the synthesis of zirconium, titanium and hafnium chiral proline-based ligand complexes. The zirconium compound **5.7** is shown in Scheme 5.1. Group IV metals are an inexpensive alternative to precious metals such as Pd, Pt, Rh and Ir. They are generally biologically inactive and earth abundant.[12-17] Hafnium complexes often exhibit similar activities to zirconium analogues but at slower rates, providing ideal conditions for studying kinetic behavior of the hydroelementation reactions.[18-19]

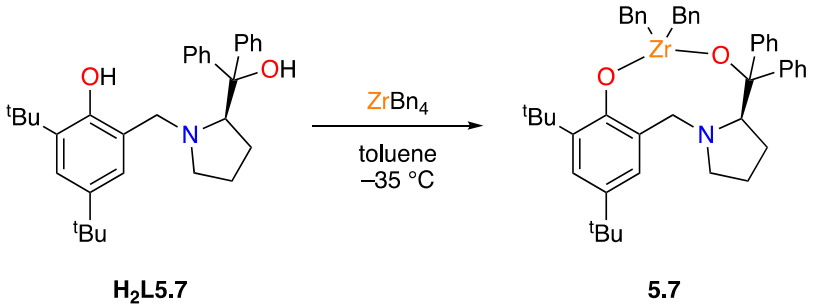

H$_2$L5.7 **5.7**

Scheme 5.3: Synthesis of chiral zirconium complex **5.7** from proligand **H$_2$L5.7**.

Rare earth (Yb, Y, Sm, Nd) complexes supported by the *S*-enantiomer of compound **L5.7** were previously reported and applied as catalysts for asymmetric epoxidation of *a,ß*-unsaturated ketones.[20] These complexes exist as heterobimetallic [Ln(*S*-**L5.7**)$_2$]$^-$ anions paired with a [(THF)$_3$Li$_2$]$^+$(μ-Cl) cation. $ZrBn_4$ was prepared according to literature procedure and stored in the dark to prevent photochemical degradation.[21] Reactions of **H$_2$L5.7** with $Zr(NMe_2)_4$ were unsuccessful in generating the bis(amido) analogue. Compound **5.7** was screened for hydroamination activity under the conditions described in Table 5.1 but was inactive. Very closely related compounds (Fig. 5.5) were shown to be active toward **5.5** at 100 °C, reaching high conversions over different reaction lengths dependent upon the R groups.[22] Compound **5.8** was the fastest, achieving 93% conversion to the Markovnikov product in 2.5 h. Similar conversion was observed using **5.9** (95%) but required 4.5 h reaction time. Using **5.10** also reached a high conversion of 96% but after 11 h. Each of the products exhibited enantiomeric excesses greater than 67% (*R*-enantiomer). However, compound **5.11** reached 85% conversion with %ee of 13% (*S*-enantiomer) and required 59.5 h to reach completion. Clearly, the R groups have an impact on the enantioselectivity of this product as well. It would be prudent to extend reactions with **5.7** to

60 h and elevate the temperature to 100 °C. This would also provide information on the influence of the *ortho*-aryl substituent (e.g. CPh_3).

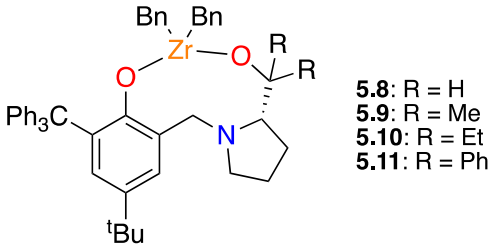

Fig. 5.5: Chiral zirconium complexes for hydroamination of **5.5** at 100 °C (C_6D_6). Compound **5.9** was also applied toward other *gem*-disubstituted aminoalkenes.[22]

As described above, the proposed hydroelementation reactions catalyzed by **5.7** could be an excellent research project if the activity of the catalyst exhibits similar activity to those above.[22] Hydroelementation reactions catalyzed by zirconium complexes is well studied compared to the other group IV metals, particularly hafnium. Regioselective hydroelementation is also of interest but only a few examples of such group IV metal complex catalyzed processes have been reported.[23-27] Some of these reports involve zirconium amino-bis(phenolate) complexes (Fig. 5.6) and the Kozak group has extensive experience with this class of ligand and thus provides a prime opportunity to capitalize on the transformation. Due to the nature of such reactions, the substrate scope is enormous – whether the substrates are primary or secondary amines and phosphines, and terminal or internal alkenes and alkynes – with mechanistic and kinetic studies relying on the synthons that return positive results. As such, separating the research goals into groups comprised of

metal choice, ligand design, inter or intramolecular reactions, and phosphine or amine coupling with alkenes or alkynes is necessary.

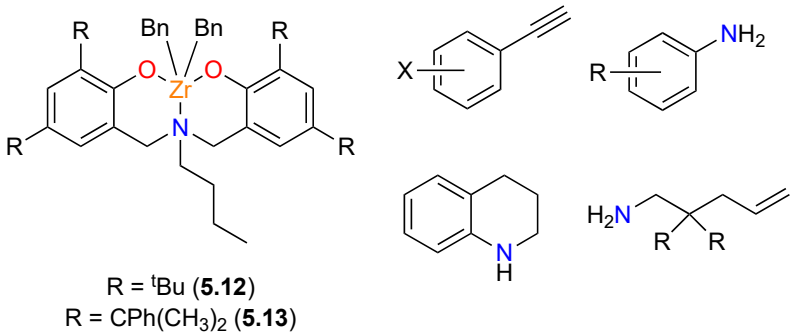

Fig. 5.6: Zirconium amino-bis(phenolate) complexes used for intermolecular hydroamination of alkynes and amines.[27] Examples of substrates throughout the literature are shown on the right.

5.3. Zinc amino-bis(phenolate) catalysts for polymerization reactions

In Chapter 2, the activity of **2.1** for CO_2 and epoxide copolymerization is described, and although some of the molecular weights of the polymers obtained were quite high, they were also more polydisperse than polymers reported by others.[28-29] However, the synthesis of poly(limonene carbonate) and the activity at 1 bar of CO_2 with CHO are worthy of further investigation. Development of an isolable alkoxo zinc complex would be desirable as I believe the generation of alkoxide initiator from BnOH and **2.1** *in situ* is limiting initiation toward ROP of epoxides. Furthermore, as activity was observed at 1 bar of CO_2, further study into activity toward other epoxides at low pressures is worthwhile. Unfortunately, as

ROP of CHO is rapid with compound **2.1**, selectivity toward poly(carbonate) at low pressures is unlikely. Also, the chiral amino-phenolate ligand **H_2L5.7** with zinc (or other transition metals) may be suitable for copolymerization of CO_2 and asymmetric epoxides (such as propylene oxide) for stereoselective polymerization.

5.4. Iron catalyzed polymerization reactions

As described in Chapter 4, compounds **4.8** and **4.9** have afforded promising results for copolymerization reactions involving cyclic esters and anhydrides with epoxides and further development of this chemistry should be prioritized because the synthesis of well-controlled CO_2 and epoxide copolymerization catalysts by other metal complexes is well developed.[30-31] Also, although several reports of iron catalyzed CO_2/epoxide copolymerization exist,[32-34] iron catalysts typically result in the production of cyclic carbonate rather than polymer.[30-31,35] Chapter 4 showed that the nature of the pendent donor groups of the iron complexes described therein dictated the activity toward CHO and CO_2 copolymerization. Should less bulky pendent donor groups (i.e. **4.5**) or sp^2 donors (i.e. **4.1a**) be employed carbonate units may be incorporated into the polymer as selectivity toward PCHC was observed with **4.5** at modest conversions (48%) and **4.1a** at 99% conversion. As such, for the purposes of these or other complexes in Chapter 4, diversifying the substrate scope to include cyclic esters and anhydrides alongside the more active epoxides should allow for terpolymer synthesis of various chemical compositions (Scheme 5.4).

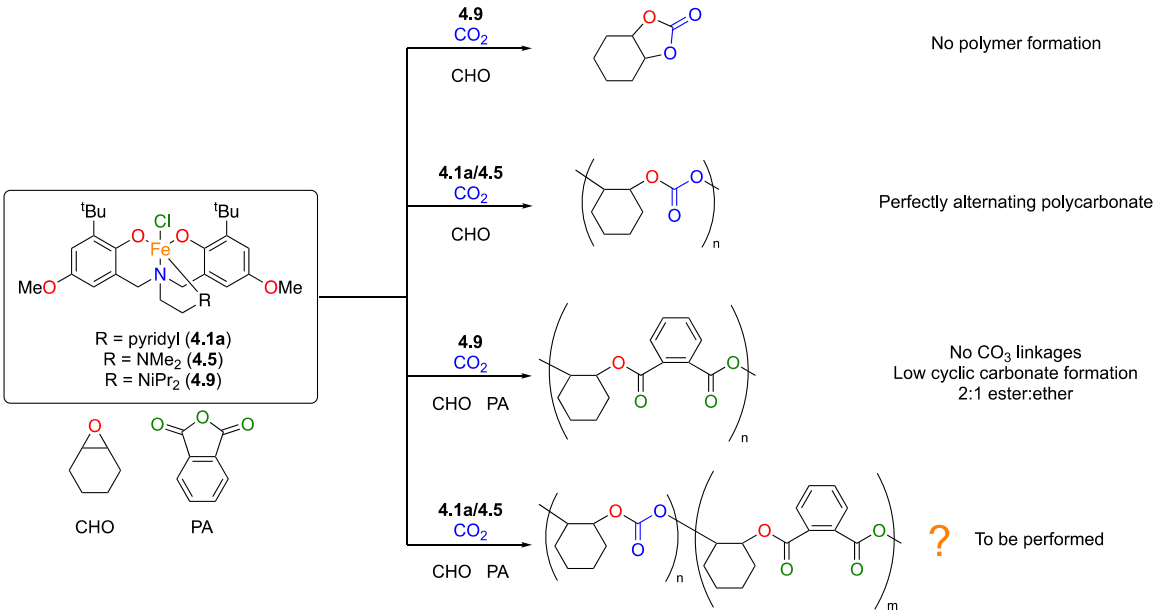

Scheme 5.4: Potential carbonate enchainment by **4.1a** and **4.5** due to activity toward CHO and CO_2 copolymerization. Details on the reactions can be found in Chapter 4.

5.5. Peroxo metal complexes for epoxidation and subsequent copolymerization with CO_2

The alkylperoxo zinc chemistry described in Chapter 3 represents the beginning of what could be a rich project for further development. Although the synthesis the alkylperoxo zinc analogue of **5.3** was elusive, it is believed that this is due to the highly flexible behavior of the aza-crown-ether fragment of the ligand encouraging σ-bond metathesis with **5.3** (Scheme 5.1). Isolation of the expected zinc-alkoxide from such a transformation was not achieved. As Lewiński and others have shown, metal complexes of alkylperoxo ligands are not limited to zinc, as magnesium and cobalt complexes have been reported.[36-38] The stability of these complexes is likely heavily influenced by the strength of the O–O bond but also the

enthalpy of formation of the corresponding metal oxidation products, typically metal oxides. To my knowledge, the most thermodynamically "unfavourable" peroxo metal complexes that have been isolated and structurally characterized are cobalt complexes as the enthalpy of formation of Co_3O_4 is –891 kJ mol^{-1}.[39] The 3d metal oxides where $\Delta_f H$ [oxide] < 891 kJ mol^{-1} include TiO, VO_2, MnO, MnO_2, FeO, Fe_2O_3, CoO, Ni_2O_3, Cu_2O, CuO and ZnO.[39] If the limitation on peroxo metal complex formation is governed by the enthalpy of formation of the corresponding metal oxides, any of these metals could be suitable. For copolymerization of epoxides and CO_2, it is sensible to focus upon those in which catalysts derived from those metals have exhibited high activity toward polymer formation.[31] Therefore, zinc and cobalt are the ideal candidates and examples of alkylperoxo metal complexes with these metals have been reported (Chapter 3 and below).

In Chapter 3 it was shown that the one-pot synthesis of poly(carbonate) from epoxidation of alkene substrates followed by reaction with CO_2 was viable. The investigation of individual reactions contained within the proposed catalytic cycle remains to be performed. Specifically, the epoxidation of alkenes by the alkylperoxo metal complexes formed under controlled reaction with oxygen may provide an alternative source of epoxides to conventional methods or allow for expanded epoxide scope. As more examples of alkylperoxo metal complexes are reported, the opportunity presents itself to apply these toward less functionalized alkenes. Of particular interest as catalysts are alkylperoxo cobalt complexes. Cobalt catalysts for CO_2 and epoxide ROCOP are well known.[31] Therefore, applying such analogous catalysts toward epoxidation of alkenes may be a feasible method of simple epoxide synthesis and subsequent polymerization or coupling with CO_2. Alkylperoxo

cobalt complexes have been known for some time, the earliest report of a structurally characterized complex was in 1985 (Fig. 5.7).[36,40]

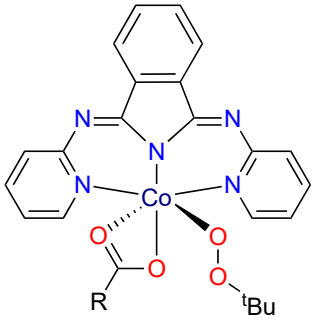

R = Ph (**5.14**)
R = Me (**5.15**)

Fig. 5.7: The first structurally characterized alkylperoxo cobalt complex, **5.14**, and related compound **5.15** that was not structurally characterized.[36]

The bonding environments of **5.14** and **5.15** contain a planar tridentate monoanionic ligand that enforces a meridional coordination mode in octahedral Co(III) complexes. This leaves three coordination sites and two charges for ancillary ligands, in these examples, carboxylate and alkylperoxo ligands. Although the coordination number of this ligand differs from that of the tetradentate salen ligands that are common to CO_2 and epoxide copolymerization, both are strong donor ligands with typically planar orientations around a coordinated metal. Much like **5.14** and **5.15**, Co(III) salen complexes may be suitable for alkylperoxo cobalt complex synthesis. Compounds **5.14** and **5.15**, as well as other related compounds that could not be structurally characterized, were synthesized by addition of ^{t}BuOOH solution to the Co(II) ligand complexes in C_6H_6. Each of these species exhibited conversion of sp^2 and sp^3 hybridized carbon containing compounds to various oxidation

products (i.e. alcohols, ketones, epoxides) with selectivity at sp^2 carbon sites over sp^3. Compound **5.15** produced epoxides in much greater yields than **5.14** from unsaturated starting materials and complete selectivity for epoxides over other oxidation products if there were one or fewer allylic protons present. Evidently the carboxylate ligand plays an important role toward reactivity. Whether this is strictly due to electronic or steric differences between **5.14** and **5.15** or the ligand participates in the reaction is unknown. The proposed reaction mechanism is shown below and suggests that the carboxylate ligand is ancillary (Scheme 5.5). Although not speculated upon in the report, it is possible that resulting *tert*-butoxy radical can bind with the Co(II)L species by electron donation from the metal, forming a Co(III) alkoxide complex – possibly an active initiator for ROP of epoxides. If so, peroxo ligand regeneration from cobalt alkoxide may also be possible in the presence of ^{t}BuOOH (or other alkyl hydroperoxide) as described in Chapter 3.

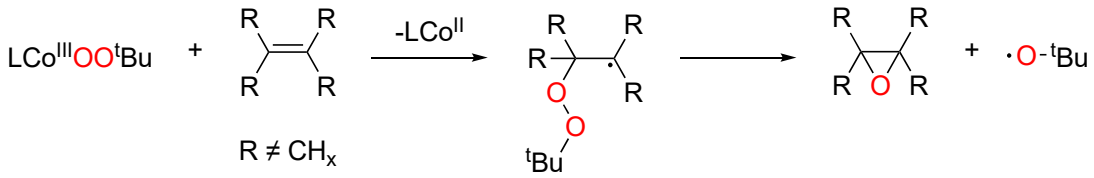

Scheme 5.5: Proposed mechanism for epoxidation of alkenes.[36]

Thus far the discussion of peroxo-metal complexes has relied on discrete peroxo ligands, but recently an example of an alkylperoxo cobalt complex (**5.16**) was reported that generates the peroxo ligand intramolecularly – tethering one oxygen to the chelating ligand (Fig. 5.8).[37] Whether such a species would be suitable for epoxidation of unfunctionalized alkenes is unknown. Other first row transition metals, including cobalt, have been studied for

CO_2 and epoxide ROCOP by members of the Kozak and Kerton groups, and others, and the reports of alkylperoxo cobalt complexes highlights the potential of this metal toward one-pot epoxidation-polymerization reactions.[41]

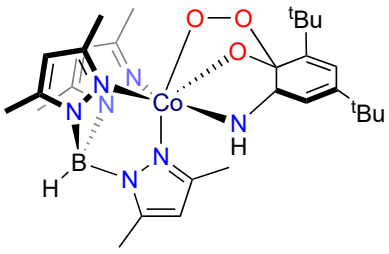

5.16

Fig. 5.8: Cobalt complex with intramolecular alkylperoxo ligand.[37]

A study modelling the reaction mechanism of cobalt-substituted homoprotocatechuate 2,3-dioxygenase enzyme (Co-HPCD) examined the supposed active site of the enzyme and highlighted several intermediates of interest.[42] Foremost among these are the alkylperoxo radical complex (**5.17**) and the epoxide containing complex (**5.18**) shown below (Fig. 5.9). As the histidine are nitrogen donors, the similarities between the enzymatic ligand system and that of **5.14 – 5.16** above can be seen. However, perhaps due to the lack of hydrogen bonding to weaken it, the O–O bond remains intact. Furthermore, as the indole (tryptophan in the enzymatic macrostructure) acts as a "radical sponge", it may be possible to isolate the epoxides that form as shown in compound **5.18**, although this may again limit the substrate scope if coordination of the substrate is required. However, unlike the alkylperoxo zinc complexes in Chapter 3, this would not rely on the generation of alkylperoxo metal

complexes prior to epoxidation. Rather, substrate-metal coordination complexes could be developed first, with peroxide source introduced to those which exhibit ligand behaviour.

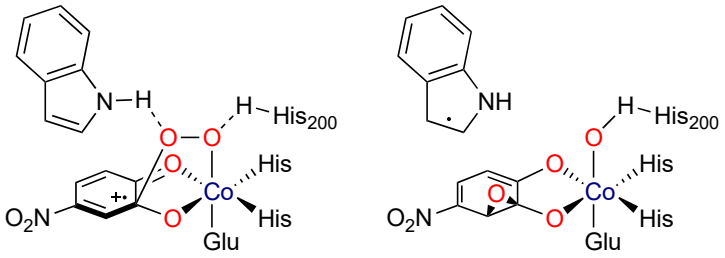

5.17 **5.18**

Fig. 5.9: Intermediate species of Co-HPCD modelled by quantum mechanical/molecular mechanical calculations.[42] Glu refers to glutamate and His to histidine as a simplified representation of the enzyme active site.

A Co(II) salen complex exhibited activity toward triethylsilylperoxidation of terminal alkenes.[43] A cobalt alkyl complex is required to incorporate elemental oxygen and was generated *in situ* via insertion of terminal alkenes into a Co–H bond. This preparation of the hydride complex results in oxidation to Co(III) but many alkyl Co(III) salen complexes are known.[44,45,46,47] It is also known that Co(II) salen complexes are oxidized by O_2, thus preparation of the alkyl complexes prior to O_2 addition is key.[48] Nojima and coworkers propose a mechanism suggesting the release of an alkyl radical via homolytic cleavage and subsequent reaction of the alkyl radical with O_2.[43] The resulting alkylperoxo radical then reacts with a Co(II) complex leading to the formation of a Co(III) alkylperoxo complex. Addition of triethylsilane at this stage completes the triethylsilylperoxidation, but there was no mention of whether the alkylperoxo complexes could be isolated. Additionally, while the

cobalt salen complex was suitable for this reaction, only 33% conversion was observed over 6.5 h, while cobalt "acac" and functionalized "acac" complexes were much more active, reaching 95% and 100% conversions respectively over 3.5 h. This may suggest that the peroxo species were much more reactive in the "acac" complexes, perhaps due to higher electron density at the metal of these two species than would be the case in the salen complex due to the electron withdrawing imine groups of the ligand. As the electronic properties of such ligands can be influenced rather easily, these compounds are excellent candidates for alkylperoxo cobalt complex synthesis and characterization. Co(II) peroxo complexes may exhibit limited substrate scope if homolytic cleavage of Co–C bonds occurs readily, particularly of those containing *ß*-protons as described in Scheme 5.5. Due to the probable presence of radical species *in situ* and that the theorized alkylperoxo cobalt complexes are all diagmagnetic, EPR and NMR spectroscopy would be excellent tools to monitor and characterize the compounds. Among the cobalt complexes synthesized previously in the Kozak group, K. Ambrose prepared a series of Co(II) amino-bis(phenolate) complexes of which two examples, **5.19** and **5.20** (Fig. 5.10), are mononuclear.[49] Studying the feasibility of these compounds for peroxo complex synthesis is a suitable starting point for such a project.

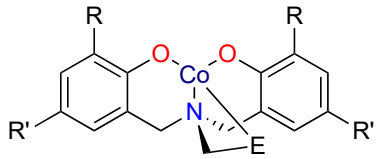

E = CH_2NMe_2 (**5.19**)
E = C_5H_4N (**5.20**)

Fig. 5.10: Co(II) amino-bis(phenolate) complexes from the Kozak group.[49]

As this project is still in its infancy, focusing on the development of alkylperoxo complexes can be performed first. Although isolation of compound **3.1** was an exciting result, the uncertainty surrounding its structure in solution suggests that simpler mononuclear zinc alkyl complexes may be better candidates for such transformations, particularly those with *ß*-diketiminate ligands (i.e. **1.41**) that encourage dimer formation in the alkylperoxo complexes. Well defined complexes will allow for controlled stoichiometry and better mechanistic understanding as multimetallic complexes may involve cooperative mechanisms that are difficult to elucidate. This is where I believe compounds **5.19** and **5.20** to be interesting subjects of study. Information gleaned from such studies would improve further ligand design. Similarly, cobalt salen (and salan) compounds are strong candidates for alkylperoxo complex isolation and the Kozak group has a deep understanding and a wide library of such compounds to study. The focus here can be on peroxo complex generation rather than ligand design and will provide excellent data regarding the influence of the electronic effects of the ligands. Furthermore, I believe alkylperoxo cobalt complexes to be excellent candidates for enhanced alkene scope. As shown by the oxidative addition process above, there is interaction with the unsaturated bond at the metal and this may encourage reactivity with an alkylperoxo ligand.

Alkylperoxo zinc complexes for epoxidation reactions are thus far limited to enones. This is reportedly due to the enhanced electrophilicity of the alkene in the enol tautomer, suggesting that alkylperoxo ligands with zinc exhibit reduced nucleophilicity compared to the cobalt complexes above. If the substrate scope of peroxo zinc complexes cannot be expanded, it is possible that heterodinuclear complexes of zinc and cobalt (or another metal

known to activate alkenes) could provide a suitable environment for peroxo complex formation and controlled reactivity. Heterodinuclear complexes of zinc and other metals have been used in CO_2 and epoxide copolymerization to great effect, seemingly retaining the benefits of each metal while mitigating the shortfalls (see Chapter 2).[50-52] As copolymerization of *in situ* synthesized epoxides is the ultimate goal of this project, it stands to reason that development of catalysts that mimic the most active in the field is worthwhile, although a deep understanding of the epoxidation process is required first. Should salen or amino-phenolate ligands prove fruitful, design of macrocyclic analogues incorporating one or both is possible, and the spatial arrangement of the active sites may encourage a cooperative effect between the metals. Ideally, this work will expand the epoxide substrate scope for copolymerization of CO_2 and epoxides and provide alternative methods for synthesizing epoxides in a more efficient and less wasteful manner.

5.6. Conclusions

The development of sustainable polymers is an expansive area of research. Conversion of carbon dioxide and renewable reagents into polymers represents a key step in reducing our environmental footprint as well as providing a route to new polymers with unique physical properties. Transition metal catalysts have demonstrated exceptional ability to catalyze such transformations. The first chapter of this Thesis discussed the importance of polymers to our society and how these robust materials impact the environment. Current poly(carbonate) production relies on toxic reagents and fossil fuel resources. A thorough overview of 3d transition metal-based catalysts for the production of poly(carbonate) and

cyclic carbonate from CO_2 and epoxides as an alternative to the current methods of production was provided with a focus on zinc and iron-catalyzed systems. Transition metal-catalyzed poly(ester) synthesis from cyclic substrates was also reviewed and the ability of iron-based catalysts to facilitate such reactions was highlighted. The advantages and limitations of the catalysts developed to date was provided along with discussions on the mechanisms behind each process. Each of these classes of polymers has been studied extensively and recently the metal-catalyzed synthesis of copolymers and terpolymers that incorporate the substrates from each has been developed. Literature review shows that the ability of any particular metal to catalyze polymerization reactions can be heavily dependent on the ligand(s), the steric effects they impart, and the influence they hold over the Lewis acidity at the metal centre. Alkylperoxo zinc complexes and the catalytic epoxidation of alkenes was also introduced.

Chapter 2 discussed the activity of an amino-bis(phenolate) zinc complex, **2.1**, for copolymerization of CO_2 and epoxides. The Kozak group had previously demonstrated the activity of complex **2.1** toward ring-opening polymerization of *rac*-lactide for poly(ester) synthesis. Homopolymerization of cyclohexene oxide catalyzed by **2.1** was observed in the presence of 2 equiv BnOH co-catalyst over a wide range of temperatures. Copolymerization of CHO and CO_2 by **2.1** and 2 equiv BnOH was selective for polymer and afforded poly(ether-*co*-carbonate) with high molecular weights. Temperature and pressure dependence on this reaction was studied, and copolymerization was achievable at 1 bar of CO_2 with low carbonate incorporation. Limonene oxide and propylene oxide could be incorporated as a co-monomers with CHO and CO_2 to afford poly(ether-*co*-carbonate).

Chapter 3 described the synthesis and characterization of an alkylperoxo zinc complex **3.1**. This compound and alkylperoxo zinc *β*-diketiminate complex **1.41** were applied toward the epoxidation of alkenes followed by copolymerization of the epoxide with CO_2 in one-pot. Both species demonstrated epoxidation activity toward *trans*-chalcone and **1.41** catalyzed the ROP of the epoxide. Introducing 20 bar CO_2 after epoxidation of *trans*-chalcone by **1.41** resulted in poly(ether) and poly(carbonate) production, identified via MALDI-TOF MS. Epoxidation of carvone by **1.41** was also observed by ^{1}H NMR and IR spectroscopy. Conversion to poly(ether) and poly(carbonate) was also observed by these techniques and is the first example of one-pot epoxidation-copolymerization and the first identification of carvone-based poly(carbonate).

Chapter 4 consists of the synthesis and application of 17 different iron amino-bis(phenolate) and salan complexes for CHO and CO_2 copolymerization. Many of the catalysts selectively yielded poly(carbonate), the most active of which was determined to be the iron amino-bis(phenolate) complex **4.1a**. Studies of pressure and co-catalyst dependence of this reaction were performed, and it was found that PPNCl co-catalyst could switch the selectivity to cyclic carbonate. Iron amino-bis(phenolate) complexes **4.8** and **4.9** were investigated as catalysts for lactide ROP. Compound **4.9** did not require co-catalyst addition (PPNCl) to achieve high conversion to poly(ester) and was applied toward more complex mixtures of lactide, phthalic anhydride and epoxides. Complete conversion of phthalic anhydride could be observed in epoxide solvents (CHO, PO, LO) with limited or no poly(ether) production. Epoxides were deemed necessary to form a metal-alkoxide through

ring-opening reaction of the axial chloride ligand with an epoxide. Molecular weights of the resulting poly(ester-*co*-ether)s were lower than anticipated but dispersities were fairly narrow.

Chapter 5 provides a summary of other catalyst development and reactions. The synthesis of complexes analogous to **2.1** from different zinc starting materials was attempted but ultimately unsuccessful. A zinc aza-crown-ether-phenolate complex **5.3** was synthesized and applied toward copolymerization of CHO and CO_2 affording low conversions to poly(carbonate) with few ether linkages. An ionic zinc borate species **5.4** was synthesized from reaction of **5.3** with Brookhart's acid. This species was inactive toward catalytic hydroamination of **5.5**. Compound **2.1** exhibited low activity toward hydroamination of **5.5**. A chiral zirconium amino-phenolate complex **5.7** was also applied toward hydroamination of **5.5** but was inactive.

In summary, this thesis has shown a zinc amino-bis(phenolate) catalyst **2.1** for homopolymerization of CHO and for CO_2 and epoxide copolymerization producing high molecular weight polymer. Reaction of **2.1** with O_2 resulted in the synthesis of a novel alkylperoxo zinc complex, **3.1**, that demonstrated activity toward epoxidation of enones. Compound **3.1** and another alkylperoxo zinc complex, **1.41**, were able to epoxidize carvone as well. Compound **1.41** was also able to homopolymerize the epoxides and copolymerize them with CO_2. Several iron complexes exhibited activity toward CO_2 and epoxide copolymerization and coupling. Compounds **4.8** and **4.9** were found active toward lactide ROP and **4.9** toward phthalic anhydride, epoxide and lactide terpolymerization reactions.

5.7. Experimental

General Methods: All reagents were purchased from Sigma-Aldrich, Alfa-Aesar, or Caledon. All epoxides were dried over CaH_2 and distilled. Unless otherwise stated, all reactions were performed under inert atmosphere of N_2. ^{1}H NMR spectra were recorded at 300 MHz on a Bruker Avance III spectrometer with BBO probe and ^{13}C at 500 MHz on a Bruker Avance I spectrometer with a TCI inverse gradient probe. *In situ* FTIR monitoring was performed using a 100 mL Parr Instruments 4560 stainless steel mini reactor vessel with motorized mechanical stirrer and a heating mantle. The vessel was modified with a bottom-mounted Mettler Toledo SiComp Sentinel ATR sensor, which was connected to a ReactIR 15 base unit through a silver-halide Fiber-to-Sentinel conduit. Profiles of the absorbance height at the desired frequency (e.g. 1089 cm^{-1} and 1750 cm^{-1}) were measured every 60 – 120 s. Similar methods for reaction monitoring via *in situ* IR have been reported elsewhere.[53-55]

Synthesis of **5.3**: Following the procedure to synthesize **2.1**, a solution of $ZnEt_2$ (6.9 mL, 1.0 M solution in hexanes) was added dropwise to a solution of **5.2** (3.00 g, 6.86 mmol) in THF (30 mL) at –35 °C. The reaction mixture was stirred for 1 h while warming to 25 °C. The solvent was then removed under reduced pressure and the resulting solid washed with pentane (3 × 10 mL). The colourless solid was then dried under reduced pressure affording **5.3** (3.10 g, 5.83 mmol). ^{1}H NMR spectroscopy analysis agreed with reported synthesis.[6]

Synthesis of **$[H(OEt_2)_2]^+[B((m\text{-}CF_3)_2C_6H_3)_4]^-$**: Brookhart's acid was prepared according to literature procedure.[9]

Synthesis of **5.4**: A solution of Brookhart's acid (101.1 mg, 0.099 mmol) in diethyl ether was added slowly to a solution of **5.2** (43.4 mg, 0.099 mmol) in toluene (10 mL) and cooled to -35 °C to yield the diacid. A solution of $ZnEt_2$ (0.11 mL, 1.0 M solution in hexanes) was added dropwise to the reaction mixture. This was stirred for 1 h while warming to 25 °C. The solvent was then concentrated to ~5 mL and cooled to –35 °C yielding single-crystals suitable for X-ray diffraction. The structure was solved by Dr. Michael Katz at Memorial University of Newfoundland. The remaining solvent was removed under reduced pressure and the remaining solid washed with pentane (3 × 10 mL). The resulting colourless powder was dried under reduced pressure affording **5.4** (0.11 g, 0.081 mmol).

^{1}H NMR (CD_3CN, 300 MHz): ∂ 7.70 (4 H, br t, B–ArH), 7.68 (8 H, br s, B–ArH), 7.20 (1 H, d, ArH), 6.89 (1 H, d, ArH), 4.10 (4 H, m, OCH_2CH_2O) 3.98 – 3.66 (12 H, m, CH_2CH_2), 3.54 (4 H, m, $ArCH_2N$), 2.94 (4 H, NCH_2CH_2), 1.42 (9 H, s, $C(CH_3)_3$), 1.24 (9 H, s, $C(CH_3)_3$). Diethyl ether contamination (∂ 3.42, 1.12) and ethane (∂ 0.84) are present in the spectrum (Fig. A5.1). ^{19}F NMR spectroscopy produced a single signal at ∂ –63.34 (24 F, s, CF_3).

Synthesis of **5.7**: A solution of $ZrBn_4$ (0.2340 g, 0.5134 mmol) in toluene (10 mL) was added slowly to a solution of **L5.7** (0.2387 g, 0.5061 mmol) in toluene (20 mL) at –35 °C yielding an orange solution. The reaction mixture was stirred for 3 h while warming to 25 °C. The solvent was removed under reduced pressure affording **5.7** as a yellow powder (0.2277 g, 61%).

^{1}H NMR (C_6D_6, 300 MHz): ∂ 7.84 (1 H, m, ArH), 7.49 (1 H, m, ArH), 7.21 (1 H, t, ArH), 7.17 – 6.92 (6 H, m, ArH), 6.89 – 6.82 (1 H, m, ArH), 6.38 (2 H, m, ArH), 4.54 (1 H, d,

CHN), 4.00 (1 H, m, ArCH$_2$N), 3.26 (1 H, d, ArCH$_2$N), 2.69 (2 H, m, CH$_2$N), 2.57 (2 H, m, CH$_2$CH$_2$), 2.37 (2 H, m, CH$_2$CH$_2$), 1.27 (9 H, s, C(CH$_3$)$_3$), 1.13 (9 H, s, C(CH$_3$)$_3$) (Fig. A5.2). ^{13}C{^{1}H} NMR (C$_6$D$_6$, 75 MHz): ∂ 158.30 (ArC), 150.20 (ArC), 149.41 (ArC), 139.46 (ArC), 139.12 (ArC), 136.86 (ArC), 130.97 (ArC), 128.74 (ArC), 127.89 (ArC), 126.67 (ArC), 126.09 (ArC), 125.91 (ArC), 125.70 (ArC), 125.27 (ArC), 124.52 (ArC), 123.91 (ArC), 123.66 (ArC), 123.50 (ArC), 87.42 (*C*(Ph)$_2$O), 77.69 (Ar*C*H$_2$N), 72.43 (N*C*H$_2$CH$_2$), 61.76 (N*C*CPh$_2$O), 55.85 (NCH$_2$*C*H$_2$), 34.96 (*C*(CH$_3$)$_3$), 34.16 (*C*(CH$_3$)$_3$), 31.95 (C(*C*H$_3$)$_3$), 30.30 (C(*C*H$_3$)$_3$), 20.67 (ZrCH$_2$).

5.8. References

1. Liu, Y.; Dawe, L. N.; Kozak, C. M., Bimetallic and trimetallic zinc amino-bis(phenolate) complexes for ring-opening polymerization of rac-lactide. *Dalton Trans.* **2019**, *48*, pp 13699-13710.

2. Chamberlain, B. M.; Cheng, M.; Moore, D. R.; Ovitt, T. M.; Lobkovsky, E. B.; Coates, G. W., Polymerization of Lactide with Zinc and Magnesium β-Diiminate Complexes: Stereocontrol and Mechanism. *J. Am. Chem. Soc.* **2001**, *123*, pp 3229-3238.

3. Piesik, D. F. J.; Range, S.; Harder, S., Bimetallic Calcium and Zinc Complexes with Bridged β-Diketiminate Ligands: Investigations on Epoxide/CO_2 Copolymerization. *Organometallics* **2008**, *27*, pp 6178-6187.

4. Anderson, T. S.; Kozak, C. M., Ring-opening polymerization of epoxides and ring-opening copolymerization of CO_2 with epoxides by a zinc amino-bis(phenolate) catalyst. *Eur. Polym. J.* **2019**, *120*, p 109237.

5. Chen, M.-T.; Chen, Y.-Y.; Li, G.-L.; Chen, C.-T., Diverse Coordinative Zinc Complexes Containing Amido-Pyridinate Ligands: Structural and Catalytic Studies. *Front. Chem.* **2019**, *6*.

6. Poirier, V.; Roisnel, T.; Carpentier, J.-F.; Sarazin, Y., Zinc and magnesium complexes supported by bulky multidentate amino-ether phenolate ligands: potent pre-catalysts for the immortalring-opening polymerisation of cyclic esters. *Dalton Trans.* **2011**, *40*, pp 523-534.

7. Sergeeva, E.; Press, K.; Goldberg, I.; Kol, M., Zinc Complexes of Bipyrrolidine-Based Diamine-Diphenolato and Diamine-Diolato Ligands: Predetermination of Helical Chirality Around Tetrahedral Centres. *Eur. J. Inorg. Chem.* **2013**, *2013*, pp 3362-3369.

8. Alonso-Moreno, C.; Garcés, A.; Sánchez-Barba, L. F.; Fajardo, M.; Fernández-Baeza, J.; Otero, A.; Lara-Sánchez, A.; Antiñolo, A.; Broomfield, L.; López-Solera, M. I.; Rodríguez, A. M., Discrete Heteroscorpionate Lithium and Zinc Alkyl Complexes. Synthesis, Structural Studies, and ROP of Cyclic Esters. *Organometallics* **2008**, *27*, pp 1310-1321.

9. Brookhart, M.; Grant, B.; Volpe, A. F., [(3,5-(CF3)2C6H3)4B]-[H(OEt2)2]+: a convenient reagent for generation and stabilization of cationic, highly electrophilic organometallic complexes. *Organometallics* **1992**, *11*, pp 3920-3922.

10. Wu, G.-P.; Wei, S.-H.; Ren, W.-M.; Lu, X.-B.; Xu, T.-Q.; Darensbourg, D. J., Perfectly Alternating Copolymerization of CO_2 and Epichlorohydrin Using Cobalt(III)-Based Catalyst Systems. *J. Am. Chem. Soc.* **2011**, *133*, pp 15191-15199.

11. Sarazin, Y.; Poirier, V.; Roisnel, T.; Carpentier, J.-F., Discrete, Base-Free, Cationic Alkaline-Earth Complexes – Access and Catalytic Activity in the Polymerization of Lactide. *Eur. J. Inorg. Chem.* **2010**, *2010*, pp 3423-3428.

12. Wataha, J., Palladium, Biological Effects. In *Encyclopedia of Metalloproteins*, Kretsinger, R. H.; Uversky, V. N.; Permyakov, E. A., Eds. Springer New York: New York, NY, 2013; pp 1628-1635.

13. Medici, S.; Peana, M.; Nurchi, V. M.; Lachowicz, J. I.; Crisponi, G.; Zoroddu, M. A., Noble metals in medicine: Latest advances. *Coord. Chem. Rev.* **2015**, *284*, pp 329-350.

14. Leung, C.-H.; Zhong, H.-J.; Chan, D. S.-H.; Ma, D.-L., Bioactive iridium and rhodium complexes as therapeutic agents. *Coord. Chem. Rev.* **2013**, *257*, pp 1764-1776.

15. Ghosh, S.; Sharma, A.; Talukder, G., Zirconium. *Biol. Trace Elem. Res.* **1992**, *35*, pp 247-271.

16. Ding, Y.; Zhang, S.; Liu, B.; Zheng, H.; Chang, C.-c.; Ekberg, C., Recovery of precious metals from electronic waste and spent catalysts: A review. *Resour. Conserv. Recy.* **2019**, *141*, pp 284-298.

17. Fitzpatrick, R. W.; Chittleborough, D. J., Titanium and Zirconium Minerals. In *Soil Mineralogy with Environmental Applications*, 2002; pp 667-690.

18. Clark, W. D.; Cho, J.; Valle, H. U.; Hollis, T. K.; Valente, E. J., Metal and halogen dependence of the rate effect in hydroamination/cyclization of unactivated aminoalkenes: Synthesis, characterization, and catalytic rates of CCC-NHC hafnium and zirconium pincer complexes. *J. Organomet. Chem.* **2014**, *751*, pp 534-540.

19. Watson, D. A.; Chiu, M.; Bergman, R. G., Zirconium Bis(Amido) Catalysts for Asymmetric Intramolecular Alkene Hydroamination. *Organometallics* **2006**, *25*, pp 4731-4733.

20. Qian, Q.; Tan, Y.; Zhao, B.; Feng, T.; Shen, Q.; Yao, Y., Asymmetric Epoxidation of Unsaturated Ketones Catalyzed by Heterobimetallic Rare Earth–Lithium Complexes Bearing

Phenoxy-Functionalized Chiral Diphenylprolinolate Ligand. *Org. Lett.* **2014**, *16*, pp 4516-4519.

21. Zucchini, U.; Albizzati, E.; Giannini, U., Synthesis and properties of some titanium and zirconium benzyl derivatives. *J. Organomet. Chem.* **1971**, *26*, pp 357-372.

22. Zhou, X.; Wei, B.; Sun, X.-L.; Tang, Y.; Xie, Z., Asymmetric hydroamination catalyzed by a new chiral zirconium system: reaction scope and mechanism. *Chem. Commun.* **2015**, *51*, pp 5751-5753.

23. Chong, E.; Qayyum, S.; Schafer, L. L.; Kempe, R., 2-Aminopyridinate Titanium Complexes for the Catalytic Hydroamination of Primary Aminoalkenes. *Organometallics* **2013**, *32*, pp 1858-1865.

24. Bielefeld, J.; Kurochkina, E.; Schmidtmann, M.; Doye, S., New Titanium Complexes and Their Use in Hydroamination and Hydroaminoalkylation Reactions. *Eur. J. Inorg. Chem.* **2019**, *2019*, pp 3713-3718.

25. Lauzon, J. M. P.; Schafer, L. L., Tethered Bis(amidate) and Bis(ureate) Supported Zirconium Precatalysts for the Intramolecular Hydroamination of Aminoalkenes. *Z. Anorg. Allg. Chem.* **2015**, *641*, pp 128-135.

26. Sun, Q.; Wang, Y.; Yuan, D.; Yao, Y.; Shen, Q., Zirconium catalysed intermolecular hydroamination reactions of secondary amines with alkynes. *Chem. Commun.* **2015**, *51*, pp 7633-7636.

27. Sun, Q.; Wang, Y.; Yuan, D.; Yao, Y.; Shen, Q., Zirconium complexes stabilized by amine-bridged bis(phenolato) ligands as precatalysts for intermolecular hydroamination reactions. *Dalton Trans.* **2015**, *44*, pp 20352-20360.

28. Lehenmeier, M. W.; Kissling, S.; Altenbuchner, P. T.; Bruckmeier, C.; Deglmann, P.; Brym, A. K.; Rieger, B., Flexibly tethered dinuclear zinc complexes: a solution to the entropy problem in CO_2/epoxide copolymerization catalysis? *Angew. Chem. Int. Ed.* **2013**, *52*, pp 9821-9826.

29. Cheng, M.; Lobkovsky, E. B.; Coates, G. W., Catalytic Reactions Involving C1Feedstocks: New High-Activity Zn(II)-Based Catalysts for the Alternating Copolymerization of Carbon Dioxide and Epoxides. *J. Am. Chem. Soc.* **1998**, *120*, pp 11018-11019.

30. Andrea, K. A.; Kerton, F. M., Iron-catalyzed reactions of CO_2 and epoxides to yield cyclic and polycarbonates. *Polym. J. (Tokyo, Jpn.)* **2020**.

31. Kozak, C. M.; Ambrose, K.; Anderson, T. S., Copolymerization of carbon dioxide and epoxides by metal coordination complexes. *Coord. Chem. Rev.* **2018**, *376*, pp 565-587.

32. Buchard, A.; Kember, M. R.; Sandeman, K. G.; Williams, C. K., A Bimetallic Iron(III) Catalyst for CO_2/Epoxide Coupling. *Chem. Commun.* **2011**, *47*, pp 212-214.

33. Taherimehr, M.; Al-Amsyar, S. M.; Whiteoak, C. J.; Kleij, A. W.; Pescarmona, P. P., High Activity and Switchable Selectivity in the Synthesis of Cyclic and Polymeric Cyclohexene Carbonates with Iron Amino Triphenolate Catalysts. *Green Chem.* **2013**, *15*, pp 3083-3090.

34. Nakano, K.; Kobayashi, K.; Ohkawara, T.; Imoto, H.; Nozaki, K., Copolymerization of Epoxides with Carbon Dioxide Catalyzed by Iron–Corrole Complexes: Synthesis of a Crystalline Copolymer. *J. Am. Chem. Soc.* **2013**, *135*, pp 8456-8459.

35. Andrea, K. A.; Kerton, F. M., Iron-catalyzed reactions of CO_2 and epoxides to yield cyclic and polycarbonates. *Polym. J. (Tokyo, Jpn.)* **2021**, *53*, pp 29-46.

36. Saussine, L.; Brazi, E.; Robine, A.; Mimoun, H.; Fischer, J.; Weiss, R., Cobalt(III) alkylperoxy complexes. Synthesis, x-ray structure, and role in the catalytic decomposition of alkyl hydroperoxides and in the hydroxylation of hydrocarbons. *J. Am. Chem. Soc.* **1985**, *107*, pp 3534-3540.

37. Kumar, P.; Lindeman, S. V.; Fiedler, A. T., Cobalt Superoxo and Alkylperoxo Complexes Derived from Reaction of Ring-Cleaving Dioxygenase Models with O_2. *J. Am. Chem. Soc.* **2019**, *141*, pp 10984-10987.

38. Bailey, P. J.; Coxall, R. A.; Dick, C. M.; Fabre, S.; Henderson, L. C.; Herber, C.; Liddle, S. T.; Loroño-González, D.; Parkin, A.; Parsons, S., The First Structural Characterisation of a Group 2 Metal Alkylperoxide Complex: Comments on the Cleavage of Dioxygen by Magnesium Alkyl Complexes. *Chem. Eur. J.* **2003**, *9*, pp 4820-4828.

39. Sun, C.; Yan, L.; Yue, B.; Liu, H.; Gao, Y., The modulation of metal–insulator transition temperature of vanadium dioxide: a density functional theory study. *J. Mater. Chem. C* **2014**, *2*, pp 9283-9293.

40. Chavez, F. A.; Mascharak, P. K., Co(III)−Alkylperoxo Complexes: Syntheses, Structure−Reactivity Correlations, and Use in the Oxidation of Hydrocarbons. *Acc. Chem. Res.* **2000**, *33*, pp 539-545.

41. Ambrose, K.; Robertson, K. N.; Kozak, C. M., Cobalt amino-bis(phenolate) complexes for coupling and copolymerization of epoxides with carbon dioxide. *Dalton Trans.* **2019**, *48*, pp 6248-6260.

42. Cao, L.; Dong, G.; Lai, W., Reaction Mechanism of Cobalt-Substituted Homoprotocatechuate 2,3-Dioxygenase: A QM/MM Study. *J. Phys. Chem. B* **2015**, *119*, pp 4608-4616.

43. Tokuyasu, T.; Kunikawa, S.; Masuyama, A.; Nojima, M., Co(III)−Alkyl Complex- and Co(III)−Alkylperoxo Complex-Catalyzed Triethylsilylperoxidation of Alkenes with Molecular Oxygen and Triethylsilane. *Org. Lett.* **2002**, *4*, pp 3595-3598.

44. Hirota, S.; Kosugi, E.; Marzilli, L. G.; Yamauchi, O., The Co-CH_3 bond in Shiff base B12 models: influence of the trans and equatorial ligands as assessed by Fourier transform Raman spectroscopy. *Inorg. Chim. Acta* **1998**, *275-276*, pp 90-97.

45. van Arkel, B.; van der Baan, J. L.; Balt, S.; Bickelhaupt, F.; de Bolster, M. W. G.; Kingma, I. E.; Klumpp, G. W.; Moos, J. W. E.; Spek, A. L., Intramolecularly alkylated salen complexes: new models for coenzyme B12 with a cobalt-to-ligand carbon bridge. *J. Chem. Soc. Perkin Trans. 1* **1993**, pp 3023-3032.

46. Costa, G.; Mestroni, G.; Stefani, L., Organometallic derivatives of cobalt(III) chelates of bis(salicylaldehyde) ethylenediimine. *J. Organomet. Chem.* **1967**, *7*, pp 493-501.

47. McAllister, R. M.; Weber, J. H., Preparation and reactions of alkyl-cobalt complexes containing schiff base ligands. *J. Organomet. Chem.* **1974**, *77*, pp 91-105.

48. Talsi, E. P.; Zimin, Y. S.; Nekipelov, V. M., Coordination of molecular oxygen by Co(II) β-diketonates. *React. Kinet. Catal. Lett.* **1985**, *27*, pp 361-364.

49. Ambrose, K. Cobalt and chromium amino-bis(phenolate) complexes for epoxide homopolymerization and copolymerization with carbon dioxide. Memorial Unversity of Newfoundland, 2019.

50. Trott, G.; Garden, J. A.; Williams, C. K., Heterodinuclear zinc and magnesium catalysts for epoxide/CO_2 ring opening copolymerizations. *Chem. Sci.* **2019**, *10*, pp 4618-4627.

51. Garden, J. A.; White, A. J. P.; Williams, C. K., Heterodinuclear titanium/zinc catalysis: synthesis, characterization and activity for CO_2/epoxide copolymerization and cyclic ester polymerization. *Dalton Trans.* **2017**, *46*, pp 2532-2541.

52. Trott, G.; Saini, P. K.; Williams, C. K., Catalysts for CO_2/epoxide ring-opening copolymerization. *Philos. Trans. Royal Soc. A* **2016**, *374*.

53. Ni, K.; Paniez-Grave, V.; Kozak, C. M., Effect of azide and chloride binding to diamino-bis(phenolate) chromium complexes on CO_2/cyclohexene oxide copolymerization. *Organometallics* **2018**, *37*, pp 2507-2518.

54. Andrea, K. A.; Kerton, F. M., Triarylborane-catalyzed formation of cyclic organic carbonates and polycarbonates. *ACS Catal.* **2019**, *9*, pp 1799-1809.

55. Darensbourg, D. J.; Yarbrough, J. C.; Ortiz, C.; Fang, C. C., Comparative kinetic studies of the copolymerization of cyclohexene oxide and propylene oxide with carbon dioxide in the presence of chromium salen derivatives. In situ FTIR measurements of copolymer vs cyclic carbonate production. *J. Am. Chem. Soc.* **2003**, *125*, pp 7586-7591.

5.9. Appendix

Table A5.1: Crystallographic data table for compound **5.4**.

	5.4
Empirical formula	$C_{57}H_{54}BF_{24}NO_5Zn$
Crystal colour	Colourless
Formula weight	1365.20
Temperature/K	100
Crystal system	Monoclinic
Space group	P $2_1/c$
a/Å	13.42069(3)
b/Å	18.38759(3)
c/Å	24.43495(3)
α/°	90.0
ß/°	98.366(4)
γ/°	90.0
Volume/Å^3	5965.75(6)
Z	3
ϱ_{calc}g/cm^3	1.520
μ/mm^{-1}	0.535
F(000)	2776.000
Crystal size/mm^3	0.1 × 0.1 × 0.1
Radiation	MoKα (λ = 0.71073)
2θ range for data collection/°	3.068 to 59.034
Index ranges	$-18 \leq h \leq 18$, $-25 \leq k \leq 23$, $-33 \leq l \leq 31$
Reflections collected	91458
Independent reflections	15513 [R_{int} = 0.0864, R_{sigma} = 0.2007]
Data/restraints/parameters	5339/146/832
Goodness-of-fit on F^2	1.0063
Final R indexes [I>=2σ(I)]	R_1 = 0.1730, wR_2 = 0.2977
Final R indexes [all data]	R_1 = 0.0864, wR_2 = 0.2007
Largest diff. peak/hole / e Å^{-3}	1.97/–0.86

Table A5.2: Selected bond lengths for compound **5.4**.

Atom	Atom	Length/Å	Atom	Atom	Length/Å	Atom	Atom	Length/Å
Zn1	O2	1.919(6)	C23	C26	1.527(14)	C72	C73	1.412(13)
Zn1	O9	2.198(6)	C27	C28	1.367(13)	C72	C77	1.382(13)
Zn1	O12	2.174(6)	C28	C29	1.550(12)	C72	B43	1.667(14)
Zn1	O15	2.251(6)	C29	C30	1.540(13)	C73	C74	1.403(12)
Zn1	O18	2.196(6)	C29	C31	1.524(13)	C74	C75	1.373(12)
Zn1	N6	2.162(8)	C29	C32	1.538(13)	C74	C82	1.506(10)
O2	C3	1.322(11)	C34	C37	1.509(10)	C75	C76	1.377(12)
O9	C8	1.436(11)	C37	C38	1.383(12)	C76	C77	1.395(12)
O9	C10	1.470(11)	C37	C42	1.392(12)	C76	C78	1.493(11)
O12	C11	1.451(11)	C38	C39	1.419(13)	C34	F33	1.331(7)
O12	C13	1.417(12)	C39	C40	1.379(12)	C34	F35	1.328(7)
O15	C14	1.465(11)	C39	C86	1.495(10)	C34	F36	1.340(7)
O15	C16	1.465(11)	C40	C41	1.402(13)	C47	F48	1.330(8)
O15	C16	1.440(11)	C41	C42	1.405(12)	C47	F49	1.326(8)
O18	C17	1.442(11)	C41	B43	1.654(14)	C47	F50	1.343(8)
O18	C19	1.431(11)	C44	C45	1.389(13)	C54	F55	1.345(8)
C3	C4	1.426(13)	C44	C53	1.368(13)	C54	F56	1.340(8)
C3	C28	1.457(13)	C44	B43	1.630(14)	C54	F57	1.341(8)
C4	C5	1.490(13)	C45	C46	1.384(13)	C64	F65	1.334(7)
C4	C21	1.374(13)	C46	C47	1.505(11)	C64	F66	1.339(7)
C5	N6	1.481(12)	C46	C51	1.406(14)	C64	F67	1.333(7)
C7	C8	1.510(13)	C51	C52	1.373(13)	C68	F69	1.361(8)
C7	N6	1.488(12)	C52	C53	1.405(12)	C68	F70	1.317(8)
C10	C11	1.488(14)	C52	C54	1.479(10)	C68	F71	1.317(8)
C13	C14	1.509(14)	C58	C59	1.406(13)	C78	F79	1.345(7)
C16	C17	1.497(13)	C58	C63	1.406(13)	C78	F80	1.337(8)
C19	C20	1.517(13)	C58	B43	1.617(15)	C78	F81	1.338(8)
C20	N6	1.488(11)	C59	C60	1.384(13)	C82	F83	1.331(8)
C21	C22	1.401(13)	C60	C61	1.386(13)	C82	F84	1.338(7)
C22	C23	1.529(14)	C60	C68	1.516(11)	C82	F85	1.332(8)
C22	C27	1.420(13)	C61	C62	1.383(13)	C86	F87	1.341(8)
C23	C24	1.542(13)	C62	C63	1.388(12)	C86	F88	1.333(8)
C23	C25	1.542(14)	C62	C64	1.507(10)	C86	F89	1.340(8)

Table A5.3: Selected bond angles for compound **5.4**.

Atom	Atom	Atom	Angle/°
O2	Zn1	O9	112.8(2)
O2	Zn1	O12	95.9(2)
O9	Zn1	O12	73.2(2)
O2	Zn1	O15	89.2(2)
O9	Zn1	O15	142.4(2)
O12	Zn1	O15	74.6(2)
O2	Zn1	O18	150.0(2)
O9	Zn1	O18	95.3(2)
O12	Zn1	O18	102.4(2)
O15	Zn1	O18	73.2(2)
O2	Zn1	N6	95.4(3)
O9	Zn1	N6	77.6(3)
O12	Zn1	N6	150.8(3)
O15	Zn1	N6	132.4(2)
O18	Zn1	N6	80.1(3)

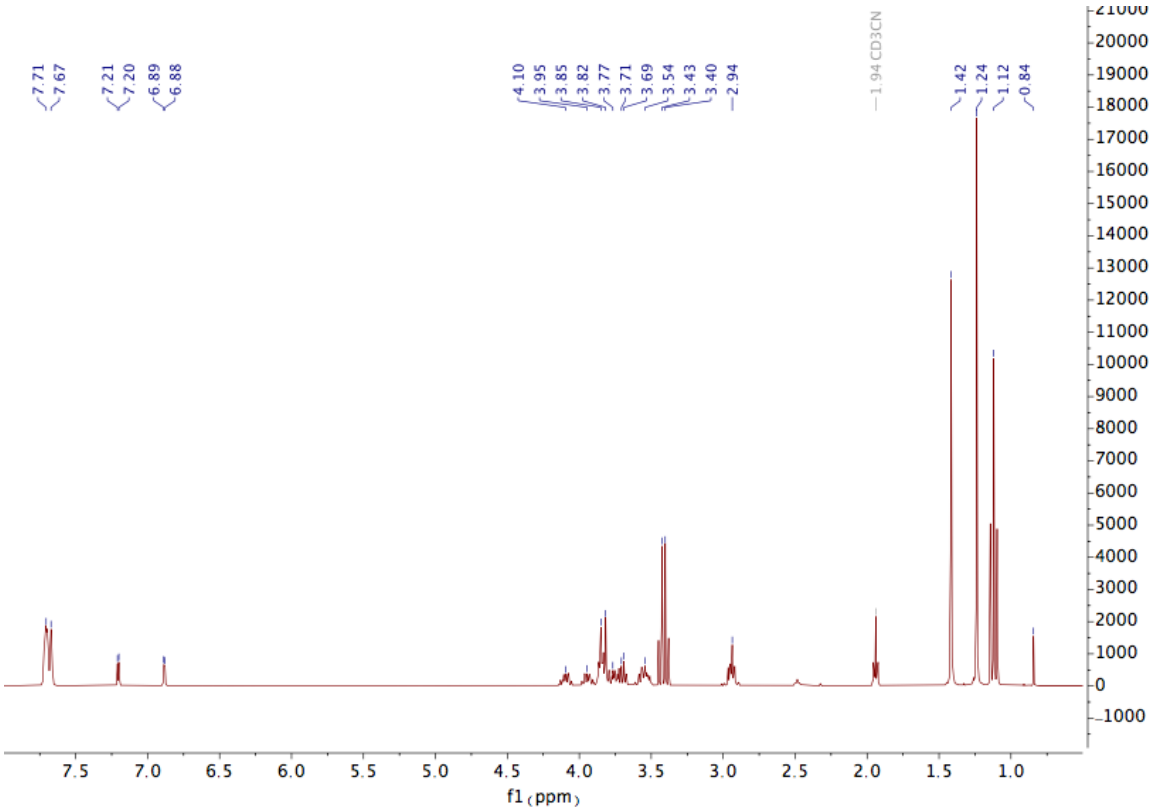

Fig. A5.1: ^{1}H NMR spectrum (CD_3CN, 300 MHz) of compound **5.3**.

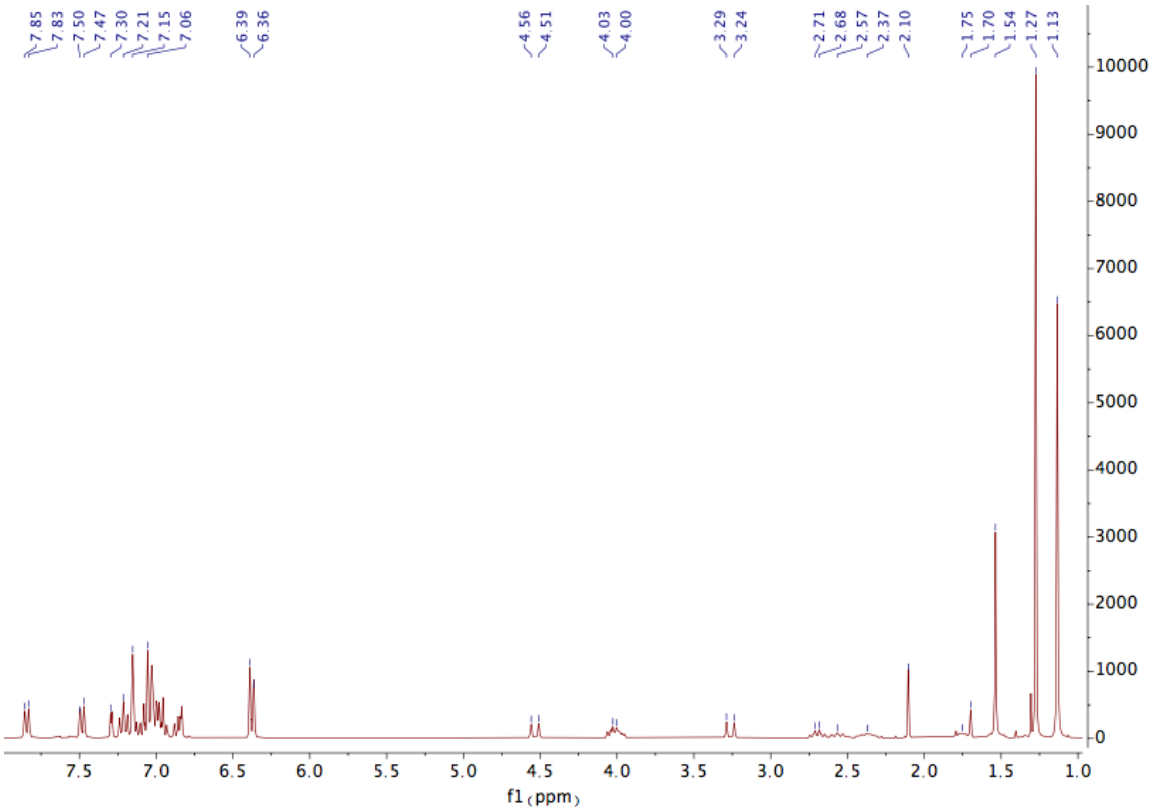

Fig. A5.2: ^{1}H NMR spectrum (C_6D_6, 300 MHz) of compound **5.6.** Small amounts of unreacted **H_2L5.6** are present at ∂ 7.30, 1.54, 1.28 and other positions overlapping with the product (91% conversion to **5.6**).